REPORT DOCUMENTATION PAGE	AFRL-SR-AR-TR-04- 0421

The public reporting burden for this collection of information is estimated to average 1 hour per response, including the tim gathering and maintaining the data needed, and completing and reviewing the collection of information. Send comments regar of information, including suggestions for reducing the burden, to Department of Defense, Washington Headquarters S (0704-0188), 1215 Jefferson Davis Highway, Suite 1204, Arlington, VA 22202-4302. Respondents should be aware that notwithstanding any other provision of law, no person shall be subject to any penalty for failing to comply with a collection of information if it does not display a currently valid OMB control number.

PLEASE DO NOT RETURN YOUR FORM TO THE ABOVE ADDRESS.

1. REPORT DATE (DD-MM-YYYY)	2. REPORT TYPE	3. DATES COVERED (From - To)
	FINAL REPORT	01 aug 1999 to 30 Apr 2004 - FINAL

4. TITLE AND SUBTITLE (MURI-99) Innovative Vacuum Electronics	**5a. CONTRACT NUMBER**
	5b. GRANT NUMBER
	5c. PROGRAM ELEMENT NUMBER
6. AUTHOR(S) Dr McDermott	**5d. PROJECT NUMBER**
	5e. TASK NUMBER
	5f. WORK UNIT NUMBER F49620-99-1-0297
7. PERFORMING ORGANIZATION NAME(S) AND ADDRESS(ES) UNIVERSITY OF CALIFORNIA SPONSORED PROGRAM 118 EVERSON HALL DAVIS CA 95616	**8. PERFORMING ORGANIZATION REPORT NUMBER**
9. SPONSORING/MONITORING AGENCY NAME(S) AND ADDRESS(ES) AFOSR/NE 4015 WILSON BLVD SUITE 713 ARLINGTON VA 22203	**10. SPONSOR/MONITOR'S ACRONYM(S)**
	11. SPONSOR/MONITOR'S REPORT NUMBER(S)

12. DISTRIBUTION/AVAILABILITY STATEMENT
DISTRIBUTION STATEMENT A: Unlimited

20040907 013

13. SUPPLEMENTARY NOTES

14. ABSTRACT
This report covers the period May 1, 1999- April 30, 2004 and contains a detailed description of the work conducted by the FY'99 MURI Consortium on Innovative Microwave Vacuum Electronics (MVE). The participating institutions were the University of California, Davis (Lead Institution); MIT; Stanford University; University of Maryland, College Park; University of Michigan, Ann Arbor; and the University of Wisconsin. The program was tightly focused on the critical need for a multi-disciplinary basic research program focused on 21st Century MVE devices and the education and training essential to the continuation of US preeminence. To ensure the accomplishment of the associated research and teaching goals, the Consortium developed a broad and well- integrated program involving close coordination with Industry and DoD laboratories. The strongly coordinated program drew on the institutions' strengths in microwave vacuum electronics, plasma physics, antennas, computational science and engineering, materials science, and thermal engineering, thereby resulting in a multiplicative factor significantly exceeding the sum of the individual programs. The participating institutions possess unparalleled facilities ranging from state-of-the-art measurement and diagnostic instrumentation to complete prototype manufacturing capability as well as strong analytic theory and computational

15. SUBJECT TERMS
modeling capability.

16. SECURITY CLASSIFICATION OF:			17. LIMITATION OF ABSTRACT	18. NUMBER OF PAGES	19a. NAME OF RESPONSIBLE PERSON
a. REPORT	b. ABSTRACT	c. THIS PAGE			19b. TELEPHONE NUMBER (Include area code)
			UL		

Standard Form 298 (Rev. 8/98)
Prescribed by ANSI Std. Z39.18

BEST AVAILABLE COPY

8-6-04

MURI'99
Innovative Microwave Vacuum Electronics Initiative Consortium

massachusetts institute of technology

Stanford University

UC DAVIS

UNIVERSITY OF MARYLAND

University of MICHIGAN

university of WISCONSIN

Director
Defense
Research
&
Engineering

Final Progress Report
May 1, 1999 – April 30, 2004
Dr. Robert Barker
Program Manager
Air Force Office of Scientific Research

Investigators:
J. Booske, G. Caryotakis, R. Gilgenbach, V. Granatstein, N.C. Luhmann, Jr., R. Temkin

TABLE OF CONTENTS

1.0 DIRECTORS OVERVIEW

This report covers the period May 1, 1999- April 30, 2004 and contains a detailed description of the work conducted by the MURI Consortium on Innovative Microwave Vacuum Electronics. The participating institutions were the University of California, Davis (Lead Institution); MIT; Stanford University; University of Maryland, College Park; University of Michigan, Ann Arbor; and the University of Wisconsin. The program was tightly focused on the MURI'99 Topic #11 description which succinctly identified the critical need for a multi-disciplinary basic research program focused on 21st Century MVE devices and the education and training essential to the continuation of US preeminence. To ensure the accomplishment of the associated research and teaching goals, the Consortium developed a broad and well- integrated program involving close coordination with Industry and DoD laboratories. The strongly coordinated program drew on the institutions' strengths in microwave vacuum and solid state electronics, plasma physics, antennas, computational science and engineering, materials science, and thermal engineering, thereby resulting in a multiplicative factor significantly exceeding that of the sum of the individual programs. The participating institutions possess unparalleled facilities ranging from state-of-the-art measurement and diagnostic instrumentation to complete prototype manufacturing capability as well as strong analytic theory and computational modeling capability. As described in more detail in the body of the Report, this has been an extremely productive endeavor. In the following, highlights from the past five years are briefly enumerated.

1.1.1 Fast Wave Device Research

Fast wave device research was conducted at UC Davis, MIT, and the University of Maryland. The aim of these activities was to provide a fundamental understanding of device physics and to develop new concepts to satisfy DoD needs for coherent amplifiers for applications such as imaging radar as well compact, oscillators for nonlethal defense applications.

Five innovative gyro-devices were investigated in the MURI-MVE program at UC Davis and which were designed for operation in W-Band and Ka-Band, the most important bands for future DoD millimeter-wave applications. A major emphasis these experimental activities has been aimed at a (potentially) high average power W-Band gyro-TWT operating in the low-loss TE_{01} mode, which significantly improves upon the characteristics of the recent NRL-industry high average power W-Band TE_{01} gyro-klystron amplifier with the focus being the need for wide bandwidth sources for imaging radar. The UCD gyro-TWT is driven by a 100 kV, 5 A, $v_{\perp}/v_Z=1.0$ MIG electron beam with $\Delta v_Z/v_Z=2.2\%$ reduce this to 2.2% with attendant increases in gain and bandwidth. The single-stage amplifier has been fabricated and is predicted by a large-signal simulation code to generate 140 kW at 94 GHz with 28% efficiency, 50 dB saturated gain and 5% bandwidth. Hot testing of the gyro-TWT continues with 61.2 kW saturated output power, 40 dB gain, 17.9 % efficiency, and 1.5 GHz (1.6%) bandwidth under zero drive stable conditions obtained for an 87 kV, 3.9 A beam and a magnetic field of 35.1 kG. Significant improvements are expected (both in bandwidth and power) when the testing of the seventh version is completed in July.

A dual mode gyro-BWO has been designed to yield high power over a broad bandwidth for future ECM applications. The two tuning modes of the gyro-BWO are fast tuning by changing

the cathode voltage and slow tuning by changing the magnetic field. It will utilize much of the TE_{01} gyro-TWT circuit. The TE_{01} gyro-BWO has been modeled with a self-consistent particle-tracing simulation code. The tapered device has been fabricated and is predicted to generate 100 kW near 94 GHz with over 10% tuning capability. Testing will commence following the completion of the gyro-TWT tests.

The UC Davis second-harmonic peniotron experiment is designed to demonstrate high device efficiency (~47%) and power output (~125 kW) at 34 GHz. It is intended as a first step towards higher frequency devices and an amplifier based on the peniotron interaction with the goal being stable operation at 94 GHz. The device incorporates a four-vane slotted circuit which supports the interaction of the fundamental cavity mode with the second-harmonic of the 70 kV, 3.5 ampere, axis-encircling electron beam. The circuit has been delivered and verified on cold test. The cusp electron gun is supplied by Northrop Grumman. Recent effort has concentrated on the re-design of the magnetic field to ensure high beam quality and safe operation. The magnetic assembly is complete and has been verified by measurement. Simulation of the beam, incorporating the new magnetic field profile, predicts greatly improved beam quality. Continuing efforts are focused on effort completing design of the collector, finishing assembly and verifying performance of the device. An Invited Talk on this work was presented by Ph. D student Larry Dressman at the Int. Conf. on Infrared and Millimeter Waves held in Toulouse, France.

A high-harmonic W-Band slotted gyrotron was designed and constructed at UCD in collaboration with the Air Force Phillips Laboratory that will be driven by a 70 kV, 3.5 A, axis-encircling electron beam from a Northrop Grumman Cusp gun provided under a DURIP grant. The 94 GHz, slotted sixth-harmonic gyrotron has been fabricated and is predicted to generate 40 kW with a device efficiency of 16%. Resumed testing awaits the completion of the W-Band gyro-TWT and BWO studies.

A second-harmonic Ka-Band TE_{21} gyro-TWT amplifier with an axis–encircling electron beam is being developed that is intended to address the need for high power broadband compact lightweight sources for DOD radar and communications applications. The device utilizes harmonic operation to reduce magnetic field requirements and to obtain higher power and greater stability. The gyro-TWT incorporates a Cusp gun developed by Northrop Grumman under DURIP/MURI funding which provides a 70 kV, 3.5 A axis-encircling electron beam. The device is predicted to nearly double the efficiency of the previous UC Davis 200 kW, 12% efficient, MIG second-harmonic Ku-Band gyro-TWT since the new device will avoid the loss in efficiency due to off-axis electrons interacting with a linearly polarized mode. The second-harmonic TE_{21} gyro-TWT amplifier has been designed, simulated and built and is being assembled for test and is predicted by our large signal code to produce 50 kW in Ka-band with 20% efficiency, 30 dB saturated gain and 3% bandwidth.

At the University of Maryland, interest has centered on the nonlinear behavior of vacuum electronic devices. They have been studying both theoretically and experimentally a harmonic doubling gyro-TWT with a clustered cavity bunching section. An output power of 40 kW was realized with 13% efficiency in K_a band; the amplifier frequency range was 1 GHz. Such an amplifier is inherently nonlinear and is directly applicable only in systems employing amplifiers working in saturation (e.g., high power radar); however, where applicable it has been shown to have certain practical advantages. They have also developed a theory which explains recently observed nonstationary behavior in gyro-BWOs and have carried out a theoretical study (with separate but related NRL support) of chaos in a conventional TWT with feedback. Nonstationary

and chaotic behavior in gyro-BWOs and TWTs and gyro-TWTs is recommended for future study. There is direct relevance to such DOD interests as jam resistant radar and secure communications.

A major event in the MIT MURI program was the successful operation of a novel 140 GHz quasioptical gyrotron traveling wave tube (gyro-TWT) amplifier at a record high power level, namely 30 kW, a significant advancement in the state-of-the-art in gyrotron amplifiers. The gyro-TWT produced up to 30 kW of peak power in 2 μs pulsed operation at 6 Hz achieving a peak gain of 29 dB, a peak efficiency of 12 % and a bandwidth of 2.3 GHz.

1.1.2 Slow Wave, Linear Beam Device Research

TWTs are nearly ubiquitous in DoD systems finding application in communications, radar, and ECM. This has motivated research activities at both the University of Wisconsin and UC Davis.

TWT phase noise reduction techniques have been investigated by UC Davis MURI Ph.D student Jae Seung Lee in cooperation with Teledyne Microwave Electronic Components. Phase modulation based communications, such as multi-PSK, Doppler radar and MTI (Moving Target Indicator) radar all requires extremely low phase noise TWTAs. One of the approaches which yielded excellent results utilizes an envelope feedback loop, which has the advantage of correcting the slow phase variation. This method resembles the conventional phase-locked loop (PLL) in which the detected output phase noise is compensated through a voltage controlled phase shifter

The importance of the TWT is reflected in the strong emphasis in the University of Wisconsin program. There, the activities are broad and comprehensive and include:

- Developing and operating a novel, multi-sensored TWT for research of fundamental nonlinear physics in MPM-class TWTs,

- Advancing a new understanding of the physics of nonlinear distortions in TWTs,

- Developing a new computational method to model 1-D linear-beam VEDs with Eulerian formulations, including the effects of charge overtaking,

- Establishing the fundamental physical mechanisms of harmonic and distortion product injection for linearization of TWTs,

- Identifying a novel TWT transmitter configuration enabling extremely linear amplification of digitally-modulated signals while operating saturated and thus at maximum efficiency,

- Completing the first combined experimental and simulation study of impulse amplification in TWTs revealing realistic prospects for novel applications to impulse radar, impulse communications, and impulse response measurements of small signal gain characteristics,

- Conducting investigations of X-ray LIGA, UV LIGA and deep reactive ion etching methods for microfabricating millimeter wave and THz regime TWTs, and

- Developed and disseminated a suite of 1-D TWT simulation codes for teaching and research of TWTs, making them available as open source software at http://www.lmsuite.org.

1.1.3 Microfabricated Miniature Millimeter Wave and THz Sources and Systems

A significant emphasis area of the MURI99 Innovative Vacuum Electronics program has been in the use of advanced microfabrication techniques to develop miniature millimeter wave and THz sources. This makes use of a variety of approaches including LIGA, SU-8, and advanced milling/etching techniques. A wide variety of complimentary activities have taken place at Stanford, UC Davis, and the University of Wisconsin.

Unquestionably, the leader in the microfabricated MVED field has been Stanford who have not only successfully fabricated and cold tested structures, but who have also propagated beams through them. A major thrust of the Stanford research has been directed toward the development of a 100 kW peak power, 1 kW average power,W-band klystrino. The goal of the research is to produce significant average power at W- band (95 GHz) in a compact lightweight package which has application in both radar and nonlethal defense systems. While researching alternative fabrication methods for the klystrino project, two alternate methods of lithographic circuit manufacturing were investigated by the Stanford team. The original klystrino circuit required dozens of post-LIGA machining steps because it used a roughened aluminum substrate for a base material and because the gold lithographic mask was bonded to the top of the PMMA photoresist. Attempts at using a smooth copper substrate failed because of poor adhesion of the PMMA and undercutting due to x-ray scattering from the copper base. Substituting SU-8 epoxy as the photoresist provides multiple benefits. First, the SU-8 is 200 times more sensitive to x-rays than PMMA. This means that the exposure times can be cut by two orders of magnitude and the effects of backscattering are negligible. Second, SU-8 is also sensitive to UV exposure which means that the LIGA process can be divorced from the synchrotron light sources that were its major shortcoming. Two 1 mm tall test circuits were made using SU-8. One was fabricated at SRRC with their x-ray source, the second was done at a small business using a commercial UV source. Both produced good results with specular surface finish.

Other Stanford activities have included the design of a microfabricated W-Band sheet-beam klystron. In addition, a collaboration involving UCD, Stanford, and Seoul National University is pursuing the development of LIGA fabricated TWTs. Yet another endeavor involves a collaboration which has the goal of making a dramatic advance beyond the MPM wherein an entire microfabricated TWT based millimeter wave transmitter is fabricated on a single substrate.

The University of Wisconsin group has specifically focused on the folded waveguide (FWG) TWT as one whose circuit is naturally suited to planar microfabrication methods. To date, they have successfully demonstrated the feasibility of fabricating 400 GHz FWG TWT circuits using conventional X-ray LIGA, novel UV LIGA, and deep reactive ion etching (DRIE).

A significant UCD emphasis area is in the use of advanced microfabrication techniques to develop miniature millimeter wave and THz sources. This makes use of both LIGA and advanced milling/etching techniques. The collaborative activities with Stanford aimed at the development of LIGA fabricated W-band klystrinos is described below under their portion of the overview. In parallel, a collaboration aimed at involving UCD, Stanford, and Seoul National University is pursuing the development of LIGA fabricated TWTs. Yet another endeavor involves collaboration with Profs. R.J. Hwu and L. Sadwick, which has the goal of making a

dramatic advance beyond the MPM wherein an entire microfabricated TWT biased millimeter wave transmitter is fabricated on a single substrate.

A major disadvantage of MPM/MMPM based phased arrays is that despite their small size, it is physically impossible to place them sufficiently close ($d<\lambda/2$) at frequencies above X-Band. Consequently, UC Davis is investigating two approaches to alleviate this problem. The first involves the development of further miniaturized tubes as mentioned above. The second involves the development of MEMS based delay lines and piezoelectric transducer perturbed lines to provide high power beam steering and shaping capability with the requisite spacing, thereby permitting the use of conventional MVEDs.

In addition to the above, a novel extension for the millimeter wave power module (MMPM) was investigated by UC Davis. The objective is to efficiently multiply the 26-40 GHz, 100 W output power of the MMPM to higher frequencies for use in a wide variety of DoD and commercial high frequency applications. This is achieved utilizing spatially power combined grid arrays of frequency multipliers. Preliminary results included Multi-Quantum Barrier Varactor and Schottky Quantum Barrier Varactor based 94 GHz frequency tripler arrays and a Schottky varactor based frequency doubler grid array at 63 GHz.

1.1.4 Crossed Field Device Research

University of Michigan graduate students and faculty have made a major breakthrough by discovery of an innovative technique to dramatically reduce the noise in magnetron oscillators (2 patent applications filed). The technique utilizes an azimuthally-varying axial magnetic field. Microwave measurements show dramatic reductions in the noise of kW oven magnetrons operating near 2.45 GHz. The noise reduction near the carrier is some 30 dB. Microwave sidebands are reduced or eliminated. Noise reduction occurs at all anode currents, but is particularly significant at low current near the start-oscillation condition. Further, this technique has been shown to be effective in noise reduction regardless of the magnetron current or age. Magnetic-Priming of magnetrons in the pi-mode has been discovered by use of N/2 magnetic perturbations (where N is the number of magnetron cavities).

MIT has extended the theoretical analysis of two-dimensional non-axisymmetric equilibrium flow in crossed-field devices, in collaboration with Mission Research Corporation. It is their hope that an improved understanding of the equilibrium flow will help us to identify the origin of noise in crossed-field amplifiers (CFAs). As the electron density approaches the (critical) Brillouin density, they found that a vortex structure with regions of negative potential forms near the cathode surface.

1.1.5 Field Emitter and Carbon Nanotube Arrays

Considerable progress was made at UC Davis on the development of photo-enhanced field emitter arrays, which will eliminate the bulky heater required in conventional microwave tubes and will also reduce their size due to the prebunching. In addition, a significant benefit of photo-excitation with short optical pulses is the opportunity to produce prebunched electrons where the use of optical gating bypasses speed-limiting capacitance of gridded cathodes. A key to the development of practical sources is the ability to utilize back-side illumination; this was successfully demonstrated together with high quantum yield (~50%). Other UC Davis work involved the successful fabrication of carbon nanotube arrays in collaboration with LLNL researchers.This work will continue under a newly established MURI Consortium on the

NanoPhysics of Electron Dynamics near Surfaces in High Power Microwave Devices and Systems.

MIT has successfully fabricated gated carbon nanotube emitter arrays using two different methods. The field emission mechanism of a carbon nanotube was studied and the FEED spectrum obtained agreed with experiment quite well.

1.1.6 Thermionic Cathodes

Another research area addressed at Stanford was the fabrication of improved thermionic cathodes for RF sources. As the frequency and power requirements of RF sources increase, the cathode area decreases. As an example, the klystrino above requires 15 A/cm^2 for a very low perveance device. An oxide cathode running 150°C cooler would have 25 times the expected life due to reduced barium evaporation.

The original Stanford/ UC Davis plasma deposition program for oxide cathodes produced a 30 A/cm^2 cathode operating at 960°C before problems with plasma triggering and available manpower sidetracked the research. An equivalent M-type dispenser cathode would operate at least 100°C hotter. With the use of a DURIP funded, excimer laser the triggering problems will not be an issue and significant improvements beyond the previous cathode results are expected. Under a newly established MURI Consortium on the NanoPhysics of Electron Dynamics near Surfaces in High Power Microwave Devices and Systems, Stanford, UC Davis, and the Naval Postgraduate School will collaborate on studies of oxide and scandate, low temperature/high current density cathodes produced via laser deposition. The intended applications are both conventional MVEDs and HPM sources.

1.1.7 Theory and Computational Modeling

A major accomplishment of the Stanford program was the completion of the parallel processing version of the 3D MAGIC PIC code. This is critical to future RF source development because realistic 3D modeling of RF interactions requires hundreds of hours of processing time on current state of the art workstations. Three dimensional modeling is required for new sheet beam and multiple beam devices as well as for lithographically fabricated round beam RF sources. A collaboration between Stanford and Mission Research Corporation was concerned with the development of parallel processing versions of MAGIC on both Windows and Linux platforms. Validation of the recently completed code produced nearly identical results for a single CPU run compared to a model run on a 24 processor Beowulf Linux Cluster.

In collaboration with Stanford, UC Davis student has been conducting 3-D Magic simulations of millimeter wave linear beam devices. Specifically, she has focused on Ka-Band extended interaction klytrons (EIKs) and Ka-Band TunneLadder TWTs.

In the area of code development, the University of Maryland participated in developing a new time dependent simulation code, TESLA, for linear beam microwave vacuum electronic devices The goal was to improve code efficiency and reduce computation time. Typically, TESLA can complete a design run in 15 minutes that would have taken 40 hours with MAGIC; thus TESLA is very valuable for optimizing designs after an initial MAGIC simulation of the precise geometry. The TESLA code has been transitioned to NRL and to industry (CPI, L3). University of Maryland researchers have also focused on the development of analytical methods to provide relatively rapid “zero order approximations” of the performance of microwave vacuum electronic devices.

In addition to the above, the University of Maryland developed a suite of codes supporting the design of multi-stage depressed collectors (MSDC) in gyro-devices. These codes take secondary electron emission into account. They typically allow for enhancement of device efficiency from ~30% to greater than 50%. This suite of codes has been called "the world's most sophisticated for MSDC analysis" and it has been transferred to U.S. industry for improving the performance of commercially produced gyrotrons.

MIT has developed a self-consistent technique for analytical calculation of dispersion curves in two-dimensional (2D) metallic photonic band gap (PBG) structures representing square and triangular arrays of metal rods.

University of Michigan has solved a 90-year old problem by finding a 2-dimensional Child-Langmuir Law, which gave the maximum current density that can be emitted over a finite patch of the cathode surface before the onset of a virtual cathode.

University of Michigan has also developed a general theory that accurately evaluates the intermodulation products that result from an input signal with multiple frequency components. The UM code has been validated with a series of collaborative experiments with MURI partner, University of Wisconsin. Also with UW, a novel method, by injecting a weak-signal, to suppress 3rd order intermodulation has been demonstrated.

In further activities, the University of Michigan has quantified to what extent a thin film of contaminants would lead to excessive heating of high power rf windows, by a scaling law. The University of Michigan scaling law surprisingly predicts that a thin film of contaminants (<< skin depth) may absorb up to a 50 percent of incident rf power.

1.1.8 MVED Materials Research

The University of Maryland MURI99 efforts to develop new materials as replacements for carcinogenic BeO composites in microwave power tubes proved successful. Using microwave sintering and chemical additives they have produced materials which exceed the thermal conductivity of the BeO composites and have the required dielectric properties.

1.1.9 MURI Book Project

A major emphasis over the past several years and involving the entire MURI Consortium as well as contributors from Industry and Government Laboratories has the preparation of a definitive book entitled "Modern Microwave and Millimeter-Wave Power Electronics" to be published by IEEE Press. The table of contents is provided in the body of this report. It is noteworthy that by unanimous agreement of the coeditors and all the coauthors, all royalties from this book will be used to fund graduate student involvement and activities in the field of microwave vacuum electronics device (MVED) research. The overall university leadership for this project rested with UC Davis, Maryland, and Wisconsin. The intended audience of this cutting edge book is primarily comprised of electrical engineers and/or systems engineers interested in long-distance (high power) communications and/or radar systems as well as those involved in nonlethal microwave defensive systems. At the time of this report, the book manuscript has been completed and submitted to IEEE Press for review. Galley proofs are expected in August and the book publication is scheduled for the end of the year. Another outcome of this book project has been the initiation of a UC Davis/Maryland collaboration to write a comprehensive historical survey of microwave tube R&D including little known Russian activities.

1.10 Education and Outreach

On the educational front, Stanford has been significantly involved in several ways. The major benefit to students is the exposure to state of the art experimental devices and tools. MURI students at Stanford have actively participated in the design, development, and operation of RF breakdown experiments, klystrons for the Next Linear Collider, the W-band klystrino, multiple beam and sheet beam klystron design, vector network analyzers from UHF to W-band, plasma deposition of oxide cathodes and surface science analysis for both RF breakdown and oxide cathodes. Stanford equipment has been used by several universities to provide hands-on experience with RF sources and components. Stanford has also provided MURI students with significant exposure to modeling and simulation of RF devices and components. The students have worked with state of the art simulation tools such as MAFIA, MAGIC, and ANSYS and actively participated in the development of MAGIC as a design code for klystrons. Furthermore, Stanford has actively participated in the curriculum development of the microwave courses provided at UC Davis. Most recently, Stanford conducted an extensive series of lectures (both life and in streaming video) on the physical principles and theory of klystrons, including their design and fabrication. The topics included klystron theory, electron gun design, beam focusing, computational modeling, vacuum and processing techniques, power supplies and modulators. The complete set of Stanford lecture notes and streaming video of the presentations may be found at:

http://www-group.slac.stanford.edu/kly/Old_web_site/slac_klystron_lecture_series.htm.

MIT hosted most of the student conference calls during the MURI program. These were very successful and popular with the students. More than twenty students were listening in on many of these calls. In addition, the talks were heavily attended by industry and government researchers.

Finally, it should also be noted that there is a main MURI99 MVE website located at http://tempest.das.ucdavis.edu/muri99/. Here, additional information including copies of presentations from the Annual Reviews may be found. In addition, a Networked Electronic Resource for Vacuum Electronics (NERVE) website is located at http://nerve.ece.wisc.edu.

N.C. Luhmann, Jr.
University of California, Davis
July 2004

2.0 SIGNIFICANT ACHIEVEMENTS May 1, 1999 – April 30, 2004

2.1 University of California, Davis

2.1.1 Wide Band, High Gain W-Band Gyro-TWT

2.1.1.1 Need

DoD radar applications increasingly require more precise tracking as well as higher resolution in range, angle, and Doppler. This is crucial for applications such as inverse synthetic aperture radar (ISAR) target imaging and jet engine modulation (JEM) classification electronic protection radar adjunct, detection of low cross section threats, and accurate tracking of sea skimming missiles. Although inferior to visible and IR systems in high humidity and rain, the millimeter wave portion of the spectrum (particularly the 94 GHz and 140 GHz "windows") offers superior performance through clouds, fog and smoke. As one example, this need motivated the NRL development of the WARLOC (*W-band Advanced Radar for Low Observable Control*) radar which is a transportable, land- or sea-based system, based on the use of a high-power 94 GHz Gyro-Klystron. This has been successfully demonstrated and is currently finding extensive service as a "cloud" radar. Despite the success, there remains a critical for an amplifier with considerably wider bandwidth to support the use of appropriately chirped pulses with pulse compression for high range resolution. In addition, increased gain is desired since the current NRL system must utilize a TWT driver, thereby adding cost and increasing weight as well as compared to a higher gain device which could employ a solid-state driver. Other applications include the Lincoln Laboratory millimeter wave radar located at the U.S. Army Kwajalein Atoll/Kwajalein Missile Range where they track and collect metric/signature data on missiles and provide tracking information on space objects. To respond to the increasing miniaturization of satellites, an upgrade to the Haystack radar is required over the 92 to 100 GHz band. However, as noted in the July 2001 report by the Ad Hoc Tri-Service Committee studying the DoD R&D investment strategy, no current rf amplifier technology can provide the required power. As further noted in the report, the Air Force Space HUSIR requirements may require the use of wideband gyro-TWT technology to satisfy the 8 GHz instantaneous bandwidth requirement. Explicitly noted in the report is the proposed W-Band TE_{01} gyro-TWT development solution.

2.1.1.2 MURI Activity and Achievement

To satisfy the above needs, a high power, TE_{01} mode, W-Band gyro-TWT has been successfully designed and fabricated at UCD and even in its still un-optimized state, it has provided impressive performance. The initial amplifier design is predicted to generate 140 kW at 94 GHz with 50 dB saturated gain, 28% efficiency and 5% bandwidth and it appears that with continued optimization (see Sec. 4.1.1.1) these figures will be reached. Note that this represents more than a factor of three increase in bandwidth over the current WARLOC sources while the gain is within the capability of currently available waveguide combined InP HEMT drivers. For the longer term, a more ambitious device is planned which would have ultrahigh gain (70 dB) which completely eliminates the burden on the driver. Efficiency will be increased via the use of a depressed collector. The table below compares the predicted and currently realized performance of the UC Davis TE_{01} gyro-TWT with the state-of-the art for W-Band sources. Additional perspective may be obtained by comparing the predicted (and anticipated) performance of the

UC Davis W-Band gyro-TWT to the state-of-the-art for gyro-TWTs of all frequencies as done in Fig. 2.1.1 below.

Year	**Institution**	**Device**	**V_b (kV)**	**3dB Bandwidth (MHz)**	**Peak Power (kW)**	**Average Power (kW)**	**Saturated Gain (dB)**	**□ (%)**
1982	Varian	Gyro-TWT	50	1880	20	-	30	8
2003	CPI	Gyro-Klystron	55	700	100	10	35	30
2003	CPI	Gyro-Twystron	65	1600	60	0.3*	34	15
2003	UC Davis (Designed)	Gyro-TWT	100	4625	140	14 **	50	28
2003	UC Davis (Measured)***	Gyro-TWT	87	1500	61	-	45	18

*Limits of current testing-9 kW predicted
** Potential with high power absorber and collector
*** Not yet optimized

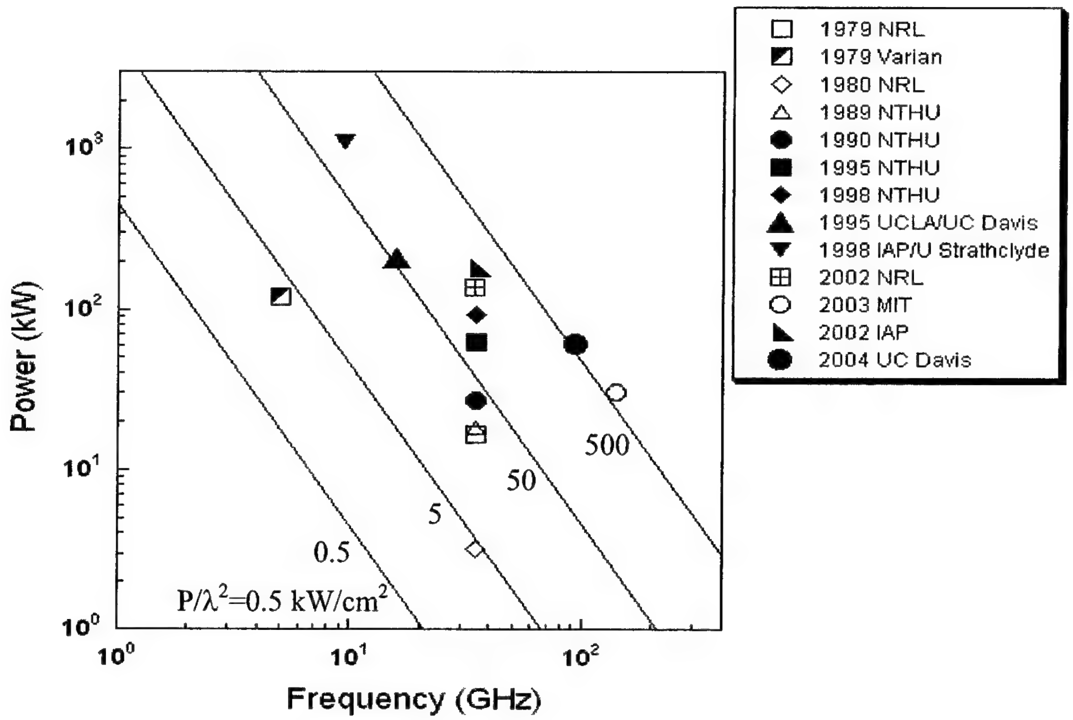

Fig2.1.1. Gyro-TWT state-of-the-

2.1.2 Compact, High Efficiency 40 to 160 GHz Sources

2.1.2.1 Need

As noted in the July 2001 report "DoD Investment Strategy for Vacuum Electronics R&D and Investment Balance for RF Power Vacuum Electronics and Solid-State R&D" by the Ad Hoc Tri-Service Committee, there is a current need for compact, efficient sources in the 50 to 100 W range in the 40 to 160 GHz region with longer term needs rising to 500 W with 50 % power added efficiency. Representative application areas include the AN/TSC-154 Secure Mobile Anti-Jam Reliable Tactical Terminal (SMART-T), the Advanced EHF satellite (AEHF) which is a follow-on to MILSTAR, Wideband Gap Filler, GPS III, the Navy's Advanced Narrow Band System/Mobile User Objective System, and satellite cross-links. As explicitly noted in the 2001 report, the current SMART-T transmitter is based on a solid-state pHEMT transmitter which can only provide 25 to 30 W of power, thereby resulting in difficulties in link closure under adverse weather conditions.

Although it is clear that only VEDs can satisfy these DoD 50 -500 W power requirements, it is equally clear that as the features in the tube interaction circuits get smaller, and as long as the methods of their fabrication and assembly remain traditional, their cost remains prohibitive, except for very special situations. For example, the cost of MMPMs, or "Millimeter Microwave Power Modules" in small quantities is $75,000 a copy. At this price, the quantities are bound to remain small. This is not a price tag that is likely to generate a new market, nor are the manufacturing methods involved amenable to mass production. Regarding commercial spin-offs

which would concurrently reduce costs for military systems, it is noted that communication system houses would prefer MMPM prices closer to $1000, in very large quantities.

2.1.2.1 MURI Activity and Achievement

To satisfy the above needs, Stanford and Davis have devoted considerable resources to both the development of new microfabrication techniques as well as computational modeling and design (also see the Stanford section of the Annual report). In the modeling area, it is essential to have a rapid 3-D simulation capability so that this can be employed as a design tool and not simply a verification technique. This motivated the Stanford-MRC parallel MAGIC-3D activities as well as the Davis TWT and EIK modeling studies. In the latter, MURI student Hsin-Lu Hsu has begun work on the simulation of a structure which is amenable to microfabrication and for which there is ample experimental data, namely the Karp/TunneLadder circuit. Here, we have great benefited from the fact that Dr. Karp lives only 5 minutes from Stanford. The initial work has focused on the design and fabrication of a Ka-Band proof-of-principle device.

Fig. . 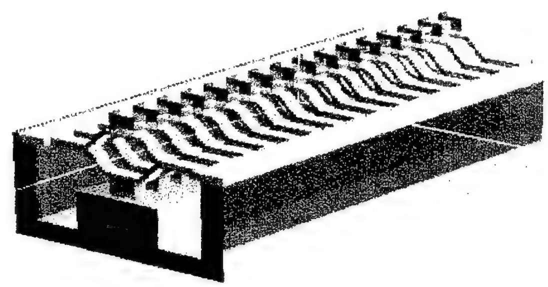 *adder TWT*

2.2 Stanford University

2.2.1 Parallel Processing for Magic 3D Simulations

2.2.1.1 DoD Need

Two specific applications where 3D models of device behavior are critical are the multiple beam klystron designs for the SPY-1 low noise upgrade to the AEGIS radar and millimeter-wave, high-average-power, sheet beam klystron designs for active denial systems. These devices require 3D modeling to optimize designs and predict performance. Given the hundreds of hours required for full 3D modeling of these devices using single processor PCs, the development of a parallel processing capability for MAGIC is mandatory. In addition to the specific needs noted above, the general trend to higher performance devices makes 3D modeling a necessary tool to insure that non-axisymmetric modes, circuit geometry, magnetic circuits, etc. do not cause failures that are only detected after the devices are built and tested.

2.2.1.2 MURI Achievement

Stanford University, in collaboration with Mission Research Corporation (MRC), the developers of the MAGIC code group, has been working on a parallel processing version of MAGIC. The goal of the program is to be able to adequately model the sheet beam klystron designs at the Stanford Linear Accelerator Center at X-band and at W-band. Sheet beam devices cannot be modeled accurately in two dimensions as significant issues with electron gun design, beam

focusing, cavity geometry, device stability, spurious modes, heat transfer and power extraction require 3D analysis. The task had multiple components, all of which had to be completed successfully in order to produce a workable parallel processing version of MAGIC. Since the multiple processor cluster used the Linux operating system, the first task was to produce a port of MAGIC to Linux that would return exactly the same results for a given input file. This was a significant effort in itself as multiple bugs were discovered and corrected in both versions of the code. Once an accurate Linux version was obtained, the code was modified to deal with slices of the problem with the information at the boundaries passed to other processors in the cluster. In essence, each processor solved its own version of MAGIC except that data on fields and particles at the problem boundaries were not static. When all processors complete the problem section assigned to them, it is the job of the master processor to sew together all the individual data sets into a seamless model of the device behavior.

The acid test for this endeavor is to model a given device using the single processor version of MAGIC3D and then split the problem into "n" pieces and assign each piece to a separate processor. With Stanford's 24 processor Beowulf Linux Cluster, "n" varied from 2 to 24. Successful completion of the project was achieved when a comparison of the six electric and magnetic field components for a two-cavity, sheet beam klystron, single processor run versus an "n" processor run produced an average error of less than $1*10^{-5}$. The figure below shows a plot of elapsed time versus number of processors. The diminishing return for additional processors is caused by the amount of information that must be passed between processors as the number of processors increases as well as the overhead of recombining the individual solutions from each processor. The message passing bottleneck consumes roughly 50% of the computational time so replacing the 10 Mb/sec Ethernet cards with gigabit Ethernet should produce much better performance with larger number of processors.

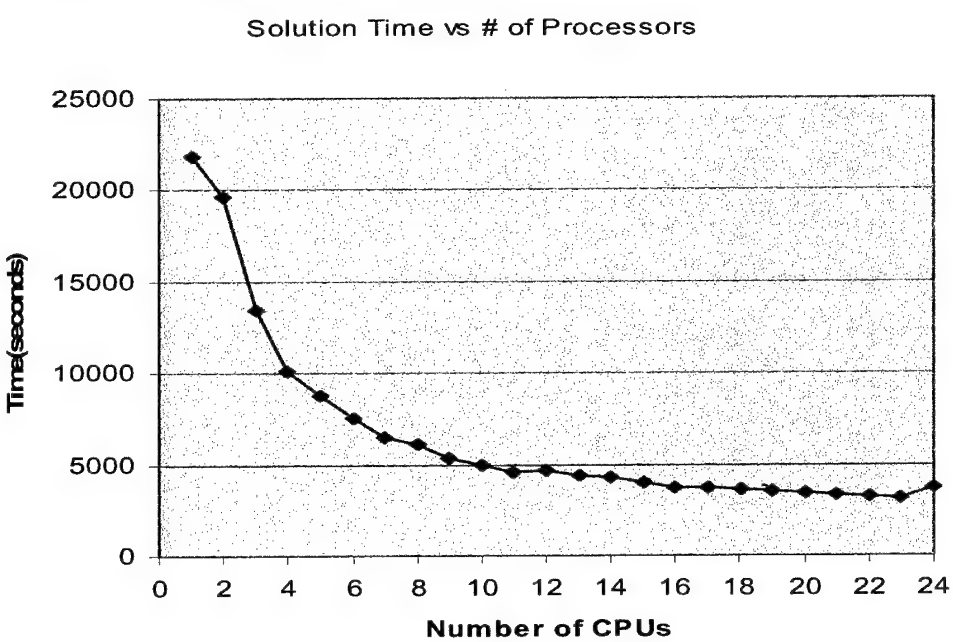

Fig. 2.2.1 Plot of Parallel MAGIC3D solution time vs # of processors.

2.2.2 Klystrino Circuit Microfabrication Improvements

2.2.2.1 Dod Need

The 95 GHz klystrino has multiple potential applications as an RF source for both high average power and high peak power applications. There are significant, immediate DoD needs for high average power millimeter wave sources for programs such as Active Denial. High peak power applications such as imaging radar and missile seekers require RF sources with significantly more peak power than is available with solid state systems. These high peak power needs can only be met with millimeter wave vacuum electronic devices.

The circuit microfabrication methods described below are applicable to a wide variety of millimeter wave sources including klystrons, coupled cavity TWTs and magnetrons.

2.2.2.2 MURI Achievement

The original klystrino circuit was fabricated using LIGA. A thick PMMA photoresist was exposed to x-rays from a synchrotron lightsource. This approach produced klystron cavities with intrinsic Q's approaching theoretical limits, but it required an excessive number of post-LIGA machining steps to produce the finished circuit. The first circuits made used a roughened aluminum plate as the substrate material for the LIGA process. To expose a full millimeter thick PMMA photoresist, multiple x-ray exposures were required. This meant that the gold x-ray mask had to be bonded to the PMMA surface to maintain registration over repeated exposure and etch cycles. Therefore, both top and bottom surfaces of the LIGA assembly had to be machined away and replaced by a diffusion bonded copper plate.

To overcome these circuit fabrication difficulties, several attempts were made to use a smooth copper plate as the substrate for the LIGA process. Experiments at both Sandia, Livermore and the Synchrotron Radiation Research Center in Hsinchu, Taiwan came up with the same results. The higher atomic number substrate (Cu – 29 vs Al – 13) resulted in significant x-ray backscatter with the copper substrate. The backscattered x-ray photons damaged the PMMA under the mask and resulted in undercutting of the PMMA columns which subsequently lifted off the copper surface during the etch process. The problem was the long exposure times required to break down the long chain polymers in the PMMA. The solution was to use a much more sensitive photoresist material.

The epoxy SU-8 is a negative photoresist that is 200 times more sensitive to x-ray exposure than PMMA. This cut the exposure times from tens of hours to minutes. After etching, the SU-8 columns remained bonded to the smooth copper surface. Figure 2.2.2 is a photograph of an SU-8 LIGA structure after etching. The exposure and etching were done at SRRC. Electroplating, planarization and final machining will be done at Stanford.

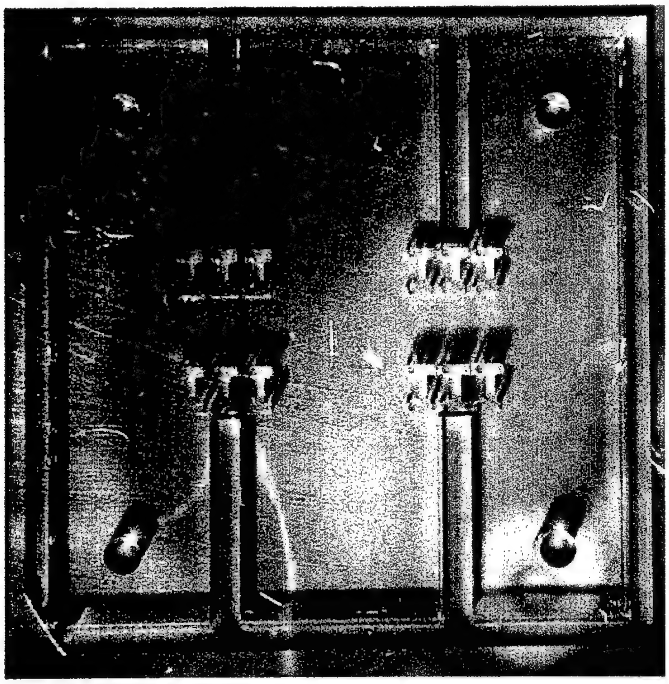

Fig. 2.2.2 SU-8 LIGA W-band circuit on smooth copper after exposure and etch steps.

The surface finish of the SU-8 columns was measured to be less than 200 nm. This is better than a diamond turned surface and comparable to LIGA surface finish. Cold tests on the completed test cavities are expected to show intrinsic Q's very close to the LIGA values.
Since synchrotron x-ray sources are unlikely to be readily available for production of millimeter wave circuits, an attempt was made to expose the SU-8 LIGA circuits with UV from equipment using in commercial integrated circuit processing. A small business involved in translating semiconductor techniques to vacuum device manufacturing is involved in a collaboration with Stanford to produce klystrino circuits with commercially available lithographic equipment. They were given the same mask geometry as SRRC and produced duplicate 1 mm tall SU-8 LIGA structures. Prior state of the art for UV SU-8 lithography was limited to structures less than 250 μm tall. The UV SU-8 structures have been electroplated, planarized and a beam tunnel has been machined. They are currently at the small business to have the exposed SU-8 removed with a proprietary process that doesn't etch the exposed copper surfaces. Figure 2.2.3 below shows several steps in the UV SU-8 circuit fabrication.

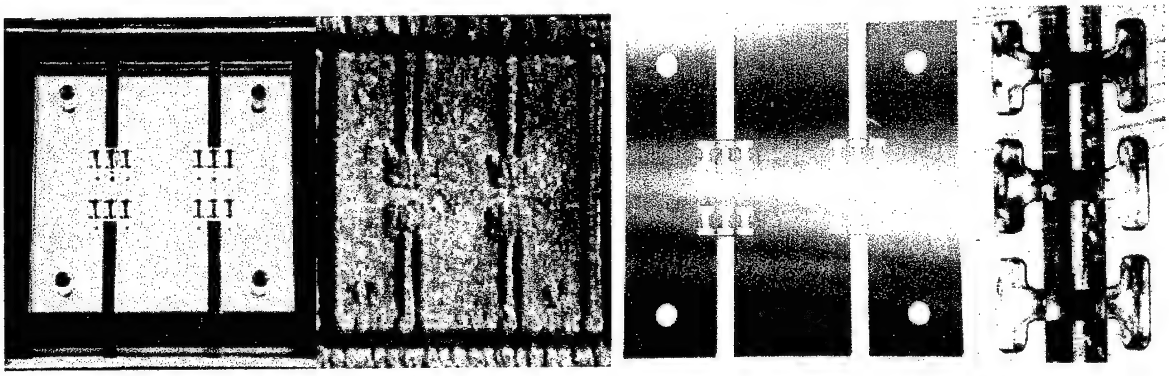

Fig. 2.2.3 Four images of processing steps for UV exposed SU-8 LIGA fabrication. From left to right, the exposed and etched SU-8 on diamond turned copper, after electroplating, after planarization, closeup of machined beam tunnel.

The final validation of the UV SU-8 LIGA circuits depends on cold testing to be completed shortly. Based on the visual evidence, the new fabrication method is a great improvement over LIGA using PMMA. Both quality of the finished circuit and cost of fabrication will benefit from using this method. But by far the major advantage is that this fabrication method can be done using relatively inexpensive commercial equipment without requiring access to a synchrotron light source.

2.2.3 Advances in Understanding of RF Breakdown

2.2.3.1 Dod Need

The High Power Microwave community is developing a variety of RF sources for directed energy applications. The goal of these programs is to produce pulse energies greater than one kilojoule that can be directed at military electronics targets to disable operation. The major problem with all of the sources currently being developed is pulse shortening. The desired pulsewidth is 1 μs but RF breakdown limits microwave generation to a few hundred nanoseconds. Research into the physics and limits of RF breakdown is critical to the successful development of these high power devices.

2.2.3.2 MURI Achievement

Initial MURI funded RF breakdown experiments at the Stanford Linear Accelerator Center defined limits for RF breakdown in single cavities and evaluated processing techniques that increased the RF breakdown threshold field values. Continued research by S. Tantawi and V. Dolgashev of the Accelerator Research Department has determined that breakdown threshold fields vary with the amount of energy available to the breakdown event. High Q, single cavity breakdown thresholds are much higher than accelerator structure breakdown thresholds. In similar accelerator structures with differing group velocities, the breakdown threshold is highest for the structure with the lowest group velocity.
Modeling of RF breakdown using 3D PIC codes has produced good agreement with measured diagnostics of RF breakdown events. Surprisingly, tests on different materials in waveguide breakdown studies have shown stainless steel waveguides to perform significantly better than either copper or gold (plated) waveguides. Figure 2.2.4 below shows some of the results of

Stanford research on RF breakdown. Under a newly established MURI Consortium on the "NanoPhysics of Electron Dynamics near Surfaces in High Power Microwave Devices and Systems", Stanford, UC Davis, and the Naval Postgraduate School will collaborate on continued studies of this important HPM issue.

Single cavity experiments by Scheitrum, Laurent, Sprehn

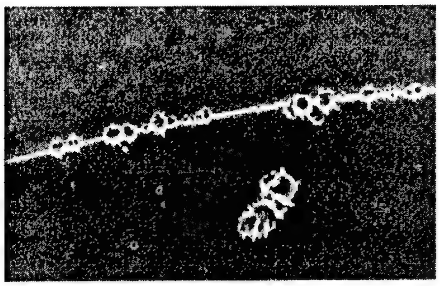

Breakdown along grain boundaries

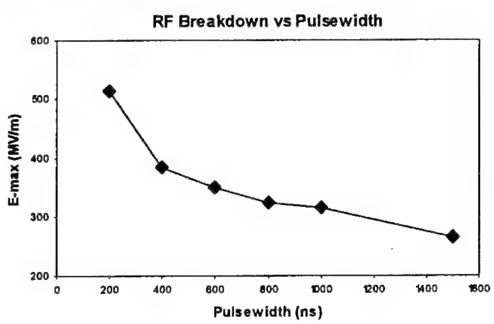

Waveguide experiments and modeling by Tantawi, Dogashev

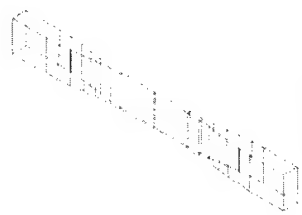

Reduced height waveguide

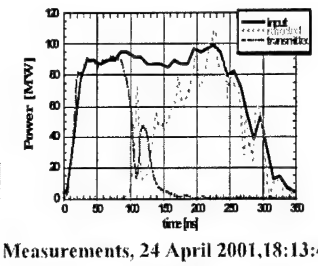

Measurements, 24 April 2001,18:13:40, shot 45

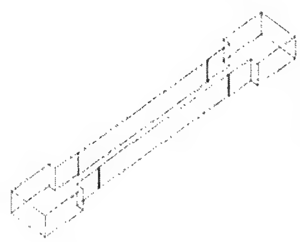

Reduced width waveguide

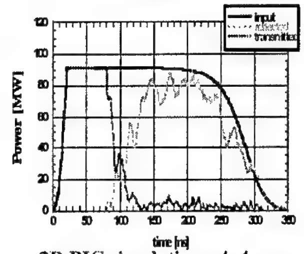

3D PIC simulations, 4x4 mm emitting spot, electron current 7kA, copper ion current 30A

Fig. 2.2.4 Images from RF breakdown experiments and 3D PIC models of a breakdown event.

2.3 University of Wisconsin, Madison

The major University of Michigan MURI research breakthroughs to date include:

- Developing and operating a novel, multi-sensored TWT for research of fundamental nonlinear physics in MPM-class TWTs,
- Advancing a new understanding of the physics of nonlinear distortions in TWTs,
- Developing a new computational method to model 1D linear-beam VEDs with Eulerian formulations, including the effects of charge overtaking,
- Establishing the fundamental physical mechanisms of harmonic and distortion product injection for linearization of TWTs,
- Identifying a novel TWT transmitter configuration enabling extremely linear amplification of digitally-modulated signals while operating saturated and thus at maximum efficiency,
- Completing the first combined experimental and simulation study of impulse amplification in TWTs revealing realistic prospects for novel applications to impulse

radar, impulse communications, and impulse response measurements of small signal gain characteristics,

- Conducting pioneering investigations of xray LIGA, UV LIGA and deep reactive ion etching methods for microfabricating mmwave and THz regime TWTs, and
- Developed and disseminated a suite of 1D TWT simulation codes for teaching and research of TWTs, making them available as open source software at http://www.lmsuite.org.

2.4 Massachusetts Institute of Technology

The MIT research program has concentrated on the following tasks: fast wave amplifier/ gyro-TWT research; photonic bandgap structures for vacuum electron devices, novel cathode research, and the theory of crossed field amplifiers.

A major event in the MIT MURI program was the successful operation of a novel 140 GHz quasioptical gyrotron traveling wave tube (gyro-TWT) amplifier at a record high power level, namely 30 kW, a significant advancement in the state-of-the-art in gyrotron amplifiers. The gyro-TWT produced up to 30 kW of peak power in 2 μs pulsed operation at 6 Hz achieving a peak gain of 29 dB, a peak efficiency of 12 % and a bandwidth of 2.3 GHz.

MIT has extended the theoretical analysis of two-dimensional non-axisymmetric equilibrium flow in crossed-field devices, in collaboration with Mission Research Corporation. It is their hope that an improved understanding of the equilibrium flow will help us to identify the origin of noise in crossed-field amplifiers (CFAs). As the electron density approaches the (critical) Brillouin density, they found that a vortex structure with regions of negative potential forms near the cathode surface.

MIT has successfully fabricated gated carbon nanotube emitter arrays using two different methods. The field emission mechanism of a carbon nanotube was studied and the FEED spectrum obtained agreed with experiment quite well.

MIT has developed a self-consistent technique for analytical calculation of dispersion curves in two-dimensional (2D) metallic photonic band gap (PBG) structures representing square and triangular arrays of metal rods.

2.5 University of Maryland, College Park

As noted above, the University of Maryland activities have focused on five areas: (1) Frequency multiplying gyro-amplifiers; (2) Development of analytical methods to provide relatively rapid "zero order approximations" of the performance of microwave vacuum electronic devices; (3) Development of a suite of codes to support the design of multi-stage depressed collectors (MSDC) in gyro-devices; (4) The use of microwave sintering to fabricate ceramics with high thermal conductivity and controllable electromagnetic loss; and (5) The exploitation of controlled chaos in microwave tubes.

In the analytical methods area, the first device class which was analyzed is that of multi-stage gyro-amplifiers including frequency multiplying devices. The frequency doubling gyro-amplifier, when compared with gyro-amplifiers operating at the second harmonic in all stages, has the practical advantage of requiring a lower frequency driver, and also, has stronger beam-

wave interaction in the input stage so that this stage may be made shorter and more stable. The second analysis topic was non-stationary phenomena in gyrotron oscillators including the discovery of a second region of stable oscillation at very high current in a gyrotron with tapered circuit walls.

In the code development area, a suite of codes was developed supporting the design of multi-stage depressed collectors (MSDC) in gyro-devices. These codes take secondary electron emission into account. They typically allow for enhancement of device efficiency from ~30% to greater than 50%. This suite of codes has been called "the world's most sophisticated for MSDC analysis" and it has been transferred to U.S. industry for improving the performance of commercially produced gyrotrons.

The frequency multiplying gyro-amplifier work has focused on the design and experimental testing of frequency doubling gyrotrons. First, the incorporation of mode converters into a gyro-amplifier circuit with the aim of improving stability was carried out; a frequency-doubling inverted gyro-twystron with internal mode converters achieved stable operation in Ka-band with an output power of 410 kW. Next, the use of an extended interaction output cavity was shown to be effective in increasing bandwidth. Finally, extensive studies were conducted on the analytical and experimental study of noise in a frequency-doubling gyro-TWT. It was shown that the average noise density may be significantly lower at the second harmonic frequency than at the fundamental. Finally, a new configuration for a wideband mode launcher for use in gyro-TWTs was realized.

Successful studies were conducted on the use of microwave sintering to fabricate ceramics with high thermal conductivity and controllable electromagnetic loss. Such materials are potentially useful as support structures and output windows in microwave tubes. They have been shown to have thermal conductivity equal to BeO which they would replace since BeO is carcinogenic. In addition, they would be much less costly than diamond.

The final area involved the investigation of the potential for exploiting controlled chaos in microwave tubes. Communication systems using such tubes could potentially operate with higher efficiency and with lower probability of intercept. Radar systems using chaotic signals would have higher resistance to jamming and reduced detection probability. While some of these concepts have been investigated at lower frequency relatively little has been done in the microwave regime. Thus, microwave controlled chaos is a ripe topic for future study.

2.6 University of Michigan, Ann Arbor

The University of Michigan's effort focused on the following four (4) areas, with significant collaboration with other universities, DoD labs, and industries:

a. Investigation of noise generation in crossed-field-microwave devices,

b. First simple analytic theory of Child-Langmuir Law,

c. Intermodulation in a klystron – theory, simulation, and comparison with experiments,

d. Excessive heating of high power rf windows due to thin film of contaminants.

University of Michigan graduate students and faculty have made a major breakthrough by discovery of an innovative technique to dramatically reduce the noise in magnetron oscillators (2 patent applications filed). The technique utilizes an azimuthally-varying axial magnetic field. Microwave measurements show dramatic reductions in the noise of kW oven magnetrons operating near 2.45 GHz. The noise reduction near the carrier is some 30 dB. Microwave sidebands are reduced or eliminated. Noise reduction occurs at all anode currents, but is particularly significant at low current near the start-oscillation condition. Further, this technique has been shown to be effective in noise reduction regardless of the magnetron current or age. Magnetic-Priming of magnetrons in the pi-mode has been discovered by use of N/2 magnetic perturbations (where N is the number of magnetron cavities).

Univesity of Michigan solved a 90-year old problem by finding a 2-dimensional Child-Langmuir Law, which gave the maximum current density that can be emitted over a finite patch of the cathode surface before the onset of a virtual cathode.

University of Michigan developed a general theory that accurately evaluates the intermodulation products in a multi-cavity klystron that result from an input signal with multiple frequency components. The UM code has been validated with a series of collaborative experiments with our MURI partner, U of Wisconsin. Also with UW, a novel method, by injecting a weak-signal, to suppress 3rd order intermod has been demonstrated.

University of Michigan quantified to what extent a thin film of contaminants would lead to excessive heating of high power rf windows, by a scaling law. The U Michigan scaling law surprisingly predicts that a thin film of contaminants (<< skin depth) may absorb up to a 50 percent of incident rf power.

3.0 QUAD CHARTS

Note: To view the following Power Point Presentation – Right Click the powerpoint slide of the presentation then choose "Presentation Object" and "Show" The slide show will then act as any Power Point Presentation. Hit "Esc" to go back to the main report.

3.1 University of California, Davis

MVRI Millimeter Vacuum Electronics

UCD W-Band TE_{01} Gyro-TWT Amplifier

Objectives

- Extend the state-of-the-art wide bandwidth, high power millimeter wave amplifier technology by developing a stable W-band gyro-TWT (Performance Goal: P_{out}=110 kW, Gain=45 dB, η=22%, BW_{3dB}=5%)

Overall system setup for hot test of the W-band TE_{01} gyro-TWT

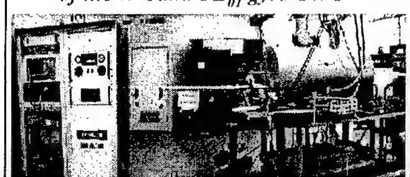

Approach

- Gyro-TWT's offer wide bandwidth
- TE_{01} mode transmits high power
- Distributed wall loss configuration stabilizes amplifier

Accomplishments

- Recent gyro-TWT under hot test with 61.2 kW saturated output power, 40 dB gain, 17.9 % efficiency, 1.5 GHz (1.6%) bandwidth in zero drive stable condition (unoptimized)

3.2 Stanford University

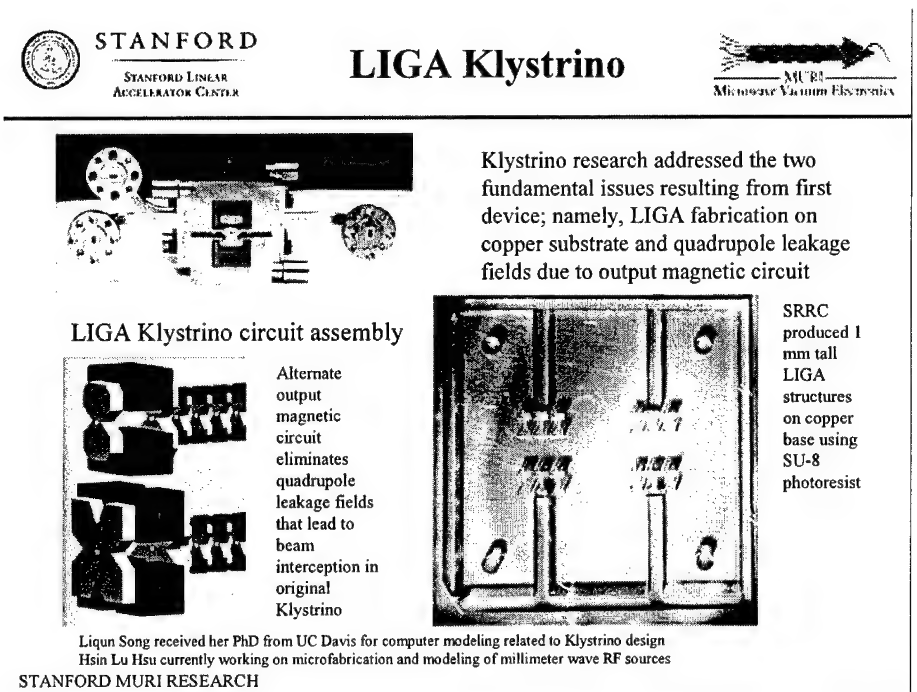

3.3 University of Wisconsin, Madison

Multi-sensored Research TWT

University of Wisconsin

Innovative Microwave Vacuum Electronics MURI99 Consortium

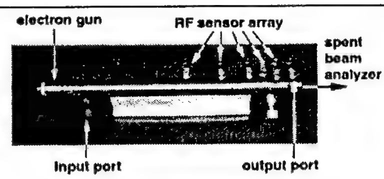

Multi-sensored research "XWING" TWT, for fundamental research of nonlinear physics in MPM-class TWTs

MURI Objectives

- Develop a new research TWT for experimental investigation of nonlinear distortion mechanisms in MPM-class TWTs.
- Obtain research results that enable industry to manufacture lower cost, ultrawideband, ultralinear, high efficiency, compact microwave amplifiers for radar, communications and electronic warfare
- Assess reliability and performance of rf-sensored TWTs

Scientific/technical approaches

- Specify, acquire, and make operational a state-of-the-art, sensor-laden, MPM-class TWT research amplifier
- Establish fundamental understanding of nonlinear TWT physics and identify strategies to suppress distortions and increase data rate capacity at high electronic efficiency

Most Significant Accomplishments

- Successful collaboration with Northrop Grumman to innovate, manufacture, and make operational a first-of-its-kind, multisensored research TWT.
- Successful experimental verification of new breakthrough understanding of nonlinear distortion mechanisms in TWTs.

7/21/2004 R.J. Barker, Program Manager

MURI Microwave Vacuum Electronics

3.4 Massachusetts Institute of Technology

MIT PHOTONIC BANDGAP CAVITY RESEARCH

Innovative Vacuum Electronics MURI

P.I., Richard Temkin - MIT

Started 1 May 99 internet: temkin@psfc.mit.edu http://www.psfc.mit.edu/wab/personnel/temkin.html

Photonic Bandgap Cavity (140 GHz)

Accomplishments

- Novel Photonic Bandgap cavity invented.
- Revolutionary new idea in vacuum electronics: highly overmoded, yet single mode cavity.
- Unprecedented range of single mode operation demonstrated at 25 kW, 140 GHz.
- Applicable to other devices: TWT, Klystron, etc.

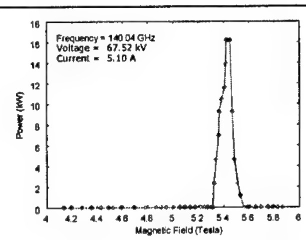

Power vs. Magnetic Field

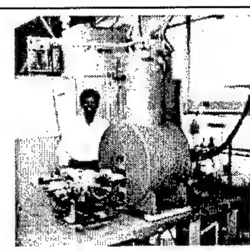

Experimental System

R.J. Barker, Program Manager

3.5 University of Maryland, College Park

Innovative Microwave Vacuum Electronics MURI Consortium

University of Maryland

email: vlg@glue.umd.edu Web URL:http://ireap.umd.edu

Started 1 August 99 Completed 30 April, 2004

Most Significant Accomplishments

- **HARMONIC DOUBLING GYRO-AMPLIFIERS** found advantageous for operation in nonlin. saturation regime. Compared to 2nd harmonic amplifier, lower frequency driver has advantage in price and availability; also, stronger interaction results in shorter input section length and improved stability. Compared to a fundamental gyro-amplifier, the bare noise (without input signal) ~10x smaller in a frequency-doubling gyro-amplifier with the same output frequency. Harmonic doubling gyro-TWT exper. demonstrated 125 kW output power in Ka band with 3% bandwidth and was verified analytically.
- **DEMONSTRATED NOVEL CIRCUIT GEOMETRIES TO IMPROVE PERFORMANCE OF GYRO-AMPLIFIERS.** These include internal mode converter chains to improve stability and extended interaction output cavities to enhance bandwidth.
- **DEVELOPED THEORY OF NON-STATIONARY PHENOMEMA IN GYRO-BWO** which explained previous experimental results that were not understood.
- **EVALUATED USING CLUSTER CAVITIES IN GYROKLYSTRONS.** Gain-bandwidth product doubled compared with usual gyroklystron configuration with little degradation in efficiency.
- **DEVELOPED THEORY OF CHAOTIC OPERATION IN TWT WITH FEEDBACK.** Potential advantage for anti-jamming, secure communications, etc.
- **FABRICATED CREDIBLE REPLACEMENTS FOR TOXIC BeO/SiC** for structural elements in MVEDs. Al/TiB_2 & AlN/SiC fabricated with pressureless microwave sintering to have thermal conductivity comparable to BeO/SiC and to be much lower cost than diamond.
- **DEVELOPED SUITE OF CODES FOR CAD OF DEPRESSED COLLECTORS** in high power MVEDs. Codes track multiple generations of backscattered electrons and are considered best in world. Codes have been transferred to Industry.

3.6 University of Michigan, Ann Arbor

Innovative Microwave Vacuum Electronics MURI Consortium

University of Michigan

email: rongilg@umich.edu

Started 1 August 99

Aug '02 - July '03

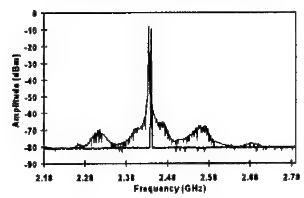

UM-Demonstrated Noise Suppression in a magnetron

MURI Objectives

- Investigate the fundamental mechanisms of noise generation in crossed field devices
- Find a cure for crossed-field-noise
- Explore the mechanisms and suppression of intermodulation distortion
- Analyze current limitations on temporally and spatially restricted electron bunches

Scientific/ Technical Approaches

- Utilize magnetrons with efficiencies of 80-90%
- Characterize microwave spectrum as a function of magnetron parameters and innovative geometries
- Theoretically investigate techniques for suppression of intermodulation distortion
- Compare experimental data to both analytical and computational results

Most Significant Accomplishments

- Breakthrough in magnetron noise suppression
- Theory for intermodulation product suppression (successfully compared to UW Experiments)
- First simple, analytic theory for 2D Child-Langmuir Law
- First theory of crossed-field-limiting current in relativistic diodes
- Theory of RF losses in contaminated RF windows

7/22/2004

R.J. Barker, Program Manager

MURI

Microwave Vacuum Electronics

4.0 PROGRESS

4.1 University of California, Davis

MURI
Microwave Vacuum Electronics

May 1, 1999 – April 30, 2004

Principal Investigator: N.C. Luhmann, Jr.:
University of California, Davis
TEL: 530-752-5414; FAX: 530-754-9070
Email: ncluhmann@ucdavis.edu

Senior Participants:

C.W. Domier
J.P. Heritage
E. Landahl
D.B. McDermott

4.1.1 Fast Wave Device Research

The UC Davis fast wave activity is aimed at critical DoD needs for radar, ECM, and nonlethal microwave weapons including Active Denial technology. In the following, progress in devices relevant to these needs is discussed.

4.1.1.1 UCD Heavily Loaded W-Band TE_{01} Gyro-TWT

DoD radar applications increasingly require more precise tracking as well as higher resolution in range, angle, and Doppler. This is crucial for applications such as inverse synthetic aperture radar (ISAR) target imaging and jet engine modulation (JEM) classification, electronic protection radar adjunct, detection of low cross section threats, and accurate tracking of sea skimming missiles. Although inferior to visible and IR systems in high humidity and rain, the millimeter wave portion of the spectrum (particularly the 94 GHz and 140 GHz "windows") offers superior performance through clouds, fog and smoke. As one example, this need motivated the NRL development of the WARLOC (*W-band Advanced Radar for Low Observable Control*) radar which is a transportable, land- or sea-based system, based on the use of a high-power 94 GHz Gyro-Klystron. This has been successfully demonstrated and is currently finding extensive service as a "cloud" radar. Despite the success, there remains a critical for an amplifier with considerably wider bandwidth to support the use of appropriately chirped pulses with pulse compression for high range resolution. In addition, increased gain is desired since the current NRL system must utilize a TWT driver, thereby adding cost and increasing weight as well as compared to a higher gain device which could employ a solid-state driver. Other applications include the Lincoln Laboratory millimeter wave radar located at the U.S. Army Kwajalein Atoll/Kwajalein Missile Range where they track and collect metric/signature data on missiles and provide tracking information on space objects. To respond to the increasing miniaturization of satellites, an upgrade to the Haystack radar is required over the 92 to 100 GHz band. However, as noted in the July 2001 report by the Ad Hoc Tri-Service Committee studying the DoD R&D investment strategy, no current rf amplifier technology can provide the required power. As further noted in the report, the Air Force Space HUSIR requirements may require the use of wideband gyro-TWT technology to satisfy the 8 GHz instantaneous bandwidth requirement. Explicitly noted in the report is the proposed W-Band TE01 gyro-TWT development solution.

To satisfy the above need, a high power, TE01 mode, W-Band gyro-TWT has been designed and fabricated under the MURI99 Innovative Vacuum Electronics program by MURI student Heather Song and is currently being tested and optimized at UCD. It is driven by a 60-100 kV, 5 A magnetron injection gun with a simulated velocity ratio of $v_{\perp}/v_z$=1.0 and velocity spread of 2.2%. The amplifier is predicted to generate 140 kW at 94 GHz with 50 dB saturated gain, 28% efficiency and 5% bandwidth. To suppress the potential backward wave oscillations, the circuit has been loaded with loss so that the one-way attenuation is 90 dB at 93 GHz. A coaxial input coupler with ~1 dB insertion loss and 3% bandwidth is employed. The output power is monitored with crystal detector through a 10 dB coaxial coupler.

In the initial stages of the experiment, the search for the small and large signal characteristics was hampered by poor electron beam quality due to misalignment of the old MIG. The old MIG was subsequently disassembled and carefully inspected. The alignment of the old MIG was determined to be off by ~35 mils and hot spots were observed on the surface of the cathode due

to cathode surface poisoning. Misalignment of the old MIG together with cathode surface roughening are believed to have been the main factors in the increased beam axial velocity spread over the EGUN predictions. The new optimized MIG with a predicted velocity spread of 2.2% was employed for all of the subsequent experimental tests of the various versions of the W-Band TE01 gyro-TWT and immediately yielded dramatic improvements in performance. Figure 1 shows the cathode assembly of the modified MIG with improved predicted beam parameters.

The overall system setup for the hot tests is shown in Fig. 2. The 50 kG superconducting magnet together with the SLAC-UC Davis W-Band modulator/driver is shown. The refrigerated superconducting magnet is capable of producing 50 kG $\pm$ 0.1% over 50cm and it is composed of 4 independent coils. A 100 W, 5% bandwidth Hughes folded waveguide continuous wave TWT is used as an input driver and it is connected to the gyro-TWT circuit through a 10 foot long Ka-Band overmoded waveguide feed. The input driver is pulsed to produce 1μs duration signals with a repetition rate of 1~2 Hz which is sufficient for data acquisition purposes. An HP synthesized sweeper which drives the folded waveguide TWT determines the input frequency. The RF diagnostics are designed such that the RF input power, output power and the oscillation power can be monitored separately through a directional coupler, rotary attenuator and crystal detector. The output power and input drive power are varied using a precision rotary attenuator and a cavity frequency meter is used to identify the frequency of the output signal.

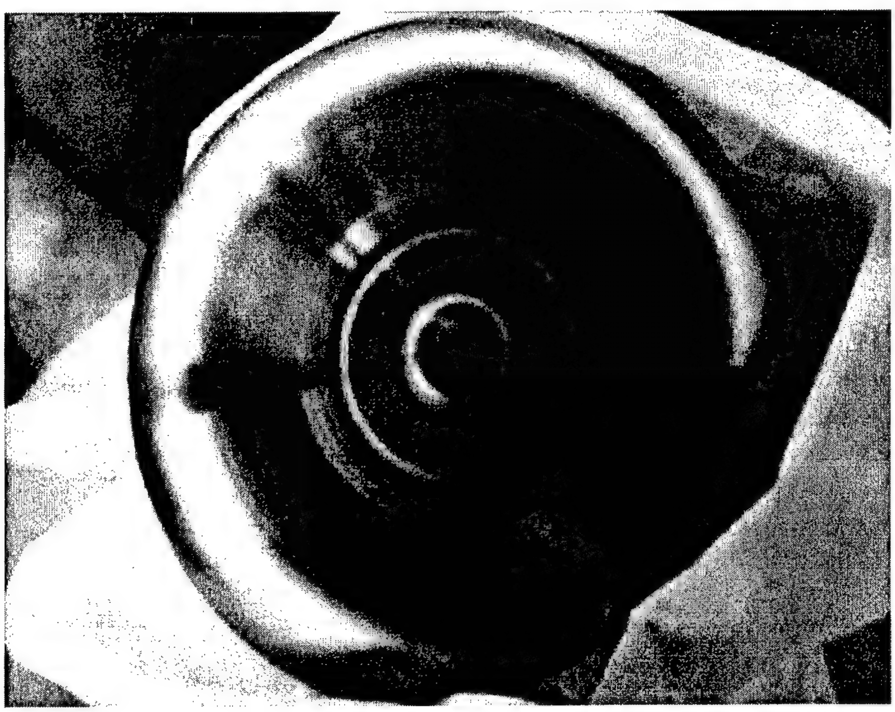

Fig. 4.1.1: Cathode assembly of optimized MIG with predicted velocity spread of 2.2%

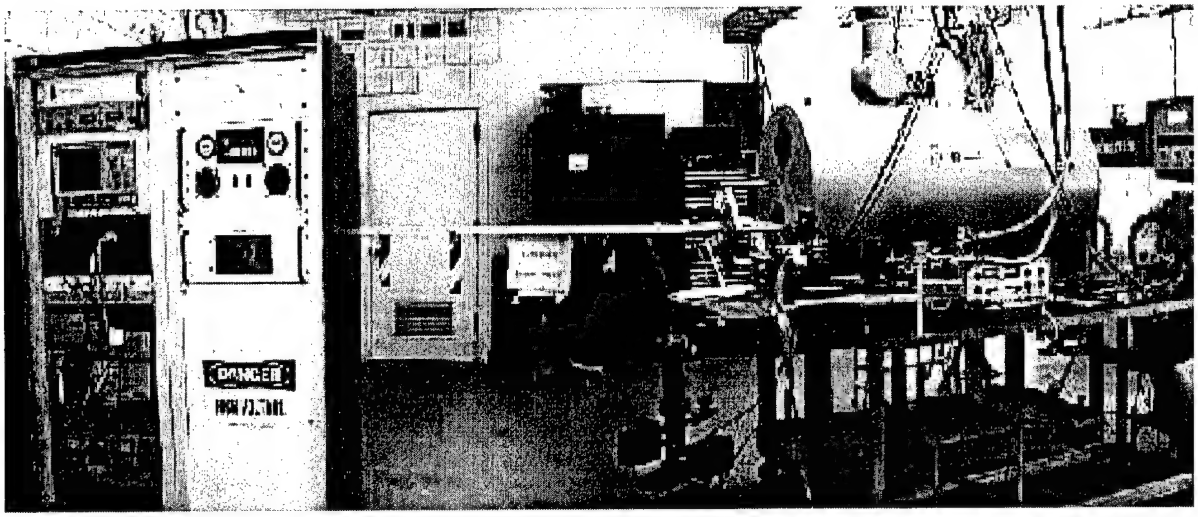

Fig. 4.1.2 Overall system setup for hot tests of the heavily loaded W-Band TE_{01} gyro-TWT

Figures 3 and 4 show the output power versus input power of the second version of the W-Band TE_{01} gyro-TWT measured at 92.2 GHz with slightly different beam voltage, beam current and magnetic field values. The saturated gain is in excess of 40 dB at an output power of ~50 kW. In these transfer characteristic plots, the amplifier output power is seen to grow linearly with increasing input power in the small signal regime, but eventually reaching a maximum in the large signal saturated regime as expected. The measured saturated bandwidth of the W-Band TE_{01} gyro-TWT is shown in Fig. 5. A saturated bandwidth of only ~1.0 GHz is measured at 63 kV, 6A and 34.2 kG. The peak power was measured at ~92.2 GHz with ~50 kW saturated output power with 14% efficiency. As the drive frequency approaches the waveguide cutoff of the interaction circuit of 91 GHz, the output power decreases. The performance of the gyro-TWT at higher frequencies is limited due to the current input coupler's upper limit frequency of 97 GHz. Figure 6 shows the dependence of output power on beam voltage measured at 92.2 GHz, 6.0A and 34.6 kG. A beam voltage of 72~73 kV yielded the maximum power under this operating condition. As the beam voltage is further increased beyond 73 kV, the output signal is observed to become jumpy and erratic giving rise to difficulties in accurately measuring the output power, attributed to various instabilities uncovered in subsequent investigations.

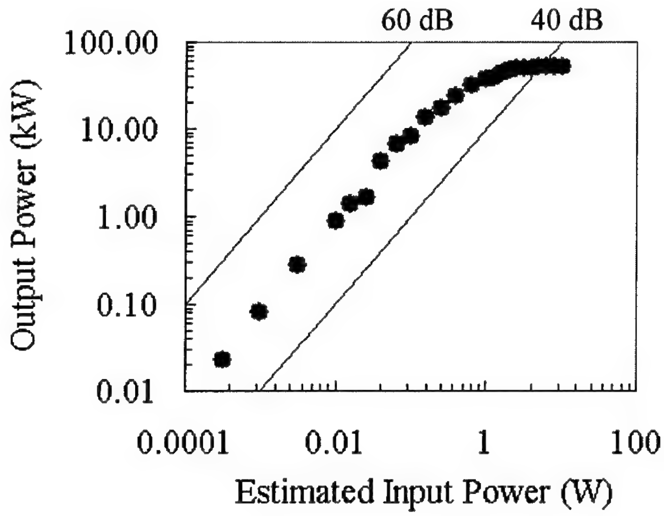

Fig. 4.1.3 Output power versus input power (63 kV, 6.0 A, 34.2 kG, 92.2 GHz)

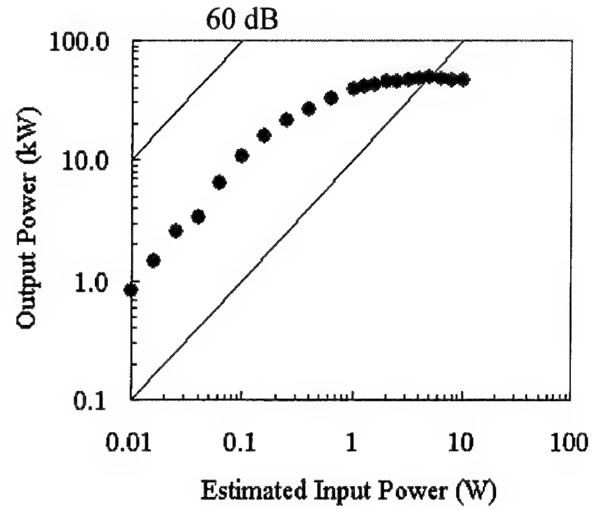

Fig .4.1.4 Output power versus input power (61.2 kV, 5.2 A, 34.1 kG, 92.2 GHz)

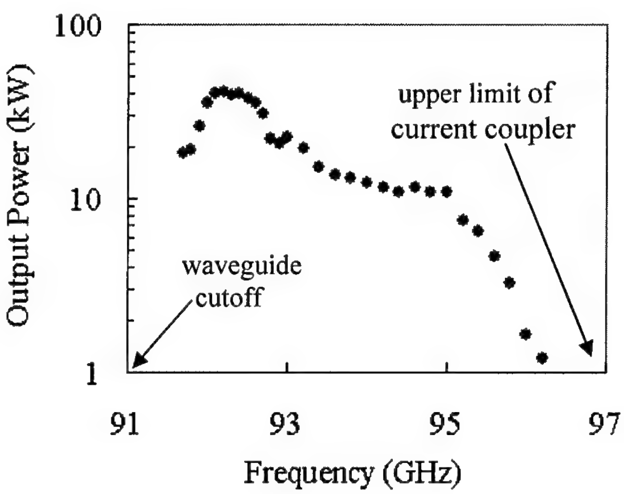

Fig. 4.1.5: Output power versus input drive frequency under saturated operation

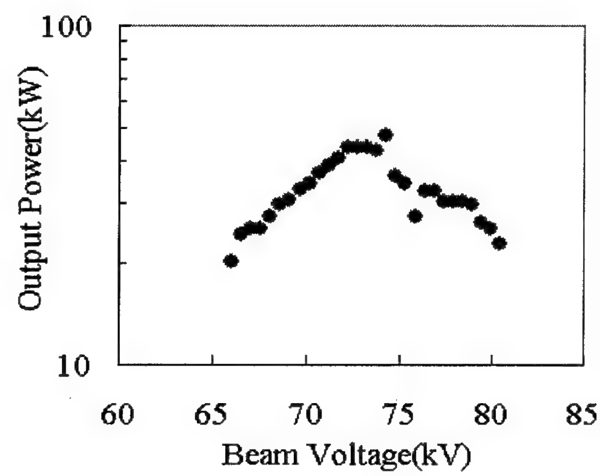

Fig. 4.1.6: Saturated output power versus beam voltage (6.0 A, 34.6 kG, 92.2 GHz)

In this initial series of hot test measurements of Version #2, the operating voltage was limited to values below 75 kV because of oscillations encountered at higher voltages. As shown in Fig. 7, the computed start oscillation current values for the $TE_{11}^{(1)}$ and $TE_{02}^{(2)}$ modes are below 5.0 A for a velocity spread of less than 5%. As the velocity spread increases, the start oscillation current value for the $TE_{11}^{(1)}$ mode increases; however, for the $TE_{02}^{(2)}$ mode it remains constant at ~1.2 A for velocity spreads up to 8%. The oscillation may occur at 167 GHz for the $TE_{02}^{(2)}$, 66 GHz for the $TE_{11}^{(1)}$, and 75 GHz for the $TE_{21}^{(1)}$ mode, respectively. To identify the most likely $TE_{02}^{(2)}$ competing mode at 167 GHz, a Fabry-Perot interferometer has been fabricated as shown in Fig. 8. This interferometer employs two 114 μm thick GaAs wafers, two W-Band horn antennas and a translation stage with micrometer attached. By measuring the distance between the adjacent detected signal peaks, the frequency of the signal can be determined.

These initial hot tests of Version #2 taken at reduced voltages from the design value showed that the UCD W-Band TE01 Gyro-TWT offered performance at the very frontiers of the state-of-the-art. As a consequence, it was felt that it was highly desirable to pursue the various causes for the instabilities and to optimize the device so that it could operate at the higher design voltages thereby permitting the achievement of the predicted performance. To suppress the competing modes, a reduced length unloaded section of the interaction circuit was employed in the next version of the W-Band TE_{01} gyro-TWT with additional loading. Figures 9 and 10 show the predicted output power, efficiency, and saturated gain versus frequency for the modified gyro-TWT circuit. For a velocity spread of 5%, 110 kW output power, 22% efficiency and 45 dB of saturated gain are predicted. Also, for future experiments the wider bandwidth (5%) input coupler that we have fabricated will be employed. In addition, we have initiated discussions with the Maryland Group to collaborate with John Rodgers who has a different coupler design which offers the promise of yet broader bandwidth.

The W-band TE_{01} gyro-TWT has undergone numerous modifications with each version extensively hot tested. Five separate versions were tested thus far in the quest to improve electron beam quality and to eliminate sources of instability. Modifications have included modifications of the input drift section to eliminate oscillation, replacement of windows containing magnetic materials which degraded the electron beam quality, and improving the rf matching. Thus far, the amplifier has produced 61.2 kW saturated output power, 40 dB gain, 17.9 % efficiency, 1.5 GHz (1.6%) bandwidth in zero drive stable condition (unoptimized). The narrow bandwidth, etc. has been traced to instabilities associated with the design of the output drift section which has since been redesigned. Currently, the 6th version of the W-band TE_{01} gyro-TWT is under hot test which is expected to increase the stability thresholds and permit the device to operate at the full design values.. In the 6th version, to eliminate the oscillations encountered in the previous version, a modified up-tapered output section has been employed. The 7th version is scheduled to be tested with the optimized 7% bandwidth input coupler to add additional stability to the amplifier.

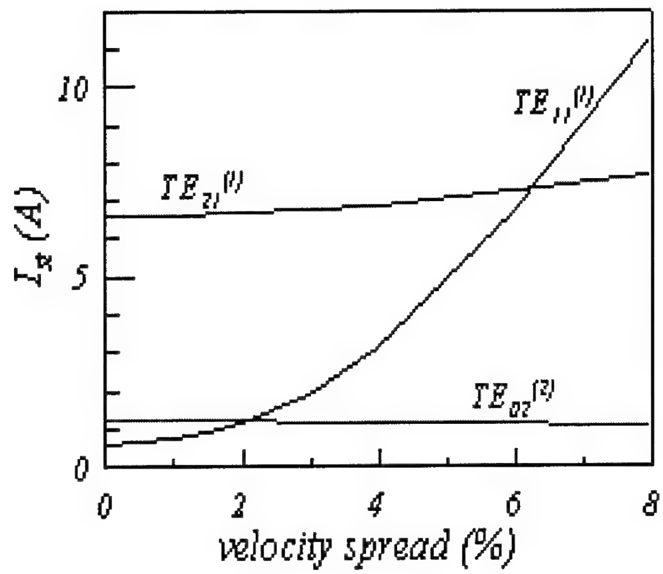

Fig. 4.1.7 Calculated start oscillation currents of the most likely competing modes as functions of velocity spread.

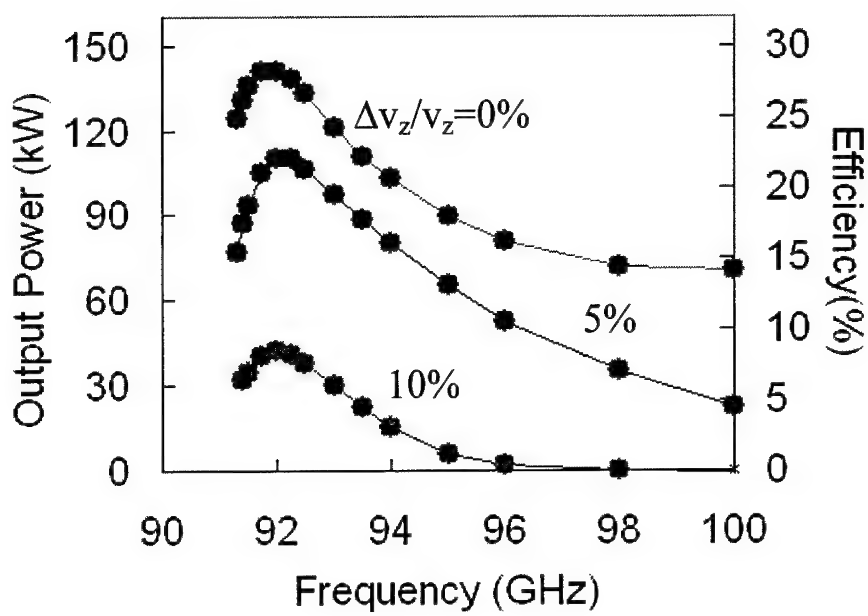

Fig.4.1. 9 Output power and efficiency versus frequency for next generation TE_{01} W-Band gyro-TWT circuit.

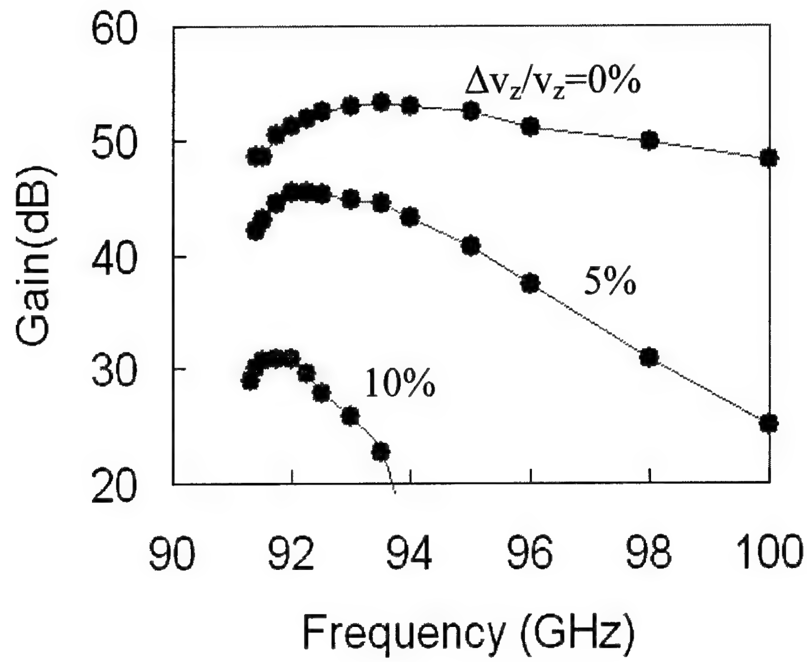

Fig. 4.1.10: Gain versus frequency for next generation TE01 W-Band gyro-TWT circuit

4.1.1.2 34 GHz Second-Harmonic Peniotron

The 34 GHz second-harmonic peniotron experiment of MURI student Lawrence Dressman is designed to demonstrate the well known predicted efficiency advantages inherent in the device and its suitability for harmonic applications at millimeter wavelengths. The long-term goals of this program are the development of highly efficient, compact, millimeter wave harmonic oscillators (for non-lethal HPM applications) and amplifiers (for radar) employing reduced magnetic fields. Prototype high-resolution radar and non-lethal HPM systems have recently proven the viability of the technology. However, system size (which is largely determined by the efficiency of the primary mm-wave power source) inhibits use except in fixed locations. Furthermore, space applications inherently require extremely high efficiencies and traditionally ground-based applications such as telecommunications transmitters (which see almost continuous use) realize substantial cost savings by increases in operational efficiency.

The UCD peniotron project was conceived to expand on the demonstrated high efficiency of the peniotron interaction. Electronic conversion efficiencies as high as 75% have been demonstrated and the device has long been suggested as suitable for harmonic operation (which decreases over-all system size). This experiment is designed to achieve a high device efficiency (~47%) while extracting useful output power levels (~125 kW) and maintaining stable operation. The device is being developed as a first step towards higher frequency operation and development of a penio-amplifier.

The 34-GHz peniotron exploits an interaction of the second harmonic of an axis-encircling electron beam with the fundamental cavity mode of a slotted resonator. The operating mode is inherently free from mode competition. The device will operate at 70 kV and 3.5 amperes with a confining axial magnetic field of 6.5 kG in the interaction region (see Fig. 11). The design has been optimized for high device efficiency and power output with values of 47% and 125 kW predicted by large-signal simulation. Simulation also predicts that the overall efficiency can be increased to 57% with the addition of a depressed collector. The device requires a 6.5 kG axial magnetic field, a value still within the limits of conventional magnet technology.

The beam is produced by a Northrop Grumman cusp gun and the recently re-designed (and tested) magnet system should provide high beam quality. The experiment has been described in the Special Issue on High Power Microwave Generation, IEEE Transactions on Plasma Science (June 2000) and in an invited talk at the 26th International Conference on Infrared and Millimeter Waves (IRMMW), Toulouse, France, 2001. The current status has been presented at both IVEC2004 and ICOPS 2004.

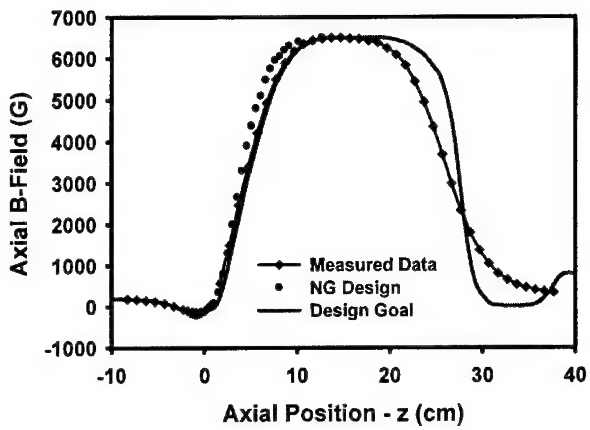

Fig.4.1.11. Measured, simulated and Northrop Grumman provided (optimum) magnetic field profile.

The circuit of the UCD device is a slotted cylindrical (magnetron-like) resonant cavity which contributes to the efficiency and enhances the stability of the device. The operating mode of the peniotron, the $\pi/2$ mode, is unique to this device. Simulation indicates that the device will be highly immune to competing gyrotron modes - a problem which has limited earlier research - as well as higher order peniotron modes. The RF output transforms easily to the desirable TE_{11} mode in circular waveguide. Key device parameters are given below in Table 1.

The crucial circuit block, circuit vacuum housing, and output irises have been machined, delivered, and tested. Testing included incoming inspection of the individual piece parts to verify conformance with the design drawings and cold test with a 50 GHz HP 8510 vector network analyzer. Inspection was performed using a measuring microscope with 0.1 mil resolution. Major circuit components are shown in Figure 12 below.

Cold test of the peniotron circuit were critical in verifying the large amount of simulation data obtained during design of the circuit (using HFSS). Because the circuit has two planes of symmetry and incorporates diagnostic couplers in each plane (two each for a total of four), cold testing was a laborious task. Furthermore, two output irises were fabricated, one for critical coupling (to compare with other experimental devices) and one for the desired over-coupling. Both output configurations were cold tested. Results were extremely positive, agreeing well with the design simulations, and indicated that the design is sound and that the experiment can proceed to final assembly.

A significant hurdle to be overcome for success of this experiment was the design and implementation of the magnetic field. The experiment is designed to exploit the advantages of the axis-encircling beam produced by the Northrop Grumman cusp gun. The cusp gun requires a

magnetic field profile (both off-axis as well as on-axis) unlike any other gun type and the beam quality, and hence the device efficiency, is heavily dependant upon these fields. This places a significant burden on the magnetic field design.

Previous efforts to use the superconducting magnet for cusp gun based experiments have been disastrous since they resulted in damage to the gun ceramic (a problem resulting from the difficulty in mounting and supporting the gun in the confined space of the magnet bore). Consequently, a major effort was undertaken this year to re-design the magnetics. This effort is complete and appears to be fully successful. Alternate coils were identified, design simulations performed, pole pieces designed and fabricated, and the magnet system assembled. The newly designed magnetic field profile, as compared to the field recommended by Northrop Grumman, was shown above in Fig. 11. The new design provides a superior magnetic field profile as compared with the old design and closely matches the recommended profile, especially in the critical gun region. Furthermore, the new design is more compact, allows greater access to the circuit assembly and incorporates an easily adjustable axial pole piece which adjusts the taper of the interaction field in a nearly linear fashion. This was previously not possible and could result in improved efficiency of the device. The magnet assembly is shown in Fig. 13

Currently, the major components of the device have been delivered and are ready for assembly. The circuit has been cold tested and shows good agreement with design simulations. The magnet, crucial to good beam quality has undergone a complete redesign. Testing of the axial magnetic field showed excellent agreement with design. The vacuum system is in place and ready for final assembly. The collector (the only remaining significant component), which is heavily dependant on the magnet design, is being designed and will be ready shortly. Waveguide components have been delivered and final assembly will be complete in the near future. The complete device is shown schematically in Fig. 14.

Future work will include increasing the frequency and harmonic number with 94 GHz as the goal. Concurrently, extended interaction configurations will be explored to determine if the interaction is suitable for efficient mm-wave amplifiers.

Table 4.1.1 - Peniotron Design Parameters

Beam Voltage	V_b	70.0 kV
Beam Current	I_b	3.5 a
Velocity Ratio	$v_\perp/v_\parallel = \alpha$	1.5
Magnetic Field	B_z	6.5 kG
Velocity Spread	$\Delta v_\parallel/v_\parallel$	5%
Guiding Center Spread	$\Delta r_c/r_L$	10%
Mode		$\pi/2$
Axial Mode Number	l	1
Vane Depth	b/a	1.45
Electron-Vane Ratio	r_L/a	0.65
Inner Vane Radius	a	1.82 mm
Outer Vane Radius	b	2.639 mm
Cavity Length	L	31 mm
Slot Angle	θ_0	22.5
Unloaded Q	Q_0	1900
Loaded Q	Q_L	357

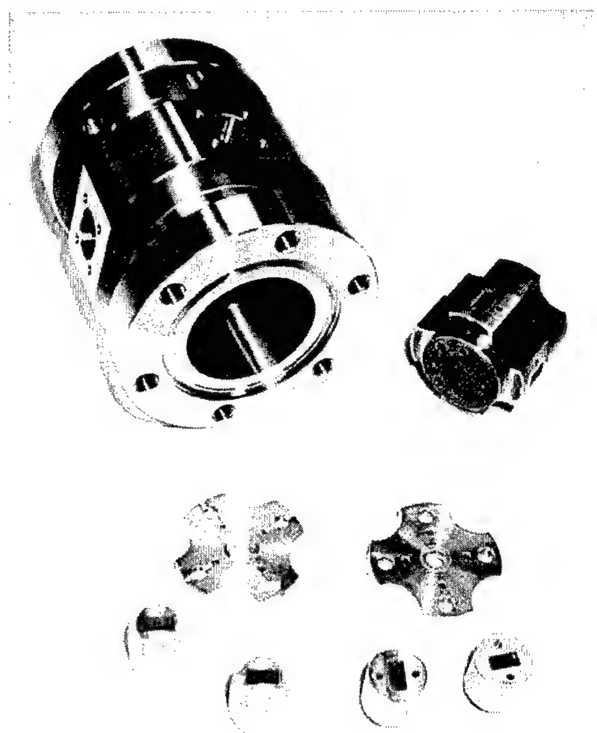

Fig. 4.1.12 Key circuit components including the vacuum housing (upper left), circuit block (upper right), irises (center), and waveguide outputs (bottom).

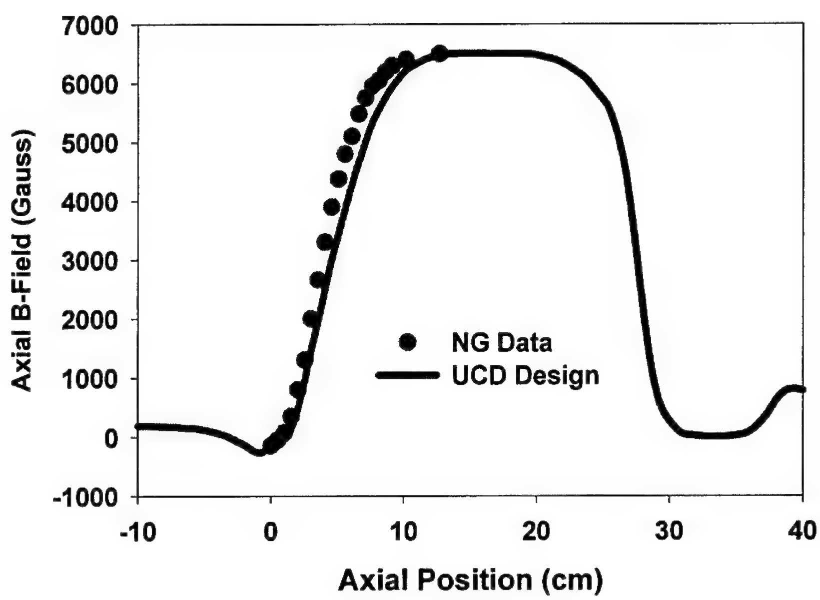

Fig. 4.1.13 Design axial magnetic field profile compared to the Northrop Grumman recommended field.

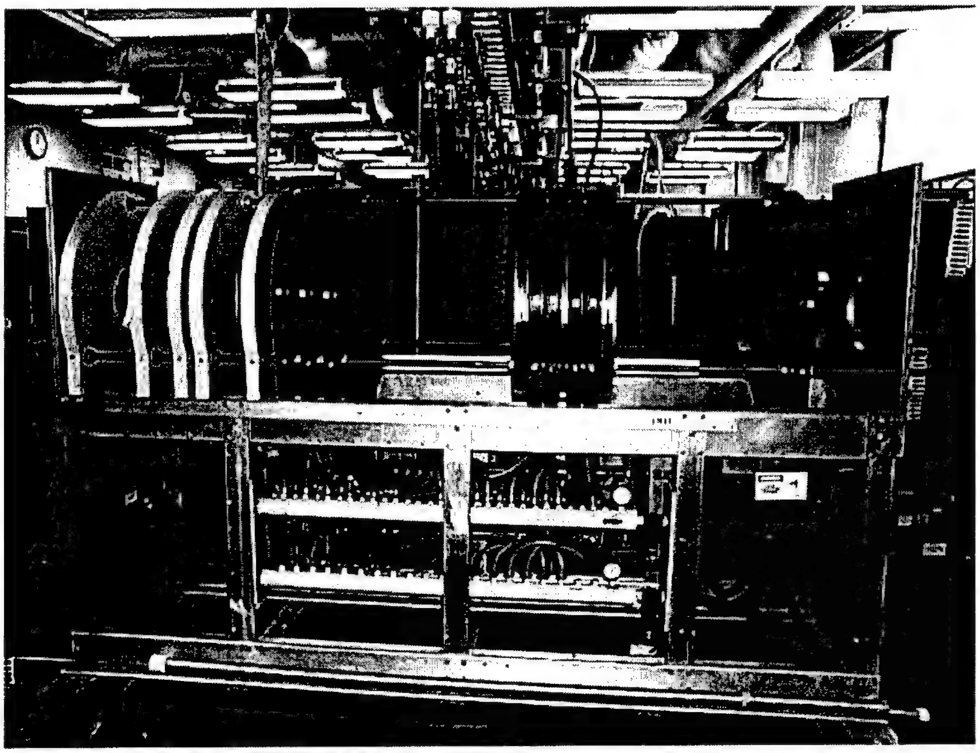

Fig. 4.1.14 Magnetic assembly showing pole pieces (blue) and four pancake coils (other coils present are not needed for this oscillator experiment, but are essential for amplifier studies).

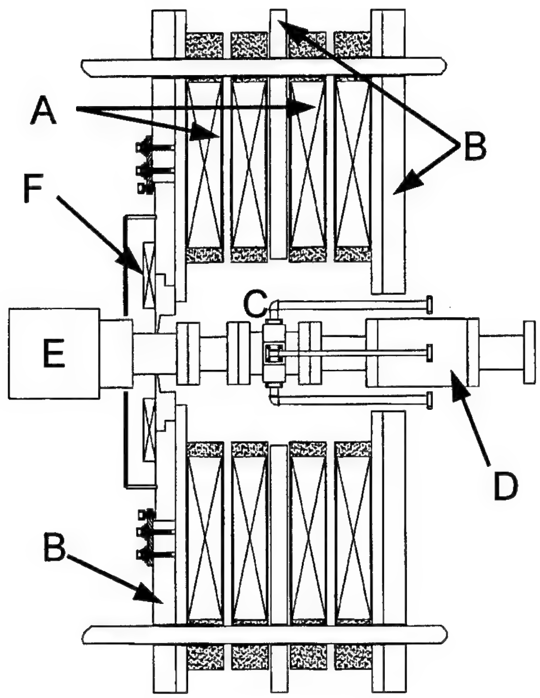

Fig. 4.1.15. Magnet and device assembly with the coils and pole pieces shown in cross-section to reveal the vacuum device assembly. Shown are: four conventional high-current coils (A) and multiple pole pieces (B); an intra-coil pole piece (B) between the second and third coils which serves to flatten the field at the interaction circuit (C); an axial pole piece (D) which compensates for the opening in the collector end pole pieces and can also be used to taper the interaction field; the cusp gun (E); and the gun coil (F) which, in conjunction with the pole pieces determines the critical magnetic field profile in the gun region.

4.1.1.3 UCD Ka-Band Second-Harmonic Gyro-TWT Amplifier

There is an increasing need for wide-band, high power millimeter-wave gyro-TWT amplifiers for DoD radar applications such as the WARLOC (*W-band Advanced Radar for Low Observable Control*) radar. There has recently been significant achievement in the development of gyro-TWTs for such applications however these gyro-TWTs have been fundamental-mode devices which require strong magnetic fields and cryogenic super-conducting magnets. For DoD applications where size and weight are limited there is a need for compact devices. By operating at cyclotron harmonics the magnetic field strength requirement is reduced significantly by a factor of the harmonic number. Another advantage of harmonic operation is that gyro-TWT amplifiers can stably operate at higher beam current and therefore produce higher power at higher harmonics because the weaker harmonic interactions yield a higher threshold electron beam current for the absolute instability at the cutoff frequency of the operating mode.

To address these needs, UC Davis graduate student Stephen Harriet is designing, building and testing a TE_{21} second-harmonic gyro-TWT with a large-orbit axis-encircling beam that is predicted to double the efficiency of our previous small-orbit 200 kW TE_{21} second-harmonic MIG gyro-TWT and which is aimed at DOD applications such as the WARLOC radar as discussed previously. The gyro-TWT is predicted by our large signal code to produce 50 kW in Ka-band with 20% efficiency, 30 dB saturated gain and 3% bandwidth.

Although the previous UC Davis second-harmonic TE_{21} gyro-TWT produced impressive results by using off-axis electrons from a MIG, the efficiency was reduced due to the essentially constant guiding-center azimuth of the electrons in the linearly polarized mode. This caused some electrons to experience a weak RF field, while others oversaturated in a strong field. In the axis-encircling beam electrons rotate through both the peaks and nulls of the linearly polarized mode as illustrated in Fig. 15 so the efficiency is predicted to nearly double in the new device.

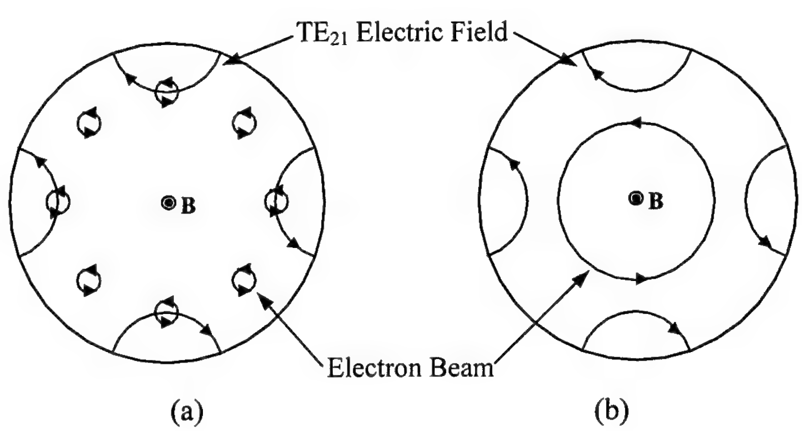

Fig. 4.1.16. Schematic of electrons interacting with a TE_{21} mode in a circular waveguide for (a) a non-axis-encircling beam and (b) an axis-encircling beam

A novel cusp electron gun shown in Fig. 16, developed and delivered by Northrop Grumman under combined MURI/DURIP funding, is used to produce the axis-encircling beam in the device. The gun employs a convergent Pierce gun with a spherical annular cathode. The initially axial electron beam starts to spin due to $v_z \times B_r$ forces in a magnetic field reversal region.

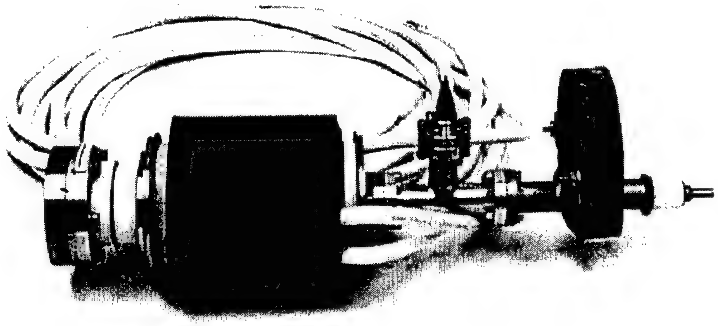

Fig. 4.1.17 Novel Northrop Grumman cusp electron gun that produces the axis encircling beam in the second-harmonic TE_{21} gyro-TWT.

The second-harmonic TE21 gyro-TWT amplifier was designed for optimal power efficiency, gain and bandwidth, while maintaining a safe margin for stability. The design parameters that were determined from the optimization are shown in Table 2. The amplifier was designed using linear theory to provide a 30% margin from absolute instability. To ensure amplifier stability, the device employs a sliced mode-selective circuit to suppress odd-order azimuthal circuit modes by interrupting their wall currents as shown in Fig. 17. Surrounding the interaction circuit is a lossy cylinder to absorb the radiated power. Furthermore, distributed loss with a wall resistivity 2300 times copper is added to the first 30.5 cm of the interaction circuit to suppress the $TE_{41}^{(4)}$ mode gyro-BWO. The last 11.5 cm of the 42 cm circuit does not have loss added so that the high power wave is not attenuated. The device incorporates identical multi-hole 0 db RF input and output couplers designed with the HFSS code. The coupler contains an array of slots connecting the narrow wall of the TE10 rectangular input waveguide to the TE21 circular interaction waveguide. The fabricated coupler and breakout assembly for the coupler are shown in Fig. 18. The magnetic circuit for the gyro-TWT is designed to provide both the magnetic field reversal required in the cusp gun region and at the same time a constant axial magnetic field of 5.48 kG in the interaction circuit region over the 42 cm length of the circuit. In addition, the axial magnetic field is designed to ensure that each section of the device is free from oscillation. The magnetic circuit consists of water cooled copper magnet coils and iron waveguide. The fabricated coupler and breakout assembly for the coupler are shown in Fig. 2. The magnetic circuit for the gyro-TWT is designed to provide both the magnetic field reversal required in the cusp gun region and at the same time a constant axial magnetic field of 5.48 kG in the interaction circuit region over the 42 cm length of the circuit. In addition, the axial magnetic field is

designed to ensure that each section of the device is free from oscillation. The magnetic circuit consists of water cooled copper magnet coils and iron pole pieces as shown in Fig. 19.

Table 4.1.2. Parameters for the second-harmonic TE_{21} gyro-TWT amplifier.

Beam Voltage	70 kV
Beam Current	3.5 A
$\alpha = v_{\perp}/v_Z$	1.2
$\Delta v_Z/v_Z$	7%
Magnetic Field, B_O	5.48 kG
B_O/B_g	0.99
Wall Resistivity	2300 x copper
Cutoff Frequency	28.6 GHz
Guiding Center Radius, r_C	0
Circuit Radius, r_W	0.509 cm
Lossy Circuit Length	30.5 cm
Circuit Length	42 cm

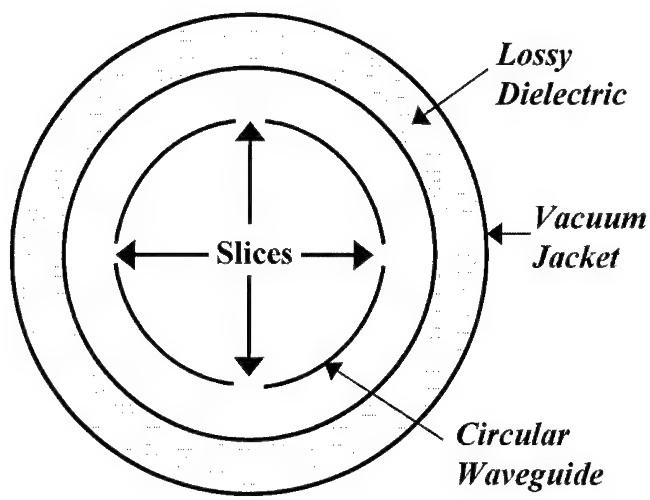

Fig. 4.1.18. Schematic of linearly polarized Second-Harmonic TE21 gyro-TWT circuit cut with two orthogonal slices through the axis

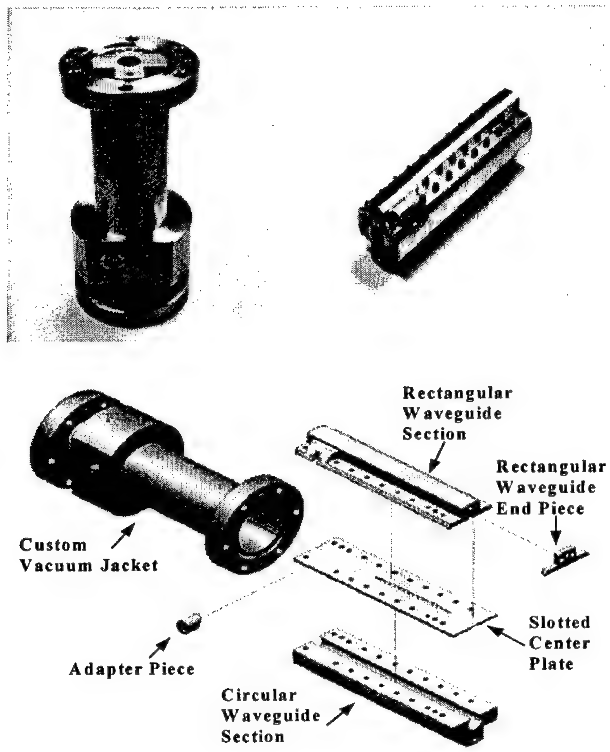

Fig. 4.1.19. Second-harmonic TE21 gyro-TWT amplifier coupler and breakout assembly.

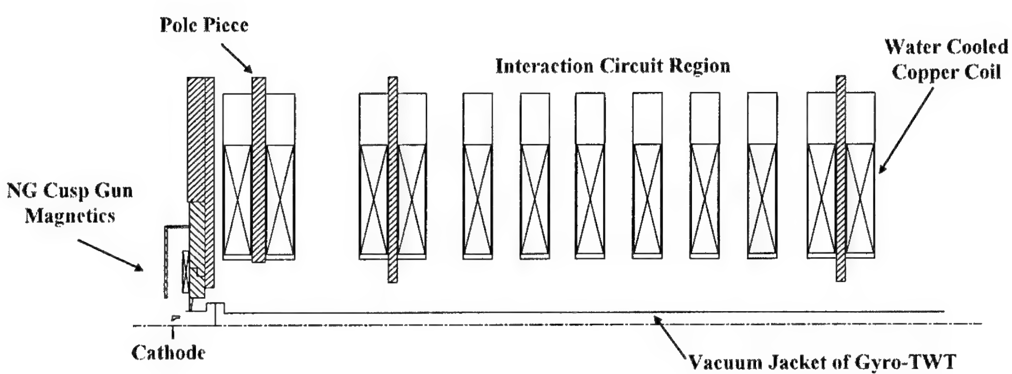

Fig. 4.1.20. Magnetic field circuit for the second-harmonic TE21 gyro-TWT amplifier

An important aspect of the device is the ability to couple RF energy in and out of the device efficiently. Multi-hole RF input and output couplers were designed using HFSS. The coupler

contains an array of slots connecting the narrow wall of the TE10 rectangular input waveguide to the TE_{21} circular interaction waveguide. HFSS simulation results predict that the input directional coupler will have less than 0.5 dB insertion loss over the bandwidth of the amplifier as shown in Fig. 20. There is excellent selectivity of 98% to the TE_{21} mode. Figure 21 shows the HFSS intensity plot showing the coupling from the TE_{10} rectangular mode to the TE_{21} circular mode.

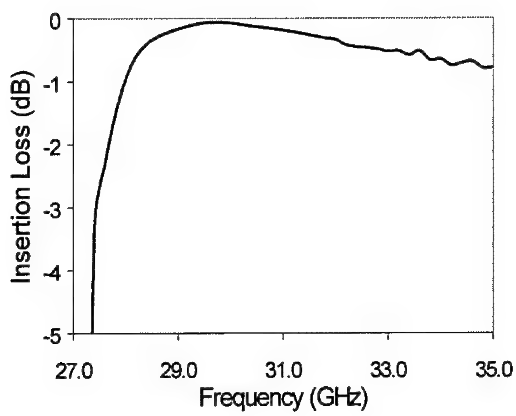

Fig. 4.1.21. Dependence of the insertion loss on frequency for the TE_{21} mode in the multi-slot coupler.

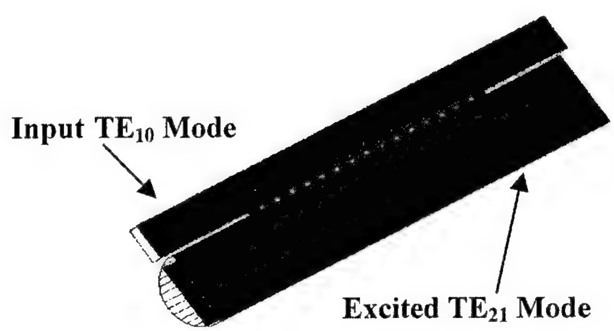

Fig. 4.1.22. HFSS intensity plot of the TE_{10} rectangular waveguide mode input and TE_{21} circular waveguide mode excited waves of the multi-slot coupler.

The TE_{21} second-harmonic gyro-TWT will be driven by the 80 W CPI Ka-Band TWT shown in Figure 22(b). The ETM modulator shown in Fig. 22(a) will supply the Ka-Band TWT. The Ka-Band TWT is being tested and characterized.

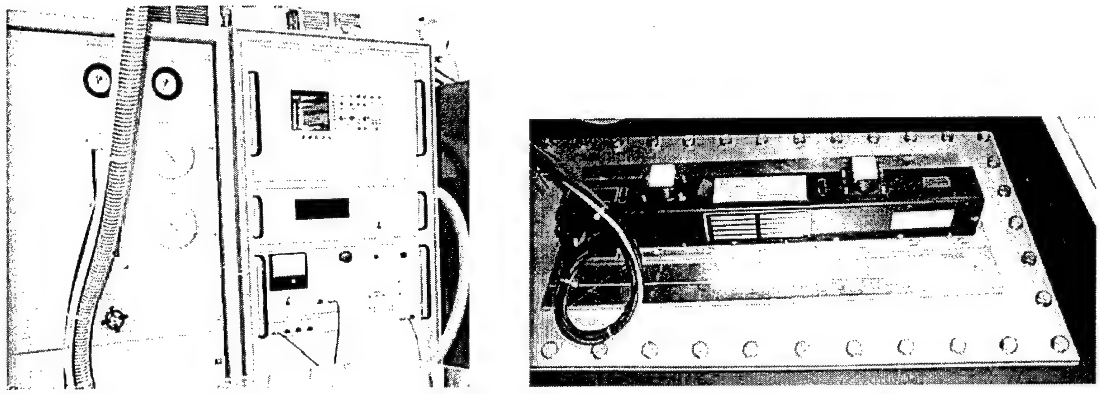

(a) (b)

Fig. 4.1.23 (a) ETM Modulator Supply, (b) 80 W CPI Ka-Band TWT driver.

As noted above, the Ka-Band TE_{21} second-harmonic gyro-TWT amplifier is being developed at UC Davis to further advance the relatively untapped potential of harmonic gyro-TWTs and to address the DoD needs for compact high power wide-band millimeter wave sources. The device has been designed and built and is being assembled for test. The design features of the gyro-TWT are published in the IEEE Transactions on Plasma Science June 2002 Special Issue on High Power Microwave Generation in an article entitled *Cusp Gun TE_{21} Second Harmonic Gyro-TWT Amplifier*. The current status has been presented at both IVEC2004 and ICOPS 2004. The device is a step in the development of a compact harmonic W-Band high power wide-band, efficient gyro-TWT amplifier. The single stage Ka-Band TE_{21} second-harmonic gyro-TWT amplifier which operates with 70 KV beam voltage and 3.5 A beam current is predicted to produce 50 kW with 20% efficiency, 30 dB saturated gain and 3% saturated bandwidth. The magnetic field requirements are reduced by a factor of two and the magnetic field is produced using water cooled copper coils. The eventual W-Band device will operate at higher harmonics taking further advantage of the characteristics of harmonic operation discussed above.

4.1.2 Slow Wave Device Research

As noted in the Director's Overview, TWTs and klystrons are nearly ubiquitous in DoD systems finding application in communications, radar, and ECM. This has motivated research activities at both the University of Wisconsin and UC Davis. At UCD, there are two lines of research: (a) design and modeling of millimeter wave TWTs and klystrons compatible with microfabrication techniques, and (b) TWT phase noise and linearization methods for the improvement of radar performance.

4.1.2.1 UCD Ka-Band TunneLadder TWT

As mentioned previously, Stanford and Davis have devoted considerable resources to both the development of new microfabrication techniques as well as computational modeling and design (also see the Stanford section of the report). In the modeling area, it is essential to have a rapid 3-D simulation capability so that this can be employed as a design tool and not simply a verification technique. This motivated the Stanford-MRC parallel MAGIC-3D activities as well

as the Davis TWT modeling studies. In the latter, MURI student Hsin-Lu Hsu has begun work on the simulation of a structure which is amenable to microfabrication and for which there is ample experimental data, namely the Karp/TunneLadder circuit. In addition to the experimental data, there have been previous simulations by a number of researchers including Carol Kory which facilitated initial comparisons before Ms. Hsu embarked on more realistic geometries. The geometry is shown below in Figs. 23 and 24.

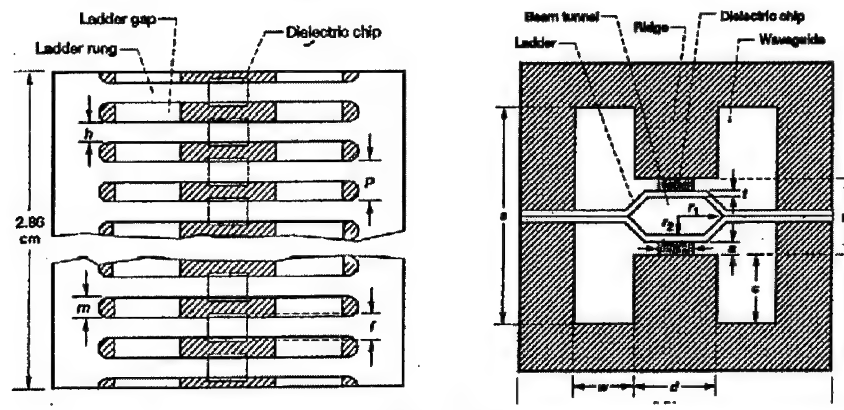

Top View Side View

Fig. 4.1.24. Initial TunneLadder geometry. (Three-Dimensional Simulation of Traveling-Wave Tube Cold-Test Characteristic using MAFIA., C. L. Kory, NASA Technical Paper 3513, 1995)

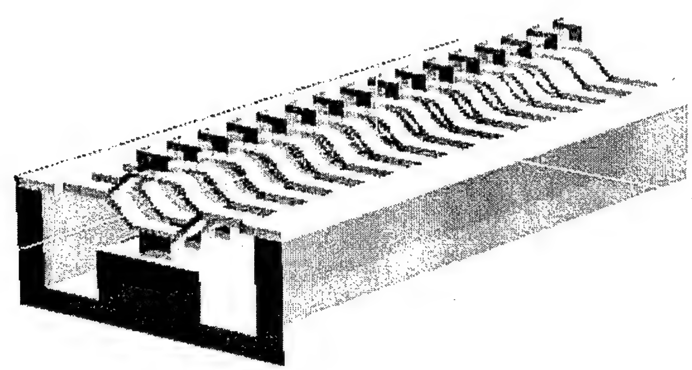

Fig. 4.1.25. Magic 3D computer modeling

Initial design simulation results have been obtained with MAGIC 3D and are in agreement with previously measured data as shown below in Fig.25.

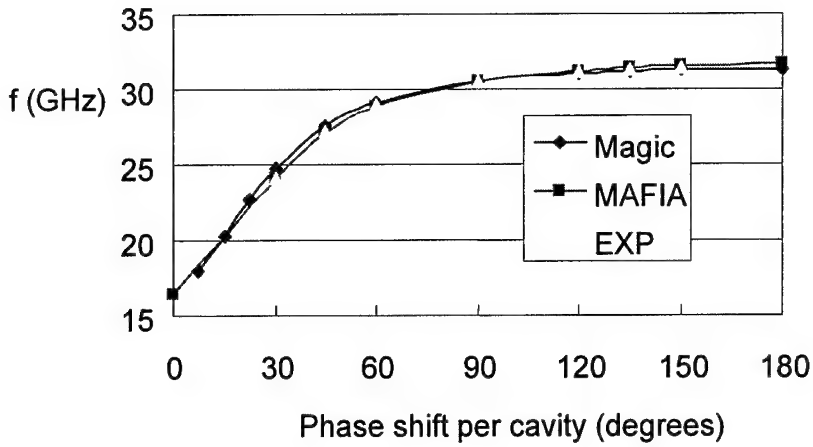

Fig.4.1.26 Initial design simulation result using MAGIC 3D and comparison with experimental data and MAFIA simulation result of Carol Kory.

The interaction impedance has been calculated and the predicted maximum gain is around 30 GHz. The attenuation has been obtained as well.

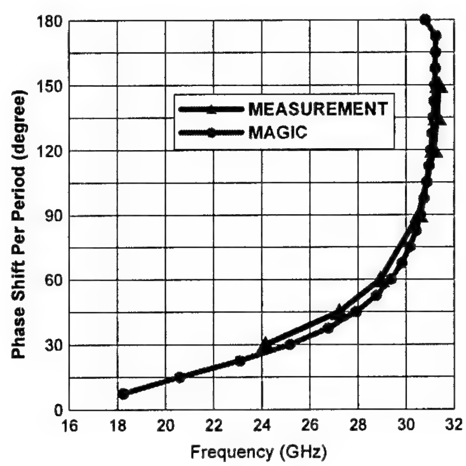

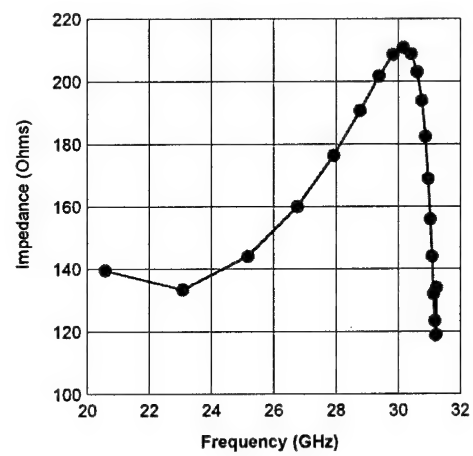

Fig. 4.1.27. Dispersion results (left figure) and the impedance simulation/calculation (right figure) which shows the maximum gain would be around resonance 30 GHz.

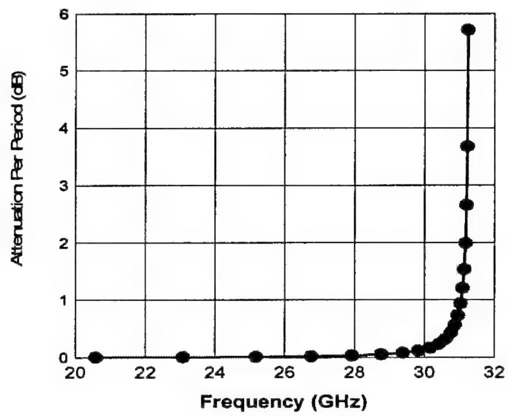

Fig. 4.1.28 Attenuation results were obtained where the conductivity of the wall, ridge and ladder were assumed to be S/m. In addition, the dielectric constant of the dielectric support was set equal to 5.5 and no loss tangent was input.

The couplers and transitions have been added and modeled by MAGIC 3D. The results are currently under examination.

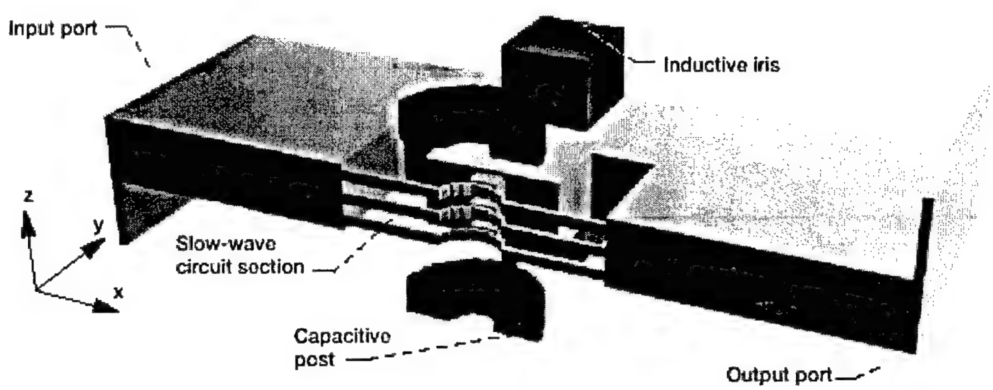

Fig. 4.1.29 Simulation of TunneLadder Traveling-Wave Tube Input/Output Coupler Characteristics Using MAFIA, C. L. Kory, NASA Contractor Report 198505, Sep, 1996

4.1.2.2 3D Magic Modeling of a Millimeter Wave EIK

MURI student Hsin-Lu Hsu has also been working under the direction of Glenn Scheitrum and George Caryotakis to carry out a full 3D Magic modeling of a millimeter wave EIK. The motivation for investigating the elliptic extended interaction klystron is to widen the bandwidth beyond that available from conventional klystrons. The device under study is aimed at

relatively high power output which is facilitated by the use of a coupled cavity configuration. The required tuning of the individual cavity resonant frequencies is greatly simplified by the use of an elliptic shape. As can be seen from an examination of Fig. 29, the flat, deformable surface permits easy tuning and easy fabrication using a standard end mill.

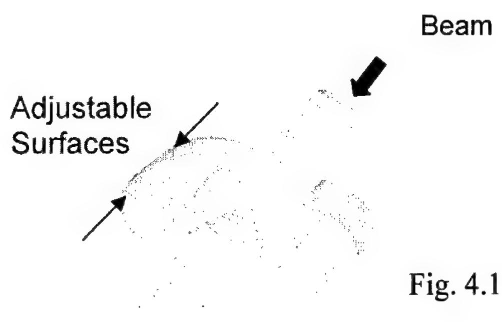

Fig. 4.1.30. Single elliptic cavity

By using the standard one dimensional small signal and large signal codes, an initial design achieves 1kW at 35 GHz and 200 MHz bandwidth. However, three dimensional modeling is obviously necessary since the geometry is not symmetrical with respect to any of the axes. By using Magic 3D, a complete tube structure has been built which requires an enormous amount of computer memory (see Fig. 30 below). By dividing it to individual cavities, it was possible for the initial modeling to run on single CPU, albeit extremely slowly with a typical run taking about one week. A parallel Linnux in SLAC will be used to handle the hot test simulation for a complete modeling of the EIK.
The status of the modeling activity was given by Ms. Hsu in an Invited talk: "Computer modeling of elliptic EIK using Magic 3D", MAGIC User Group meeting, April, 27, 2004, Monterey.

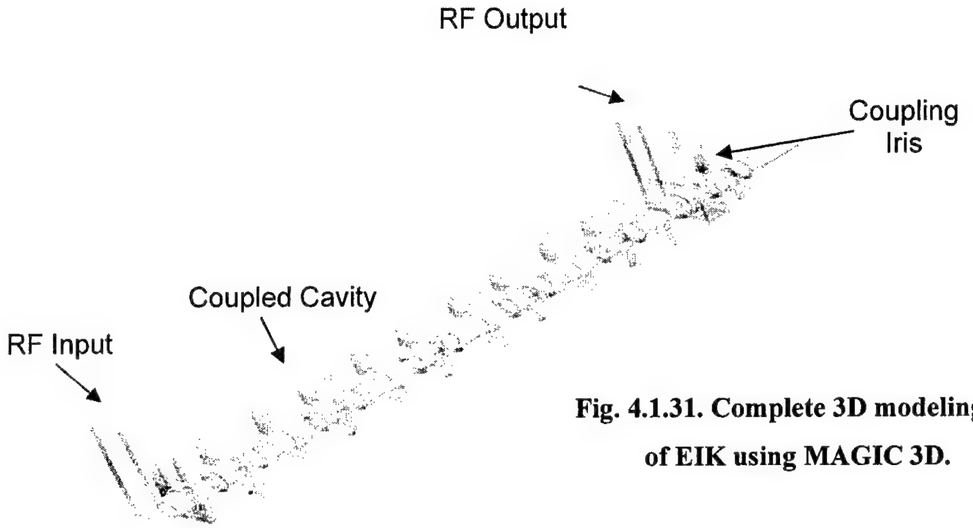

Fig. 4.1.31. Complete 3D modeling of EIK using MAGIC 3D.

4.1.2.3 Phase Noise Reduction in Radar TWTs

TWT phase noise reduction techniques have investigated by MURI Ph.D student Jae Seung Lee in cooperation with Teledyne Microwave Electronic Components. Phase modulation based communications, such as multi-PSK, Doppler radar and MTI (Moving Target Indicator) radar all require extremely low phase noise TWTAs. One of the approaches which has yielded excellent results utilizes an envelope feedback loop, which has the advantage of correcting the slow phase variation. This method resembles the conventional phase-locked loop (PLL) in which the detected output phase noise is compensated through a voltage controlled phase shifter
Although solid state amplifiers typically have smaller volume, lower noise figure and easier implementation capability compared with tube based RF amplifiers, the limited output power available in the higher frequency ranges has resulted in the continued dominance of t vacuum power amplifiers for many applications, especially low to medium PRF (Pulse Repetition Frequency) pulse radars. The larger metallic structure and collector of tube amplifiers allow higher terminal power handling and higher efficiency, respectively. The specific amplifier studied by Mr. Lee is part of a radar transmitter and is an MTG-5336 triband (C, X, Ku band) communication TWT provided by Teledyne Microwave Electronic Component Inc. The typical operation conditions are: cathode voltage and current for continuous wave output 10.94 kV and 340 mA, respectively. The output power is 58 dBm and the power gain is around 42 dB over X-band.
Radar receivers respond not only to the desire target signal, but also to strongly reflected cutter. Figure 31 illustrates two targets with different speeds and different cross sections. The solid line over the offset frequency band is redrawn clutter which hides desired low level target reflections. This research work proposes and proves that a phase locking feedback can increase probability of detection reducing inherent phase noise of TWT by the dotted line in the figure.

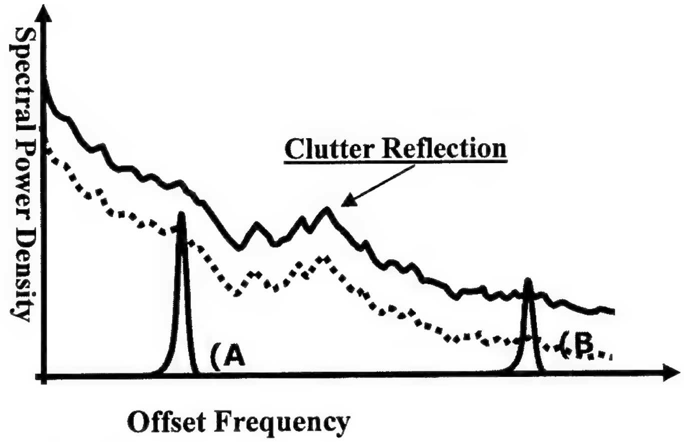

Target (A): Not detectable
Target (B): Detectable, but must be sufficiently fast

Fig. 4.1.32. Radar target reception

Radar, in general, is operated in the deeply saturated regime where phase noise becomes an extremely important factor. The phase noise can be determined on the basis of a basic FM (frequency modulation) theory. If a signal of interest is phase modulated, one can express its phase noise as follow;

Phase modulated signal; $V(t)=V\cos(2f(t))^{0}+\Delta^{\varphi}\, t$

Phase noise spectral density; $L(f)=\dfrac{\Delta_{\varphi}^{2}(f)}{2BW}$

$\Delta\varphi(t)$

The phase variation term, can be a random noise signal. The single side band spectral density expression of phase noise is expressed in standardized terminology in units of dBc/Hz. Figure 32 shows the dissertation goal of the TWT phase noise reduction. The green line indicates IESS (Intelsat Earth Station Standards) and specifies the phase noise spectral density from 10 Hz to 1 MHz of offset frequency for oscillators, amplifiers, and up-down converters used in satellite communication. It is of interest to note that the inherent TWT phase noise, plotted as the black dotted line, is about 40dB below the IESS specification. The aim of Mr. Lee's work is to obtain an additional 20dB of improvement, which will significantly improve the overall efficiency of radar transmitter, reduce transmitter size (via the relaxation in power supply filtering requirements) and allow multi-channel use in radar.

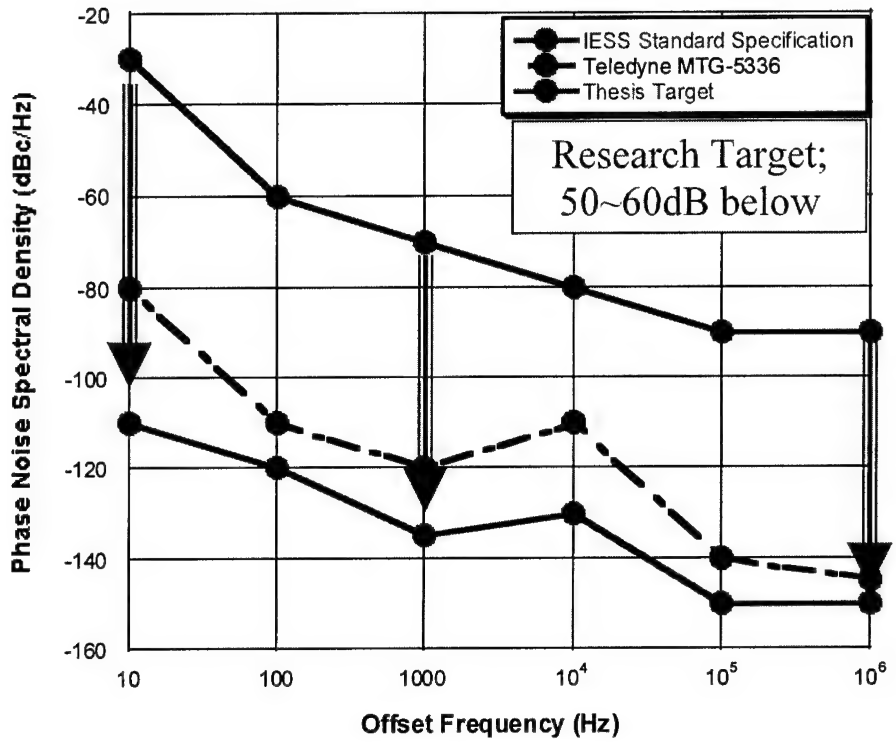

Fig 4.1.33. Phase noise spectral density versus offset frequency illustrating the research goals.

The major phase noise source is the unstable dc voltage of the HVPS (High Voltage Power Supply). The jitter on top of the cathode voltage causes beam velocity modulation which is, in turn, converted into phase jittering. One can simply derive the relation between the voltage fluctuation on HVPS and the followed phase change,, with the aid of electron motion theory. Ignoring nonlinear effects, the electrons are assumed to $\Phi(t)$ move in the influence of a static electric field. The velocity of the electron and the phase of RF signal are:

$$v=\sqrt{\frac{2eV}{m}} \text{ and, } \Phi(t)=\frac{2\pi f}{v}L$$

For $V=V_{DC}+v_{ripple}$, the phase change becomes:

$$\Phi(t)=\pi fL\sqrt{\frac{2m}{e(V_{DC}+v_{ripple})}}$$

The common method to reduce this voltage fluctuation is to employ a regulator together with large capacitive filtering. This conventional method is rather simple and effective, but results in large space requirements and increased weight. In addition, additional factors arise in the case of pulsed mode operation. Since the Fourier frequency response of a rectangular pulse extends from dc to infinity, frequency domain filtering loses effectiveness. Consequently, Mr. Lee's research has focused on real-time detection of phase jitter and compensation by the required amount. As shown in Fig 33, a double balanced mixer discriminates the phase difference between the "clean"

input signal and the phase noise added output signal of the TWT amplifier. With 16 V/degree of conversion, the converted video voltage signal is readily able to drive a voltage controlled phase shifter prior to TWT input. This video signal experiences two conversions; phase to voltage and voltage to phase in mixer and voltage controlled phase shifter, respectively. Therefore, the video amplifier is designed to compensate for this total conversion loss. In the mean time, nonlinear effect of the mixer creates dc bias and harmonics so that dc blocking and a low pass filter are also required in the transition. The manual phase shifter in the left hand side of system adjusts the fine difference of time delay between the two paths towards the mixer. Phase noise measurement is performed with an HP L1500A spectrum analyzer and E5500 software. The first result demonstrates phase noise reduction in CW (Continuous Wave) mode operation. As shown in Fig 34, 20~25 dB of improvement was achieved.

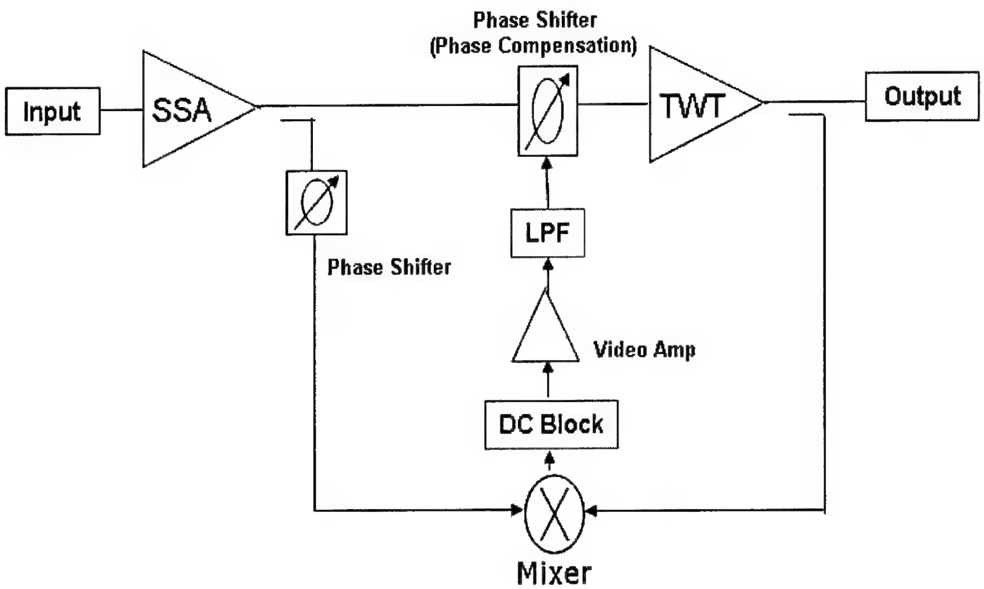

Fig 4.1.34. Phase locking feedback loop method system schematic

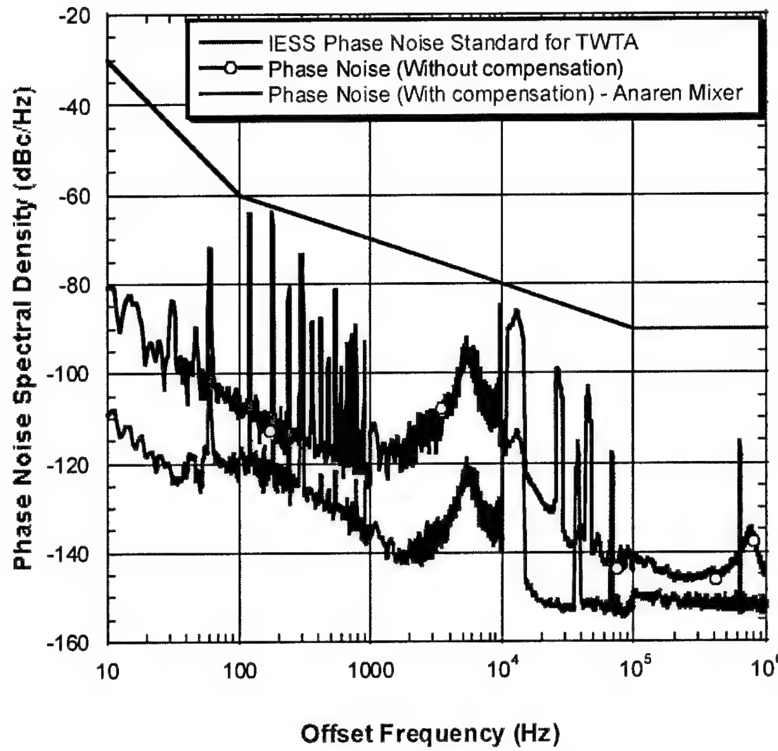

Fig 4.1.35. Phase noise reduction for CW operation, carrier frequency is 8 GHz

In pulsed radar, PRF is an important parameter as long as both Doppler and range ambiguities are concerned. To verify phase noise reduction for high PRF operation, two case studies were performed; 20% duty cycle with 50μs pulse width, and 5% duty cycle with 25μs pulse width. For both cases, the tuned system is maintained in the same state for the entire frequency sweeping measurement. The carrier frequency was swept from 7.7 to 8.3 GHz, because 500MHz of bandwidth is the maximum required in general radar operation. In Fig 35 and Fig 36 are measured results in the 20% duty case. Figure 35 shows the inherent phase noise spectral density in the green line and the reduced noise in red for 8.0GHz carrier operation. Five sets of reference noise and reduced noise spectra were measured, respectively. The amount of reduction versus offset frequency is plotted in Fig 36. Over 500MHz of bandwidth, about 20 dB of consistent improvement was achieved. Similarly, results for the 5% duty case are also presented in Fig 37 and 38.

These preliminary results were presented by Mr. Lee at both the 5th IEEE International Vacuum Electronics Conference, Monterey, California, USA, April 2004 and the IEEE International Microwave Symposium, Fort Worth, Texas, USA, June 2004.

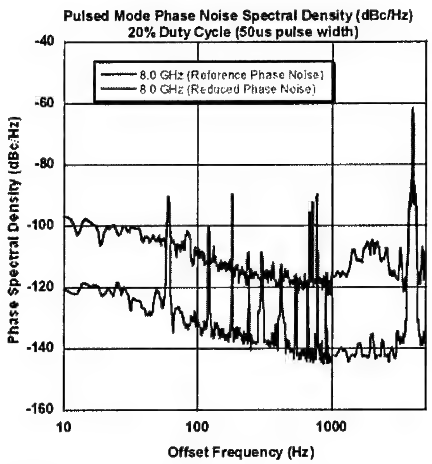

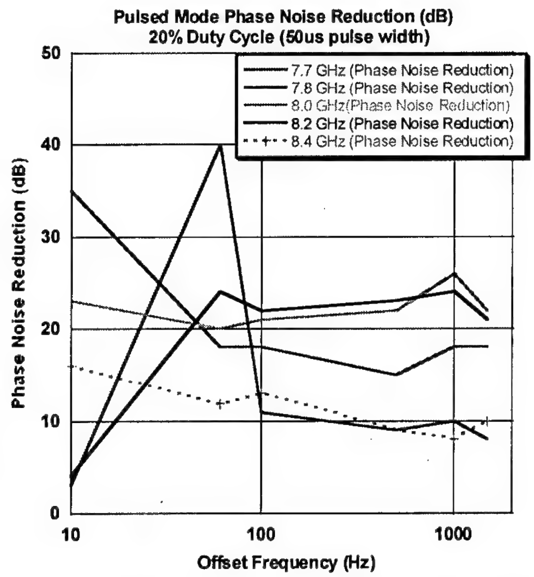

Fig. 4.1.36 Phase noise measured for pulsed mode operation with 20% duty cycle (50 μs pulse), carrier frequency is 8GHz

Fig. 4.1.37 Phase noise reduction for pulsed mode with 20% duty cycle (50 μs pulse) carrier frequency from 7.7~8.4 GHz

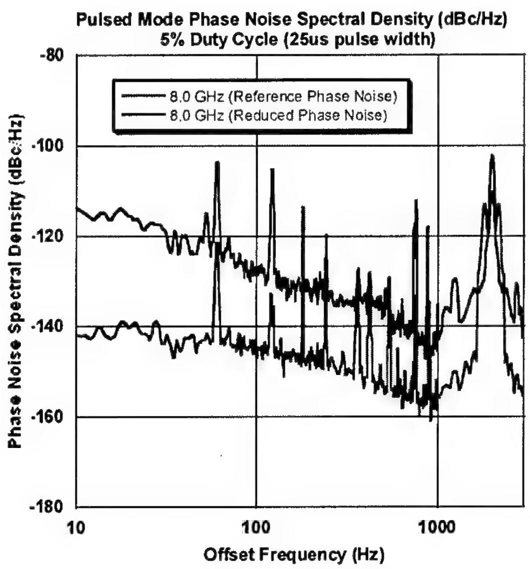

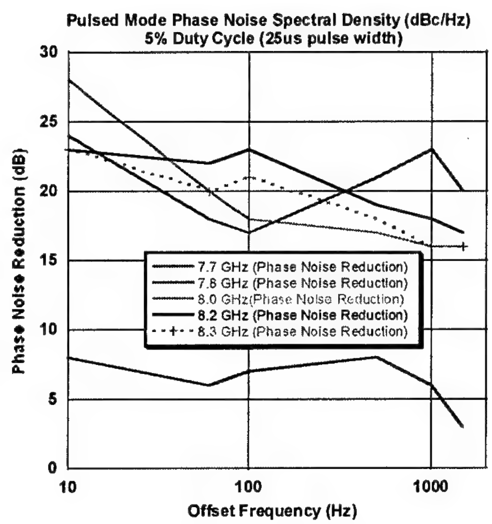

Fig. 4.1.38 Phase noise measured for pulsed mode operation with 5% duty cycle (25 μs pulse), carrier frequency is 8GHz

Fig. 4.1.39 Phase noise reduction for pulsed mode with 5% duty cycle (25 μs pulse) carrier frequency from 7.7~8.3 GHz

4.1.2.4 UCD High Power Millimeter Wave Beam Steering/Shaping Antenna Arrays

MURI students Chia-Chan Chang and Yaping Liang have been focused on the development of novel millimeter wave beam steering/shaping phased antenna arrays (PAAs) at Ka-band and W-band which are intended to be used with millimeter wave vacuum electron beam sources. The major problem with conventional millimeter wave tubes is that their size poses a serious impediment since this prevents them from being spaced less the requisite maximum $\lambda/2$ value. Investigations at NRL have concluded that even such measures as removing the covers from TWTs restrict conventional approaches to a maximum frequency of approximately. This has led them, as well as researchers in the MURI Vacuum Electronics Program, to investigate novel approaches involving microfabricated arrays (see Sec. 4). The conventional approach to high frequency PAAs is to utilize solid-state T/R modules since they offer the possibility of greatly reduced element spacing. However, they suffer from a number of serious limitations such as cost and power, particularly at high frequencies. In fact, even the highest frequency devices (i.e., InP HEMTs) are restricted to considerably lower operating frequencies than VEDs in addition to offering much lower output powers. The approach taken by Ms. Chang, in contrast, employs high power VED sources followed by compact and efficient power splitters and delay lines which can handle high powers and which feed antenna radiators spaced less than $\lambda/2$ apart. This approach satisfies the growing need for radar and communication systems both in military defense and commercial applications which employ phased array based beam steerers and beam shapers.

Two phased antenna arrays are currently under development in these initial basic studies. The operation frequency for the first system is set as 18 GHz for initial testing. The second PAA system is designed to operate in the Ka-band range (38 GHz). Furthermore, a W-band PAA is also currently under design and is intended to operate at power levels appropriate for current DoD applications including Active Denial systems.

A major function of a PAA is to scan the main beam into the desired direction as well as to provide beam-shaping capability by appropriate arrangement of the feed signals. This is accomplished by appropriately changing the relative phases of the antenna elements or by programming time delays between elements. In this MURI research, considerable attention is given to a system employing the true time delay approach developed by K. Chang [1] which utilizes a piezoelectric translator (PET)-driven perturber to vary the propagation velocity along low loss transmission lines. A programmable DC bias causes the PET to move the dielectric layer, thereby perturbing the electromagnetic field of the transmission line. The variation in effective dielectric constant results in the change of propagation constant, $\Delta\beta$, and consequently results in a time delay type phase shift $\Delta\phi$.

$$\Delta\phi = L_P \cdot \Delta\beta$$

$$\Delta\beta = \frac{2\pi}{\lambda_0} \cdot \left(\sqrt{\varepsilon_{eff}(f)} - \sqrt{\varepsilon_{eff}'(f)}\right)$$

Here, $\varepsilon_{eff}(f)$ is the frequency dependent effective dielectric constant under maximum perturbation, while $\varepsilon'_{eff}(f)$ is the value under the minimum perturbation, while L_P is the length of dielectric perturber.

The piezoelectric material, which is comprised of Lead Zirconate Titanate ceramic, was purchased from Piezo System, Inc. The maximum free deflection is about ± 1300 μm when applying ± 90 volts. Figure 39 shows the photograph of microstrip line-based PET phase shifter and Fig. 40 shows the measured phase shifts for different frequencies and different air gaps.

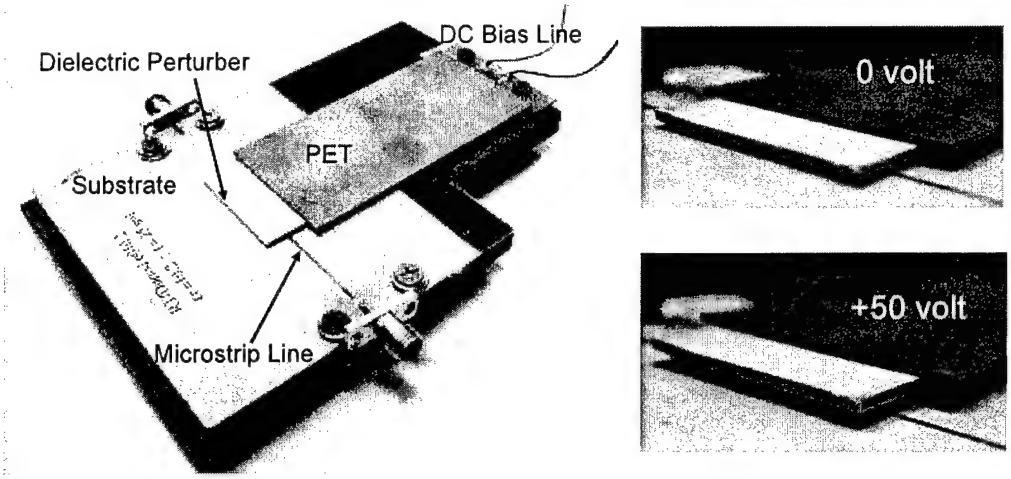

Fig. 4.1.40 True-time delay type, microstrip line-based PET phase shifter

PET perturbers based on different transmission media have been investigated. For the case of a transmission line with the ground on the same surface with the signal line (eg. coplanar waveguide, coplanar stripline and slot line), the density of the electric and magnetic field lines in the air is greater than in the microstrip lines. Therefore, the perturbation effect is more significant. Figure 41 shows the comparison of different transmission media. The simulation results indicate that both coplanar waveguide and coplanar stripline can generate greater phase shift as compared to microstrip line. In this beam steering/shaping antenna array design, coplanar stripline (CPS) has been chosen. In addition to the attractive perturbation characteristics, the balanced structure of CPS also facilitates connection to the transmitting antennas without introducing additional baluns.

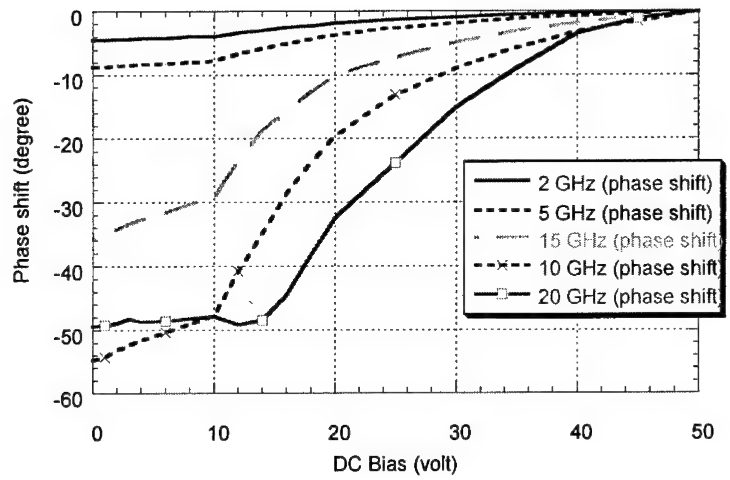

Fig. 4.1.41. Measurement results for microstrip line based PET phase shifter. The microstrip line was designed as 55Ω (21 mil) at 20 GHz and fabricated on 25-mil, RT/Duriod 6010.2 (ε_r =10.2). The perturber used the same material and was 0.8" long and 50 mil thick.

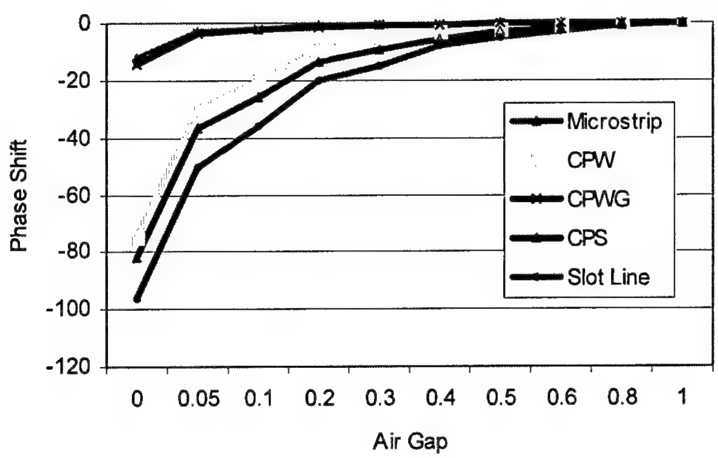

Fig. 4.1.42 Simulation comparison of the phase shift caused by PET perturber based on different transmission media

For the proof-of-principle studies, an 18 GHz PAA has been designed and fabricated on 20-mil GML1000 substrate (εr =3.05). The entire system layout is shown in Fig. 42. The microwave signal is first fed via an 8-way microstrip-based power divider, and then passes through the microstrip to CPS transition. The CPS-based, PET perturber, which is controlled by the DC bias, provides the true time delay. Finally, the resultant RF signal is then fed directly to a planar tapered slot antenna with half wavelength spacing between each channel. The overall system size is about 5″ × 8″. Figure 43 shows a photograph of the fabricated circuit.

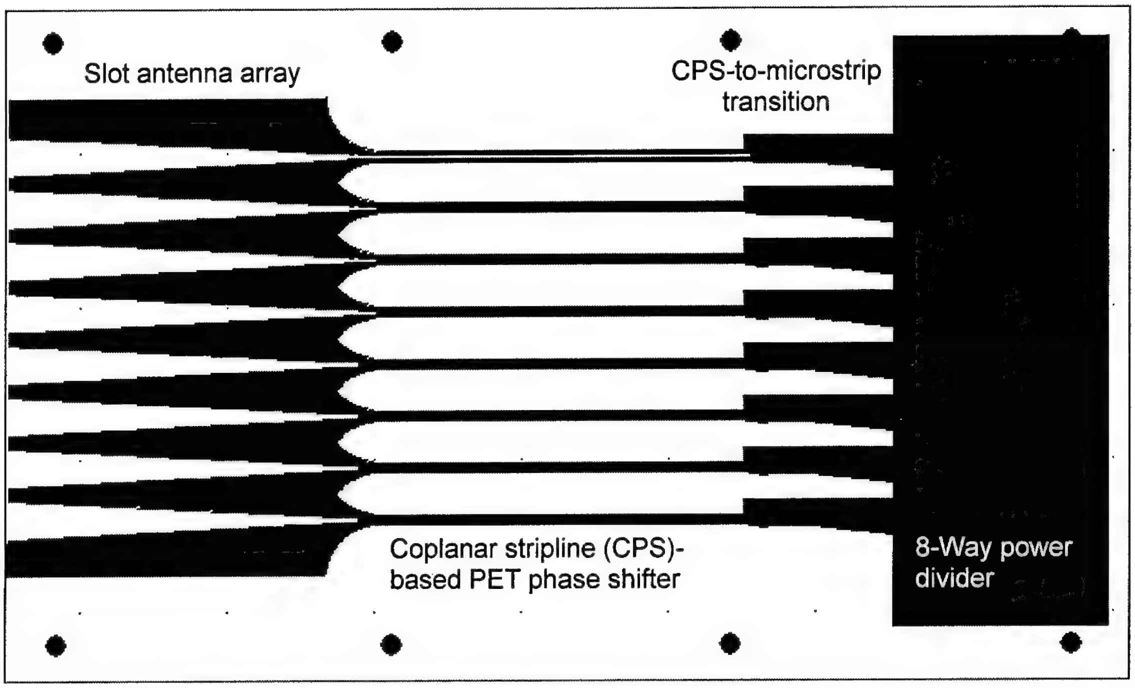

Fig 4.1.43 Circuit layout of 18 GHz beam steering/shaping phased antenna array

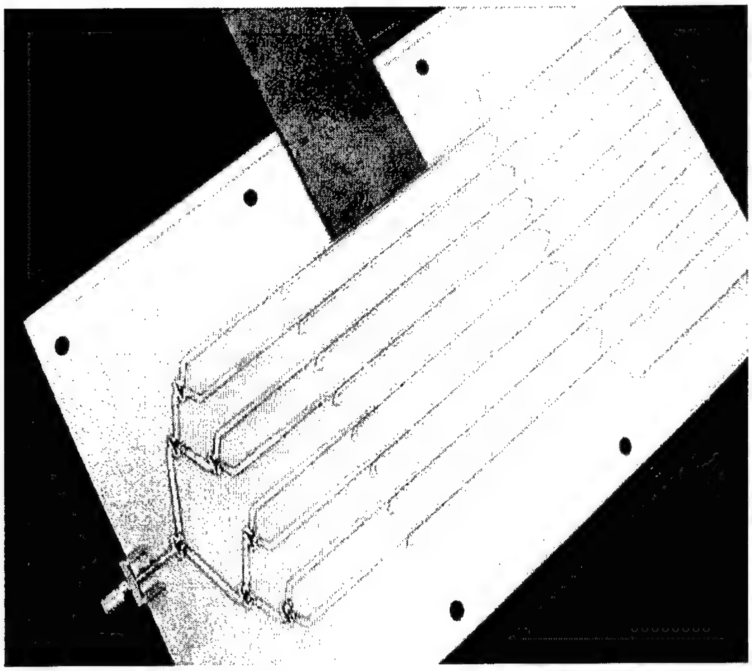

Fig. 4.1.44. Photograph of 18 GHz, beam steering/shaping antenna array (5" × 8")

For the 38 GHz PAA system, the entire structure will be similar to the 18 GHz system, except that the substrate material has been replaced by 10-mil RO3203 ($\varepsilon r = 3.02$). To achieve 100W output power, the major consideration of the entire system design is the power handling capability. The power-handling capability of a transmission line is limited by dielectric voltage breakdown and by excessive heating due to attenuation. The electrical breakdown limits the peak power, which is mainly considered under pulsed operation. Under continuous wave (CW) operation condition, the increase in temperature due to conductor and dielectric losses limits the average power. When the operating temperature is too high over prolonged periods of time, the concern is that the traces will loose adhesion to the base dielectric and eventually delaminate. Therefore, it is crucial to ensure that the operating temperature is maintained below the rated value for the given material.

For this Ka-band, 100W output PAA design, the entire system will remain the same as the previous 18 GHz PAA design except for the CPS-based PET perturber and feeding method. In the previous 18 GHz PAA design, the CPS structure was chosen in the PET perturber region instead of microstrip line to generate more time delay. However, according to previous studies, microstrip line has the highest power handling capability comparing to other transmission media in this general category. Hence, microstrip line should be chosen over CPW and CPS here to accommodate the high output power requirement.

The maximum average power (P_{ave}) under CW conditions was addressed in detail by Gupta [2] and is given by

$$P_{ave} = \theta / \Delta T \qquad (W)$$

where θ is the temperature rise above ambient (°C), In general, maintaining the continuous operating temperature below 125°C is recommended which means that θ should be less than 100°C (assuming 25°C ambient temperature). Here, ΔT is defined as the temperature rise to indicate the density of heat flow caused by power absorption per unit length

$$\Delta T = \frac{0.2303 \cdot h}{K}\left[\frac{\alpha_C}{W_{eff}} + \frac{\alpha_D}{2W_{eff}(f)}\right] \qquad (oC/W)$$

In the above, h is the substrate thickness, K is the thermal conductivity of the substrate, α_C and α_D are the conductor and dielectric losses, and W_{eff} and $W_{eff}(f)$ are the effective microstrip widths. As expected, the substrate material dominates the temperature rise as well as the maximum average power for CW power transmission conditions. Therefore, it is obviously advantageous to select a material with higher thermal conductivity K when it comes to power handling. Additionally, the thinner substrate and larger microstrip geometries will result in improvements in power handling.

In this 38 GHz PAA system, the substrate was chosen as 10-mil RO3203 (εr =3.02, K= 0.47 W/m-K; Rogers Corp.). The 50Ω transmission line design will result in a temperature rise ΔT given by 5.2837 °C/W [3]. In other words, 18.93 W incident RF power will cause a 100°C temperature increase. If the system is still fed by a coaxial connector through a 1-to-8 power divider, approxiamately150 W input power is required to overcome all losses and to provide the required output power level. Consequently, there will be overheating at the input port. Therefore, we need to employ a different RF signal feed configuration. The proposed method is to use a custom designed oversized waveguide with a gradual transition from the standard WR-28, Ka-band waveguide. The individual receiving antenna elements, which are spaced half a wavelength apart, will replace the coaxial connector and power divider. The entire PAA will be driven by a Ka-band high power tube. The system schematic is shown in Fig. 44.

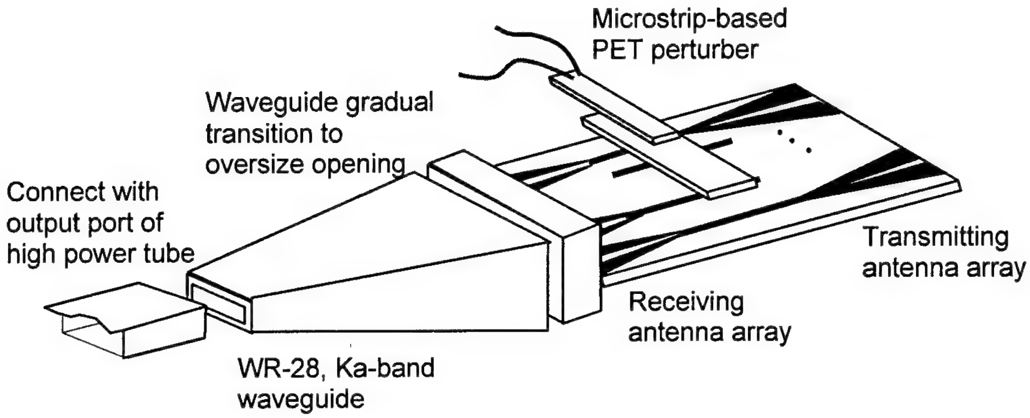

Fig. 4.1.45. Schematic of proposed Ka-band, 100 W output power, phased antenna array

A standard WR-28 waveguide can usually drive 22-31 kW power, and therefore should be able to readily handle the high power level coming from the tube. The possible power losses through the entire system could come from the waveguide transition, antenna radiation loss, microstrip line loss, and/or possible mode conversion problems due to the multi-mode operation. Accounting for all possible losses, at least 12 channels are required to ensure 100 W output power. The overall size has been predicted as 2.5″ × 4″.

For the W-band PAA system, it seems prudent to utilize a high dielectric constant substrate and a slow wave propagation velocity; this reduces the radiation loss from the circuits. However, at the higher frequencies of future interest to the DoD, the circuits get impossibly small, which restricts the power handling capability as well as increases the fabrication difficulties. Additionally, the piezoelectric controlled phase shifter will not be suitable for use at such a high frequency range due to its large size. Microelectromechanical systems (MEMS) switch based delay hence is a good candidate to generate the required time delay. 10-mil fused quartz (ε_r=3.8, K=1.4 W/m-K) has been chosen as the substrate material in this W-band PAA design based on its compatibility with standard microfabrication techniques. Calculation shows that 50Ω transmission line designs (assuming a center frequency of 88 GHz) will result in a temperature rise ΔT of 2.2739 °C/W, which means that a maximum of 43.98 W RF power is allowed to flow through each channel before reaches 100°C temperature increases. Here we note that the recent availability of large, high quality CVD diamond substrates makes this attractive for even higher power operation. CVD diamond exhibits remarkable dielectric properties including a low dielectric constant of 5.7, a loss tangent below 0.00005 at 145GHz and a high thermal conductivity of 2000-2500 W/m-K. This thermal conductivity value has been found as the highest of any material at room temperature. Assuming that 10-mil CVD diamond is chosen as substrate material for W-band PAA design, the 50Ω transmission line at 88 GHz designs will result in a temperature rise ΔT of 2600 °C/W, which makes a single channel be able to handle maximum 37780 watt before reaches 100°C temperature increases, almost 85 times larger than fused quartz.

Similar to the previous cases, an endfire tapered slot antenna is still chosen here because it has many advantages including wide bandwidth, high gain and narrow beam width. Other researchers have shown that the effective substrate thickness normalized to the free-space wavelength must satisfy the following relationship to exhibit traveling-wave characteristics [4]: At high frequencies, this results in a fragile structure. To improve the mechanical stability,

$$t_{eff}/\lambda_0 = [(\sqrt{\varepsilon_r} - 1)\cdot t/\lambda_0] \leq 0.03$$

micro-machining holes can be employed to remove a portion of the underlying substrate, thereby reducing the effective thickness and effective dielectric constant but still maintaining good mechanical properties. This method was first presented by researchers at the Radiation Lab. at the University of Michigan, and successfully demonstrated at 94 GHz [5].
Figure 45 shows the Agilent HFSS simulation model for this micro-machining substrate. The related effective dielectric constant can be calculated by the following equation:

$$\varepsilon_{eff} = \frac{\pi}{2}\cdot(\frac{D}{W}) + \varepsilon_r \cdot \left[1 - \frac{\pi}{2}\cdot(\frac{D}{W})^2\right]$$

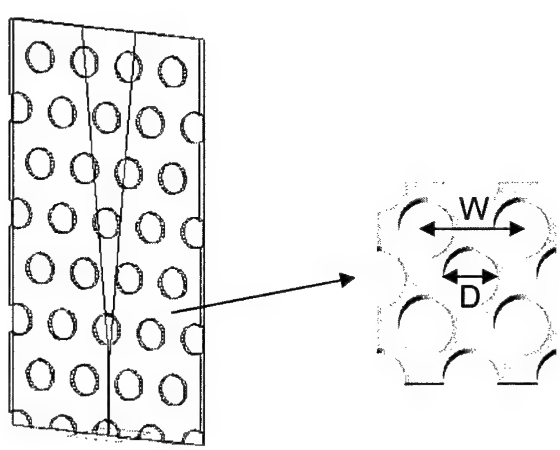

Fig. 4.1.46. HFSS simulation model for W-band single slot antenna with the micro-machining substrate

The simulation results shown in Fig. 46 reveal that the 10-mil thick substrate (green curve) generated the undesired patterns; reducing the substrate thickness to 4.24 mils will efficiently improve the antenna patterns (blue curve). Using the 10-mil thick substrate, but removing a portion of the underlying substrate, will also generate good patterns (orange curve).

The need for MEMS switches for microwave and millimeter applications has dramatically arisen in the past decades based on their numerous advantages including low cost fabrication, extremely high ON/OFF contrast ratios, low insertion loss, high isolation and relatively high power handling capability. The MEMS switch can be configured to generate phase shift by switching between two different signal paths (digital-type), or can be used as a distributed capacitive switch to change the effective capacitance of the transmission line (analog-type). Figure 47 shows the digital-type MEMS switched delay line. The phase shift is determined by the difference between the two path lengths, which is selectively controlled by DC bias.

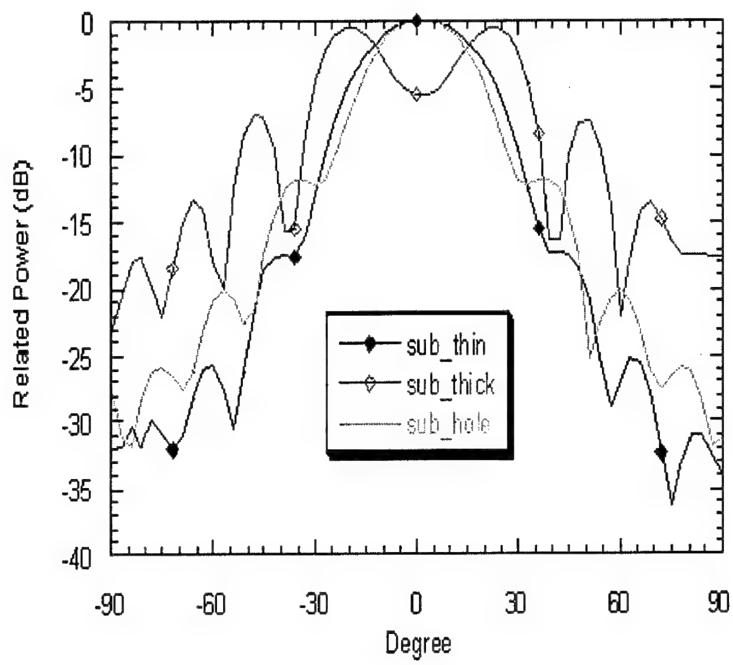

Fig. 4.1.47. HFSS W-band single antenna pattern simulation results for three different cases (a) 10-mil quartz substrate (b) 10-mil quartz substrate with micro-machining holes (Resulted in ε_{eff}=1.969) (c) Corresponding substrate thickness = 4.24mil, which satisfies:

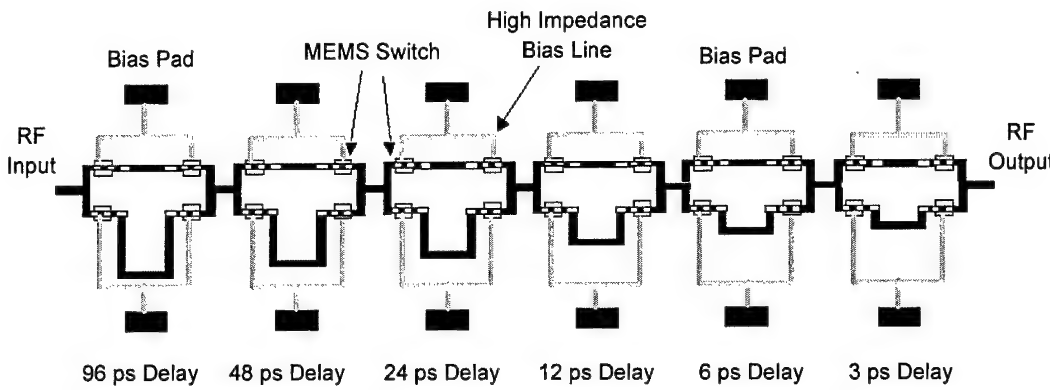

Fig. 4.1.48. Schematic of a 200 ps digital-type MEMS switched delay line

Bridge-type MEMS devices used in high power switching arrays have been studied at UC Davis, and recently the group has successfully demonstrated an E-band MEMS quasi-optical switching array (see Fig. 48) with < 15dB isolation at 76 GHz [6]. It shows the ability and confidence to fabricate high frequency MEMS devices for the related applications in the near future.

From the previous calculation, it was seen that each channel can handle a maximum of 44 W RF power. Including all possible losses including the waveguide transition loss, antenna radiation loss and the MEMS delay line insertion loss, at least 8 channels are needed to ensure 100 W output power. Each channel will be spaced half a wavelength apart. The proposed system schematic is shown in Fig. 49.

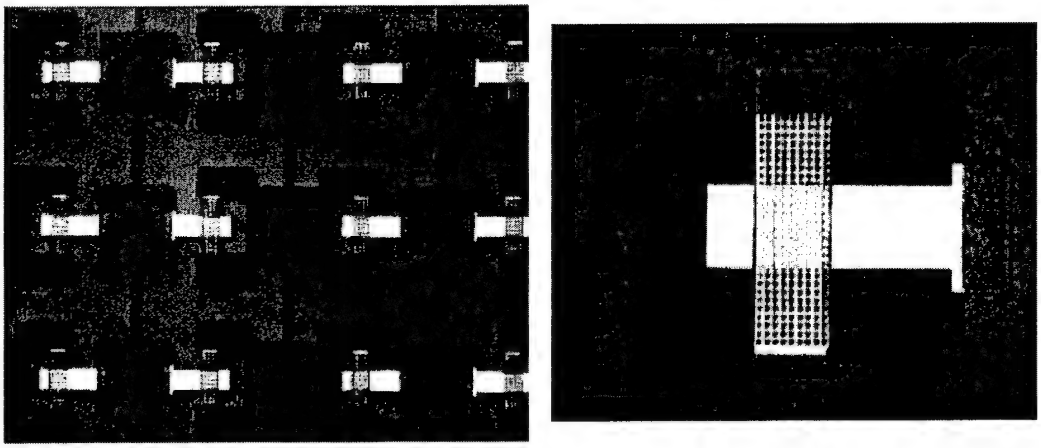

Fig.4.1.49. Photographs of E-band, bridge-type MEMS used in high power switching arrays have been conducted in the UC Davis Microfab Lab. The left one is MEMS quasi-optical switching array. The right one is a single switch.

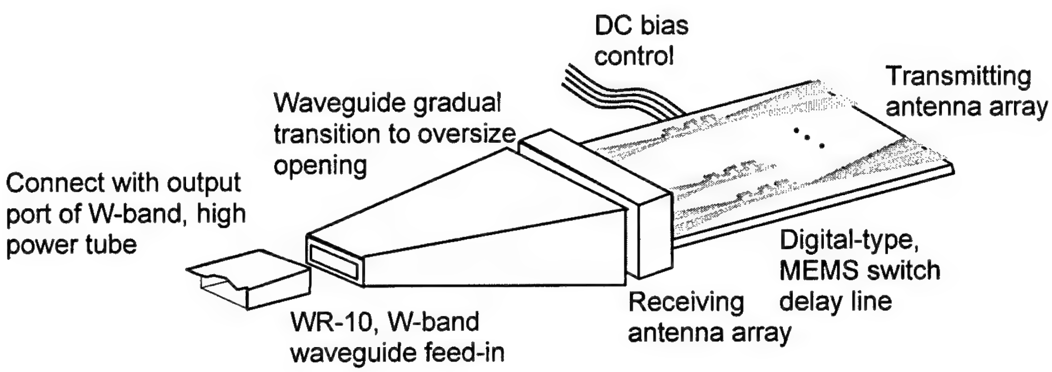

Fig. 4.1.50 Schematic of proposed W-band, 100 W output power, phased antenna arrav fabricated on 10-mil fused auartz substrate

In addition to MEMS switch based delay lines, we are also investigating the use of MEMS varactors in nonlinear delay lines. The approach taken by UC Davis student Yaping Liang is to begin with the varactor design conceived by the Katehi group [7,8]. This addresses the so-called "pull-in" effect which is a major limitation in MEMS varactor designs. This effect occurs upon the addition of sufficient DC bias to cause the air gap to decrease beyond 1/3 of the distance of the entire gap. Beyond that point, the two metal plates will quickly snap into contact. This effect causes nonlinearity and also decreases the capacitance variation ratio of the MEMS varactors. The solution adopted by the Katehi group is to employ a two-parallel-plate MEMS varactor design. As shown in Fig. 50, The design consists of two metal beams with different thickness. The lower beam is 0.7μm thick and is suspended 2μm above the CPW line. The upper beam is 13μm thick and is suspended 8μm above the bottom actuation pads. Upon addition of bias between the upper beam and the actuation pads, the lower beam deflects. Because the pull-in effect will happen when the upper beam moves about 2.7μm, since the upper beam is connected with the lower beam, the maximum deflection for this varactor is 2μm. That means there is essentially no pull-in effect in this design. Figure 51 shows the HFSS model employed for the 3D simulations of the new MEMS varactors (this version utilizes a "standard" configuration). Currently, we expect to fabricate the first devices by the end of the summer.

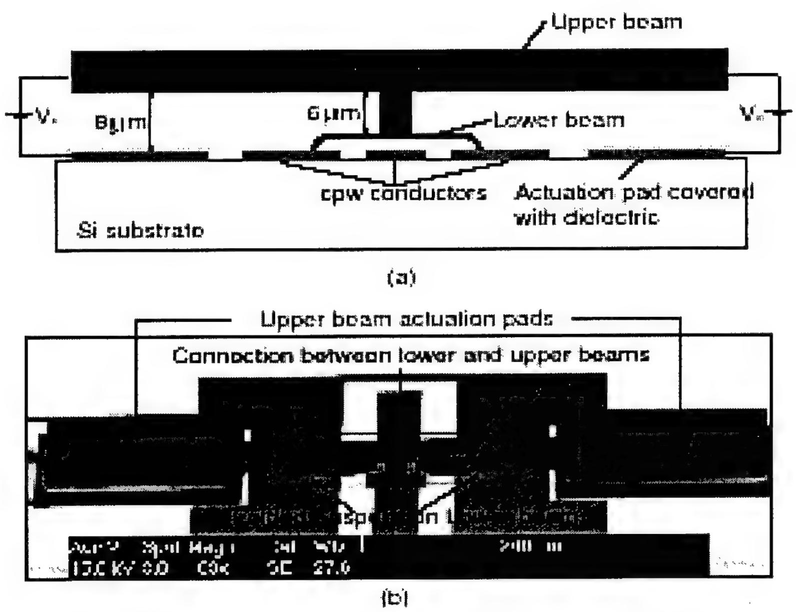

Fig. 4.1.51.. Katehi group's two-parallel-plate MEMS varactor design.

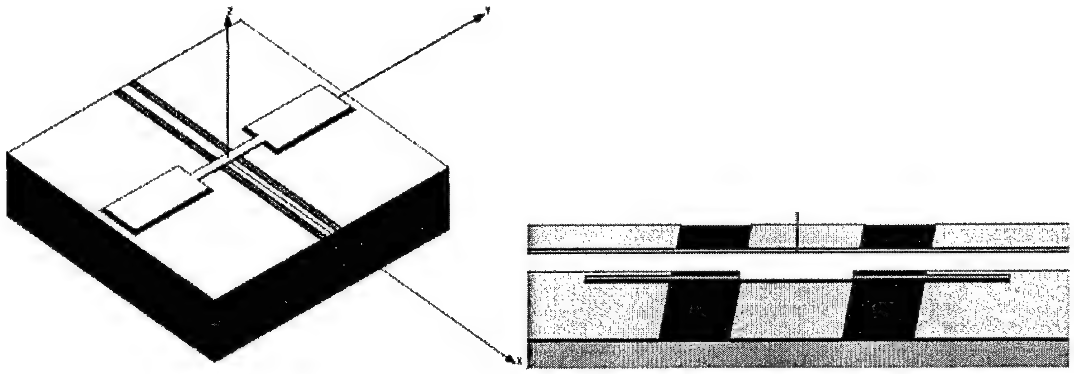

Fig. 4.1.52. HFSS model of MEMS varactor

1. T. Yun, and K. Chang, "A Low-Cost 8 to 26.5 GHz Phased Array Antenna Using a Piezoelectric Transducer Controlled Phase Shifter," *IEEE Tran. On Antenna and Propagation*, Vol. 49, No. 9, pp.1290-98, Step. 2001.

2. K.C. Gupta, R. Garg, , I. J. Bahl, and P. Bhartia, " Microstrip Lines and Slotlines," 2nd edition, *Artech House Inc.*, Norwood, MA 1996.

3. G. Robert Traut, MWI Simulation Code, *Rogers Corporation* , Feb., 2003

4. K. S. Yngvesson, T. L. Korzeniowski, Y-S Kim, E. L. Kollerg, and J. F. Johnsson, " The Tapered Slot Antenna – A New Integrated Eleement for Millimeter-Wave Applications," *IEEE Trans. Microwave Theory Tech.*, Vol.37, No.2, pp.365-374, 1989.

5. J.B. Muldavin and G.M. Rebeiz, "Millimeter-Wave Tapered-Slot on Synthesized Low-Permittivity Substrates," *IEEE Trans. Antennas Propag.*, Vol. 47, pp. 1276-1280, Aug. 1999.

6. K. Zheng, C. W. Domier, N.C. Luhmann, Jr., "Quasi-Optical E-Band MEMs Switching Arrays," *IEEE Microwave Symposium*, Seattle, U

7. Dimitrios Peroulis and Linda P. B. Katehi, "Electrostatically-Tunable Analog RF MEMS Varactors with Measured Capacitance Range of 300%," IEEE MTT-S Digest, pp. 1793-1796, 2003.

8. Dimitrios Peroulis, Yumin Lu and Linda P. B. Katehi, "Highly Reliable Analog RF MEMS Varactors ," IEEE MTT-S Digest, pp. 869-872, 2004.

4.1.3 Field Emitter and Carbon Nanotube Arrays

Field emitter arrays (FEAs) are widely investigated because of their high current density capability, ease of fabrication and their inherent nonthermal tunneling emission. At the University of California, in a class-100 cleanroom, MURI student Kendrick Liu has successfully

fabricated optically sensitive gated silicon FEAs. Figure 52 below shows an SEM view of a typical emitter tip with a radius of ≅ 15 nm. Such photo sensitive FEAs could have potential applications in RF guns, microwave electronics, image tubes and others. In the microwave area, this offers the promise of high frequency, optically pre-bunched devices resulting in light-weight, extremely short devices (see Fig. 53).

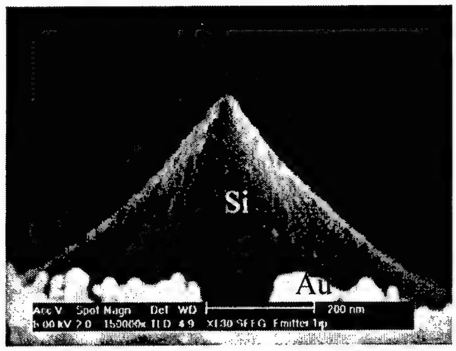

Fig. 4.1.53. SI FEA fabricated at UC Davis

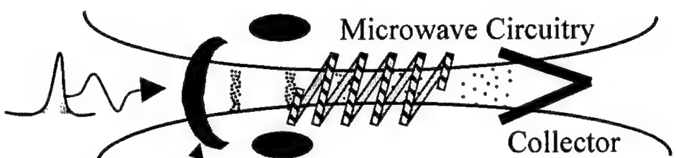

Fig. 4.1.54. Schematic of photo-enhanced FEA for use in prebunched TWTs.

Kendrick has made tremendous improvements in the microfabrication process resulting in reduced leakage currents to the gate that, in turn, allows field emission from p-type Si FEA to occur without interference from current heating and dielectric breakdowns. Furthermore, the devices fabricated by the improved process are operable after merely baking in vacuum, without having to burn any shorts between the gate electrode and the substrate. The field emission and photo-enhanced field emission data from such a device are shown in figures 54 and 55 under various levels of optical illumination. Figure 54 shows the total current (dark current plus photo-current) versus the applied gate voltage. Figure 55 shows the same set of data in the form of the Fowler-Nordheim plots (logarithm of the total current versus inversed gate voltage). Without contaminations on the surface and thermal effects, the field emission region at low fields and the saturation region at high fields are clearly evident.

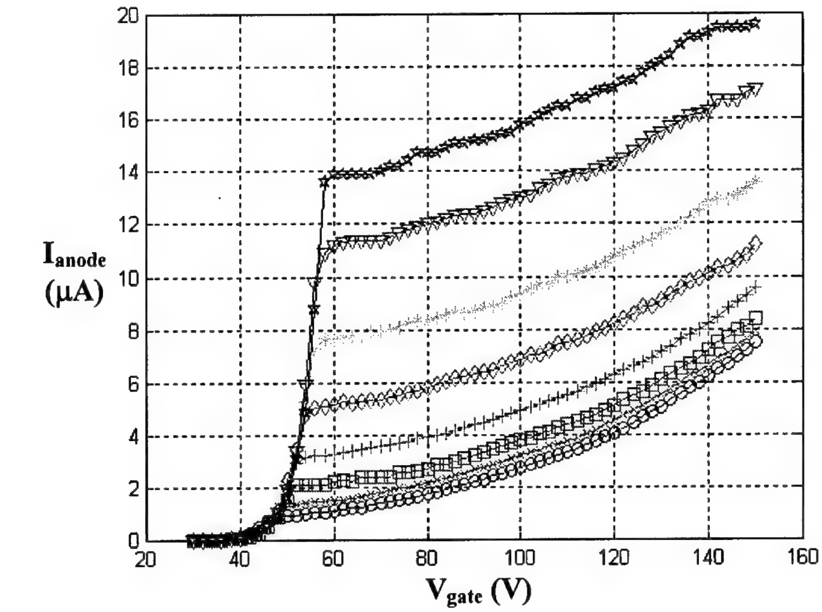

Fig. 4.1.55. Current-voltage plots of anode currents with increasing optical powers. ○ ***dark current;*** × ***0.06 relative optical power;*** □ ***0.11; + 0.22;*** ◊ ***0.33;*** ∗ ***0.56;*** ▽ ***0.78;*** □ 1.00.

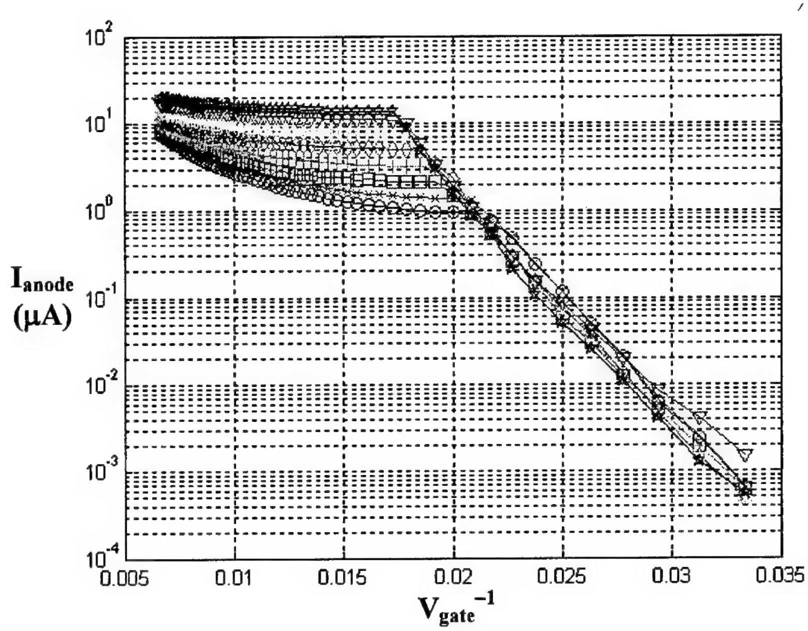

Fig.4.1.56. Fowler-Nordheim plots of anode currents with increasing optical powers. ○ ***dark current;*** × ***0.06 relative optical power;*** □ ***0.11; + 0.22;*** ◊ ***0.33;*** ∗ ***0.56;*** ▽ ***0.78;*** □ 1.00.

Kendrick has also demonstrated field emission of up to 0.5 mA from a 1mm-by-1mm active area (50-by-50 emitters) device, thereby showing attractive scalability for MVED applications. In addition, up to 80% quantum efficiency has been recorded from a CW optical excitation at 800nm wavelength. Optical pulse modulation has been observed using excitation by a Q-switched Nd:YAG laser (1064 nm wavelength, 10 ns pulsewidth at 2kHz repetition). The configuration is shown below in Fig. 55. The resultant anode current pulse profile is displayed in Fig. 56 and reveals further areas for improvements in our FEA devices. Specifically, the two distinct slopes on the rise are indicative of contributions from fast drift electrons and slow diffusion electrons. For faster response, we would need to increase the contributions from the drift electrons by increasing the depletion region thickness. This could be done be using high resistive silicon substrates. The fall time was a result of the RC time constant. For improvement, we needed to decrease the series resistance of our device. This could be achieved by optimizing the bottom substrate conductivity and the electrical contacts.

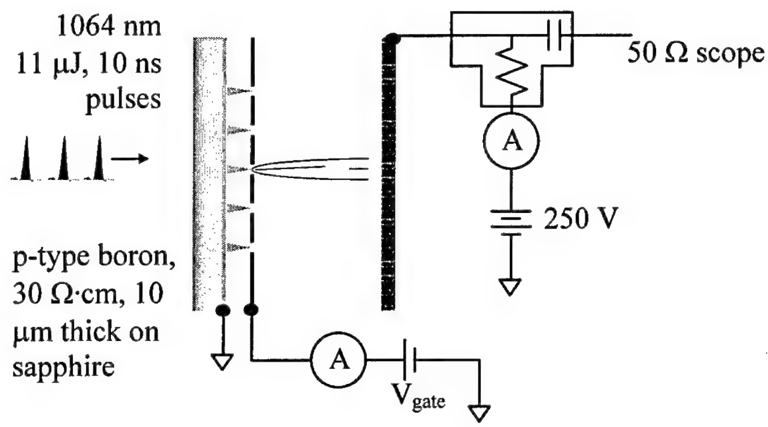

Fig. 4.1.57. Experimental arrangement for the study of photo-enhanced field emitter arrays.

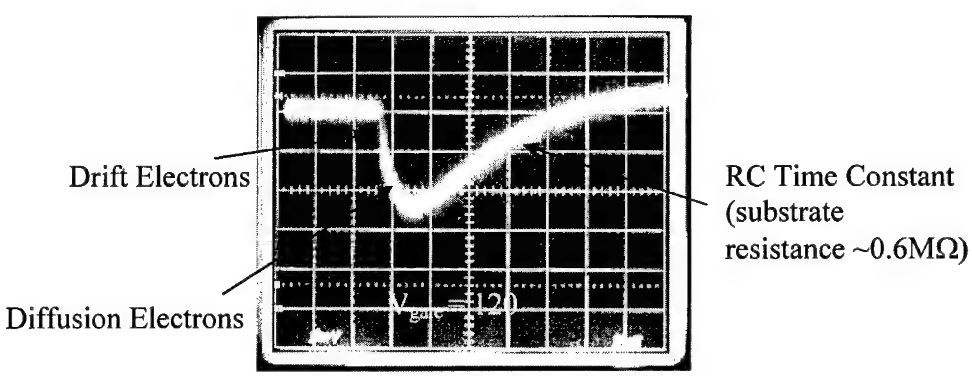

Fig. 4.1.58 Optically excited anode current pulse profile.

Finally, Kendrick, in collaboration with LLNL researchers has been fabricating carbon nanotube cathodes. Figure 57 below contains an SEM of some of their cNTs fabricated on semi-intrinsic Si substrates. These are extremely attractive due to their potential for stable emission and long life.

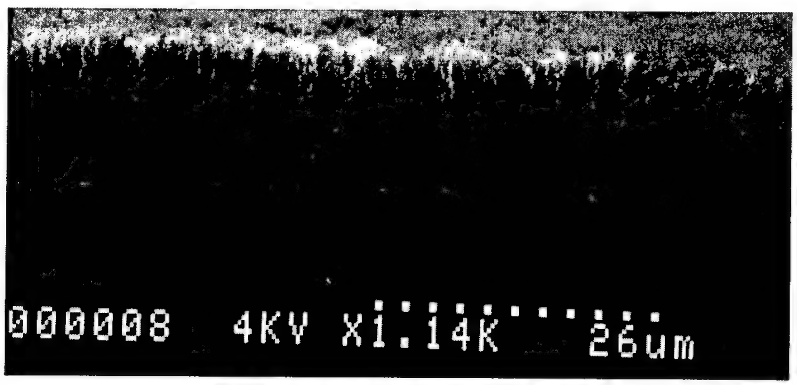

Fig. 4.1.59 cNTs fabricated on semi-intrinsic Si substrates.

To summarize: In our efforts to develop an efficient photocathode based on photo-enhanced field emission, we have made significant contribution to the field of vacuum nano-electronics. We have improved on the microfabrication process to repeatedly produce functional and low-leakage current gated devices. An anode-to-gate current ratio has been increased to about 1800 by dramatic reduction in the gate current. Our results have been consistently demonstrated without having to "burn in" the device. We have also explored other possibilities to reduce field emission fluctuations and increase the lifetime and emission currents, such as, incorporating carbon nanotubes. Field emission characterization of *p*-type silicon field emitter arrays has revealed the onset of a clearly defined saturation region in the Fowler-Nordheim plots previously partially masked by heating from large gate currents. This feature is consistent with a reported model in which an insufficient supply of electrons allows field penetration into the *p*-type material forming a depletion layer at the surface. In the saturation region, the emission current is limited by the generation of electrons relatively independent of the applied field. Optical excitation in this region results in photo-enhanced field emission currents, also evident in the Fowler-Nordheim plots. Up to 80% quantum yield has been obtained. Pulsed optical excitation has also revealed two distinct features in the rise of the emission current pulse: We attribute the fast rise to drift electrons and the slower rise to diffusion electrons. Findings gathered from the experiments have helped us to propose an optimized ultra-fast device: a near-intrinsic silicon device with about 10 μm of depletion layer. This device has potential to have a rise time of about

100 ps and a quantum yield of over 60% at 600-nm excitation wavelength. We have reported our findings in conferences and journal publications. This work will continue under a newly established MURI Consortium on the NanoPhysics of Electron Dynamics near Surfaces in High Power Microwave Devices and Systems.

4.1.4 Graduate Students Supported by MURI

Student	Type and Date of Degree	Dissertation Title	Status
Liang, Cheng	Ph.D. September 2001	"Novel Microwave and Millimeter-Wave Technologies & Applications"	Harris Co.
Steven Rosenau	Ph.D. September 2001	Quasi-Optical Overmoded Waveguide Frequency Multiplier Grid Arrays	Engineer, Agilent Research Lab
Lisa Laurent**	Ph.D. June 2002	High Gradient RF Breakdown Studies	Engineer, Stanford Linear Accelerator Center
Liqun Song**	Ph.D. September 2002	W-Band LiGA Fabricated Klystron	Engineer, Calabazas Creek Research, Inc.
Chia-Chan Chang	Ph.D. December2003	Microwave and Millimeter Wave Beam Steering/Shaping Phased Antenna Arrays and Related Applications	Professor ???
Anthony Troha	Ph.D. June 2003	The Chirped-Pulse Inverse Free-Electron Laser: A Novel, High-Gradient, Vacuum-Based Electron Accelerator	
Heather Song	Ph.D. Expected September 2004	W-Band Heavily Loaded TE01 Gyro-TWT	UCD Grad Student
Kendrick Liu	Ph.D. Expected December 2004	Photo-Assisted Field Emission of Gated Silicon Field Emitter Arrays (FEA's)	UCD Grad Student
Stephen Harriet*	Advanced to Candidacy March 2003	Harmonic Cusp Gun Gyrotron Traveling Wave Tube Amplifiers	Engineer, Naval Surface Warfare Center, Crane
Lawrence Dressman*	Ph.D. In Progress	Harmonic Peniotron Oscillators with Axis-Encircling Electron Beams	Engineer, Naval Surface Warfare Center, Crane
Yaping Liang	Ph.D. In Progress	MEMS Based Delay Lines for Millimeter Wave Phased Antenna Arrays	UCD Grad Student
Hsin-Lu Hsu	Ph.D. In Progress	Ka-band Micro-Fabricated TunneLadder TWT.	UCD Grad Student
Jae Seung Lee	Ph.D. In	Phase Noise Reduction in TWT for	UCD Grad

	Progress	Radar Applications	Student
Weiying Li	M.S. September 2000	Computer Automated High Power Millimeter Wave Test Systems for Quasi-Optics and Vacuum Electronics Research	Engineer, Motorola
Ronald Stutzman	M.S.	High Harmonic Cusp Gun W-Band Gyrotron	Engineer, Teledyne
Peter Marandos	M.S.	Eighth Harmonic Cusp Gun Gyrotron	Grad Student

* Supported by Naval Surface Warfare Center, Crane

** Stanford Research Mentors

4.1.5 Publications

PUBLICATION LIST: May 1, 1999- April 30, 2004

Books/Chapters

1. "Modern Microwave and Millimeter-Wave Power Electronics," Edited by Barker, R.J., Luhmann, N.C., Jr., Booske, J., and Nusinovich, G.S., to be published in **IEEE Press**. (In preparation)

2. Granatstein, V.L., Nusinovich, G.S., Blank, M., Felch, K.L., Gilgenbach, R., Guo, H., Jory, H., Luhmann, N.C., Jr., McDermott, D.B., Rodgers, J.M., Spencer, T.A., "Gyrotron Oscillators and Amplifiers," *High-Power Microwave Sources and Technologies,* edited by Robert J. Barker, Edl Schamiloglu, IEEE Press, ISBN 0-7803-6006-0, 2001

Journals

3. G. S. Nusinovich, O. V. Sinitsyn, J. Rodgers, T. M. Antonsen, Jr., V. L. Granatstein, and N. C. Luhmann, Jr., "Comparison of multistage gyroamplifiers operating in the frequency-multiplication regime with gyroamplifiers operating at a given cyclotron harmonic", IEEE Trans. Plasma Sci., Special Issue on high-power microwave generation, vol. 32, June 2004 (to be published).

4. W. C. Tsai, T. H. Chang, N. C. Chen, and K. R. Chu, H. H. Song and N. C. Luhmann, Jr. "Absolute Instabilities in a High-Order-Mode Gyrotron Traveling-Wave Amplifier," accepted for publication in *Physical Review E* , 2004.

5. H. H. Song, D. B. McDermott, Y. Hirata, L. R. Barnett, C. W. Domier, H. L. Hsu, T. H. Chang, W. C. Tsai, K. R. Chu, and N. C. Luhmann, Jr., Theory and Experiment of a 94 GHz Gyrotron Traveling-Wave Amplifier", Phys. Plasmas, vol. **11**, pp. 2935-2941, 2004

6. Harriet, S.B., McDermott, D.B., Gallagher, D.A., Luhmann, N.C., Jr., "Cusp Gun TE_{21} Second-Harmonic Gyro-TWT Amplifier," *IEEE Transaction on Plasma Science, Special Issue on High Power Microwave Generation,* **30,** No. 3, Pg. 909-914, June 2002

7. McDermott, D.B., Song, H.H., Hirata Y., Lin, A.T., Chang, T.H., Hsu, H.L., Chu, K.R., and Luhmann, Jr., N.C., "Design of a W-Band TE_{01} Mode Gyrotron Traveling-Wave Amplifier with High Power and Broad-Band Capabilities,'' *IEEE Transaction on Plasma Science, Special Issue on High Power Microwave Generation*, **30,** No. 3, Pg. 894-902**,** June 2002

8. Gibson, D.J., Hartemann, F.V., Landahl, E.C., Troha, A.L., Luhmann, N.C., Jr,. LeSage, G.P., Ho, C.H., "Electron Beam and RF Characterization of a Low-Emittance X-Band Photoinjector," *Physical Review Special Topics – Accelerators and Beams*, Vol. **4**, 9, 090101 September (2001)

9. Q. S. Wang, H. E. Huey, D. B. McDermott, Y. Hirata and N. C. Luhmann, Jr., "Design of a W-Band Second-Harmonic Gyro-TWT Amplifier," *IEEE Trans. on Plasma Science*, vol. **28**, no. 6, pp. 2232-2237, 2001.

10. S.A. Rosenau, C. Liang, W-K, Zhang, W-Y. Li, C.W. Domier, N.C. Luhmann, Jr., "Advances in Quasi-Optical Grid Array Technology for Millimeter-Wave Imaging Diagnostics," *Review of Scientific Instruments,* Part II, Vol. **72,** No. 1, pp. 371-374, January, 2001

11. McDermott, D.B., Hirata, Y., Dressman, L.J., Gallagher, D.A, Luhmann, N.C., Jr., "Efficient Ka-Band Second-Harmonic Slotted Peniotron," *IEEE Trans. on Plasma Science*, **28**, No. 3, pg. 953-958, June 2000.

12. Wang, Q.S., Huey, H.E., McDermott, D.B., Hirata, Y., Luhmann, N.C., Jr., "Design of a W-Band Second-Harmonic TE_{02} Gyro-TWT Amplifier," *IEEE Transactions on Plasma Science*, **28** No. 6, pg. 2232-2237, December 2000.

13. F.V. Hartemann, E.C. Landahl, D.J. Gibson, A.L. Troha, J.R. Van Meter, J.P. Heritage, H.A. Baldis, N.C. Luhmann, Jr., C.H. Ho, T.T. Yang, M.J. Horny, J.Y. Hwang, W.K. Lau, M.S. Yeh, "RF Characterization of a Tunable, High-Gradient, X-Band Photoinjector," *IEEE Transactions of Plasma Science, High Power Microwave Special Issue*, June 2000.

14. D.B. McDermott, Y. Hirata, L.J. Dressman, D.A. Gallagher and N.C. Luhmann, Jr., "Efficient Ka-Band Second-Harmonic Slotted Peniotron," *IEEE Trans. on Plasma Science*, vol. **28**, no. 3, p. 953-958, 2000.

Proceedings

15. W. C. Tsai, T. H. Chang, N. C. Chen, and K. R. Chu, H. H. Song and N. C. Luhmann, Jr. "Absolute Instabilities in a High-Order-Mode Gyrotron Traveling-Wave Amplifier," *29^{th} Int. Conf. on Infrared and Millimeter Waves*, Karlsruhe, Germany Sept. 27- Oct. 1, 2004.

16. Song, H.H., Barnett, L.R., McDermott, D.B., Hirata, Y., Hsu, H.L., Marandos, P.L., Lee, J.S., Chang, T.H., Chu, K.R., Luhmann, N.C., Jr., "High Power W-Band Gyrotron Traveling Wave Amplifier,'' *Infrared and Millimeter Wave Conference*, Sept. 29- Oct. 3, 2003, Shiga, Japan.

17. Dressman, L.J., McDermott, D.B., Hirata, Y., Gallagher, D.A., Spencer, T.A., Luhmann, N.C., Jr., "Cusp Gun Driven 34 GHz Peniotron," *Infrared and Millimeter Wave Conference*, Sept. 29-Oct. 3, 2003, Shiga, Japan.

18. Song,H.H., McDermott, D.B., Hirata, Y., Barnett, L.R., Domier, C.W., Hsu, H.L., Chang, T.H., Tsai, W.C., Chu, K.R., Luhmann, N.C., Jr., "Theory and Experiment of a 95 GHz Gyrotron Traveling Wave Amplifier," *Infrared and Millimeter Wave Conference*, Sept. 29- Oct. 3, 2003, Shiga, Japan. **(Invited)**

19. Harriet, S.B., McDermott, D.B., Luhmann, N.C., Jr., "Cusp Gun Ka-Band Second-Harmonic TE_{21} Gyro-TWT Amplifier," ," *Proceedings of the 5^{th} IEEE International Vacuum Electronics Conference, IVEC 2004*, pg. 192-193, April 2004.

20. Dressman, L.J., McDermott, D.B., Hirata, Y., Luhmann, N.C., Jr., Gallagher, D.A., Spencer, T.A., "Cusp Gun Driven Peniotron," *Proceedings of the 5th IEEE International Vacuum Electronics Conference, IVEC 2004*, pg. 240-241, April 2004

21. Lee, Jae Seung, Luhmann, N.C., Jr., Yehuda, G., "Phase Noise Reduction Techniques of Radar's TWTA," *Proceedings of the 5th IEEE International Vacuum Electronics Conference, IVEC 2004*, pg. 110-111, April 2004.

22. Lee, Jae Seung, Lally, P., Goren, Y., Luhmann, N.C., Jr., "TWT Phase Noise Reduction Techniques," *Proceedings of 2004 IEEE MTT-S Digest*, May 2004.

23. C.C. Chang, C.W. Domier, N.C. Luhmann, Jr., H. Park and T. Munsat, "A Millimeter Wave Beam Shaping Phased Antenna Array Proposed for Imaging Reflectometry", *ICOPS 2003, Proceedings of the 30th IEEE International Conference on Plasma Science,* June 2-5, 2003, pg. 238, Jeju, Korea.

24. Harriett, S.B., McDermott, D.B., Luhmann, N.C., Jr., "Investigation of a Smooth Bore Harmonic Cusp Gun Gyro-TWT,'' *Proceedings of the 4th IEEE International Vacuum Electronics Conference (IVEC)*, Seoul, Korea, May 28-30, 2003, pg. 170-171.

25. Song. H.H., Barnett, L.R., McDermott, D.B., Hirata, Y., Hsu, H.L., Marandos, P.S., Lee, J.S., Chang, T.H., Chu, K.R., Luhmann, N.C., Jr., "W-Band Heavily Loaded TE_{01} Gyrotron Traveling Wave Amplifier, *Proceedings of the 4th IEEE International Vacuum Electronics Conference (IVEC)*, Seoul, Korea, May 28-30, 2003, pg. 348-349. **(Invited)**

26. Dressman, L.J., McDermott, D.B., Luhmann, N.C., Jr., Gallagher D.A., Spencer, T.A., "Simulation and Modeling of a 34 GHz Cusp Gun Driven Peniotron,'' *Proceedings of the 4th IEEE International Vacuum Electronics Conference (IVEC)*, Seoul, Korea, May 28-30, 2003, pg.

27. Song, L., Luhmann, N.C., Jr., Scheitrum,G., Arfin, B., "Three-Dimensional Design of the Coupling Slot for a W-Band Output Structure," *Proceedings of the 27th Int. Conference on Infrared and Millimeter Waves*, San Diego, CA, Sept. 22-26, 2002, pg. 351-352.

28. McDermott, D.B., Song, H.H., Barnett, L.R., Hirata, Y., Lin, A.T., Hsu, H.L., Marandos, P.S., Lee, J.S., Chang, T.H., Chu, K.R., Luhmann, N.C., Jr., "High Power Broadband W-Band Gyrotron Traveling Wave Amplifier," *Proceedings of the 27th Int. Conference on Infrared and Millimeter Waves*, San Diego, CA, Sept. 22-26, 2002, pg. 201-202.

29. Dressman, L.J., McDermott, D.B., Hirata, Y., Luhmann, N.C., Jr., "Highly Efficient 34 GHz Peniotron," *Proceedings of the 27th Int. Conference on Infrared and Millimeter Waves*, San Diego, CA, Sept. 22-26, 2002, pg. 139-140.

30. Harriet, S.B., McDermott, D.B., Luhmann, N.C. Jr., "Cusp Gun TE_{21} Second Harmonic Gyro-TWT Amplifier," *The 27th IEEE International Conference on Infrared and Millimeter Waves,* San Diego, California, USA, September 22-26, 2002.

31. Cheng, C.-C., Liang, C., Deng, B., Domier, C.W., Luhmann, Jr., N.C., "A Beam-Shaping Phased Antenna Array Based on True-Time Delay Technologies," *The 27th IEEE International Conference on Infrared and Millimeter Waves,* San Diego, California, September 22 - 26, 2002

32. McDermott, D.B., Song, H.H., Hirata, Y., Lin, A.T., Chang, T.H., Hsu, H.L., Marandos, P.S., Lee, L.S., Chu, K.R., Luhmann, N.C., Jr., "High Power W-Band Heavily Loaded TE_{01} Gyro-TWT," *Proceedings of the 3rd International Vacuum Electronics Conference*, Monterey, CA April 23-25, 2002, pg 369-370.

33. Rosenau, S.A., Liang, Y., Liang, C., Zhang, W-K, Domier, C.W., Luhmann, N.C., Jr., "High Efficiency Frequency Multiplier Grid Arrays for Watt-Level Millimeter Wave Sources," *Proceedings of the 3rd International Vacuum Electronics Conference*, Monterey, CA April 23-25, 2002, pg 202-203.

34. Dressman, L.J., McDermott, D.B., Luhmann, N.C., Jr., Gallagher, D.A., Spencer, T.A., "Ka-Band Fundamental-Mode Peniotron with High Device Efficiency," *Proceedings of the 3rd International Vacuum Electronics Conference*, Monterey, CA April 23-25, 2002, pg 194-195.

35. Harriet, S.B., McDermott, D.B., Luhmann, N.C., Jr., "TE_{21} Second-Harmonic Gyro-TWT Amplifier with an Axis-Encircling Beam," *Proceedings of the 3rd International Vacuum Electronics Conference*, Monterey, CA April 23-25, 2002, pg 121-122.

36. C.C. Chang, C. Liang, B.H. Deng, C.W. Domier, N.C. Luhmann, Jr., "A Beam-Shaping Phased Antenna Array Based on True-Time Delay Technologies," *27th International Conference on Infrared and Millimeter Waves Conference Digest*, San Diego, CA, September 22-26, 2002, Paper MP17, pp. 99-100 (2002).

37. Harriet, S.B., McDermott, D.B., Luhmann, N.C., Jr., "Cusp Gun TE_{21} Second-Harmonic Gyro-TWT Amplifier," *Proceedings of the 27th Int. Conference on Infrared and Millimeter Waves*, San Diego, CA, Sept. 22

38. Chang, C.C., Liang, C., Deng, B., Domier, C.W., Luhmann, N.C., Jr., Park, H. and Munsat, T. "A Millimeter Wave Beam Shaping Phased Antenna Array," **Invited paper**, *Proceedings 3rd International Conference on Microwave and Millimeter Wave Technologys*, pp.11-16, Beijing, China, 17-19 August 2002

39. .S.B. Harriet, D.B. McDermott, and N.C. Luhmann, Jr., "Ka-Band Second-Harmonic Cusp-Gun Gyro-TWT Amplifier," *Digest of 2nd Int. Vacuum Electronics Conference*, 2001.

40. D.B. McDermott, H. Song, Y. Hirata, A.T. Lin, T.H. Chang, K.R. Chu, and N.C. Luhmann, Jr., "140 kW, 94 GHz Heavily Loaded TE_{01} Gyro-TWT," *Digest of 2nd Int. Vacuum Electronics Conference*, 2001.

41. L.J. Dressman, D.B. McDermott, D.A. Gallagher, T.A. Spencer and N.C. Luhmann, Jr., "High Efficiency 34 GHz Second-Harmonic Slotted Peniotron ," *Digest of 2nd Int. Vacuum Electronics Conference*, 2001.

42. R.C. Stutzman, D.B. McDermott, D.A. Gallagher, T.A. Spencer and N.C. Luhmann, Jr., "W-Band Sixth-Harmonic Slotted Cusp-Gun Gyrotron ," *Digest of 2nd Int. Vacuum Electronics Conference*, 2001

43. Hartemann, F.V., Gibson, D.J., Troha, A.L., "Coherent Synchrotron Radiation in an X-Band Photoinjector, *Proceedings of the 2001 Particle Accelerator Conference,* Chicago, 2001.

44. Hartemann, F.V., Rupp, B., Baldis, H.A., Gibson, D.J., Kerman, A.K., Le Foll, A., "Three-Dimensional Theory of Emittance in Compton Scattering and X-Ray Protein Crystallography," *Proceedings of the 2001 Particle Accelerator Conference*, Chicago, 2001.

45. S.B. Harriet, D.B. McDermott, N.C. Luhmann Jr., "Second-Harmonic Axis-Encircling-Beam TE21 Gyro-TWT Amplifier," *Digest of 28th IEEE Int. Conference on Plasma Science*, p. 513, 2001.

46. L. J. Dressman, D.B. McDermott, D. A. Gallagher, T. A. Spencer and N.C. Luhmann, Jr., "Highly Efficient Second-Harmonic Peniotron with Fundamental Mode Interaction" **Invited Talk** *The 26th IEEE International Conference on Infrared and Millimeter Waves*, Toulouse, France, 11-14 September 2001.

47. S. B. Harriet, D.B. McDermott and N.C. Luhmann, Jr., "30 GHz Cusp Gun Second-Harmonic TE_{21} Gyro-TWT Amplifier" *The 26th IEEE International Conference on Infrared and Millimeter Waves*, Toulouse, France, 11-14 September 2001.

48. D.B McDermott, H. H. Song, Y. Hirata, A. T. Lin, T. H. Chang, H. L. Hsu, K. R. Chu, and N. C. Luhmann, Jr., "Heavily Loaded W-band TE_{01} Gyro-TWT" *The 26th IEEE International Conference on Infrared and Millimeter Waves*, Toulouse, France, 11-14 September 2001.

49. R.C. Stutzman, P.S. Marandos, D.B. McDermott, D.A. Gallagher, T.A. Spencer and N.C. Luhmann, Jr., "Sixth-Harmonic W-Band Slotted Gyrotron," *The 26th IEEE International Conference on Infrared and Millimeter Waves*, Toulouse, France, 11-14 September 2001.

50. Hartemann, F.V., Rupp, B., Baldis, H.A., Gibson, D.J., Kerman, A.K., Le Foll, A., "Three-Dimensional Theory of Emittance in Compton Scattering and X-Ray Protein Crystallography," *Proceedings of Applications on Intense Lasers, 2000.*

51. L.J. Dressman, D.B. McDermott, Y. Hirata, D.A. Gallagher, T.A. Spencer and N.C. Luhmann, Jr., "Slotted Ka-Band Second-Harmonic Peniotron with Axis-Encircling Electrons," *Digest of 25th Int. Conference on Infrared and Millimeter Waves,* 2000.

52. R.C. Stutzman, D.B. McDermott, Y. Hirata, D.A. Gallagher, T.A. Spencer and N.C. Luhmann, Jr., "Slotted W-Band Sixth-Harmonic Gyrotron with Axis-Encircling Electrons," *Digest of 25th Int. Conference on Infrared and Millimeter Waves,* 2000.

53. Y. Hirata, D.B. McDermott, A.T. Lin, T.H. Chang, K.R. Chu, and N.C. Luhmann, Jr., "W-Band TE01 Gyro-TWT with Heavy Wall Loss," *Digest of 25th Int. Conference on Infrared and Millimeter Waves,* 2000.

54. S.B. Harriet, D.B. McDermott, Y. Hirata and N.C. Luhmann, Jr., "Second-Harmonic Ka-Band Gyro-TWT with Axis-Encircling Electrons," *Digest of 25th Int. Conference on Infrared and Millimeter Waves,* 2000.

55. S.A. Rosenau, C. Liang, W-Y. Li, W-K. Zhang, C.W. Domier, N. C. Luhmann, Jr., "Frequency Multiplier Grid Arrays for Satellite Applications," *2000 25th International Conference on Infrared and Millimeter Waves Conference Digest,* pp. 407-408, Beijing, China, 12-15 September, 2000.

56. W.Y. Li, S.A. Rosenau, C.W. Domier, N.C. Luhmann, Jr., "Automated Test System for Quasi-Optical Frequency Multiplier Grid Array Research," *2000 2nd International Conference on Microwave and Millimeter Wave Technology Proceedings,* pp. 646-649, Beijing, China, 14-16 September, 2000.

57. L.J. Dressman, D.B. McDermott, Y. Hirata, D.A. Gallagher, T.A. Spencer and N.C. Luhmann, Jr., "Slotted Ka-Band Second-Harmonic Peniotron with Axis-Encircling Electrons," *25th Int. Conference on Infrared and Millimeter Waves*, Beijing, China, 2000.

58. R.C. Stutzman, D.B. McDermott, Y. Hirata, D.A. Gallagher, T.A. Spencer and N.C. Luhmann, Jr., "Slotted W-Band Sixth-Harmonic Gyrotron with Axis-Encircling Electrons," *25th Int. Conference on Infrared and Millimeter Waves*, Beijing, China, 2000.

59. Y. Hirata, D.B. McDermott, A.T. Lin, T.H. Chang, K.R. Chu, and N.C. Luhmann, Jr., "W-Band TE01 Gyro-TWT with Heavy Wall Loss," *25th Int. Conference on Infrared and Millimeter Waves,* Beijing, China, 2000.

60. S.B. Harriet, D.B. McDermott, Y. Hirata and N.C. Luhmann, Jr., "Second-Harmonic Ka-Band Gyro-TWT with Axis-Encircling Electrons," *25th Int. Conference on Infrared and Millimeter Waves*, Beijing, China, 2000.

61. S.A. Rosenau, C. Liang, W-Y. Li, W-K. Zhang, C.W. Domier, N. C. Luhmann, Jr., "Frequency Multiplier Grid Arrays for Satellite Applications", *25th International Conference on Infrared and Millimeter Waves*, Beijing, China, 12-15 September, 2000.

62. F.V. Hartemann, A. Le Foll, A.K. Kerman, B. Rupp, D.J. Gibson, E.C. Landahl, A.L. Troha, N.C. Luhmann, Jr., H.A. Baldis, "Three-Dimensional Theory of Emittance in Compton Scattering," *AIP Conference Proceedings, Proc. Advanced Accelerator Concepts*, June 2000.

63. R.C. Stutzman, D.B. McDermott, Y. Hirata, D.A. Gallagher, T.A. Spencer and N.C. Luhmann, Jr., "W-Band Sixth-Harmonic Slotted Gyrotron," *Digest of Int. Vacuum Electronics Conference*, paper P1.18, 2000.

64. L.J. Dressman, D.B. McDermott, Y. Hirata, D.A. Gallagher, T.A. Spencer and N.C. Luhmann, Jr., "Highly Efficient Ka-Band Second-Harmonic Slotted Peniotron ," *Digest of Int. Vacuum Electronics Conference*, paper P1.5, 2000.

65. Y. Hirata, D.B. McDermott, A.T. Lin, T.H. Chang, K.R. Chu, and N.C. Luhmann, Jr., "Design of a Heavily-Loaded W-Band TE01 Gyro-TWT," *Digest of Int. Vacuum Electronics Conference*, paper P1.4, 2000.

66. S.B. Harriet, D.B. McDermott, Y. Hirata, T.H. Chang, K.R. Chu, and N.C. Luhmann, Jr., "30 GHz Second-Harmonic Cusp-Gun Gyro-TWT Amplifier," *Digest of Int. Vacuum Electronics Conference,* paper P1.3, 2000.

67. L.R. Dressman, D.B. McDermott, Y. Hirata, D.A. Gallagher, and N.C. Luhmann, Jr., "High Efficiency Ka-Band Second-Harmonic Peniotron ," *Digest of 27th IEEE Int. Conference on Plasma Science*, p. 170, 2000.

68. R.C. Stutzman, D.B. McDermott, Y. Hirata, D.A. Gallagher, T.A. Spencer[2] and N.C. Luhmann, Jr., "94 GHz Sixth-Harmonic Slotted Gyrotron," *Digest of 27th IEEE Int. Conference on Plasma Science*, p. 171, 2000.

69. Y. Hirata, D.B. McDermott, A.T. Lin, T.H. Chang, K.R. Chu, and N.C. Luhmann, Jr., "Heavily-Loaded W-Band TE01 Gyro-TWT," *Digest of 27th IEEE Int. Conference on Plasma Science*, p. 171, 2000.

70. S.B. Harriet, D.B. McDermott, Y. Hirata, T.H. Chang, K.R. Chu, and N.C. Luhmann, Jr., "Ka-Band Second-Harmonic Cusp-Gun Gyro-TWT," *Digest of 27th IEEE Int. Conference on Plasma Science*, p. 170, 2000.

71. Steven A. Rosenau, Cheng Liang, Weikang Zhang, Bihe Deng, Weiying Li, Chia-Chan Chang, Pei-Ling Hsu, Richard P. Hsia, Fan Jiang, Calvin W. Domier, Neville C. Luhmann, Jr., "Millimeter-Wave Solid State Devices," *Electronic Proceedings of the Materials Research Society 2000 Spring Meeting*, Millimeter/Submillimeter-Wave Technology-Materials, Devices, and Diagnostics Symposium, Materials Components and Devices Session, San Francisco, California, 24-28 April 2000.

72. S.A. Rosenau, C. Liang, W-Y. Li, W-K. Zhang, C.W. Domier, Z-T. Chen, N.C. Luhmann, Jr., "Advances in High Power Millimeter Wave Grid Array Sources", *1st IEEE International Vacuum Electronics Conference*, Monterey, California, 2-4 May 2000, pp. 16.1.

73. D.B. McDermott, Y. Hirata, R.C. Stutzman, S.B. Harriet, C.K. Chong, D.A. Gallagher, C.M. Armstrong, T.A. Spencer and N.C. Luhmann, Jr., "Millimeter-Wave Harmonic Gyro-Devices," *Digest of Twenty-Fourth Int. Conf. on Infrared and Millimeter Waves*, paper PS-3, 1999.

74. D.B. McDermott, Y. Hirata, A.T. Lin, K.C. Leou and N.C. Luhmann, Jr., "100 kW, 94 GHz TE_{01} Gyro-TWT," *Digest of Twenty-Fourth Int. Conf. on Infrared and Millimeter Waves*, paper TH-E3, 1999.

75. C. Liang, S.A. Rosenau, W-K. Zhang, C.C. Chang, C.W. Domier, N.C. Luhmann, Jr., "New Millimeter Wave Array Technologies for Plasma Diagnostics," *9th International Symposium on Laser-Aided Plasma Diagnostics*, Lake Tahoe, California, 26 September - 1 October 1999.

Conferences

76. W. C. Tsai, T. H. Chang, N. C. Chen, and K. R. Chu, H. H. Song and N. C. Luhmann, Jr.," Study of Absolute Instabilities in the Gyrotron Traveling Wave Amplifier" *31st IEEE International Conference on Plasma Science*, June 28 – July 1, 2004, Baltimore, Maryland.

77. Lee, Jae Seung, Lally, P., Goren, Y., Luhmann, N.C., Jr., "TWT Phase Noise Reduction Techniques," Int. Microwave Symposium, Fort Worth, TX, June 6-11, 2004

78. L.J. Dressman, D.B. McDermott, Y. Hirata, D.A. Gallagher, T.A. Spencer, N.C. Luhmann, Jr., "Efficient 34 GHz Second-Harmonic Peniotron with Cusp-Gun Drive," to be presented at *29th Int. Conf. on Infrared and Millimeter Waves*, Karlsruhe, Germany Sept. 27- Oct. 1, 2004.

79. Harriet, S.B., McDermott, D.B., Luhmann, Jr., D.B., "Ka-Band Second-Harmonic Large-Orbit Axis-Encircling Beam Gyro-TWT Amplifier," ," to be presented at *29th Int. Conf. on Infrared and Millimeter Waves*, Karlsruhe, Germany Sept. 27- Oct. 1, 2004.

80. Harriet, S.B., McDermott, D.B., Luhmann, N.C., Jr., "Cusp Gun Ka-Band Second-Harmonic TE_{21} Gyro-TWT Amplifier," *5th IEEE International Vacuum Electronics Conference*, Monterey, CA April 27-29, 2004.

81. Lee, Jae Seung, Goren, Yehuda, Luhmann, N.C., Jr., ''Phase Noise Technique for Pulsed TWT,'' *The 5th International IVEC Conference,* April 2004, Monterey, California.

82. Dressman, L.J., McDermott, D.B., Hirata, Y., Luhmann, N.C., Jr., Gallagher, D.A., Spencer, T.A., "Cusp Gun Driven Peniotron," *5th IEEE International Vacuum Electronics Conference*, Monterey, CA April 27-29, 2004.

83. Dressman, L.J., McDermott, D.B., Hirata, Y., Gallagher, D.A., Spencer, T.A., Luhmann, N.C., Jr., "34 GHz Cusp Gun Driven Peniotron," *31st IEEE International Conference on Plasma Science*, June 28 – July 1, 2004, Baltimore, Maryland.

84. Harriet, S.B., McDermott, D.B., Gallagher, D.A., Luhmann, Jr., N.C., "TE_{21} Second-Harmonic Gyro-TWT Amplifier with an Axis-Encircling Beam," *31st IEEE International Conference on Plasma Science*, June 28 – July 1, 2004, Baltimore, Maryland.

85. S.B. Harriet, D.B. McDermott, D.A. Gallagher and N.C. Luhmann, Jr., "Ka-Band Second-Harmonic Cusp Gun Gyro-TWT Amplifier", *ICOPS 2003, Proceedings of the 30th IEEE International Conference on Plasma Science*, June 2-5, 2003, pg. 169, Jeju, Korea.

86. L.J. Dressman, D.B. McDermott, Y. Hirata, D.A. Gallagher, T.A. Spencer, and N.C. Luhmann, Jr., "Cusp Gun Driven 34 GHz Peniotron", *ICOPS 2003 Proceedings of the, 30th IEEE International Conference on Plasma Science*, June 2-5, 2003, pg. 170, Jeju, Korea.

87. Harriet, S.B., McDermott, D.B., Luhmann, N.C., Jr., TE_{21} Second-Harmonic Gyro-TWT Amplifier with an Axis-Encircling Beam," *The 28th International Conference on Infrared and Millimeter Wave Conf. Digest* Sept. 29- Oct. 3, 2003, Shiga, Japan.

88. Chang, C-C., Domier, C.W., Luhmann, N.C., Jr., Park, H., Munsat, T., "A Millimeter Wave Beam Shaping Phased Antenna Array for Imaging Reflectometry," *APS, 45th Annual Meeting of the Division of Plasma Physics*, Albuquerque, NM, October 27-31, 2003

89. H. H. Song, D. B. McDermott, Y. Hirata, L. R. Barnett, C. W. Domier, H. L. Hsu, T. H. Chang, W. C. Tsai, K. R. Chu, and N. C. Luhmann, Jr., "W-Band Heavily Loaded TE_{01} Gyro-TWT", *The American Physical Society 45th Annual Meeting of Division of Plasma Physics,* Albuquerque, New Mexico, USA, 27–31 October 2003

90. H.H. Song, D.B. McDermott, Y. Hirata, L.R. Barnett, C.W. Domier, H.L. Hsu, T. H. Chang, W.C. Tsai, K.R. Chu and N.C. Luhmann, Jr., "Theory and Experiment of a Heavily Loaded 94 GHz Gyrotron Traveling-Wave Amplifier," *The American Physical Society 45th Annual Meeting of Division of Plasma Physics,* Albuquerque, New Mexico, USA, 27–31 October 2003 **(Invited)**

91. Luhmann, N.C., Jr., "Recent Advances from the DoD Multidisciplinary University Research Initiative Consortium on Innovative Vacuum Electronics," *RF 2003*, Berkeley Springs, W. Virgina, June 22-26, 2003. **(Invited)**

92. McDermott, D.B., Song, H.H., Barnett, L.R., Hirata, Y., Hsu, T.H., Marandos, P.S., Lee, J.S., Chang, T.H., Chu, K.R., Luhmann, Jr., N.C., "A Heavily Loaded W-band TE_{01} Gyro-TWT with High Power and Broadband Capabilities," *44th Annual Meeting of the Division of Plasma Physics*, Orlando, Florida, November 11-15, 2002.

93. Dressman, L.J., McDermott, D.B., Hirata, Y., Luhmann, Jr., N.C., Gallagher, D.A., Spencer, T.A., "34 GHz Highly Efficient Peniotron with an Axis-Encircling Beam," *44th Annual Meeting of the Division of Plasma Physics*, Orlando, Florida, November 11-15, 2002.

94. Harriet, S.B., McDermott, D.B., Luhmann, Jr., N.C., Gallagher, D.A., "Ka Band TE_{21} Second-Harmonic Gyro-TWT Amplifier with a Cusp Gun," *44th Annual Meeting of the Division of Plasma Physics*, Orlando, Florida, November 11-15, 2002.

95. L. J. Dressman, D.B. McDermott, N.C. Luhmann, Jr., D. A. Gallagher and T. A. Spencer, "34 GHz Fundamental-Mode Peniotron for High Device Efficiency" *The 29th IEEE International Conference on Plasma Science*, Banff, Alberta, Canada, 26-30 May 2002.

96. S. B. Harriet, D.B. McDermott and N.C. Luhmann, Jr., "30 GHz Second-Harmonic TE_{21} Cusp-Gun Gyro-TWT Amplifier" *The 29th IEEE International Conference on Plasma Science*, Banff, Alberta, Canada, 26-30 May 2002.

97. D.B. McDermott, H.H. Song, Y. Hirata, A.T. Lin, T.H. Chang, H.L. Hsu, K.R. Chu, and N.C. Luhmann, Jr., "Design of a W-Band TE_{01} Gyro-TWT with High Power and Broadband Capabilities" *The 29th IEEE International Conference on Plasma Science*, Banff, Alberta, Canada, 26-30 May 2002.

98. D.B. McDermott, H.H. Song, Y. Hirata, A.T. Lin, T.H. Chang, K.R. Chu, and N.C. Luhmann, Jr., "94 GHz Heavily Loaded TE_{01} Gyro-TWT," *Digest of 28th IEEE Int. Conference on Plasma Science*, p. 515, 2001.

99. R.C. Stutzman, D.B. McDermott, D.A. Gallagher, T.A. Spencer and N.C. Luhmann, Jr., "94 GHz Sixth-Harmonic Slotted Gyrotron," *Digest of 28^{h} IEEE Int. Conference on Plasma Science*, p. 516, 2001.

100. L. J. Dressman, D.B. McDermott, N.C. Luhmann, Jr., D.A. Gallagher, and T.A. Spencer, "Second-Harmonic Fundamental Mode Slotted Peniotron," *Digest of 28th IEEE Int. Conference on Plasma Science*, p. 513, 2001.

101. L. J. Dressman, D.B. McDermott, N.C. Luhmann, Jr., D. A. Gallagher and T. A. Spencer, "Ka-Band Second-Harmonic Peniotron with Fundamental Mode Interaction" *The American Physical Society 43^{trd} Annual Meeting of Division of Plasma Physics,* Long Beach, California, USA, 29 October – 02 November 2001.

102. S. B. Harriet, D.B. McDermott and N.C. Luhmann, Jr., "Cusp Gun Second-Harmonic TE_{21} Gyro-TWT Amplifier" *The American Physical Society 43^{trd} Annual Meeting of Division of Plasma Physics,* Long Beach, California, USA, 29 October – 02 November 2001.

103. D.B McDermott, H. H. Song, Y. Hirata, A. T. Lin, T. H. Chang, H. L. Hsu, K. R. Chu, and N. C. Luhmann, Jr., "Stability of Heavily Loaded W-band TE_{01} Gyro-TWT" *The American Physical Society 43[trd] Annual Meeting of Division of Plasma Physics,* Long Beach, California, USA, 29 October – 02 November 2001.

104. P.S. Marandos, D.B. McDermott, D.A. Gallagher, T.A. Spencer and N.C. Luhmann, Jr., "Cusp Gun W-Band Sixth-Harmonic Slotted Gyrotron" *The American Physical Society 43[trd] Annual Meeting of Division of Plasma Physics,* Long Beach, California, USA, 29 October – 02 November 2001.

105. D.B. McDermott, H.H. Song, Y. Hirata, A.T. Lin, T.H. Chang, H.L. Hsu, K.R. Chu, and N.C. Luhmann, Jr., "Stability of Heavily-Loaded W-Band TE01 Gyro-TWT," *43[rd] Meeting of APS Div. Of Plasma Physics*, Long Beach, CA, 2001.

106. L.J. Dressman, D.B. McDermott, D.A. Gallagher, T.A. Spencer and N.C. Luhmann, Jr., "Ka-Band Second-Harmonic Peniotron with Fundamental Mode Interaction," *43[rd] Meeting of APS Div. Of Plasma Physics*, Long Beach, CA, 2001.

107. H.B. Harriet, D.B. McDermott and N.C. Luhmann, Jr., "Cusp Gun Second-Harmonic TE21 Gyro-TWT Amplifier,"*43[rd] Meeting of APS Div. Of Plasma Physics*, Long Beach, CA, 2001.

108. P.S. Marandos, D.B. McDermott, D.A. Gallagher, T.A. Spencer and N.C. Luhmann, Jr., "Cusp Gun W-Band Sixth-Harmonic Slotted Gyrotron," *43[rd] Meeting of APS Div. Of Plasma Physics*, Long Beach, CA, 2001.

109. F.V. Hartemann, D.J. Gibson, A.L. Troha, "Coherent Synchrotron Ratiation in an X-band Photoinjector," *2001 Particle Accelerator Conference*, Chicago, IL, June 18-22, 2001.

110. D.J. Gibson, F.V. Hartemann, E.C. Landahl, H.A. Baldis, C.H. Ho, A.L. Troha, N.C. Luhmann, Jr. "Electron Beam and RF Characterization of a High-Brightness X-band Photoinjector," *2001 Particle Accelerator Conference*, Chicago, IL, June 18-22, 2001.

111. F.V. Hartemann, B. Rupp, H.A. Baldis, D.J. Gibson, A.K. Kerman, A. Le Foll, "Three-Dimensional Theory of Compton Scattering and Advanced Biomedical Applications," *2001 Particle Accelerator Conference*, Chicago, IL, June 18-22, 2001.

112. Hartemann, F.V., Le Foll, A., Kerman, A. Rupp, B., Gibson, D., Troha, A., Luhmann, N.C., Jr., Baldis, A., "Three-Dimensional Theory of Emittance in Compton Scattering," *Bulletin of the American Physical Society*, September 2000.

113. L.J. Dressman, D.B. McDermott, Y. Hirata, D.A. Gallagher, T.A. Spencer and N.C. Luhmann, Jr., "Second-Harmonic Cusp-Gun Slotted Peniotron," *42[nd] Meeting of APS Div. Of Plasma Physics*, Quebec City, Canada, 2000.

114. R.C. Stutzman, D.B. McDermott, Y. Hirata, D.A.Gallagher, T.A. Spencer and N.C. Luhmann, Jr., "Cusp-Gun Sixth-Harmonic Slotted Gyrotron," *42[nd] Meeting of APS Div. Of Plasma Physics*, Quebec City, Canada, 2000.

115. D.B. McDermott, Y. Hirata, A.T. Lin, T.H. Chang, K.R. Chu, and N.C. Luhmann, Jr., "94 GHz Lossy TE01 Gyro-TWT," *42nd Meeting of APS Div. Of Plasma Physics*, Quebec City, Canada, 2000.

116. S.B. Harriet, D.B. McDermott, Y. Hirata, and N.C. Luhmann, Jr., "Second-Harmonic Cusp-Gun TE21 Gyro-TWT with Axis-Encircling Electrons," *42nd Meeting of APS Div. Of Plasma Physics,* Quebec City, Canada, 2000.

117. S.A. Rosenau, C. Liang, W-K. Zhang, W-Y. Li, C.W. Domier, N.C. Luhmann, Jr., "Advances in Quasi-Optical Grid Array Technology for Millimeter-Wave Plasma Imaging Diagnostics", *13th Topical Conference on High Temperature Plasma Diagnostics*, Tucson, Arizona, 18-22 June 2000, p. AP23.

118. L.J. Dressman, D.B. McDermott, Y. Hirata, D.A. Gallagher, T.A. Spencer and N.C. Luhmann, Jr., "Second-Harmonic Cusp-Gun Slotted Peniotron," *Bull. Am. Phys. Soc.*, vol. **45**, p. 136, 2000.

119. R.C. Stutzman, D.B. McDermott, Y. Hirata, D.A.Gallagher, T.A. Spencer and N.C. Luhmann, Jr., "Cusp-Gun Sixth-Harmonic Slotted Gyrotron," *Bull. Am. Phys. Soc.*, vol. **45**, p. 136, 2000.

120. D.B. McDermott, Y. Hirata, A.T. Lin, T.H. Chang, K.R. Chu, and N.C. Luhmann, Jr., "94 GHz Lossy TE01 Gyro-TWT," *Bull. Am. Phys. Soc.*, vol. 45, p. 136, 2000.

121. S.B. Harriet, D.B. McDermott, Y. Hirata, and N.C. Luhmann, Jr., "Second-Harmonic Cusp-Gun TE21 Gyro-TWT with Axis-Encircling Electrons," *Bull. Am. Phys. Soc.*, vol. **45**, p. 136, 2000.

122. S.A. Rosenau, C-C. Chang, C. Liang, W-K. Zhang, C.W. Domier, and N.C. Luhmann, Jr., "Advances in Millimeter-Wave Technology for Reflectometric Imaging," *Bull. Am. Phys. Soc.,* vol. **45**, p. 77, October 2000.

123. R.C. Stutzman, S.B. Harriet, D.B. McDermott, Y. Hirata, D.A. Gallagher, T.A. Spencer and N.C. Luhmann, Jr., 'Cusp-Gun Harmonic Gyro-Devices," *Bull. Am. Phys. Soc.*, vol. 44, p. 296, 1999.

124. D.B. McDermott, Y. Hirata, A.T. Lin, and N.C. Luhmann, Jr., "Heavily-Loaded 94GHz TE_{01} Gyro-TWT," *Bull. Am. Phys. Soc.*, vol. 44, p. 295, 1999.

4.2 Stanford University

G. Scheitrum, G. Caryotakis, A. Haase,
A. Burke, A. Jensen, K. Rauenbuehler
Stanford University

July 19, 2004

4.2.1 MURI Program Accomplishments

4.2.1.1 Modular Millimeter Wave Klystron Research

The W-band Klystrino program achieved several notable successes in the course of the development of a 100 kW peak, 1 kW average power, PPM focused, 95 GHz, RF source. The most important of these accomplishments was the development of lithographic (LIGA-based) fabrication methods for vacuum electronic devices. Without the 100 nm surface finish of the LIGA process, the circuit losses for the Klystrino would be unacceptable. LIGA and similar lithographic processes make it possible to produce multiple copies of a given circuit at the same time on a single substrate. This makes fabrication of millimeter wave circuits with micron tolerances relatively inexpensive. Figure 1 shows a 6 cm x 6 cm copper substrate with four Klystrino circuits. The substrate is two sided with duplicate circuit halves on the opposite side.

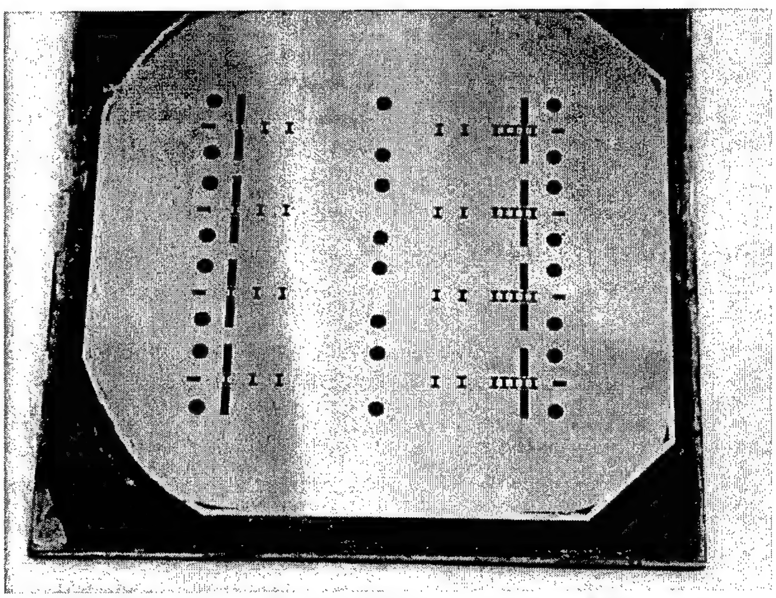

Figure 4.2.1 Copper Klystrino circuit halves fabricated using LIGA

The beam formation and transport of the 500 micron diameter beam through a 6 cm long PPM circuit was also a major accomplishment. The current density at the cathode was 15 A/cm^2 with an area convergence of 81:1 which resulted in a current density of 1200 A/cm^2 in the beam. The beam transmission was >97% through the 6 cm PPM circuit.

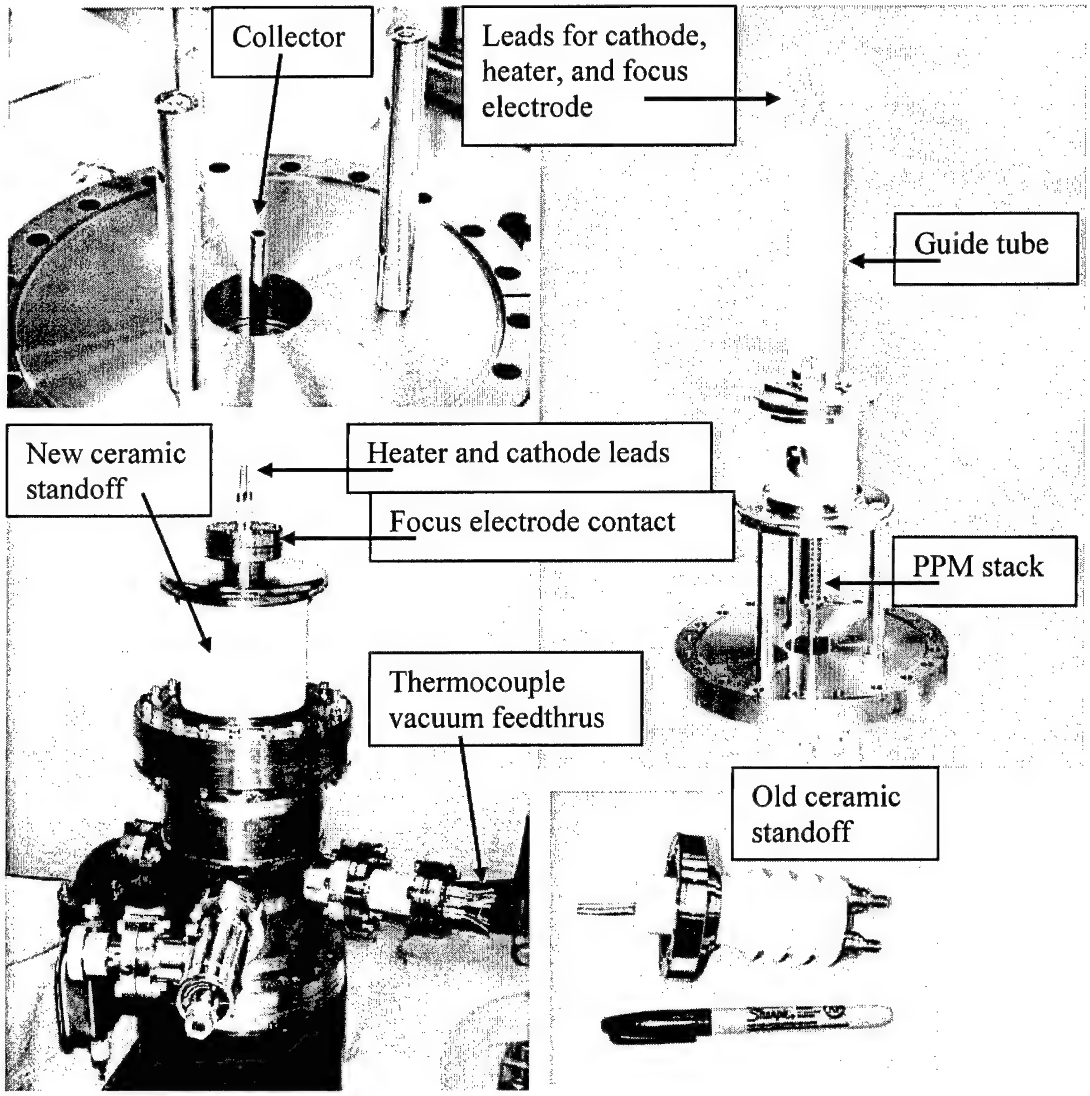

Figure 4.2.2 Photographs of the 110 kV Klystrino beamstick used to evaluate beam formation and transport in a 6 cm PPM magnetic circuit with an 800 micron drift tube.

Computer modeling of the Klystrino required extensive use of 3D modeling codes since neither the LIGA cavities nor the magnetic circuit were cylindrically symmetric. The RF interaction was simulated using GdfidL and MAFIA in 3D and then an equivalent 2D model was constructed that could be simulated in 2D MAGIC in a reasonable (50 hr) time frame. The figures below show examples of 3D modeling of output couplers using GdfidL, 3D modeling of the magnetic circuit using RADIA, and the equivalent circuit 2D MAGIC modeling of the RF interaction in the five gap output cavity.

The completed Klystrino circuit is shown in Fig. 6. It had beam transmission problems that did not occur in the beam tester experiments. The beam interception was caused by the quadrupole

leakage fields of the butterfly shaped polepieces. These quadrupole fields distorted the beam into an elliptic cross section. In the output section, the beam ellipse became large enough that it intercepted the tunnel wall and melted the copper circuit. This problem was not apparent in the 2D beam transport codes used in the original design. Three dimensional MAGIC modeling of the beam transport using the 3D magnetic field solver MAGNET demonstrated the problem. A modified polepiece shape has been designed to eliminate the quadrupole leakage fields.

4.2.1.2 Oxide Cathode Research Program

The University of California at Davis (UCD) and Stanford University have collaborated in alternate cathode technology to develop a reproducible, robust, high current density oxide cathode. Oxide cathodes have always had attractively low work functions, but they have been plagued by their variability in performance. The current oxide cathode manufacturing process either paints or sprays a barium-strontium carbonate emission layer on a nickel cathode base. The carbonate powders are mixed with a nitrocellulose binder to provide adhesion to the nickel surface. In order to activate the cathode, the nitrocellulose must be burned off and the carbonates converted to oxides by heating the cathode and drawing a current in vacuum. This activation process deposits byproducts on nearby surfaces that act as poisoning agents when they re-deposit on the cathode surface. An early experiment was performed by Sperry[1] in which the activation was done in a separate chamber and then the cathode was mounted in a clean gun structure. The pulsed emission current from the experimental cathode exceeded 100 A/cm^2 compared to 15 A/cm^2 for the standard oxide cathode.

Figure 7 shows the work function for various cathode emission materials. Oxide cathodes have the lowest work function at 1.35 eV. The best dispenser cathodes have work functions around 1.8 eV. The .45 eV difference in work function translates to roughly 300°C difference in cathode temperature for the same current density or a factor of 40 difference in current density for the same temperature.

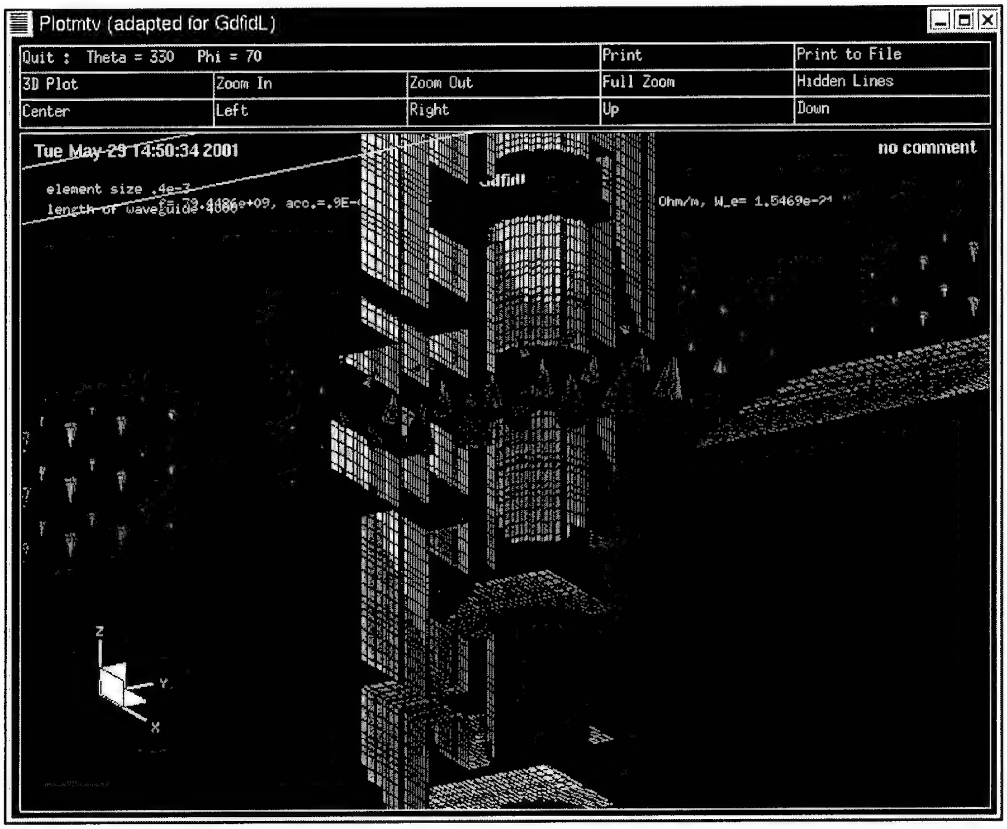

Figure 4.2.3. 3D plot of electric fields from GdfidL for output coupling iris.

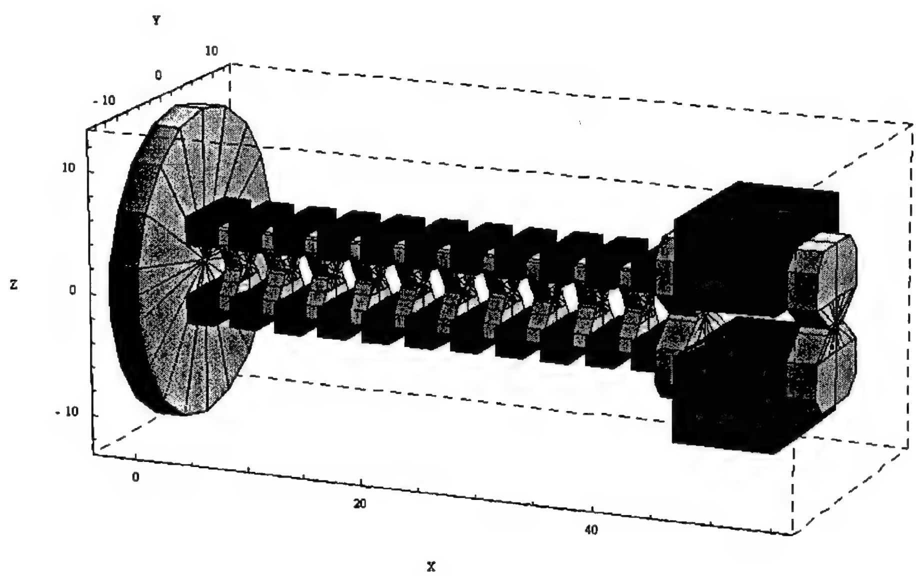

Figure 4.2.4 RADIA 3D model of the Klystrino PPM Magnetic focusing Circuit

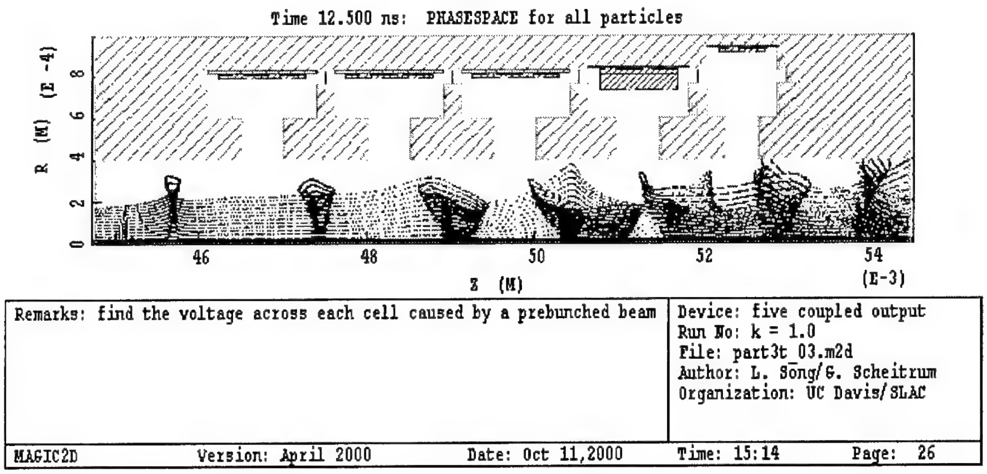

Figure 4.2.5 Simulation of a tapered 5-gap output RF circuit using MAGIC 2D

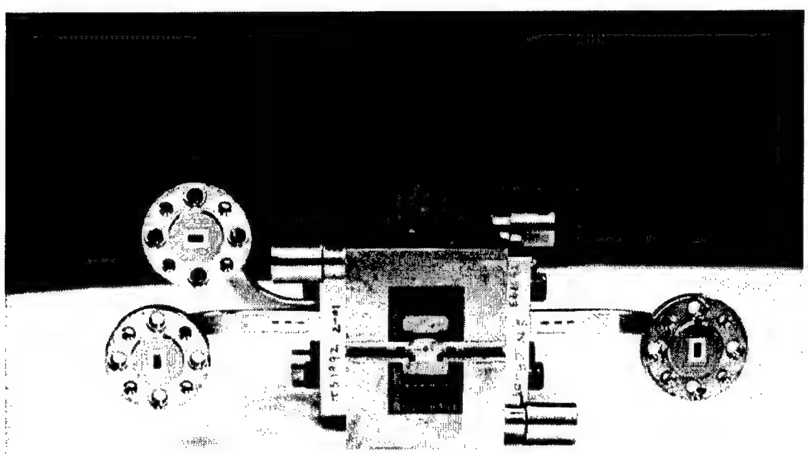

Figure 4.2.6 Photograph of the Assembled Klystrino Circuit

4.2.1.3 Plasma Deposition of Oxide Cathodes

In an earlier program, the UC Davis/Stanford team produced a few oxide cathodes using plasma deposition based on a vacuum arc plasma gun developed by Dr. Ian Brown2-4 of Lawrence Berkeley National Laboratory (LBNL). Deposition of the cathode emission layer was difficult due to triggering problems with the plasma gun. The gun was designed to operate in 10-5 torr vacuums and could not be made to work reliably in the 10-8 to 10-10 torr pressures in the oxide cathode deposition chamber. In spite of the difficulties a few cathodes were made with work functions in the 1.6 eV range.

DURIP funding was used to purchase an excimer laser to overcome the triggering problems associated with the vacuum arc plasma gun. A Lambda Physik excimer laser was purchased and installed in the cathode laboratory. The deposition system is shown in Fig. 8.

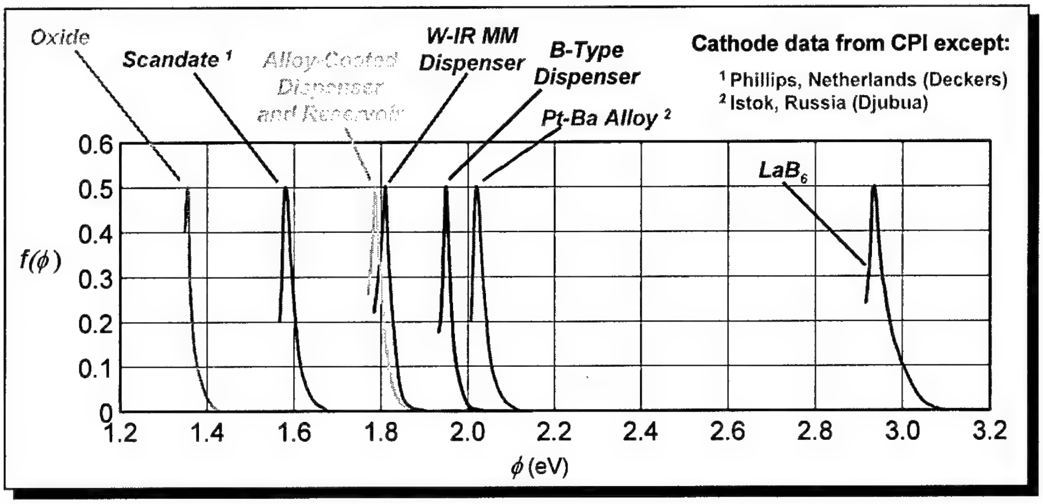

Figure 4 Practical work function distribution for various thermionic cathode types. Data from CPI cathode life tests except (1) Deckers (Phillips, Netherlands) and (2) Djubus (Istok, Russia). After Cattelino and Miram.[5]

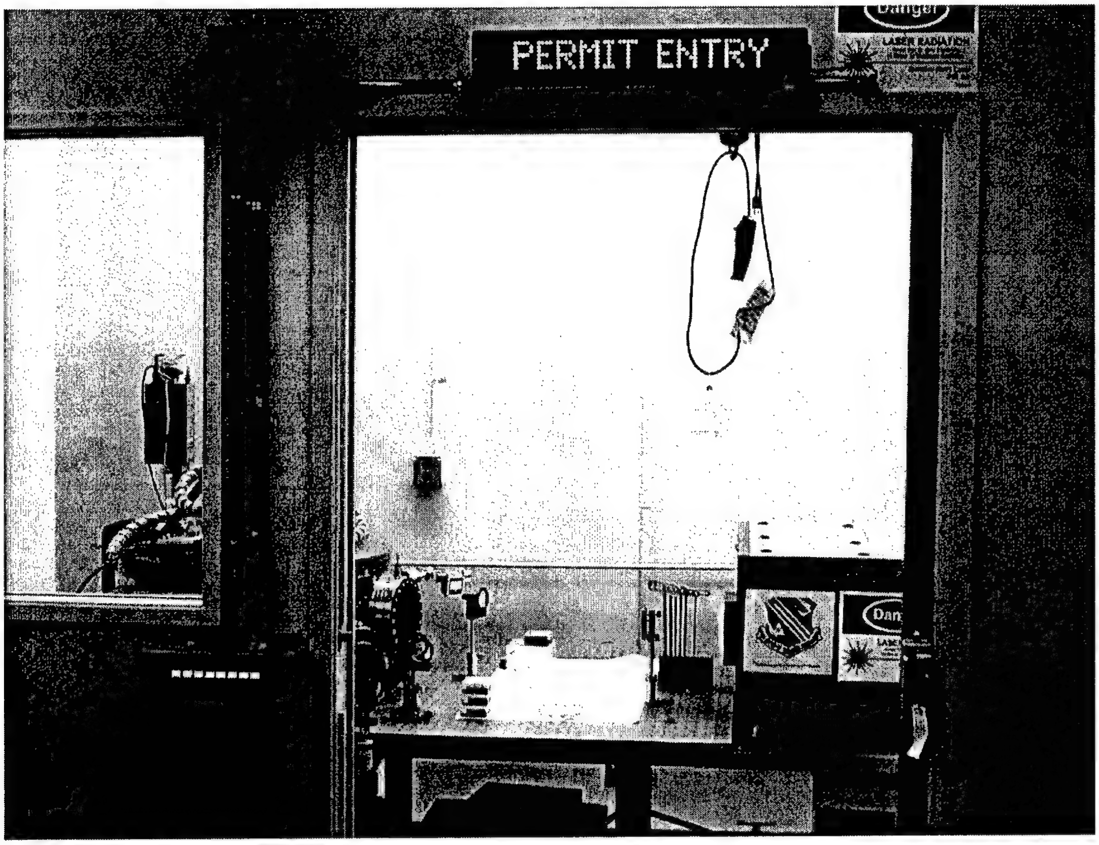

Figure 4.2.8 Photograph showing excimer laser, optical breadboard and deposition chamber in interlocked laser enclosure

4.2.1.4 Parallel Processing using 3D MAGIC on a Beowulf Cluster

A multi-processor Linux Beowulf Cluster was purchased and the particle in cell (PIC) code MAGIC was modified to enable operation on multi-processor systems. This was necessary for 3D simulation of devices such as the Klystrino. Normal 2D PIC code runtimes for a complete simulation of a multi-cavity klystron were in the 20 to 50 hour range. Extending that by the number of cells used in the added third dimension (50 to 200 cells) would push the computation time to thousands of hours. The MAGIC code was extended at Stanford to produce a parallel processing version for both Windows and Linux operating systems. The resulting code was benchmarked on a twenty-four processor Beowulf cluster. Figure 10 shows the rack mounted cluster and a plot of the reduction in execution time versus the number of processors used. Verification tests at SLAC compared results from a single processor vs 12 processors in parallel. Errors were less than 0.05% in all six field components. (Ex,Ey,Ez,Bx,By,Bz)

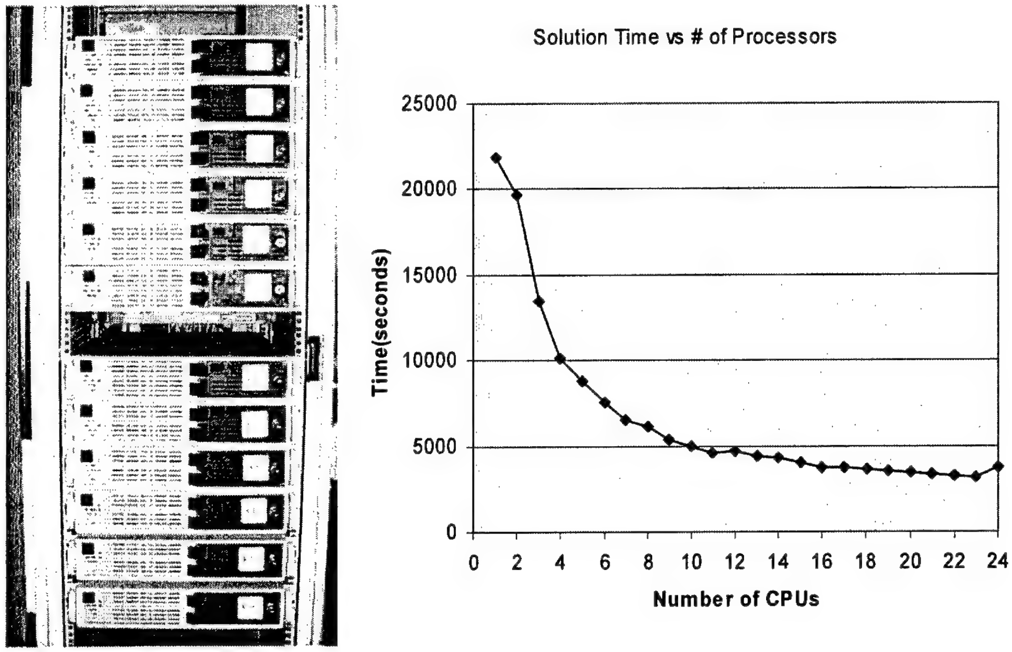

Figure 4.2.9. Photograph of 24 Processor Beowulf cluster and benchmark plot showing time to complete test case vs. number of processors used.

4.2.1.5 RF Breakdown Experiments

Lisa Laurent, a former UC Davis student, received her PhD based on the RF breakdown research she did as part of the previous MURI on High Power Microwaves. Since this area is of great importance to SLAC and increasing importance to Innovative Microwave Electronics in that millimeter wave sources are getting close to breakdown thresholds, this research was continued on a reduced scale in the current MURI Program.

In addition, the MURI funded experiments led to other related research in the Accelerator R&D Department at SLAC. Sami Tantawi and Valery Dolgashev developed both a waveguide breakdown experiment and a MAGIC model that provided some significant insights into the breakdown process.

The "Windowtron" experiments done by Laurent used a single resonant cavity to produce surface gradients up to 800 MV/m with pulse lengths from 70 ns to 1.5 μs. The achievable gradient is a monotonically decreasing function of pulselength. This can be seen in Fig. 10 where the breakdown threshold at 200 ns is > 500 MV/m.

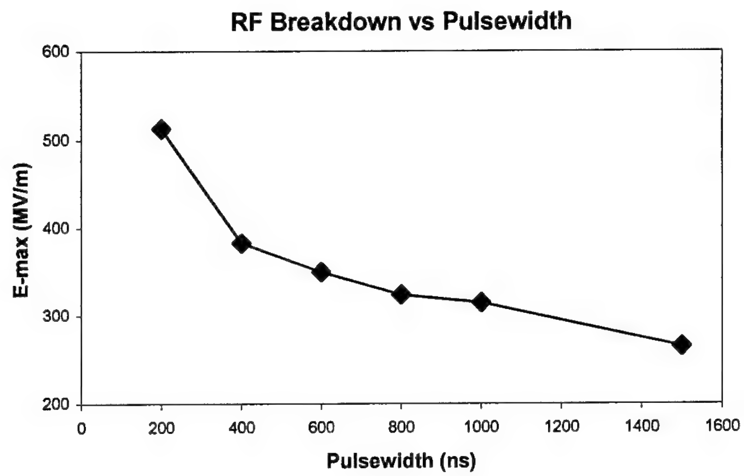

Fig. 4.2.10 Relationship between breakdown threshold and pulsewidth in single resonant cavity experiment.

Another significant finding was the role that grain boundaries in the copper surface play in RF breakdown. Figure 11 shows a close-up of the high gradient surface with a majority of the breakdown sites occurring along the grain boundary. This behavior was eliminated with a high temperature vacuum bake, leading to the conclusion that the residual gas trapped along the grain boundaries enhance the likelihood of breakdown locally.

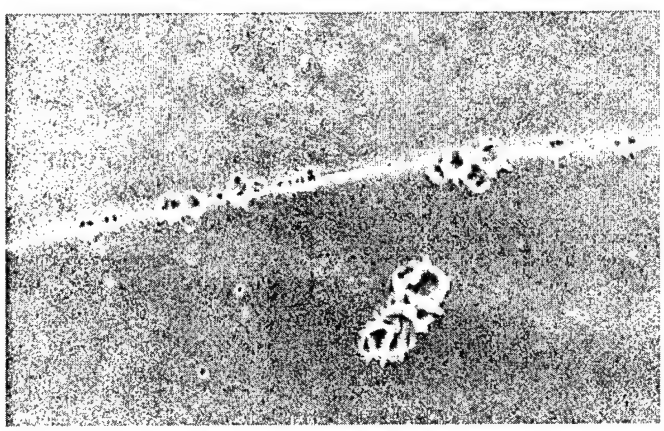

Figure 4.2.11. Waveguide RF breakdown experiments by Tantawi and Dolgashev. Breakdown threshold ~80 MV/m.

In the waveguide breakdown experiments done by Tantawi and Dolgashev, two WR90 waveguides were modified to produce the same electric field gradients over approximately the same area. In the narrow height guide, the narrow or 'b' dimension of the waveguide was reduced in height to increase the electric field gradient for a given power flow. In the narrow width guide, the wide or 'a' dimension is reduced to produce the same electric field for the same 100 MW power flow. The difference between the two experiments is the RF magnetic field which is a factor of 20 higher in the narrow height waveguide. In the series of experiments, the low magnetic field waveguide had nearly twice the breakdown threshold of the high magnetic field guide.

An attempt was made to model the breakdown transient behavior using MAGIC3D. The two plots on the right show an actual RF breakdown event captured with diagnostic probes and below it a MAGIC simulation with the ratio of electron current to ion current adjusted to produce the same time signature in the transmitted and reflected RF pulses. The 3D model is relatively crude in order to reduce the computational time with a 4 mm square emission spot but the simulation maps the behavior of transmitted and reflected power fairly well.

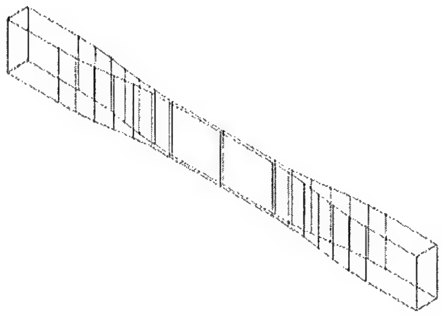

Narrow height waveguide

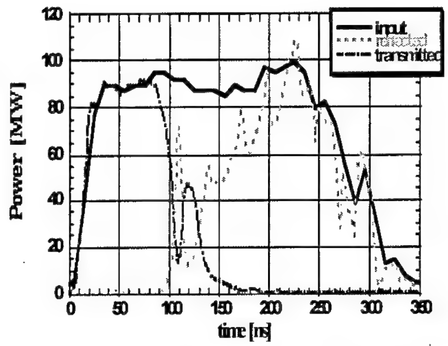

Measurements, 24 April 2001,18:13:40, shot 45

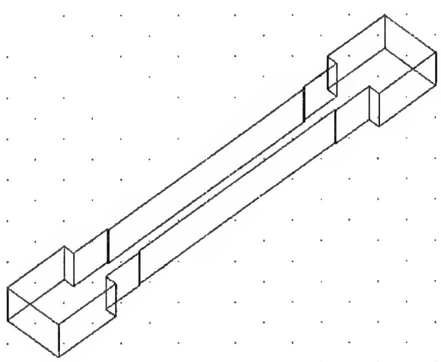

Narrow width waveguide

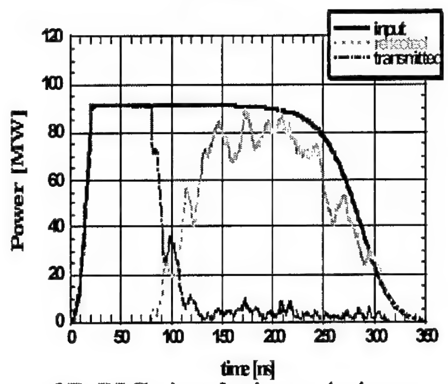

3D PIC simulations, 4x4 mm emitting spot, electron current 7kA, copper ion current 30A

Figure 4.2.12. Waveguide RF breakdown experiments by Tantawai and Dolgashev. Breakdown Threshold ~ 80 MV/m.

4.2.2 Education and Training

Stanford provided support for graduate education in microwave vacuum electronics at UC Davis including lectures, computer modeling, and design projects. At SLAC, UC Davis students were supervised while pursuing their PhD research on RF breakdown, plasma deposited oxide cathodes, microfabrication, and modeling. Students were provided hands on training in fabrication, modeling, cold test, and hot test of state of the art multi-megawatt klystrons. Two UC Davis students spent the majority of their research efforts at Stanford working on modeling and fabrication of millimeter wave sources. Liqun Song completed the PhD degree for her work on computer modeling. Hsin-Lu Hsu is currently working on her PhD on an extended interaction elliptical cavity klystron.

In a MURI collaboration with Seoul National University, Professor Gun-Sik Park sent one of his PhD students to SLAC to spend 18 months working on microfabrication and millimeter wave source design. Young-Min Shin worked on two-step LIGA fabrication of a coupled cavity TWT at 95 GHz.

Two Stanford University graduate students are currently working on PhD programs as part of the MURI program at SLAC. Aaron Jensen and Keith Rauenbuehler are both working on modeling and design of sheet beam klystrons at X-band and W-band. Aaron rewrote and corrected the venerable 1D klystron large signal code "Japandisk". The new improved version is called "AJDISK". It is written in C and uses the Windows graphics package. The code and example input files are available on the SLAC web site listed in the next section.

4.2.3 Klystron Lecture Series

In order to document and archive the decades of klystron research at SLAC, the Klystron Department has produced a series of 15 lectures on the modeling, design, fabrication and test of state-of-the-art high power klystrons. These lectures provide the student with the basic analysis and design concepts for high power klystrons which had previously only been available in an eclectic collection of published papers. The lectures are available in both streaming media and Powerpoint presentations on the SLAC Klystron Department web site.

http://www-group.slac.stanford.edu/kly/Old_web_site/slac_klystron_lecture_series.htm

In addition to the lecture material, several 1D and 2D design worksheets and computer models are available for download.

4.2.4 References

Sperry Electronic Tube Manual, 17.20 (1958)

1. I. G. Brown, J. E. Galvin, R. A. MacGill, *Applied Physics Letters* 47, 358 (1985)
2. I. G. Brown, A. Anders, S. Anders, M. R. Dickinson, R. A. MacGill, *Journal of Vacuum Science and Technology B* 12, 823 (1994)
3. I. G. Brown, A. Anders, S. Anders, M. R. Dickinson, R. A. MacGill, O. Monteiro, E. M. Oks, S. Raoux, Z. Wang, G. Yushov, *Materials Research Society Symposia Proceedings* 396, 467 (1996)
4. M. Cattelino, G. Miram, *Applied Surface Science* 111, 90 (1997)

4.2.5 Publications

1. Novel coupled-cavity TWT structure using two-step LIGA fabrication, Young-Min Shin; Gun-Sik Park; Scheitrum, G.P.; Arfin, B.; Plasma Science, IEEE Transactions on, Volume: 31 , Issue: 6 , Dec. 2003, Pages:1317 – 1324

2. Circuit analysis of Ka-band extended interaction klystron, Shin, Y.M.; Park, G.S.; Scheitrum, G.P.; Caryotakis, G.; Vacuum Electronics, 2003 4th IEEE International Conference on , 28-30 May 2003, Pages:108 – 109

3. Microfabrication of vacuum compatible millimeter wave sources, Sadwick, L.; Hwu, R.J.; Scheitrum, G.; Vacuum Electronics, 2003 4th IEEE International Conference on, 28-30 May 2003, Pages:360 – 361

4. Benchmarking the parallel magic software on small clusters, Smithe, D.; Ludeking, L.; Gray, T.; Steele, R.; Scheitrum, G.; Caryotakis, G.; Vacuum Electronics, 2003 4th IEEE International Conference on , 28-30 May 2003, Pages:120 – 121

5. An improved version of Topaz 3D, Ivanov, V.; Krasnykh, A.; Scheitrum, G.; Jensen, A.; Particle Acelerator Conference, 2003. PAC 2003. Proceedings of the ,Volume: 5 , May 12-16, 2003, Pages:3315 – 3317

6. The klystrino: a high power W-band amplifier, Scheitrum, G.; Arfin, B.; James, B.G.; Borchard, P.; Song, L.; Cheng, Y.; Caryotakis, G.; Haase, A.; Stockwell, B.; Luhmann, N.; Shew, B.Y.; Vacuum Electronics Conference, 2000. Abstracts. International , 2-4 May 2000, Pages:2 pp.

7. Modeling of beam transport in transverse magnetic fields, Shin, Y.; Scheitrum, G.; Sprehn, D.; Plasma Science, 2003. ICOPS 2003. IEEE Conference Record - Abstracts. The 30th International Conference on , 2-5 June 2003, Pages:329

8. The performance characteristics of Ka-band extended interaction klystron based on 2π-mode operation, Shin, Y.M.; Park, G.S.; Caryotakis, G.; Scheitrum, G.P.; Arfin, B.; Plasma Science, 2003. ICOPS 2003. IEEE Conference Record - Abstracts. The 30th International Conference on , 2-5 June 2003, Pages:175

9. The small and large signal analyses of the LIGA base W-band coupled cavity TWT, Shin, Y.M.; Park, G.S.; Scheitrum, G.P.; Arfin, B.; Plasma Science, 2003. ICOPS 2003. IEEE Conference Record - Abstracts. The 30th International Conference on , 2-5 June 2003, Pages:171

10. Design, fabrication and test of the Klystrino, Scheitrum, G.; Arfin, B.; Burke, A.; Caryotakis, G.; Haase, A.; Shin, Y.; Plasma Science, 2002. ICOPS 2002. IEEE Conference Record - Abstracts. The 29th IEEE International Conference on , 26-30 May 2002, Pages:200

11. Three-dimensional design of the coupling slot for a W-band output structure [klystron] Song, L.; Luhmann, N.C., Jr.; Scheitrum, G.; Arfin, B.; Infrared and Millimeter Waves, 2002. Conference Digest. Twenty Seventh International Conference on , 22-26 Sept. 2002, Pages:351 – 352

12. Initial RF testing of 95 GHz Klystrino, Scheitrum, G.; Burke, A.; Caryotakis, G.; Haase, A.; Martin, D.; Vacuum Electronics Conference, 2002. IVEC 2002. Third IEEE International , 23-25 April 2002, Pages:324 – 325

13. Design of W-band coupled-cavity TWT by LIGA fabrication, Shin, Y.M.; Park, G.S.; Han, S.T.; Kim, J.I.; Scheitrum, G.P.; Arfin, B.; Chang, S.S.; Vacuum Electronics Conference, 2002. IVEC 2002. Third IEEE International , 23-25 April 2002, Pages:50-51

14. "windowtron" RF breakdown studies at SLAC, Laurent, L.; Caryotakis, G.; Glendinning, F.; Sprehn, D.; Luhmann, N.C., Jr.; Pulsed Power Plasma Science, 2001. IEEE Conference Record - Abstracts , 17-22 June 2001, Pages:463

4.3 University of Wisconsin, Madison

4.3.1 Overview

During the five years of support from 1999 – 2004, the University of Wisconsin investigators made major research and education contributions in the following general categories:

- Multi-sensored TWTs for fundamental research of MPM-class TWTs
- Fundamental physics of nonlinear distortions in TWTs and klystron amplifiers
- Novel, improved methods for linearizing TWT and klystron amplifiers
- Microfabrication of mmwave and THz regime vacuum electronic amplifiers
- Novel operating modes of TWT amplifiers, including impulse amplification and chaos generation
- Fundamental physics of large-space-charge, MPM-class TWT amplifiers
- 1D TWT simulation codes for teaching and research of TWTs, available as open source software at http://www.lmsuite.org.
- Educated and trained 3 Ph.D., 1 post-doc, 12 M.S., and 11 B.S. students in microwave vacuum electronics.
- Published or submitted for publication 17 journal articles (with at least two more in preparation); presented 58 conference talks on subjects supported by the MURI99 funds, including a Plenary Talk and an Invited Talk at the International Vacuum Electronics Conferences of 2002 and 2003, respectively.

Our major research breakthroughs to date include:

- Developing and operating a novel, multi-sensored TWT for research of fundamental nonlinear physics in MPM-class TWTs,
- Advancing a new understanding of the physics of nonlinear distortions in TWTs,
- Developing a new computational method to model 1D linear-beam VEDs with Eulerian formulations, including the effects of charge overtaking,
- Establishing the fundamental physical mechanisms of harmonic and distortion product injection for linearization of TWTs,
- Identifying a novel TWT transmitter configuration enabling extremely linear amplification of digitally-modulated signals while operating saturated and thus at maximum efficiency,
- Completing the first combined experimental and simulation study of impulse amplification in TWTs revealing realistic prospects for novel applications to impulse radar, impulse communications, and impulse response measurements of small signal gain characteristics,
- Conducting pioneering investigations of xray LIGA, UV LIGA and deep reactive ion etching methods for microfabricating mmwave and THz regime TWTs, and
- Developed and disseminated a suite of 1D TWT simulation codes for teaching and research of TWTs, making them available as open source software at http://www.lmsuite.org.

4.3.2 Significant Achievements

4.3.2.1 Multi-sensored TWT for fundamental nonlinear physics research in MPM-class TWTs

Microwave Power Modules are a revolutionary microwave power technology that exploit the best advantages of solid state and vacuum electronics. By sequencing a low power, high gain, low noise, solid state preamplifier with a high power, modest gain, very wideband TWT, along with innovative compact power supplies and thermal management design, the MPM provides the ultimate superior combination of efficiency, bandwidth, gain, power, and low noise in an incredibly compact package. MPMs owe a significant portion of their success to the innovation of MPM-class TWTs. While the gain is modest (20-30 dB), these TWTs are extremely compact, low voltage, have very wide bandwidths, and high efficiencies. To achieve the required gain in a short length results in typically high current and charge densities in the electron beam. This results in large values space charge and thus large values of the Pierce parameter QC. The combination of extra large bandwidth and large QC results in certain unique physical responses that are less well studied, but are very important for advancing MPMs for electronic warfare, radar, and communications. For example, control of harmonic distortion at the band edges is very important, as well as prospects for linear amplification of multiple carriers in multi-target ECM applications.

To learn more about the nonlinear physics of MPM-class TWTs, UW successfully collaborated with Northrop Grumman, to innovate, manufacture, and make operational a multi-sensored, MPM-class research TWT, referred to as the "XWING" (eXperimental WIsconsin Northrop Grumman) TWT, shown in Fig. 1, below. With these sensors we can measure the evolution of the circuit wave along the TWT, and even have the capability to directly measure the beam-modified ("hot") phase velocity of the wave, a fundamental physical parameter. This new TWT has been directly responsible for experimental verification of a new breakthrough on understanding nonlinear distortion mechanisms in TWTs, the first studies of impulse amplification in a wideband TWT, and the first direct experimental measurements of hot phase velocities in a high-space-charge, MPM-class TWT.

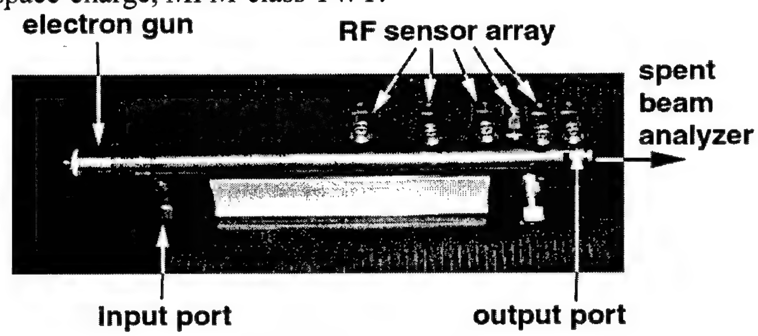

Fig. 4.3.1. Picture of the multi-sensored research "XWING" TWT, for fundamental research of nonlinear physics in MPM-class TWTs

4.3.2.2 The Physics of Nonlinear Distortions in Traveling Wave Tubes (TWTs)

Evolving communications systems need high data rates and high linearity, and make use of advanced modulation schemes. Evolving electronic warfare systems will require ultra-wide bandwidth and linearity at high power. Advanced radar transmitters envision multi-carrier operating modes for simultaneous tracking of multiple targets. Meanwhile, the traveling wave tube (TWT) amplifier has so many inherent performance advantages—bandwidth, compact power, efficiency, gain, and linearity--that it holds a dominating presence in most communications and electronic warfare systems as well as most compact radar on mobile platforms. Consequently, improving our fundamental understanding of nonlinear distortion mechanisms in TWTs can have a profound impact by pointing the way to more linear TWT amplifiers in radar, communications, and electronic warfare systems.

Our combined theoretical and experimental research has revealed a new way of understanding the nonlinear mechanisms behind fundamental and harmonic distortion in TWTs. In essence, all distortions associated with operation prior to saturation have their origin in spontaneous nonlinear second harmonic distortions on the electron beam that result from ballistic motion. All other distortions, including phase distortion at the fundamental, intermodulation distortion and higher harmonic distortion arise as intermodulation products from the second harmonic distortions on the electron beam.

In contrast to past models, this new model is quantitative and predictive, has a clearly understandable intuitive principle, and has been verified in comparisons of analytic theory and computation and experiment. It corrects a long-standing misconception that phase nonlinearity arises from slowing down of the electron beam and it provides a much firmer and clearer theoretical explanation for a recently invented method of TWT linearization [T. Chen, Y. Goren, et al, "A novel technology for linearizing traveling wave tube amplifiers, IEEE MTT-S I.M.Symposium Digest Cat No. 02CH37278, pp. 773-6, vol. 2 (2002).]. It has led to ideas for linearization using second harmonic injection that appear to have extremely high distortion suppression potential (see below and next section). Harmonic injection to suppress harmonic distortion and increase EW TWT bandwidths is clearly explained, and improved phase linearity using harmonic injection remains a possibility.

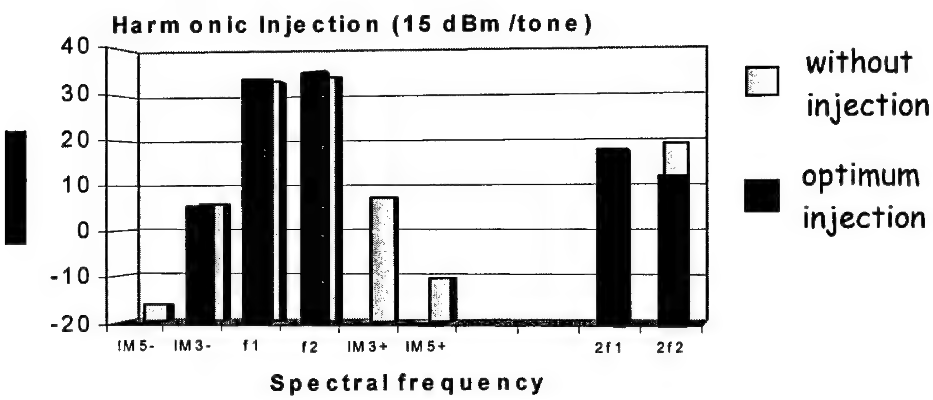

Fig. 4.3.2 Experimental verification of new nonlinear TWT theory explaining how harmonic injection suppresses 3rd and 5th order intermodulation distortions in two-tone operation.

4.3.2.3 Eulerian Modeling of Vacuum Electron Devices including charge overtaking

Advanced computer methods and hardware have contributed to the advancement of vacuum electronics technology by providing improved design codes as well as codes that lead to improved fundamental understanding of the complex physics. We have innovated a new method to model linear beam vacuum electron devices using an Eulerian formulation that accounts for particle overtaking. This new technique has been applied to and validated for klystron interactions. If applied to TWT modeling, it would enable substantially deeper insights and understanding of the complex nonlinear effects that occur when a TWT enters saturation. Moreover, the method has demonstrated dramatically greater computational speed than traditional Langrangian-type models.

It has long been understood that Eulerian (fluid-like) models provide extremely clear physical insight, but are unable to correctly model plasma, electron beam, and fluid systems when "wave-breaking" (particle overtaking) occurs. Lagrangian models use coordinate systems that are far less intuitive and therefore occasionally obscure the physical mechanisms of a phenomena. However, Lagrangian models have been powerful tools in vacuum electronics for their natural ability to handle charge overtaking phenomena that occur near saturation in TWTs, for example. We have innovated a new approach to Eulerian modeling that removes the many decades old barrier to accurately modelling charge overtaking. Our new method has been applied to modeling a klystron interaction with excellent agreement with the most exact models (e.g., kinetic theory). Moreover, the new method is dramatically faster than any alternatives and lends itself to clear intuitive physical insight regarding nonlinear mechanisms. (e.g., several days for Lagrangian vs. several minutes for Eulerian on a 1.8 GHz Gnu/Linux computer for a test case). The model is now being adopted for use in TWT simulations by Dr. J. Wöhlbier at Los Alamos National Laboratory.

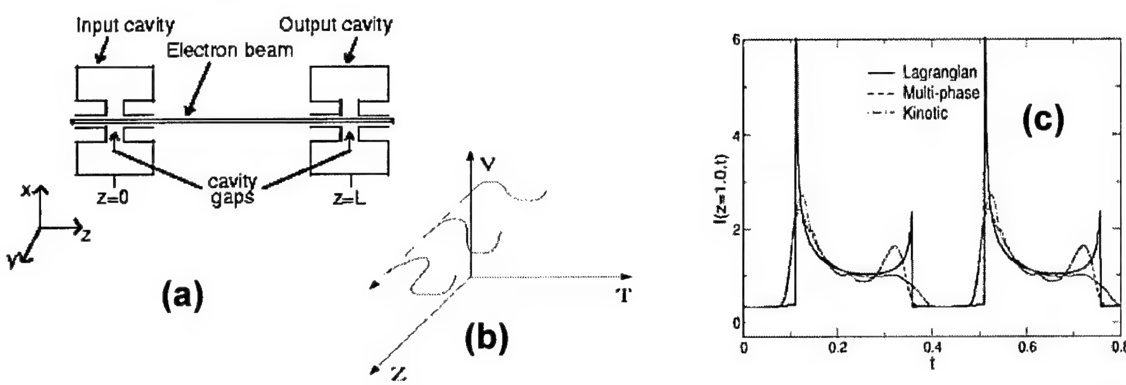

Fig.4.3 3. Demonstration for a 1D Klystron of a new computational method for modeling VEDs with an Eulerian formulation, including charge overtaking. (a) schematic of the klystron, (b) illustration of how the fluid velocity becomes multivalued with charge overtaking, (c) comparison of a traditional Lagrangian, an "exact" kinetic, and the Eulerian ("multi-phase") calculation of the beam current versus time. The differences in (c) are primarily in the height,due to use of numerical viscosity in Eulerian and gaussians for delta boundary values in kinetic, but these distinctions have negligible effect on accurate prediction of output spectra. The Eulerian calculation was ~ 3 orders of magnitude faster than other computational methods.

4.3.2.4 The Physics of Harmonic and Distortion Product Injection in TWT amplifiers

Evolving communications systems need high data rates and high linearity, and make use of advanced modulation schemes. Evolving electronic warfare systems will require ultra-wide bandwidth and linearity at high power. Advanced radar transmitters envision multi-carrier operating modes for simultaneous tracking of multiple targets. Meanwhile, the traveling wave tube (TWT) amplifier has so many inherent performance advantages—bandwidth, compact power, efficiency, gain, and linearity--that it holds a dominating presence in most communications and electronic warfare systems as well as most compact radar on mobile platforms. Consequently, improving our fundamental understanding of nonlinear distortion mechanisms in TWTs can have a profound impact by pointing the way to more linear TWT amplifiers in radar, communications, and electronic warfare systems.

We have developed a new description of harmonic (and other distortion product) injection that clearly reveals the underlying physics. Built upon the same general theoretical framework as our model for nonlinear distortions, our theory reveals that harmonic suppression results from destructive interference of two circuit voltage modes at the frequency to be cancelled, an injected mode and a nonlinearly generated mode. Contrary to previous hypotheses, the cancellation occurs only at one axial location. For linearization purposes, then, the objective is to tune the injected signal's amplitude and phase so that cancellation occurs at the tube output. Experiments (illustrated below) verify the theory as well as point out that suppression by as much as – 30 dB of harmonic and even intermodulation distortion components is achievable by proper selection of the injected signal parameters. The theory goes on to explain that concomitant increases of fundamental power seen when harmonics are suppressed is a result of constructive interference of two circuit modes at the fundamental frequency: the normal driven wave and a nonlinear mode resulting from intermodulation between the second harmonic and the fundamental excitations. Finally, the new understanding shows that injecting multiple tones (such as multiple harmonics, or second harmonic and intermodulation product frequencies) can provide even better methods for suppressing distortion products. However, the more tones one injects, the more complicated becomes the process of finding optimal injection parameters without worsening the distortion in some aspect of the output spectrum.

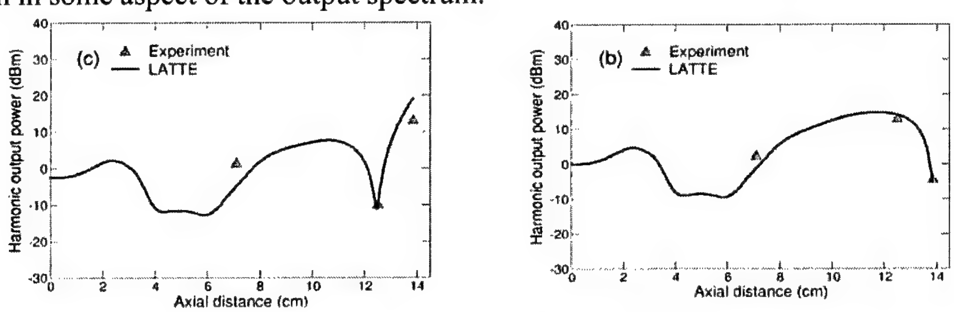

Fig. 4.4.4. Comparison of new nonlinear TWT theory with experiment distortion products. The new understanding is that the suppression results from destructive interference between two nonlinear modes in the voltage wave for the distortion product. Axial location of the suppression point depends upon the input power and phase of the injected harmonic signal.

4.3.2.5 LINC architecture for ultra-high efficiency linear transmitters of digitally modulated signals

Evolving communications systems need high data rates and high linearity, and make use of advanced modulation schemes. The most conventional method to minimize nonlinear distortion is to operate the transmitter's amplifier significantly below saturation, also called "backed-off" operation. However, operation at saturation provides maximum operating efficiency, while operating backed-off significantly reduces efficiency. The ideal situation is to realize an amplifier configuration with high linearity operating near or at saturation, and thus at peak efficiency. For TWT amplifiers the implication of such a configuration would be especially profound because of the extremely high efficiencies—between ~ 60 and 70 %—of a communications TWT operating near saturation.

Our research has identified a candidate configuration, called LINC, that would provide excellent TWT linearity at unprecendented operating efficiencies. Simulations based on DPQSK and similar modulation schemes common in North America indicate that spectral regrowth levels can be suppressed by –35 to -40 dB while operating the TWTs saturated. The LINC configuration (LINC stands for LInear amplification using Nonlinear Components) uses two TWT amplifiers, and special signal processing at the baseband to produce an unprecedented combination of linearity and efficiency. Figure 5(a) below is a block diagram of the architecture while Fig. 5(b) shows an illustration of the low-distortion amplified spectrum realized for saturated, maximum efficiency operation.

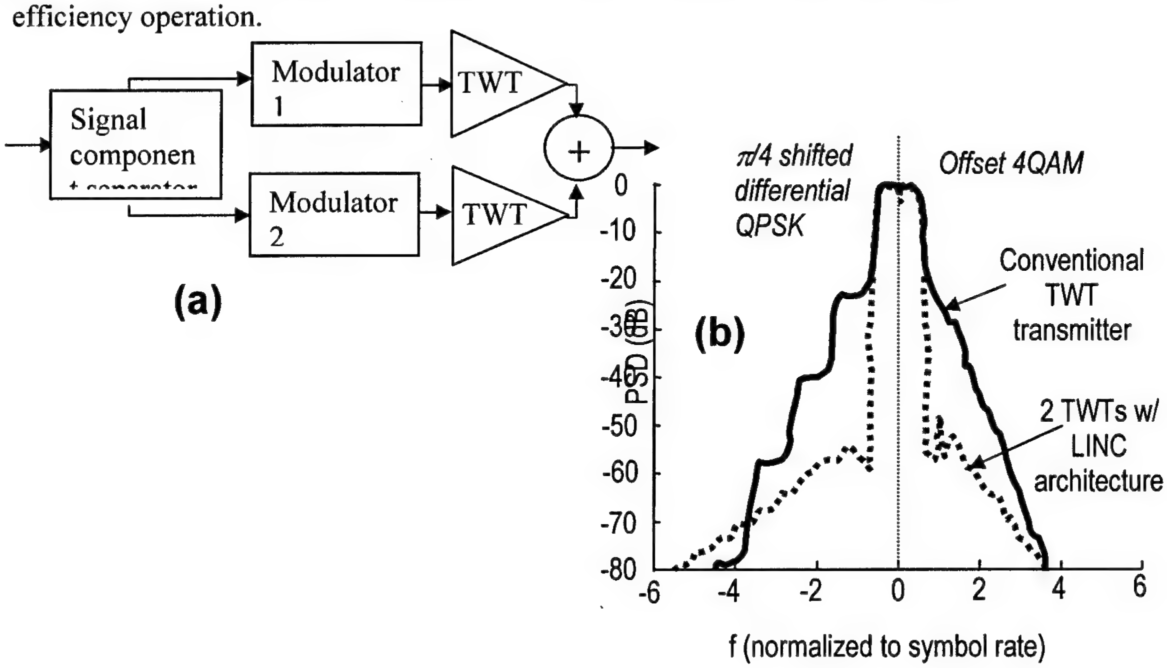

Fig. 4.3.5. TWT transmitter based on the LINC architecture (LInear amplification using Nonlinear Components). (a) LINC configuration. (b) illustrative output spectra of digitally modulated signals illustrating ~ -40 dB suppression of spectral regrowth from intermodulation distortion.

4.3.2.6 The Physics of Impulse Amplification in wideband TWT amplifiers

The amplification of an impulse by a wideband TWT has several possible exciting applications. First, wideband TWTs could make an excellent amplifier in a communications link for impulse radio communications. Impulse radio techniques are highly spectrally efficient, robustly resistant to eavesdropping (ideal for secure covert communications) and resistant to multipath fading or jamming. High power impulse radar using a TWT would provide extremely high resolution, would be highly resistant to electronic counter measures, and would provide the exciting capability to "see through" obstructions such as walls, chaff, or earth. Finally, by analyzing the time-domain "impulse response" of a TWT, we can quickly, easily, and relatively cheaply obtain the entire small signal gain characteristics, as well as several interesting nonlinear characteristics from a single data "shot".

We have completed the first experimental and computational studies of the small and large signal amplification of ultra-wideband impulses in a wideband TWT. These studies identify the exciting capability of a TWT to amplify wideband pulses for applications such as impulse radio and radar. We have also confirmed that the small signal impulse response of a TWT provides provides the entire small signal gain versus frequency characteristics of a TWT quickly, easily, and inexpensively in a single data shot. Our studies suggest that a TWT can amplify a wideband impulse with very high gain and efficiency. The reason appears to be an absence of particle trapping with impulse amplification that typically causes saturation in more conventional, single frequency carrier amplification in a TWT.

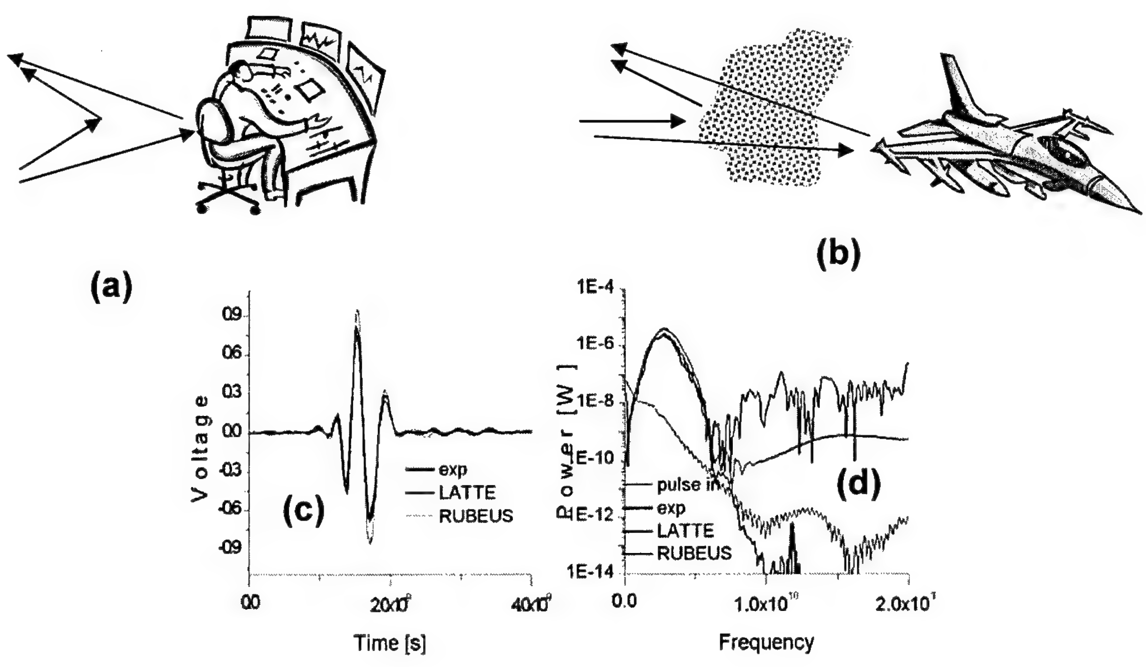

Fig. 4.3.6. Impulse amplification in wideband TWTs. Adapted for radar, one could obtain the ability to (a) conduct surveillance imaging through thick walls or (b) penetrate chaff countermeasures. In initial results good agreement between was realized between experimental measurements and computer predictions for impulse amplification in a wideband TWT, both in (c) output time-domain signal, and (d) output frequency spectrum

4.3.2.7 Microfabricated TWTs for advanced millimeter-wave and THz regime sources

Microfabrication techniques, born within the microelectronic integrated circuits industry and expanded and matured with the advent of MicroElectroMechanical Systems (MEMS) offers methods to fabricated small, sub-mm, electrical and mechanical components with high accuracy and precision, high yield, and potentially significant cost savings through batch production. Consequently, an ideal opportunity exists to marry some of the best aspects of solid state and vacuum electronics to realize low-cost, high-yield mm-wave to THz regime (100 – 3000 GHz) high power, compact sources. For mm-waves, application opportunities include close-in seeker radar, earth-space and space-space satellite communications, microsatellite cluster links, and high-data-rate wireless communications. For the THz regime (300-3000 GHz), there is a vast, untapped potential for extremely high-data-rate communications, advanced close-in radar, materials spectroscopy, space research, medicine, biology, surveillance, and remote sensing. The primary barrier to exploitation of this region of the spectrum remains the (lack of) availability of affordable compact sources (oscillators and amplifiers) of sufficient power. Vacuum electronic devices should theoretically be able to meet the needs of power and size. However,until now it has been prohibitively difficult to reliably fabricate the required small-dimensioned circuits and components.

We have conducted pioneering investigations of the applicability of modern microfabrication methods for mmwave and THz regime TWTs. We have specifically focused on the folded waveguide (FWG) TWT as one whose circuit is naturally suited to planar microfabrication methods. To date, we have successfully demonstrated the feasibility of fabricating 400 GHz FWG TWT circuits using conventional xray LIGA, novel UV LIGA, and deep reactive ion etching (DRIE). Examples are shown below. The DRIE and UV LIGA approaches are especially attractive because they obviate the need for an xray synchrotron light source.

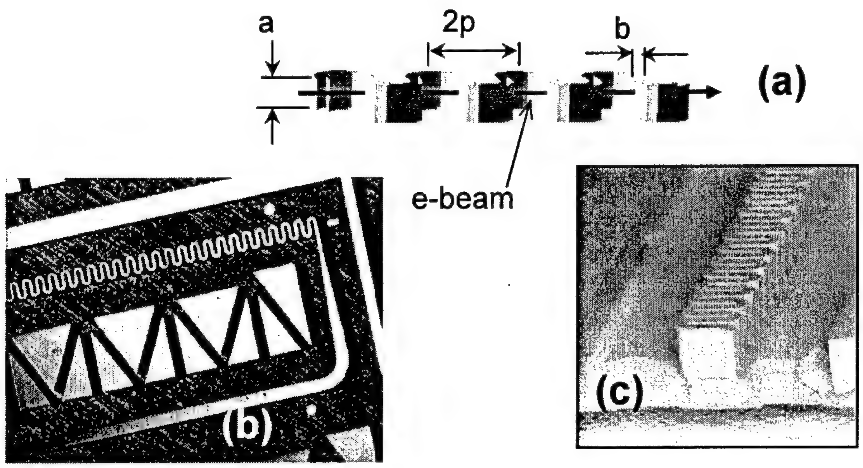

Fig. 4.3.7. Illustrations of fabrication of 400 GHz FWG TWTs using LIGA microfabrication methods. (a) basic configuration of a FWG TWT. (b) PMMA mold for a FWG TWT oscillator fabricated by xray LIGA. (c) SU-8 mold for a 400 Ghz FWG TWT circuit fabricated using UV exposure LIGA.

4.3.2.8 New Open Source Simulation Tools for TWT Research and Education

By virtue of their innate superior performance characteristics, traveling wave tubes (TWTs) hold a dominant position for microwave power amplifiers in radar, electronic warfare, and satellite communications applications. Evolving communications, radar, and electronic warfare systems require continuous improvements in transmitter technology to maintain technological superiority in the battlefield. There have been major advancements in bandwidth, linearity, frequency, efficiency, and size reduction in TWTs during the past 10 years, and there appears to be room for additional advances for several decades to come. There is both a need and an opportunity to realize these TWT technology improvements through basic university research and training of tomorrow's TWT design engineers. To that end, as a byproduct of our research on nonlinear distortion physics in TWTs, we have developed a suite of 1D TWT simulation codes that are ideal for teaching and basic research on TWTs. They are provided as open source software for all university, research laboratory or industrial scientists and engineers and can be downloaded from http://www.lmsuite.org. Over 38 user's from academia, government labs, and industry across the US and around the world have downloaded and used the codes for TWT research, education, and design studies.

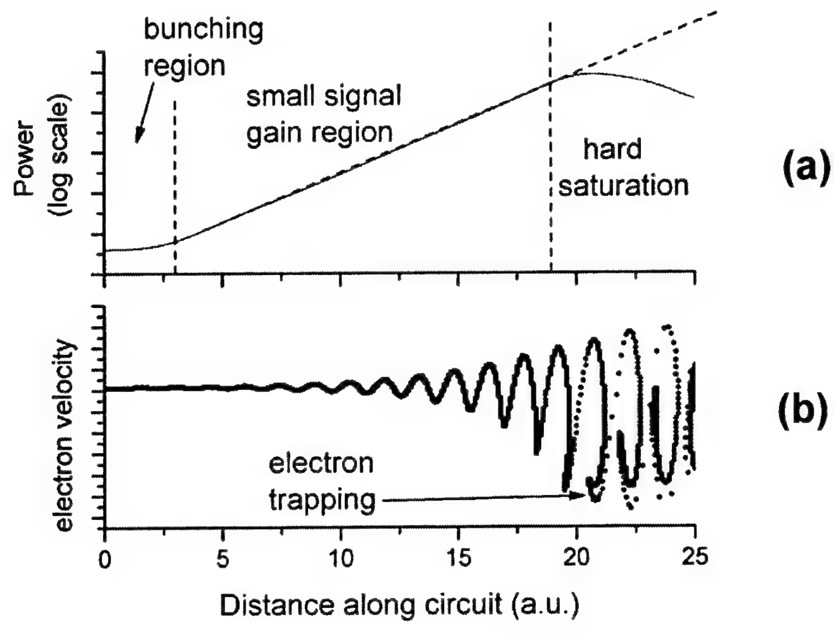

Fig. 4.3.8. Illustrations of (a) circuit wave power and (b) electron velocity evolution from a TWT simulation using the LMSUITE of open source codes available for teaching and research. Classic electron "particle trapping" responsible for saturation is illustrated by comparing figures (a) and (b). Movies of the evolution of these and other physical parameters (voltage, density, current) are available.

4.3.3 UW Students Educated under MURI'99

Student	Type and Date of Degree	Project Title	Status
John Wöhlbier	Ph.D. March 2003	Nonlinear Distortion and Suppression in Traveling Wave Tubes: Insights and Methods	Director Fellow, Scientist, Los Alamos National Laboratory
Mark Converse*	Ph.D. April 2003	Investigation of the Mechanisms of Pulse Amplification in Helical Traveling Wave Tubes	Post-doc, University of Wisconsin
Antoine Choffrut	Passed PhD qualifier and thesis proposal exams	LINC architectures for linear TWT transmitters operating at high efficiency	Work in progress
Sudeep Bhattacharjee	Post-doctoral scholar	Folded waveguide TWTs for THz applications	Will finish in Aug 2004 and assume a faculty position at Indian Institute of Technology
Mark McNeely*	M.S. 2001	Evaluation of a Method for Forming Sheet-Electron-Beams from an Initially Round-Electron-Beam using Magnetic Quadrupoles	International professional engineering consultant
Mike Wirth	M.S. 2002	Techniques in Microfabrication of a 400 GHz Folded Waveguide Travelling Wave Tube	Job with Madison startup company
Mike Neumann	M.S. 2000	Initial Experimental Investigations of Intermodulation in a Klystron Amplifier	Engineer, Agilent
John Wohlbier	M.S. 2000	Modeling and Analysis of a Traveling Wave Tube Under Multitone Excitation	Continued studies with Ph.D.
Antoine Choffrut	M.S., 2001	LINC methods for Linearizing TWT Amplifiers	Continued studies with Ph.D.
Sean Gallagher	M.S., 2003	Techniques in Microfabrication of a 400 GHz Folded Waveguide Travelling Wave Tube	Job in non-VED industry
Won-Je Lee	M.S., 2003	Reentrant Rectangular Cavity Resonator Design for Millimeter Wave and THz regime Klystrons	Continuing graduate studies in MEMS area
Aarti Singh	M.S. 2004	Suppression of Nonlinear Multitone Products in a Traveling Wave Tube Amplifier	Continuing graduate studies in digital communications theory
Ning Zhang	M.S. 2004	Studies of novel structures for THz	Continuing

		regime TWTs and BWOs	graduate studies in applied physics
Kevin McLaughlin	M.S. in progress	Hot phase velocity measurements in a TWT	In progress
Matt Genack	M.S. 2004	Novel folded waveguide circuits for mmwave and THz regime TWTs	U.S. Patent Office
John Welter	M.S. in progress	Microfabricated folded waveguide TWTs for mmwave and THz regimes	In progress, will join L3 Comm Electron Devices upon graduation
Chad Marchewka**	B.S.	Chaos in a TWT amplifier with external feedback	Graduate studies at MIT with Temkin vacuum electronics group
John Welter**	B.S., 2003	Intermodulation injection to linearize multitoned klystron	Continued graduate studies at UW
Sean Sengele**	B.S., in progress	Development of TWT software for education and research, TWT simulations for optimized velocity tapers	In progress
Jassem Shahrani	B.S., 2002	Klystron cavity measurements	Engineer in industry
Bonnie Shum	B.S., 2001	Klystron cavity simulations using MAGIC	Engineer in industry
Min Ki Choi	B.S., 2001	MVED Educational materials development	Graduate studies in applied physics
Hyun Moon	B.S., 2001	MVED Educational materials development	Graduate studies in applied physics
Jean Nguyen	B.S., 2003	Studies of TWT helix circuits using HFSS	Graduate studies in applied physics
Al Mashal**	B.S., in progress	Experimental studies of novel klystron cavities for THz regime applications	In progress
Paul Larsen**	B.S., in progress	Chaos in a driven TWT oscillator with external feedback	In progress
Adam Bush	B.S., in progress	Experimental studies of TWTs in LINC architectures for linear amplification at high efficiency	In progress

* Industrial Intern with Northrop-Grumman, Rolling Meadows, IL
** Industrial Intern with L3-Communications ED, San Carlos, CA
*** Note that two of UW's undergraduate MVE students have ended up at other MVE schools: Jim Anderson was an undergraduate student educated in our UW laboratory who went on to attend first the University of Maryland and then the MIT MVE groups. Chad Marchewka has finished his undergraduate studies in our laboratory in Fall 2003 and joined the MIT MVE group in January 2004.

4.3.4 List of Publications and presentations

4.3.4.1 Journal Papers

1. "The Multifrequency Spectral Eulerian (MUSE) Model of a Traveling Wave Tube," J.G. Wöhlbier, J.H. Booske, I. Dobson, IEEE Trans. Plasma Science, 30 [3],1063-1075 (2002).

2. "Third-Order Intermodulation Reduction by Harmonic Injection in a TWT Amplifier," M. Wirth, A. Singh, J. Scharer, and J. Booske, IEEE Trans. Electron Devices, Vol. 49, No. 6, 1082 – 1084 (2002).

3. "TWT Linearization using LINC architecture," A. Choffrut, B. VanVeen, and J.H. Booske, IEEE Trans. Electron Devices, Vol. 50, No. 5, pp. 1405 – 1408 (2003).

4. "Generation and growth rates of nonlinear distortions in a traveling wave tube," J.G. Wöhlbier, I. Dobson, and J.H. Booske, PHYS REV E 66 (5): art. no. 056504, NOV 2002.

5. "Suppression of third-order intermodulation in a klystron by third-order injection," S. Bhattacharjee, C. Marchewka, J. Welter, R. Kowalczyk, C.B. Wilsen, J.H. Booske, Y.Y. Lau, M.W. Keyser, A. Singh, J.E. Scharer, R.M Gilgenbach, M.J. Neumann, Phys. Rev. Lett., vol. 90, No. 9, paper 098303, 4 pages (2003).

6. "An Eulerian method for computing multi-valued solutions of the Euler-Poisson equations and application to wave breaking in klystrons," Xiantao Li, John G. Wöhlbier, Shi Jin, and John H. Booske, Phys Rev. E (to be published, 2004).

7. "Experimental Verification of the Mechanisms for Nonlinear Harmonic Growth and Suppression by Harmonic Injection in a Traveling Wave Tube," A. Singh, J. G. Wöhlbier, J. H.Booske, J. E. Scharer, Phys. Rev. Lett. Vol. 92, paper 205005 (2004).

8. "Insights from one-dimensional linearized Pierce theory about wideband traveling wave tubes with high space charge," J.H. Booske and M.C. Converse, IEEE Trans. Plasma Sci. (to be published, 2004).

9. "Mechanisms for phase distortion in a traveling wave tube," J.G. Wöhlbier and J.H. Booske, Phys. Rev. E, Vol. 69 [6], article 066502 (2004).

10. "On the physics of harmonic injection in a traveling wave tube,"J.G. Wöhlbier, J.H. Booske, and I. Dobson, IEEE Trans. Plasma Science, (to be published, 2004).

11. "Folded Waveguide Traveling Wave Tube Sources of THz Radiation," S. Bhattacharjee, J. H. Booske, D. W. van der Weide, C. L. Kory, S. Limbach, S. Gallagher, J.D. Welter, M. R. Lopez, R. M. Gilgenbach, R.L. Ives, M. E. Read, R. Divan, and D. C. Mancini, Trans. Plasma Sci. (to be published, 2004).

12. "Impulse Amplification in a Traveling Wave Tube I: Simulation and Experimental Validation," M.C. Converse, J.H. Booske, and S.G. Hagness, Trans. Plasma Sci (to be published, 2004)

13. "Impulse Amplification in a Traveling Wave Tube II: Large Signal Physics," M.C. Converse, J.H. Booske, and S.G. Hagness, Trans. Plasma Sci., (to be published, 2004)

14. "Improvements in Graphite-Based X-ray Mask Fabrication for Ultra-Deep X-ray Lithography," R. Divan, D.C. Mancini, S. M. Gallagher, J. Booske, and D. van der Weide, J. Microsystem Technologies (to be published, 2004).

15. "Minimizing Spectral Leakage of Non-Ideal LINC Transmitters by Analysis of Component Impairments," A. Choffrut, B.D. VanVeen, and J.H. Booske, IEEE Trans. Vehicular Technol. (submitted, 2004).

16. "Second and Third Order Signal Injection for Nonlinear Distortion Suppression in a Traveling Wave Tube," A. Singh, J. Scharer, J. Wöhlbier, and J. Booske, IEEE Trans. Elec. Devices (Submitted, 2004).

17. "Nonlinear Space Charge Wave Theory of Distortion in a Klystron," John G. Wöhlbier and John H. Booske, IEEE Trans. Elec. Devices (to be submitted, 2004).

In addition, at least two more papers (currently in preparation) are anticipated to be submitted for publication during 2004-2005 on the subjects of chaotic TWT transmitters and microfabricated folded waveguide TWTs for millimeter-wave and THz regime amplifiers.

4.3.4.2 M.S. and Ph.D. Theses and Reports

1. Mark C. Converse, "Investigation of the Mechanisms of Pulse Amplification in Helical Traveling Wave Tubes," Ph.D. Dissertation, UW-Madison (2003)

2. John G. Wöhlbier, "Nonlinear Distortion and Suppression in Traveling Wave Tubes: Insights and Methods," Ph.D. Dissertation, UW-Madison (2003).

3. John G. Wohlbier, "Modeling and Analysis of a Traveling Wave Tube Under Multitone Excitation," M.S. Thesis, UW-Madison (2000).

4. Sean Gallagher, "Techniques in Microfabrication of a 400 GHz Folded Waveguide Travelling Wave Tube," M.S. Report, UW-Madison (2003)

5. Won-Je Lee, "Reentrant Rectangular Cavity Resonator Design for Millimeter Wave and THz regime Klystrons," M.S. Report, UW-Madison, (2003)

6. Michael J. Wirth, "Experimental Investigations of a Custom Made Helical Traveling Wave Tube amplifier", M.S. Thesis, UW-Madison (2002)

7. Aarti Singh, "Suppression of Nonlinear Multitone Products in a Traveling Wave Tube Amplifier", M.S. Thesis, UW-Madison (2003).

8. Mark N. McNeely, "Evaluation of a Method for Forming Sheet-Electron-Beams from an Initially Round-Electron-Beam using Magnetic Quadrupoles," M.S. Project Report, UW-Madison (2001).

9. Michael J. Neumann, "Initial Experimental Investigations of Intermodulation in a Klystron Amplifier," M.S. Report, UW-Madison (2000).

10. Antoine Choffrut, "LINC methods for Linearizing TWT Amplifiers," M.S. Report, UW-Madison (2001).

11. Ning Zhang, "Conceptual Investigation and Performance Estimation of a THz Micro-Backward Wave Oscillator Circuit," M.S. Report, UW-Madison (2004).

12. Matt Genack, "The Effects of a Mid-Plane Broad Wall Gap on the Electromagnetic Properties of a Folded Waveguide," M.S. Report, UW-Madison (2004).

13. John Welter, "MEMs Microfabrication of THz TWTs and Millimeter-Wave TWT Components," M.S. Report, UW-Madison (to be completed, 2004).

14. Kevin McLaughlin, "Measurements of hot phase velocity and space charge reduction coefficient on a broadband TWT," M.S. Report, UW-Madison, (to be completed, 2005).

4.3.4.3 Conference Papers and Presentations

1. "Localized Growth Rates of Intermodulation Products in a Multitone Traveling Wave Tube Amplifier," J.G. Wohlbier, I. Dobson, J.H. Booske, and J.E. Scharer, The 26th IEEE International Conference on Plasma Science, Monterey, CA, 20-24 June, 1999.

2. "Analysis of 3D Phase Space Dynamics of Pencil-to-Sheet Electron Beam Transformation in Highly-Non-Paraxial Quadrupole Lens System," M.J. McNeely, J.H. Booske, J.E. Scharer, and M.A. Basten, The 26th IEEE International Conference on Plasma Science, Monterey, CA, 20-24 June, 1999.

3. "Simplified Model of a Multitoned Traveling Wave Tube Amplifier," J.G. Wöhlbier, J.H. Booske, I. Dobson, and J.E. Scharer, 41st Annual Meeting of Division of Plasma Physics, American Physical Society (Seattle, WA, Nov. 15-19, 1999).

4. "Traveling Wave Tube Amplifier (TWTA) Physics Using a Custom-Modified Experimental Test Device," M.M. McNeely, M.C. Converse, J.H. Booske, J.E. Scharer, G.

Groshart, B. Gannon, 41st Annual Meeting of Division of Plasma Physics, American Physical Society (Seattle, WA, Nov. 15-19, 1999).

5. "Advanced Investigations of Traveling Wave Tube (TWT) Physics Using a Custom-Modified Experimental Test Device," M.M. McNeely, M.C. Converse, M.A. Wirth, J.H. Booske, J.E. Scharer, G. Groshart, B. Gannon, and C.M. Armstrong, 1st IEEE International Vacuum Electronics Conference, Monterey, CA, May 2-4, 2000.

6. "Investigations of nonlinearities and multitone response in a broad band, high gain, helix traveling wave tube amplifier," M.C. Converse, M.M. McNeely, J.H. Booske, J.E. Scharer, C.L. Kory, and D. Zavadil, 1st IEEE International Vacuum Electronics Conference, Monterey, CA, May 2-4, 2000.

7. "Multifrequency Beam-Wave Interaction in an Idealized Broadband Vacuum Microwave Amplifier Model," J.G. Wohlbier, I. Dobson, and J.H. Booske, 27th IEEE International Conference on Plasma Science, June 4-7, 2000, New Orleans, LA.

8. "Investigations of Non-Linear Spectral Behavior in Multi-Toned Traveling Wave Tube Amplifiers," M.A. Wirth, J.E. Scharer, J.H. Booske, M.C. Converse, M.M. McNeely, J.G. Wohlbier, G. Groshart, B. Gannon, and C.M. Armstrong, 27th IEEE International Conference on Plasma Science, June 4-7, 2000, New Orleans, LA.

9. "Nonlinear Characterization and comparison with simulation of a high gain, broad band helix traveling wave tube amplifier," MM McNeely, MC Converse, JH Booske, JE Scharer, CL Kory, and D Zavadil, 27th IEEE International Conference on Plasma Science, June 4-7, 2000, New Orleans, LA.

10. "Magnetron Simulations and Experiments," M.R. Lopez, R.M. Gilgenbach, S.A. Anderson, Y.Y. Lau, M.L. Brake, C.W. Peters, W.E. Cohen, R.L. Jaynes, J.W. Luginsland, T.A. Spencer, R.W. Lemke, D. Price, J.H. Booske, M.J. McNeely, and L. Ludeking, 27th IEEE International Conference on Plasma Science, June 4-7, 2000, New Orleans, LA.

11. "Investigation of Transients and Pulses in Traveling Wave Tubes," M.C. Converse, J.H. Booske, Y.Y. Lau, S.C. Hagness, M.M. McNeely, M.A. Wirth, J.E. Scharer, and C. Wilsen, 42nd Annual Mtg, Division of Plasma Physics, American Physical Society, November, 2000.

12. "Comparison of Four Multifrequency Traveling Wave Tube Models," J.G. Wöhlbier, I. Dobson, and J.H. Booske, 42nd Annual Mtg, Division of Plasma Physics, American Physical Society, November, 2000.

13. "New Nonlinear Multifrequency TWT Model," J.G. Wöhlbier, J.H. Booske, and I. Dobson, 2nd IEEE International Vacuum Electronics Conference, Huis ter Duin, Noordwijk, Netherlands, 2-4 April, 2001.

14. "Micromachined TWTs for THz Radiation Sources: Proposal and Simulation," J.H. Booske, D. van der Weide, C.L. Kory, S.T. Limbach, S.-J. Lee, S.M. Gallagher, P.J. Gustafson, 2nd IEEE International Vacuum Electronics Conference, Huis ter Duin, Noordwijk, Netherlands, 2-4 April, 2001.

15. "Investigation of Ultrawideband Pulses in Wideband Helix Traveling Wave Tubes: Theory and Simulation," M. Converse, S.C. Hagness, J.H. Booske, M.M. McNeely, M.A. Wirth, J.E. Scharer, Y.Y. Lau, C. Wilsen, C.L. Kory, IEEE International Conference on Plasma Science, Las Vegas, NV, June 2001.

16. "Initial Experimental Investigations of Intermodulation in a Klystron Amplifier," M. Neumann, J.Booske, M. Wirth, J.E. Scharer, P.L. Shum, C. Wilsen, Y.Y. Lau, R.M. Gilgenbach, IEEE International Conference on Plasma Science, Las Vegas, NV, June 2001.

17. "LINC Transmission Using Traveling Wave Tubes," A. Choffrut, B. Van Veen, J. Booske, IEEE International Conference on Plasma Science, Las Vegas, NV, June 2001.

18. "Finite Bandwidth and Space Charge Effects in the MUSE model," J.G. Wöhlbier , J.H. Booske, and I Dobson, IEEE International Conference on Plasma Science, Las Vegas, NV, June 2001.

19. "Investigations of Nonlinear Spectral Behavior in Multi-toned Helix Traveling Wave Tubes," M. Wirth, J.E. Scharer, J.H. Booske, M.C. Converse, M.M. McNeely, G. Groshart, B. Gannon, C. Armstrong, IEEE International Conference on Plasma Science, Las Vegas, NV, June 2001.

20. "Terahertz Regime, Micro-VEDs: Evaluation of Micromachined TWT Conceptual Designs," J.H. Booske, C.L. Kory, D. Gallagher, V. Heinen, K. Kreischer, D. van der Weide, S. Limbach, P. Gustafson, W.-J. Lee, S. Gallagher, K Jain , IEEE International Conference on Plasma Science, Las Vegas, NV, June 2001.

21. "Investigations of Intermodulation in a Klystron Amplifier," M.J. Neumann, J.H. Booske, M.A. Wirth, J.E. Scharer, C. Wilsen, Y.Y. Lau, 43rd Annual Meeting of the American Physical Society's Division of Plasma Physics, Long Beach, CA (Oct 29 – Nov 2, 2001).

22. "Investigations of Non-linear Spectral Growth in a Broadband Traveling Wave Tube Amplifier," M.A. Wirth, J.E. Scharer, J.H. Booske, M.C. Converse, A. Singh, J.G. Wohlbier, and C. Armstrong, 43rd Annual Meeting of the American Physical Society's Division of Plasma Physics, Long Beach, CA (Oct 29 – Nov 2, 2001).

23. "Microfabricated TWTs as high power, wideband sources of THz radiation, " J.H. Booske, W.-J. Lee, S. Gallagher, D. van der Weide, S. Limbach, K. Jain and C.L. Kory, Proceedings of the 9th International Conference on Terahertz Electronics, (Charlottesville, VA, 15-16 October, 2001).

24. "New Opportunities in Vacuum Electronics Using Microfabrication Technologies", J.H. Booske, Third IEEE International Vacuum Electronics Conference, April 23-25, 2002, Monterey CA, USA. **Plenary Talk**

25. "Comprehensive Simulations of Compact THz Radiation Sources Using Microfabricated Folded-Waveguide TWTs," S. Bhattacharjee, W.-J. Lee, S. Gallagher, D.W. van der Weide, J.H. Booske, S. Limbach, 3rd IEEE International Vacuum Electronics Conference, (Monterey, CA, 23-25 April, 2002).

26. "Hot phase velocity measurements and modeling for a broad-band TWT," M. Converse, A. Singh, J. Scharer, M. Wirth, S. Bhattacharjee, J. Booske, C. Armstrong, 3rd IEEE International Vacuum Electronics Conference, (Monterey, CA, 23-25 April, 2002).

27. "The Physics of Harmonic Injection in a TWT," J.G. Wöhlbier, J.H. Booske, I. Dobson, 3rd IEEE International Vacuum Electronics Conference, (Monterey, CA, 23-25 April, 2002).

28. "Intermodulation Suppression in a Broadband TWT," A. Singh, J. Scharer, M. Wirth, S. Bhattacharjee, J. Booske, 3rd IEEE International Vacuum Electronics Conference, (Monterey, CA, 23-25 April, 2002).

29. "Effects of Modulator Misalignment on LINC Transmission with TWT Amplifiers," A. Choffrut, B.D. Van Veen, J.H. Booske, 3rd IEEE International Vacuum Electronics Conference, (Monterey, CA, 23-25 April, 2002).

30. "THz radiation using high power, microfabricated, wideband TWTs," C. L. Kory, J. H. Booske, W.-J. Lee, S. Gallagher, D. W. van der Weide, S. Limbach, and S. Bhattacharjee, Proceedings of the 2002 IEEE MTT-S International Microwave Symposium, Seattle, WA, June 2-7, 2002.

31. "An Eulerian method for computing multi-valued solutions of the Euler-Poisson equations," X. Li, J. Wöhlbier, S. Jin, J. Booske, Annual Meeting of the Division of Plasma Physics, American Physical Society, Orlando, FL, Nov. 11-15, 2002.

32. "Investigation of Various Techniques for Intermodulation Suppression in a TWT amplifier," A. Singh, J. Scharer, M. Wirth, S. Bhattacharjee, and J. Booske, Annual Meeting of the Division of Plasma Physics, American Physical Society, Orlando, FL, Nov. 11-15, 2002.

33. "The Physics of Phase Nonlinearity in a Traveling Wave Tube," J. Wöhlbier, J. Booske, I. Dobson, Annual Meeting of the Division of Plasma Physics, American Physical Society, Orlando, FL, Nov. 11-15, 2002.

34. "A compact folded waveguide traveling wave tube oscillator for the generation of Terahertz radiation," S. Bhattacharjee, J.H. Booske, W.-J. Lee, C.L. Kory, S. Gallagher, M.

Genack, S. Limbach, M.R. Lopez, R.M. Gilgenbach, Annual Meeting of the Division of Plasma Physics, American Physical Society, Orlando, FL, Nov. 11-15, 2002.

35. "THz Radiation using Compact Folded Waveguide TWT Oscillators," S. Bhattacharjee, J. H. Booske, C. L. Kory, D. W. van der Weide, S. Limbach, M. Lopez, R. M. Gilgenbach, S. Gallagher, A. Stevens, and M. Genack, IEEE MTT-S International Microwave Symposium, Philadelphia, June 8-13, 2003.

36. "LATTE/MUSE Numerical Suite: An open-source teaching and research code for traveling wave tube amplifiers," J.G. Wöhlbier, M.C. Converse, J. Plouin, A. Rawal, A. Singh, and J.H. Booske, 30th IEEE International Conference on Plasma Science, Jeju, Korea, June 2-5, 2003.

37. "Experimental observation and characterization of chaos in a driven TWT oscillator with delayed feedback," S. Bhattacharjee, C. Marchewka, J. H. Booske, and J.E. Scharer, 30th IEEE International Conference on Plasma Science, Jeju, Korea, June 2-5, 2003.

38. "Folded Waveguide Traveling Wave Tube Sources of THz Radiation," S. Bhattacharjee, J. H. Booske, D. W. van der Weide, C. L. Kory, S. Gallagher, A. Stevens, M. Genack, M. Lopez, R. M. Gilgenbach[2], J. Wöhlbier, S. Limbach, R.L. Ives, M. E. Read, 30th IEEE International Conference on Plasma Science, Jeju, Korea, June 2-5, 2003.

39. "Injection schemes for TWT linearization" A. Singh, J.G. Wöhlbier, J.E. Scharer and J.H. Booske, 30th IEEE International Conference on Plasma Science, Jeju, Korea, June 2-5, 2003.

40. "Investigations of Folded Waveguide TWT Oscillators for THz Radiation," S. Bhattacharjee, J.H. Booske, C.L. Kory, D.W. van der Weide, S. Limbach, S. Gallagher, A. Stevens, M. Genack, J. Welter, M. Lopez, R.M. Gilgenbach, J. Wöhlbier, R.L. Ives, M.E. Read, R. Divan, D.C. Mancini, 4th IEEE Intl. Vacuum Electronics Conference, Seoul, Korea, May 28-30, 2003. **Invited Talk**

41. "LATTE/MUSE Numerical Suite: An Open Source Teaching and Research Code for Traveling Wave Tube Amplifiers," J.G. Wöhlbier, M.C. Converse, J. Plouin, A. Rawal, A. Singh, and J.H. Booske, 4th IEEE Intl. Vacuum Electronics Conference, Seoul, Korea, May 28-30, 2003.

42. "Experimental observation and characterization of chaos in a driven TWT amplifier with Delayed feedback," S. Bhattacharjee, C. Marchewka, J.H. Booske, and J.E. Scharer, 4th IEEE Intl. Vacuum Electronics Conference, Seoul, Korea, May 28-30, 2003.

43. "Injection schemes for TWT linearization," A. Singh, J.G. Wöhlbier, J.E. Scharer, and J.H. Booske, 4th IEEE Intl. Vacuum Electronics Conference, Seoul, Korea, May 28-30, 2003.

44. “A New View of Phase Distortion in a Traveling Wave Tube,” J.G. Wöhlbier, J.H. Booske, and I. Dobson, 4th IEEE Intl. Vacuum Electronics Conference, Seoul, Korea, May 28-30, 2003.

45. “Investigations of Ultrawideband Pulses in Wideband Helix Traveling Wave Tubes,” M.C. Converse, J.H. Booske, S.C. Hagness, and J. Wöhlbier, 4th IEEE Intl. Vacuum Electronics Conference, Seoul, Korea, May 28-30, 2003.

46. “Experimental observation and characterization of chaos in a driven TWT oscillator with delayed feedback,” S. Bhattacharjee, C. Marchewka, J. H. Booske, and J.E. Scharer, 30th IEEE International Conference on Plasma Science, Jeju, Korea, June 2-5, 2003.

47. “Folded Waveguide Traveling Wave Tube Sources of THz Radiation,” S. Bhattacharjee, J. H. Booske, D. W. van der Weide, C. L. Kory, S. Gallagher, A. Stevens, M. Genack, M. Lopez, R. M. Gilgenbach[2], J. Wohlbier, S. Limbach, R.L. Ives, M. E. Read, 30th IEEE International Conference on Plasma Science, Jeju, Korea, June 2-5, 2003.

48. “Injection schemes for TWT linearization” A. Singh, J.G. Wöhlbier, J.E. Scharer and J.H. Booske, 30th IEEE International Conference on Plasma Science, Jeju, Korea, June 2-5, 2003.

49. “A new look at the nonlinear physics of Traveling Wave Tubes,” J.G. Wohlbier, J.H. Booske, I. Dobson, A. Singh, and J.E. Scharer, 45th Ann. Mtg of Amer. Phys. Soc. Division of Plasma Phys, (Albuquerque, NM, Oct 27-31, 2003).

50. “Experimental observation and characterization of chaos in a driven TWT amplifier with delayed feedback,” S. Bhattacharjee, C. Marchewka, J. Booske, 45th Ann. Mtg of Amer. Phys. Soc. Division of Plasma Phys, (Albuquerque, NM, Oct 27-31, 2003).

51. “Generation of chaotic radiation in a driven TWT amplifier with delayed feedback”, C. Marchewka, P. Larsen, S. Bhattacharjee, J. H. Booske, N. M. Ryskin, V. N. Titov, 5th IEEE Intl. Vacuum Electronics Conference, Monterey, CA, April 27-29, 2004.

52. “Measurements of microwave electrical characteristics of folded waveguide circuits,” M. Genack, S. Bhattacharjee, J.Booske, C. Kory, S.-J. Ho, D. van der Weide, L. Ives, M. Read, 5th IEEE Intl. Vacuum Electronics Conference, Monterey, CA, April 27-29, 2004.

53. “A modal description of intermodulation injection in a klystron,” J.G. Wöhlbier and J.H. Booske, 5th IEEE Intl. Vacuum Electronics Conference, Monterey, CA, April 27-29, 2004.

54. “Sensitivity of Harmonic Injection and its Spatial Evolution for Nonlinear Distortion Suppression in a TWT,” A. Singh, J.E. Scharer, J.G. Wöhlbier, and J.H. Booske, 5th IEEE Intl. Vacuum Electronics Conference, Monterey, CA, April 27-29, 2004.

55. “MEMS-Microfabricated Components for Millimeter-Wave and THz TWTs,” John Welter, John Booske, Hongrui Jiang, Sudeep Bhattacharjee, Steve Limbach, Dan van der Weide,

Ning Zhang, John Scharer, Matt Genack, and Al Mashal, Carol Kory, Lawrence Ives, Mike Read, 5th IEEE Intl. Vacuum Electronics Conference, Monterey, CA, April 27-29, 2004.

56. "Phase Velocity Measurements on a Broadband TWT," K.G. McLaughlin, J.H. Booske, and J.E. Scharer, 31st IEEE International Conference on Plasma Science, June 28 – July 1, Baltimore, MD (2004)

57. "Sensitivity of Harmonic Injection and its Spatial Evolution for Nonlinear Distortion Suppression in a TWT," A. Singh, J.E. Scharer, J.G. Wohlbier, and J.H. Booske, 31st IEEE International Conference on Plasma Science, June 28 – July 1, Baltimore, MD (2004).

58. "Synchronization and Generation of Chaos in a Driven TWT Amplifier with Delayed Feedback," C. Marchewka, P. Larsen, S. Bhattacharjee, J.H. Booske, N.M. Ryskin, and V.N. Titov, 31st IEEE International Conference on Plasma Science, June 28 – July 1, Baltimore, MD (2004).

4.3.4.4 Publicity

Feature Story on Madison ABC Affiliate Channel 27 evening news, "DoD-sponsored Research at the UW-Madison helps save lives of soldiers in the battlefield", Thursday, March 20, 2003.

Feature Story on Wisconsin Public Radio News, "DoD-sponsored Research at the UW-Madison could help improve radar jamming," Friday, April 4, 2003. http://clipcast.wpr.org:8080/ramgen/wpr/news/news030404gh.rm

4.4 Massachusetts Institute of Technology

June, 2004

Richard Temkin, Principal Investigator
MIT Plasma Science and Fusion Center
MIT Building NW16-186
167 Albany Street
Cambridge, MA 02139
Tel. 617-253-5528; Fax: 617-253-6078
Email: temkin@mit.edu

MIT MURI Collaborators (Staff and Students)

A. Akinwande, J. Anderson, R. Bhatt, C. Chen, E. Choi, J. Davies, M. Hess, C. Joye, I. Mastovsky, G. Sha, M. Shapiro, J. Sirigiri, J. Smirnova, R. J. Temkin, P. Woskov, J. Zhou

4.4.1 Summary of MIT Achievements

4.4.1.1 W- Band Gyrotron Amplifier Research

We have reported the successful operation of a novel 140 GHz quasioptical gyrotron traveling wave tube (gyro-TWT) amplifier at a record high power level, namely 30 kW, a significant advancement in the state-of-the-art in gyrotron amplifiers. The gyro-TWT produced up to 30 kW of peak power in 2 μs pulsed operation at 6 Hz achieving a peak gain of 29 dB, a peak efficiency of 12 % and a bandwidth of 2.3 GHz.
This gyro-TWT uses a novel concept of a highly overmoded yet mode-selective structure capable of up to 100 kW of average power operation at W-band (94 GHz). A quasioptical confocal waveguide interaction structure is chosen for its mode selectivity which is very important for operation in a highly overmoded circuit. This research was reported in "High-power 140-GHz quasioptical gyrotron traveling-wave amplifier," J. R. Sirigiri, M. A. Shapiro, and R .J. Temkin, Physical Review Letters, 90, 258302 (2003).

4.4.1.2.Photonic Bandgap Theoretical Research

In PBG modeling research, we have made extensive progress in the development and application of the Photonic Band Gap Structure Simulator (PBGSS) code. The PBGSS code, which employs the standard real-space finite difference method and has been well benchmarked against theory in certain limits, allows for the determination of electromagnetic wave propagation characteristics, such as the dispersion relations, local and global band gaps, and eigenmode field distributions, in the bulk of the two-dimensional metallic lattices. Understanding of the wave propagation characteristics is critical to both conception and design of novel PBG-based vacuum electron devices. We successfully applied the PBGSS code in our comprehensive analysis of TE and TM wave propagation characteristics in two-dimensional square and triangular metal rod lattices. We have also developed a self-consistent technique for analytical calculation of dispersion curves in two-dimensional (2D) metallic photonic band gap (PBG) structures representing square and triangular arrays of metal rods. Major results were published in E.I. Smirnova, C. Chen, M. A. Shapiro, J. R. Sirigiri, and R. J. Temkin, "Simulation of Photonic Band Gaps in metal Rod Lattices," Journal of Applied Physics, Vol. 91, No. 3, pp. 960-968, 2002.

4.4.1.3. Photonic Band Gap Gyrotron

We have demonstrated a novel technique for building a highly overmoded gyrotron resonator which can operate at a high order mode with extremely good mode selectivity. The gyrotron resonator was made of a photonic band gap (PBG) material comprised of a triangular lattice of metal rods. This opens up avenues for building larger dimension overmoded interaction structures for microwave tubes without compromising on mode-selectivity. This technique would mitigate the problems associated with the fabrication of miniature dimension interaction structures at mm wave and sub-mm wave frequencies. The following achievements highlight the research in this area

- A 140 GHz, TE04 –like mode gyrotron oscillator was designed built and tested as proof-of-principle experiment.
- The device demonstrated an unprecedented single mode single frequency operation over a range of operating parameters corresponding to a frequency bandwidth of 30 %.
- Preliminary investigation into building a conventional microwave device with an overmoded PBG interaction structure for portable low power high frequency source development.

This research was reported in J. R. Sirigiri, K. E. Kreischer, J. Machuzak, I. Mastovsky, M. A. Shapiro, and R. J. Temkin Photonic-Band-Gap Resonator Gyrotron Phys. Rev. Letters, Vol. 86, pp. 5628-5631 (June 11, 2001). There were also the following Popular Press Articles about MIT Photonic Band Gap Gyrotron Research:

- "New Microwaves," The Boston Globe, June 12, 2001.
- "Photonic bandgap provides high-frequency gyrotron oscillator," Laser Focus World, August, 2001.
- "Lattice Sends a Crystal Clear Signal," Physical Review Focus, 7 June, 2001.

4.4.1.4 Electron Beam Transport Studies

We have published a journal article [M. Hess and C. Chen, Phys. Lett. A **295**, 305 (2002)] detailing our successful results with the prediction of beam loss in high-power periodic permanent magnet (PPM) klystrons. The physics of the current limit is due to an off-axis interaction of a bunched beam with the surrounding conducting wall. This limit could be the reason why significant beam loss was measured in the SLAC Klystrino. The success that we achieved in predicting limits for bunched pencil beams has motivated us to extend our analysis to include bunched beams of large transverse size. In particular, we have developed a fluid equilibrium model for periodic bunched annular electron beams relativistically propagating in a perfectly conducting pipe with a uniform external magnetic focusing field present. The model can be used to study the beam properties of bunched annular beam used in high-power microwave experiments.

4.4.1.5 Novel Cathode Research

We have successfully fabricated gated carbon nanotube emitter arrays using two different methods. The field emission mechanism of a carbon nanotube was studied and the FEED spectrum obtained agreed with experiment quite well. Both horizontal and vertical growth of carbon nanotubes has been achieved. We demonstrated field emission from multiple walled carbon nanotubes (MW-CNT) deposited on nickel oxide / nickel and platinum / titanium contact layers. The devices show field thresholds and have typical Fowler - Nordheim characteristics.

4.4.1.6 Theory of Crossed Field Amplifiers

We have extended the theoretical analysis of two-dimensional non-axisymmetric equilibrium flow in crossed-field devices, in collaboration with Mission Research Corporation. It is our hope that an improved understanding of the equilibrium flow will help us to identify the origin of noise in crossed-field amplifiers (CFAs). As the electron density approaches the (critical) Brillouin density, we found that a vortex structure with regions of negative potential forms near the cathode surface.

4.4.2 National Student Conference Call Presentations

MIT hosted most of the student conference calls during the MURI program. These were very successful and popular with the students. More than twenty students were listening in on many of these calls. The list of student conference calls is given below:

1. J, Sirigiri, MIT, Feb. 1, 2001, "Results on Gyrotron Research with Overmoded Resonators."

2. J. Wohlbier, Univ. WI, March 20, 2001, "Traveling Wave Tubes with Multifrequency Drive: Applications, Theory, and Research."

3. Y. Miao, Univ. MD, May 15, 2001, "Wide Bandwidth Gyro-Amplifiers Employing TE-Cluster and Extended Interaction Cavities."

4. K. Liu, UC Davis, Nov. 20, 2001, "Optically Gated Silicon Field Emitter Arrays."

5. H. Bosman, Univ MI, Feb. 5, 2002, Investigation of the heating mechanism in gyrotron diamond windows

6. J. Anderson, MIT, April 9, 2002, "Experimental Studies of Nonuniform Emission from a Gyrotron Electron Gun."

7. Aarti Singh of Univ. WI, Oct. 29, 2002, "Nonlinear behavior and intermodulation suppression in a TWT amplifier."

8. Oleksandr V. Sinitsyn, Univ. MD, Jan. 14, 2003, "Comparison of two GKL concepts: multi-cavity conventional GKL vs. cluster-cavity GKL."

9. J.G. Wohlbier, Univ. WI, Jan. 29, 2003, "On the Physics of Harmonic Injection in a TWT."

10. Mike Lopez, Univ. MI, May 20, 2003, "Relativistic Magnetron Experiments on a Microsecond E-Beam Accelerator."
11. Bogdan Neculaes, Univ. MI, March 9, 2004, "Magnetron Microwave Noise Reduction and Rapid-Startup by Azimuthally Varying Axial Magnetic Fields."

12. Heather Song, Univ. CA Davis, April 13, 2004 "Development of a W-Band Heavily Loaded TE01 Gyrotron Traveling-Wave Amplifier (Gyro-TWT) for Advanced Radar Applications"

4.4.3 Students Educated Under MURI'99: MIT

4.4.3.1 MIT Graduate Students Supported by MURI

Student	Type and Date of Degree	Dissertation Title	Status
Jagadishwar Sirigiri	Ph. D. Feb., 2003	A Novel Wideband Gyrotron Traveling Wave Amplifier	Postdoc
(Jagadishwar Sirigiri)	MS Oct., 1999	Theory and Design of a Novel Quasi-optical Gyrotron Traveling Wave Amplifier	Went on to Ph.D. (see above)
Mark Hess	Ph.D. June, 2002	Green's Function Analysis of Bunched Charged Particle Beams	Assistant Prof. Indiana Univ.
Guobin Sha	Ph. D. expected 2004	Carbon Nanotube Field Emission Cathode Arrays	Expected graduation in 2004.
Jing Zhou	Ph. D. Candidate	Intense Beam Physics (to be determined).	Qualified for Ph. D.
Evgenya Smirnova	Ph. D. Candidate	Metallic Photonic Bandgap Structures	Expected graduation in 2004
Colin Joye	MS / Ph. D. candidate	Conducting research on slow wave devices	Graduate student
Eunmi Choi	Ph. D. candidate	Conducting research on gyroamplifiers and other devices	Graduate student
Chad Marchewka	M.S. Candidate	3D Electron Beam Simulations	Graduate student
James Anderson	Ph. D. Candidate	Experimental Study of a 1.5-MW, 110-GHz Gyrotron Oscillator	Expected graduation in 2004, accepted position at MIT Lincoln Lab

4.4.4 MIT Publications

1. Novel Quasioptical Interaction Structure for a Millimeter Wave Amplifier, J. R. Sirigiri, K. E. Kreischer, M. A. Shapiro and R. J. Temkin, Paper PIERS, p. 913, Boston, MA, July 5-14, 2000.
2. Novel Quasioptical W-Band Gyro-TWT, J. R. Sirigiri, K. E. Kreischer, M. A. Shapiro and R. J. Temkin, Paper 15.3, Proc. Int. Vacuum Electronics Conf. (IVEC), Monterey, CA, May 2-4, 2000.

3. Shapiro, M.A., Brown, W.J., Mastovsky, I., Sirigiri, J.R., and Temkin, R.J. "17 GHz Photonic Bandgap Cavity with Improved Input Coupling", Physical Review – Special Topics: Accelerators and Beams Vol. 4, 042001 (2001).
4. Shapiro, M.A., Brown, W.J., Chen, C., Khemani, V., Mastovsky, I., Sirigiri, J.R., and Temkin, R.J. "Improved Photonic Bandgap Cavity and Metal Rod Lattices for Microwave and Millimeter Wave Applications", Conf. Digest: International Microwave Symposium 2000, Boston, Massachusetts, June 11-16, IEEE Microwave Theory and Techniques Society (IEEE Cat. No. 00CH37017), 2000, pt 1, p. 581-4, Vol. 1.
5. Shapiro, M.A., Brown, W.J., Chen, C., Khemani, V., Mastovsky, I., Sirigiri, J.R., and Temkin, R.J. "Photonic Bandgap Structures – Oversized Circuits for Vacuum Electron Devices", Conf. Digest: International Vacuum Electronics Conference 2000, sponsored by IEEE Electron Device Society, Monterey, California, May 2-4, 2000; Paper 16.2.
6. Novel Quasioptical W-Band Gyro-TWT, J. R. Sirigiri, K. E. Kreischer, M. A. Shapiro and R. J. Temkin, Paper 15.3, Proc. Int. Vacuum Electronics Conf. (IVEC), Monterey, CA, May 2-4, 2000.
7. J. R. Sirigiri, K. E. Kreischer, J. Machuzak, I. Mastovsky, M. A. Shapiro, and R. J. Temkin Photonic-Band-Gap Resonator Gyrotron Phys. Rev. Letters, Vol. 86, pp. 5628-5631 (June 11, 2001).
8. J. R. Sirigiri, K. E. Kreischer, M. A. Shapiro, R. J. Temkin, A novel W-band quasioptical gyro-TWT. 25th International Conference on Infrared and Millimeter Waves (Cat. No.00EX442). IEEE. 2000, pp.177-8. Piscataway, NJ, USA.
9. J. R. Sirigiri, K. E. Kreischer, J. Machuzak and I Mastovsky, "A Novel Mode-Selective Gyrotron with a PBG Resonator," 28th IEEE International Conference on Plasma Science IEEE. 2001, Paper O3G3. Piscataway, NJ, USA.
10. "Lattice Sends a Crystal Clear Signal," Physical Review Focus, 7 June, 2001.
11. "New Microwaves," The Boston Globe, June 12, 2001.
12. "Photonic bandgap provides high-frequency gyrotron oscillator," Laser Focus World, August, 2001.
13. E.I. Smirnova, C. Chen, M. A. Shapiro, J. R. Sirigiri, and R. J. Temkin, "Simulation of Photonic Band Gaps in metal Rod Lattices," Journal of Applied Physics, Vol. 91, No. 3, pp. 960-968, 2002.
14. J. R. Sirigiri, C. Chen, M. A. Shapiro, E. I. Smirnova and R. J. Temkin, "New opportunities in vacuum electronics using photonic band gap structures," in High Energy Density and High Power RF: 5th Workshop, B. E. Carlsten, editor, AIP Press, Vol. 625, pp. 151-157 (2002).
15. M. Hess and C. Chen, "Beam confinement in periodic permanent magnet focusing klystrons," Physics-Letters-A. vol.295, no.5-6; 1 April 2002; p.305-10.
16. M. Hess and C. Chen, "Equilibrium and confinement of bunched annular beams," Phys. Plasmas Vol. 9, No. 4, pp. 1422-1430 (April, 2002).
17. "High-power 140-GHz quasioptical gyrotron traveling-wave amplifier," J. R. Sirigiri, M. A. Shapiro, and R .J. Temkin, Physical Review Letters, 90, 258302 (2003).
18. Asymptotic analysis of dispersion characteristics in two-dimensional metallic photonic band gap structures, Smirnova, E.I. (Plasma Sci. & Fusion Center,

Massachusetts Inst. of Technol., Cambridge, MA, USA); Chiping Chen Source: Journal of Applied Physics, v 93, n 10, 15 May 2003, p 5859-65.
19. Experimental results from the MIT 140 GHz quasioptical gyro-TWT
20. Sirigiri, J.R. (Plasma Sci. & Fusion Center, MIT, Cambridge, MA, USA); Shapiro, M.A.; Temkin, R.J. Source: Conference Digest. Twenty Seventh International Conference on Infrared and Millimeter Waves (Cat. No.02EX561), 2002, p 235-6
21. Initial experimental results from the MIT 140 GHz quasioptical gyro-TWT
22. Sirigiri, J.R. (Plasma Sci. & Fusion Center, MIT, Cambridge, MA, USA); Shapiro, M.A.; Temkin, R.J. Source: Third IEEE International Vacuum Electronics Conference (IEEE Cat. No.02EX524), 2002, p 83-4

4.5 University of Maryland, College Park

Principal Investigator: Victor L. Granatstein

Co-Principal Investigators: Thomas M. Antonsen, Jr.
Yuval Carmel
Hezhong Guo
Isabelle Lloyd
Gregory Nusinovich
John Rodgers
Amarjit Singh
Otto Wilson

4.5.1 Executive Summary

This final report summarizes the results of five years of research at the University of Maryland on the topic of innovative microwave vacuum electronics supported by MURI'99. The body of the report is organized into four section (viz. section 3.0 to section 6.0)

Section 3.0 describes analytical methods which have been developed to allow for relatively rapid "zero order approximations' of the performance of microwave vacuum electronic devices. The first device class, which is analyzed, is multi-stage gyro-amplifiers including frequency multiplying devices; this topic is closely related to the experimental work on frequency doubling gyro-amplifiers described in section 4.0. The frequency doubling gyro-amplifier, when compared with gyro-amplifiers operating at the second harmonic in all stages, has the practical advantage of requiring a lower frequency driver, and also, has stronger beam-wave interaction in the input stage so that this stage may be made shorter and more stable. The second analysis topic is non-stationary phenomema in gyrotron oscillators including the discovery of a second region of stable oscillation at very high current in a gyrotron with tapered circuit walls.

The final topic in section 3.0 describes a suite of codes which has been developed to allow for the design of multi-stage depressed collectors (MSDC) in gyro-devices. These codes take secondary electron emission into account. They typically allow for enhancement of device efficiency from ~30% to greater than 50%. This suite of codes has been called "the world's most sophisticated for MSDC analysis" and it has been transferred to U.S. industry for improving the performance of commercially produced gyrotrons.

Section 4.0 describes design and experimental testing of frequency doubling gyrotrons. First the incorporation of mode converters into a gyro-amplifier circuit with the aim of improving stability is described; a frequency-doubling inverted gyro-twystron with internal mode converters achieved stable operation in Ka-band with an output power of 410 kW. Next, the use of an extended interaction output cavity is shown to be effective in increasing bandwidth. The third subsection (viz. 3.3) presents the results of an analytical and experimental study of noise in a frequency-doubling gyro-TWT; it is shown that the average noise density may be significantly lower at the second harmonic frequency than at the fundamental. Finally a new configuration for a wideband mode launcher for use in gyro-TWTs is described.

Section 5.0 describes successful studies of using microwave sintering to fabricate ceramics with high thermal conductivity and controllable electromagnetic loss. Such materials are potentially useful as support structures and output windows in microwave tubes. They have been shown to have thermal conductivity equal to BeO which they would replace since BeO is carcinogenic. They would be much less costly than diamond

Finally section 6.0 describes the potential for exploiting controlled chaos in microwave tubes. Communication systems using such tubes could potentially operate with higher efficiency and with lower probability of intercept. Radar systems using chaotic signals would have higher resistance to jamming and reduced detection probability. While some of these concepts have been investigated at lower frequency relatively little has been done in the microwave regime. Thus, microwave controlled chaos is a ripe topic for future study.

4.5.2 Theory and Modeling of Gyro-Devices

4.5.2.1 Analysis of multi-stage gyro-amplifiers (including frequency-multiplying devices)

Motivation: Operation of multi-stage gyro-amplifiers typically depends on a large number of parameters characterizing an electron beam and parameters of a microwave circuit. Therefore more or less complete numerical optimization of the device performance is very time consuming even with the use of parametric codes (such as MAGY or MAGYKL), while in the case of PIC codes this optimization is practically impossible. This is why, the development of some analytical methods that allow researchers to promptly identify in the "zero-order approximation" the most reasonable range of operating parameters is very important. Then, a more detailed numerical optimization in the "first- and higher-order approximations" can be accomplished much more quickly. (In a certain sense, this sequence of methods is similar to the situation in radars where first a seeking and then tracking regimes of operation are used.)

The work performed at the University of Maryland in the framework of MURI '99 can be characterized by the following results:

3.1A. The linear theory of gyro-TWTs with an initial lossy waveguide section has been developed [1]. This concept, known in linear-beam TWTs, was successfully used in gyro-TWTs first by the group at NTHU, Taiwan led by K. R. Chu where stable operation of a 70 dB, 100 kW peak power, 3% bandwidth, Ka-band gyro-TWT was demonstrated [2]. Then, a similar work was started at NRL [3]. It was shown in [1] that the developed linear theory allows one to rather accurately predict the small-signal gain and bandwidth of such devices.

3.1B. Analytical theory of frequency-multiplying gyro-TWTs has been developed [4]. This theory allows one to evaluate the performance of a two-stage gyro-TWT with a sever separating the input waveguide operating at the fundamental cyclotron resonance from the output waveguide operating at the cyclotron harmonic. Such a concept providing stable operation in each stage was used in gyro-TWT experiments first without frequency-multiplication [5] and later with the frequency multiplication feature [6].

3.1C. Use of the Kompfner dip effect in multi-stage gyro-TWTs of high average power [7]. This work was initiated by the fact that in multi-stage gyro-TWTs the electromagnetic (EM) wave amplified in the first stage should be then absorbed at the end of it. In the case of operation at high average power levels, this absorption can lead to overheating of this part of the device. Therefore, it was proposed to use in the first stage of such device the regime known in linear-beam TWTs as the Kompfner dip. The Kompfner dip occurs when the EM wave is in synchronism with the fast space charge wave of the beam. In such a regime, in the first stage of the device, the EM wave is absorbed by the beam and that greatly (if not completely) solves the problem of heat dissipation in the end of the input waveguide. Then, in the drift region the bunching of electrons modulated in the first stage by the EM wave proceeds, and the bunched beam excites the EM wave in the output waveguide stage of the device. It was shown that, although this mode of operation mitigates the problem of heat dissipation, it also slightly lowers the gain.

3.1D. Comparison of the results of semi-analytical studies with MAGY simulations [8].
In order to know how reliable are results of a simplified treatment of operation of gyrodevices, the comparison of analytical methods with the results of MAGY simulations was carried out for the Ka-band gyro-TWT designed at NRL. It was shown that the results agree very well when beam-wave interaction in the uniform part of the interaction region is considered. At the same time, the inclusion of non-uniform input and output sections into the analysis may cause departure from the simulation results. This discrepancy can, in part, be explained by the fact that, while in MAGY both forward and backward waves are taken into account, the simplified analytical approach neglects the backward waves, although in principle they can also be taken into consideration.

3.1E. Comparison of multi-stage gyro-amplifiers operating in the frequency-multiplication regime with gyro-amplifiers operating at a given cyclotron harmonic [9].
Operation of gyrodevices at cyclotron harmonics has obvious advantages, which stem from the fact that the magnetic field required for generation of electromagnetic waves at a given frequency is inversely proportional to the harmonic number. This is why the study of gyro-amplifiers operating at cyclotron harmonics was in the focus of two groups in the MURI '99 consortium; viz. the University of Maryland and UC Davis. With regard to multi-stage gyro-amplifiers, these two groups considered different approaches. The Maryland group was focused on devices operating in the regime of frequency multiplication, mostly on the case when the first stage operates at the fundamental cyclotron resonance while the output stage operates at a higher harmonic. The UC Davis group developed devices in which all stages operate at the same cyclotron harmonic. Each of these approaches has its pros and cons. The frequency multiplication approach allows one to use a lower-frequency driver, a fact that is especially important with millimeter waves where, with rising frequency, the power of available drivers rapidly decreases, while their cost rapidly increases. At the same time, however, frequency multiplication is a purely nonlinear process. Therefore, such frequency-multiplying devices cannot operate in the small-signal regime and, therefore, cannot be used in many communication systems. On the other hand, gyro-amplifiers operating at a given harmonic need higher frequency drivers, but they can operate in the small-signal regime with a reasonable linearity. Also, the region of operation with high efficiency, in the case of harmonics, corresponds to higher beam currents. Therefore, this efficiency can be realized at higher power levels.

While these simple arguments are quite obvious, the potential of both methods in terms of the achievable efficiency, gain and bandwidth are less obvious. This is why a simple theory has been developed [9], which allows researchers to do such an analysis. The results obtained show that the devices operating at a given harmonic in all stages have better potential for realizing operation with high efficiency and gain, while in the devices operating in the frequency-multiplication regime the bandwidth can be larger because the operation of the input stage at the fundamental resonance allows one to use the low-Q cavities. Without going into details of the analysis performed, it can be stated that the preference of one of these schemes stronger depends on such practical issues as a specific application, availability of drivers at different frequencies, ability to provide stable operation at a higher order mode in the input stage, etc. rather than on the details of the saturation effects.

3.1F. Analysis of new concepts of gyro-amplifiers.

In the course of the work on MURI '99, as well as in the framework of the preceding MURI '94, a number of novel concepts of gyro-amplifiers were proposed at the University of Maryland by H. Guo and V. L. Granatstein. Assessing the potential of these novel concepts is rather easy with the use of analytical methods, which allow one to compare the performance characteristics of new devices with the known ones. In particular, it was proposed [10] to use in gyrodevices the cluster-cavity concept previously suggested for use in linear-beam klystrons by R. Symons [11]. A corresponding analytical formalism was developed in [12] where it was shown that the replacement of single cavities by clusters can significantly enlarge the bandwidth and increase the gain of gyroklystrons while keeping the efficiency practically unchanged.

The use of clusters instead of single cavities constitutes, of course, a complication of a device because each individual cavity is replaced by a multiplet of closely spaced (but uncoupled) cavities. This fact caused some concerns about the validity of the comparison described above. Therefore it was decided to carry out a "one-to-one" comparison of the conventional and cluster-cavity gyroklystrons, i.e. devices, which contain the same number of cavities. For this purpose, a "conventional" gyroklystron having four cavities separated by drift tubes was compared with a clustered-cavity device consisting of single input and output cavities and an intermediate cluster consisting of two adjacent cavities with effectively no drift tube between them (So the total number of cavities in both cases was equal to 4.) The analysis done in the framework of a point-gap model was described in [13] where it was shown that the conventional device has a slightly higher efficiency, while the clustered-cavity scheme has an advantage in its bandwidth and gain. This formalism, in parallel with the code MAGY, was also used for the analysis of electron bunching effects in the design of a frequency-multiplying cluster-cavity gyro-amplifier [14].

4.5.3 Nonlinear and non-stationary phenomena in gyrotron oscillators.

In addition to the work on gyro-amplifiers described above, some studies of interesting and important non-linear and non-stationary effects in gyrotron oscillators were performed.

3.2 A. Start-up scenarios in high-power gyrotrons.

For electron cyclotron plasma heating and current drive in controlled fusion reactors, the gyrotron oscillators should deliver about 1 MW continuous wave power at frequencies above 100 GHz. To handle the thermal loads associated with ohmic losses of this power in cavities, it is necessary to operate at very high-order modes, whose frequency spectrum is very dense and, therefore, an electron beam can simultaneously excite several modes. Therefore, for such devices a proper start-up scenario, which allows one to first excite the desired mode and then to drive it into the regime of MW-level operation with high efficiency, is extremely important. The analysis of such a scenario in a 140 GHz, MW-class gyrotron developed by CPI for plasma experiments on the stellarator "Wendelstein 7-X" was carried out with the use of the code MAGY. (This work was sponsored in part by AFOSR MURI-99 and in part by the Office of Fusion Energy of the U.S. Department of Energy.) Results of the study are published in [15]. These results can be important for the design and operation of W-band, 100 kW CW gyrotrons, which are currently under development at Kirtland AFB [16].

3.2B. Non-stationary phenomena in tapered gyro-backward-wave oscillators.

This work was primarily motivated by very interesting experimental observations of the performance of a tapered gyro-backward-wave oscillator (gyro-BWO) [17]. It was shown in [17] that in the gyro-BWO, whose interaction circuit consists of a regular waveguide with uptapers at both ends, the oscillations can be stable even when the beam current exceeds the starting value by about 250 times. At first glance, these results contradict the known theory of transients in linear-beam BWOs [18], which was confirmed by experiment [19]. As shown in [18, 19], in untapered BWOs the oscillations with constant amplitude becomes unstable when the beam current exceeds the starting value by only about 3 times and then, with a further increase in current, the device exhibits a sequence of transitions to stochastic oscillations. To understand the reason for the differences between the results presented in [17] and [18-19], simulations of the non-stationary oscillations in the gyro-BWO described in [17] were performed with the use of the code MAGY. The results were published in [20] where it was shown that the sequence of events in this device are more complicated than that reported in [17]. First, when the beam current slightly exceeds the starting value, there is a region of stationary oscillations with constant amplitude. Then, at higher currents, these oscillations become unstable. Later, at even higher currents, when the waveguide tapering is strong enough, a second region of stable oscillations appears, and this region includes the operating point of [17]. In this region, the EM field of backward-wave oscillations is self-contracted and is predominantly localized in the region of the first up-taper and the entrance to the regular section of the waveguide. Clearly, such a strongly localized mode has a starting current much higher than that for the field occupying the entire waveguide. This fact explains the observations reported in [17] and elucidates the physics of operation of tapered gyro-BWOs, which may also be relevant to tapered linear-beam devices.

4.5.4 Computer Codes for Depressed Collectors in Gyro-devices (including tracing trajectories of backscattered electrons)

In high power electron tubes, one of the factors that limits the achievable power level is the heat deposited by the spent electron beam on the surfaces of the collectors; there are technological limits to the heat dissipation density that can be adequately handled by a cooling system. A method of alleviating this problem is that of energy recovery from the spent beam by sending it through retarding electrostatic fields using depressed collectors. This technique also increases the overall efficiency of the tube and reduces the soft X-rays that are generated. The method is well developed for linear beam tubes. However, high power tubes of the gyrating beam variety offer special challenges. To address this problem, we have developed a suite of codes, the main ones among these being ProfilEM and BSCAT.

The development of the BSCAT code for enhancing efficiency in vacuum electronic devices while accounting for multiple generations of backscattered electrons has been described in a series of publications, the most recent being [21,22]. Unlike some of the earlier codes, BSCAT does not make an ad hoc determination of the number of backscattered rays to be tracked for each category of backscatter; nor is the user required to insert these numbers. In BSCAT, these ratios are decided within the code by virtue of the Monte-Carlo techniques that are applied and the probability distribution functions for the different parameters of the backscatter phenomenon. The code also automatically allocates the largest number of rays to the locations where the

backscattered current is the highest by virtue of the distribution of energy and incident angle of the primaries. The modeling includes the effects of residual azimuthal motion of incident electrons.

BSCAT iterates between primary and secondary trajectories so as to assure their mutual consistency. It is possible to simulate multiple generations of backscatter, as the number of representative rays for each generation is kept to within reasonable limits by a process of truncation and renormalization. BSCAT has a graphic user interface that shows the trajectories of different generations that can be sorted by specifiable energy ranges. It also shows the collector efficiency and the current collected at different electrodes.

Calabazas Creek Research (CCR), wrote the following in a report for AFOSR concerning their work on depressed collector for an ADT high power, 95 GHz gyrotron, in March 2002: "Simulations for the backscattered trajectories are performed by Dr. Amarjit Singh at the University of Maryland, who has developed the world's most sophisticated suite of design codes for Muti Stage Depressed Collector analysis."

These codes have been applied to designing gyrotron oscillators with enhanced efficiency for both the DOD ADT program as well as for the DOD magnetic fusion program. The gyrotrons used for both these programs are similar and the development of depressed collector codes for gyrotrons has been supported both by the DOE and by MURI '99. The codes are also applicable to gyroamplifiers and to improved design of linear beam devices. The most recent developments were reported at the RF 2003 Workshop [23].

For the case of a two-stage depressed collector for 1.5 MW, 110 GHz gyrotrons, Figure 1 shows the trajectories of the 4^{th} generation of backscattered electrons, This is from a run in which relatively few primary rays were selected to help in the clarity of display for illustrative purposes.

In a typical run, starting with 116 primary rays, the number of 4^{th} generation of backscattered rays is of the order of a few thousand, which is a manageable figure. This number of course depends on the degree of resolution desired in starting points, energy and angles of emergence of the backscattered rays; and on the cumulative percentage contribution that is set, below which rays are truncated. The default percentage is 2%. Figure 2 shows the profile of heat dissipation density as vectors at different locations.

BSCAT uses EGUN as the trajectory tracing code, into which the B-field data is fed via an array of r, z, Br and Bz. It is written in Visual Basic 6, using Windows 2000 as the operating system. It runs on a PC with typical runs lasting a few minutes.

The code is applicable to other types of electron tubes, such as linear beam devices. It could be used in simulation of electron devices and experiments where the effects of backscattered electrons influence the performance and the data generated.

Fig.4.5.1 Trajectories of 4th generation of backscattered electrons in a two-stage depressed collector for a 1.5 MW 110GHz gyrotron

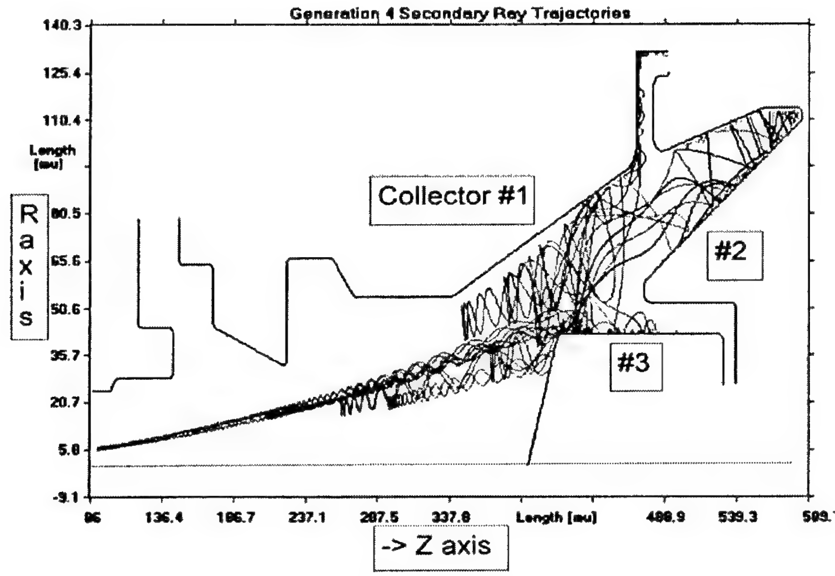

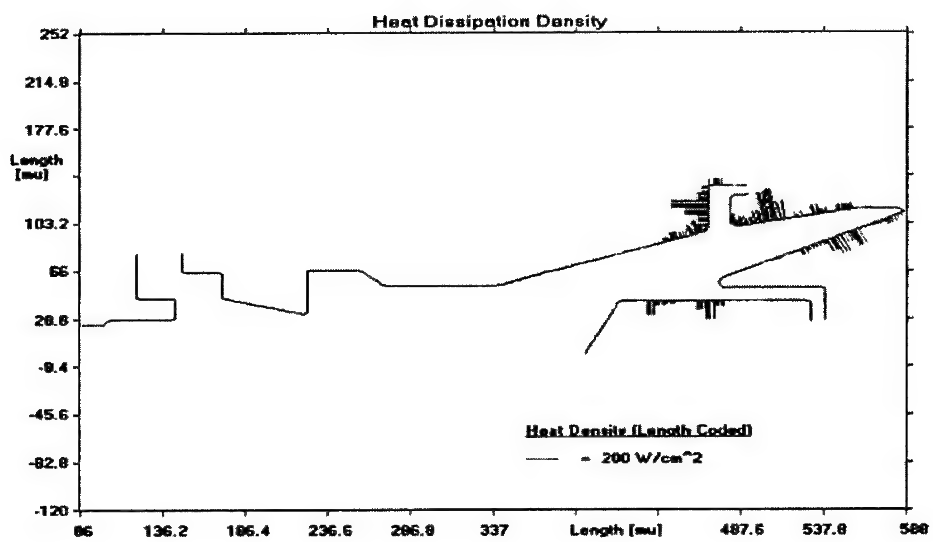

Fig.4.5.2. Heat dissipation density shown as length of vectors in a two-stage depressed collector for a 1.5 MW, 110 GHz gyrotron.

This is an update of the last report that was up to July, 2003, (attached for ready reference as an Appendix). We have described here the enhancements that have been done to the code, BSCAT, the help rendered to industry with a task of simulation of the effects of backscatter in a specific high power millimeter tube, and progress in making the code available to Industry.

During the final year of MURI'99 a number of enhancements in BSCAT and its user interface have been accomplished as follows:

- Vectors showing the direction and magnitude of impacting and emitted electrons were added in the available graphics output.
- These are shown in the r-z plane and separately as a projection on a plane perpendicular to the z-axis; thus providing insights into the azimuthal motion also. Also available is a projection on a plane transverse to the r-z plane, looking from above.
- These facilities have been used in arriving at an understanding of the effects of modifications to the electrode configuration, and feature in the paper to be published in the Trans. IEEE-PS [24].
- Brief guidance for user inputs was provided on-line as text in windows, at various steps in the simulation process

Also, during the final year of MURI'99 direct assistance was rendered to Industry for a simulation task, using BSCAT, and BSCAT was passed on to industry.
Simulations relating to the design of a 2-stage depressed collector for a 1.5 MW 110 GHz gyrotron were done as requested by Calabazas Creek Research. The collector number 2 has been specially shaped with undulations in its cone to minimize the effects of backscatter. Data and diagrams including heat dissipation profiles were simulated and transmitted to CCR. These data were found useful by CCR in updating the cooling channels/system. CCR indicated that this will result in "saving thousands of dollars"
The code BSCAT has been made available to Calabazas Creek Research, along with a User guide and a set of sample files. They are planning to use it in a number of Government sponsored projects. Analysis of the effects of backscattered electrons will be performed for high power millimeter wave tubes as well as for traveling wave tubes.
This will represent a significant step in respect of accurate simulation of backscatter in electron tubes, such that any undesirable effects are corrected at the design stage and surprises are avoided in actual operation. Enhanced accuracy and economic use of computer time are a consequence of the algorithm that has been used and advancements made in modeling of the backscatter process.

4.5.5 Design and Experimental Studies of Frequency Multiplying Gyrotrons

4.5.5.1 Frequency-doubling Inverted Gyro-twystron using Multi-mode Resonant Circuits

Choosing harmonic over fundamental operation in a gyro-device involves some tradeoffs . In general, as the harmonic number is increased, the beam wave interaction becomes weaker resulting in deceased gain and efficiuency. These drawbacks may be mitigated to some extent by increasing the interaction length to extract more energy from the beam. Once lengthened, however, the circuit may be susceptible to various instabilities arising from competing modes, reflections or backward oscillations [25]. Studies have been conducted on various combinations of concentrated and distributed loss, mode filters and mode converters to address these problems [26]

H. Guo proposed that mode converters may be employed in gyrotron cavities to create a chain of symmetric TE modes with increasing radial index n [27]. If the condition $n \geq (s = 2)$ is satisfied, where s is the harmonic number, electrons with opposite orbital phases experience fields with reversed polarity. We then write $\omega = 2\omega_c + k_z v_z$ to describe the fast wave dispersion at the second harmonic of the cyclotron frequency. The condition $n \geq (s = 2)$ also implies that a fairly high order mode is necessary, and as a result, mode competition may be a problem. At the Naval Research Laboratory, a fundamental TE01→TE04 complex cavity gyrotron was studied where it was shown that the conversion process suppressed competing modes resulting in record efficiency (63%) [28]. Studies involving many combinations of modes and harmonics can be found in the literature. We will show but a few examples of the TE0n structures that form the basis for a new family of second harmonic gyro-devices.

At the University of Maryland, a novel mode converter has been employed in both resonant and traveling wave circuits for second harmonic and frequency doubling gyro-devices, respectively. The interaction circuits include a tapered-slot mode converter joining TE0n and TE0(n+1) cavity sections with identical eigenfrequency. Therein, the electrons excite a sequence of coupled modes with similar transverse field profile and wave number. Figure 3 shows a cross-section of a second harmonic output cavity consisting of a loaded beam entrance, the TE02 and TE03 uniform circular sections with the TE02→03 transition between, the output lip and up-taper.

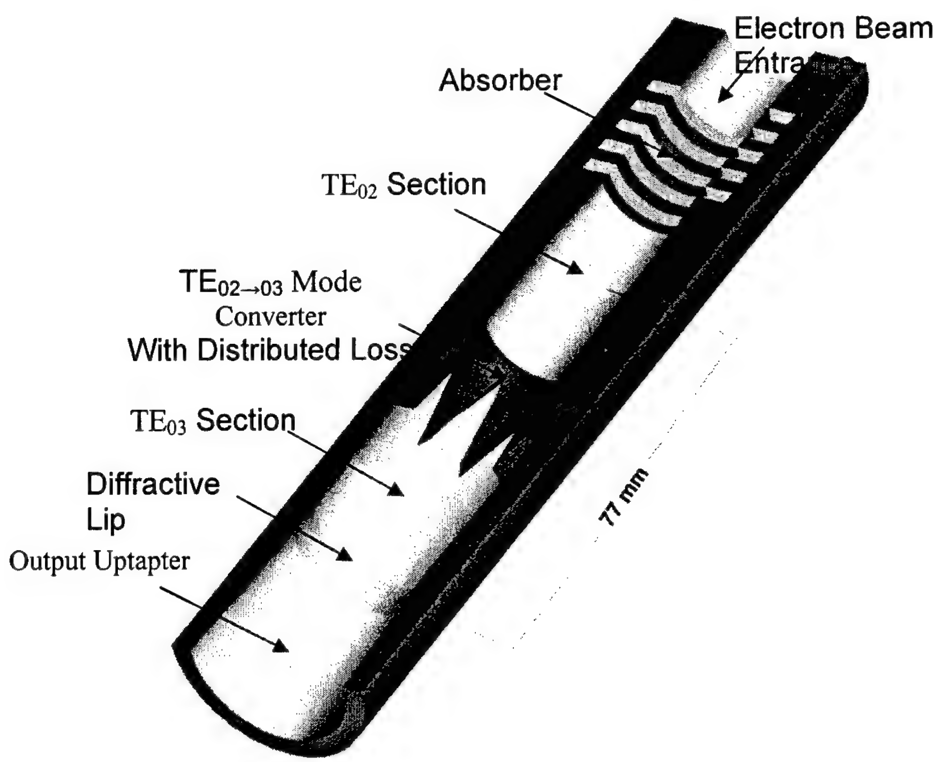

Fig. 4.5.3 35 GHz Multi-Mode Resonant Cavity

RF absorber is placed in the beam entrance tunnel before the up-taper to the TE_{02} waveguide dimension to suppress lower order modes. The effective cavity length is 77 mm, or approximately 9 free-space wavelengths at the second harmonic operating frequency. We note that this structure is uncommonly long compared to more conventional resonant cavities in gyro-monotrons and klystrons. Table 1 lists the design parameters. Figure 4 is a plot of the field intensity on either side of the mode converter from a High Frequency Structure Simulation (HFSS) of the circuit at resonance (34.67 GHz). To save computation time, the calculations were performed on a quarter section with appropriate boundary conditions applied to the cut planes. The first null in the radial field profile (innermost black ring) is nearly the center of the electron orbit (guiding radius).

Table 4.5.1 Design Parameters for Multi-Mode Cavity

TE_{02} Radius x Length (Uniform Section)	9.65 mm x 17.0 mm
TE_{03} Radius x Length (Uniform Section)	14.0 mm x 30.0 mm
Mode Converter, Number of Sections x Length	(8) x 30.0 mm
$TE_{021} \rightarrow TE_{031}$ Cold Resonant Frequency	34.67 GHz
$TE_{021} \rightarrow TE_{031}$ Cold Quality Factor	600

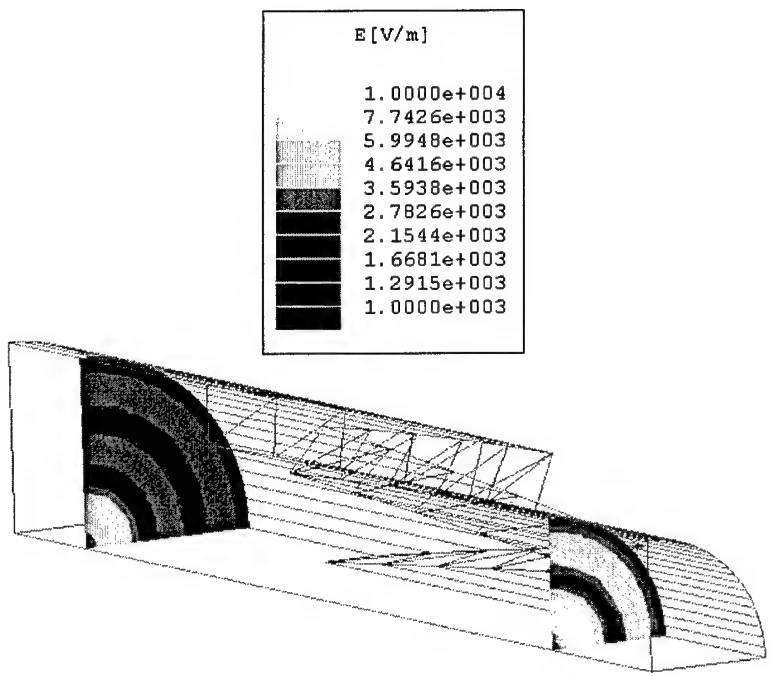

Fig. 4.5.4 Electric Field Patterns in $TE_{02\rightarrow03}$ Multi-Mode Cavity

A novel property of the structure is that the wave number of the operating mode is unaffected by its conversion to the next radial order. Thus, synchronism is maintained with the electron beam over a long distance while for competing modes it is not since their propagation characteristics change in accordance with the varying boundary conditions. This is illustrated in Fig. 5, which shows a plot of cutoff wave number verses axial distance along the converter for several modes. The data in the plot were calculated from an analytic electromagnetic theory.

In long structures, the eigenmodes may have extremely high quality factors (Q) and low self-excitation thresholds. Even at low amplitudes these parasitic modes degrade phase bunching and energy extraction, particularly in harmonic devices.

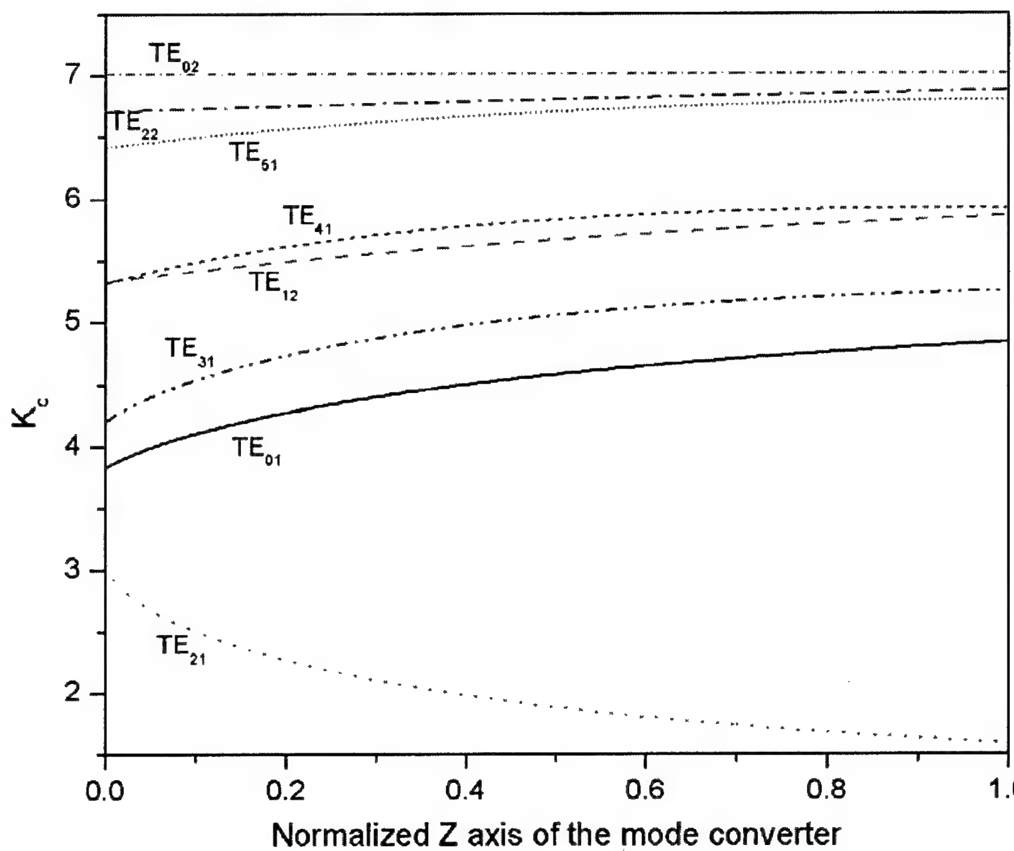

Fig. 4.5.5 ***Cutoff Wave Number (K_c) verses Axial Coordinate Along the Tapered Slots in the $TE_{02\rightarrow03}$ Converter.***

To improve stability, a thin layer of TeNiCrCoAl alloy was vapor deposited on the walls of the cavity near the beam input. Since non-symmetric modes generate higher RF wall currents than the TE0n modes, the absorber selectively lowers their Q. With minor modifications, the structure was tested at the University of Maryland in a number of gyro-devices. These included free-running and phase-locked second harmonic oscillators; phase-locked oscillator and amplifier versions of a frequency doubling, inverted gyrotwystron; and a frequency doubling gyro-TWT (lengthened and with the diffraction lip removed) [29]-[32]. A photograph of the

inverted gyrotwystron is shown in Fig. 6 and Table 2 gives the experimental results. The device was zero-drive stable up to beam currents of 30 amperes. Spurious output was measured to be at least 30 dB below carrier across the entire Ka-band. The results represent unmatched performance for this class of gyro-amplifier. Moreover, the concept has been demonstrated to improve efficiency and stability in harmonic gyro-amplifiers.

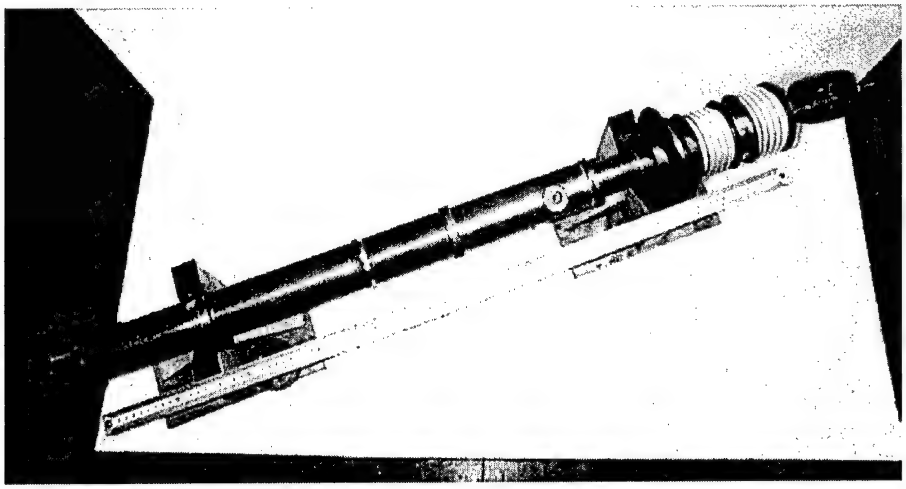

Fig.4.5. 6 Frequency Doubling Inverted Gyrotwystron

Table 4.5.2 34 GHz Frequency Doubling Gyrotwystron Results

Electron Beam Voltage, Current	50 kV, 24 A
Electron Velocity Pitch	1.5
Magnetic Field (electron gun, interaction)	1.1 kG, 6.78 kG
Output Power	410 kW
Efficiency	34 %
Bandwidth	0.7 %

4.5.5.2 Wideband Phase-locked Gyro-oscillator using Extended Interaction Output Cavity

In cavity devices, bandwidth is limited by the resonant characteristics of the circuit. In the gyro-TWT, bandwidth is the frequency range over which synchronism can be maintained between the electromagnetic and fast cyclotron waves. It would be desirable to combine the high interaction efficiency and low voltage capability of the gyro-klystron with the wide bandwidth of

traveling wave circuits. In this section, we will present such an approach using a novel cavity configuration.

Modes with the same transverse structure but many axial variations, signified by index l, are excited in extended interaction cavities such that their resonances overlap [33] The diffraction quality factors and the spacing between axial eigenfrequencies scale approximately as $Q_l \propto (L/l\lambda)^2$ and $\Delta f/f \propto (\lambda/L)^2(2l-1)$, respectively. Here, L is the cavity length; f and λ are the frequency and free-space wavelength of the radiation. Figure 7 shows Q_l and Δf verses l for a 32 GHz, multi-mode TE_{42} output cavity. The results were calculated numerically using HFSS modeling. We can see that as l increases, Q_l goes down asymptotically to zero as the wave approaches a purely propagating state as expected. In the plot, the frequency spacing is defined as $\Delta f = f_l - f_{l-1}$, where f_l is the exact resonant frequency of mode l. The actual dependence on l is not linear at high indices as the above equation approximates. This is because the simulation accurately predicts the frequency-dependent effective length and diffraction losses in the cavity.

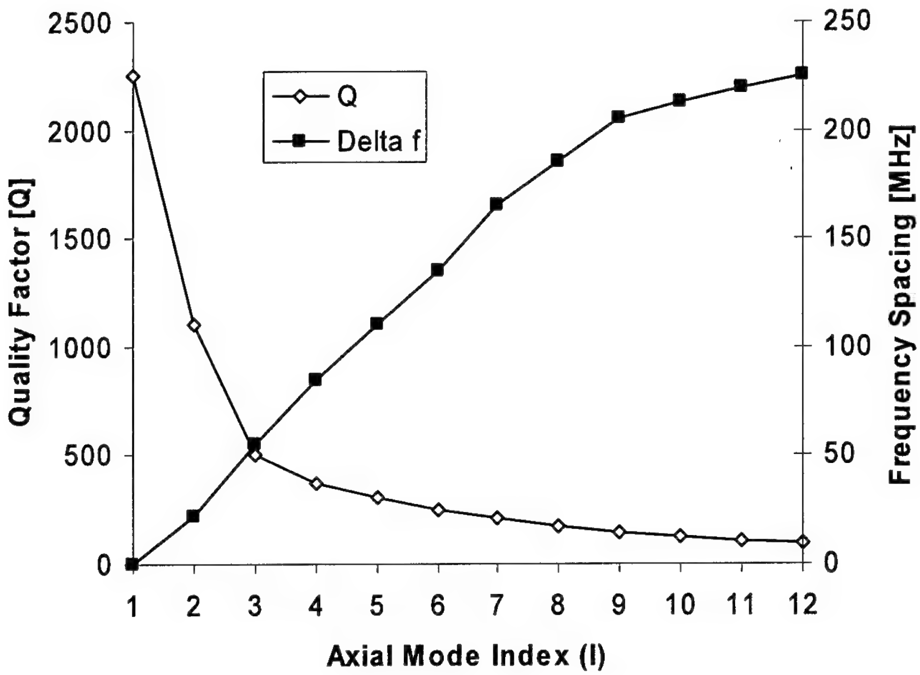

Fig. 4.5.7 Axial Modes in Extended Interaction Cavities

By proper choice of the structure dimensions, and ohmic and diffractive losses, the frequency response of a series of axial modes may overlap and couple. Figure 8 shows the axial profile of the electric field intensity in a TE_{42} extended interaction circuit resonating with the fifth axial mode (l=5).

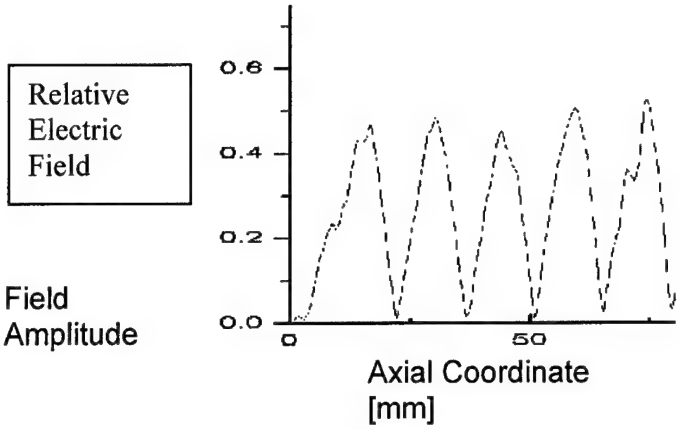

Fig. 4.5.8 Axial Profile of the RF Field in an Extended Interaction Cavity

At the University of Maryland, the concept was tested in a frequency-doubling inverted gyrotwystron operated as a phase-locked oscillator. Phase locking was accomplished by injecting RF power into a TE_{41} pre-bunching TWT section tuned near the fundamental cyclotron harmonic and at half the TE_{42} resonant frequencies of the output. Nonlinear phase bunching generated the second harmonic of the signal frequency in the beam current, which excited the output cavity with phase locked oscillations. As the input frequency was swept, phase-locking was observed in the output over a bandwidth that exceeded the frequency response of a single mode by approximately a factor of five. Figure 9 shows the experimentally measured gain and output power verses frequency. Table 3 summarizes performance of the tube.

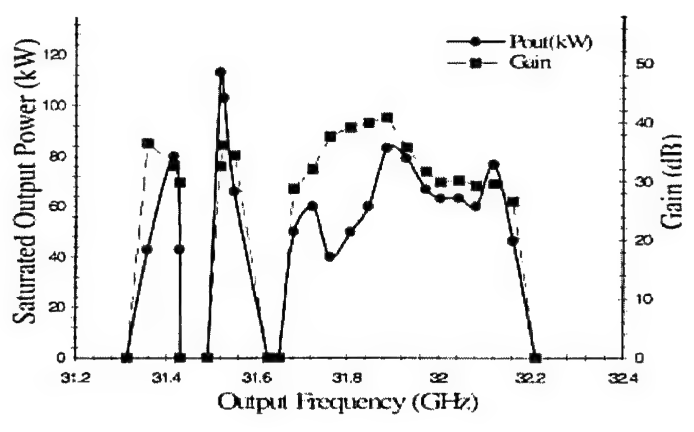

Fig. 4.5.9 Phase-locking bandwidth in a second harmonic inverted gyrotwystron showing overlapping axial modes

Clearly seen in the figure are several regions of locking bandwidth. The TE421 and TE422 modes centered at 31.39 and 31.54GHz, respectively, do not exhibit overlapping frequency response because their quality factors are too high (ref. Fig. 7) and do not overlap. However, the

TE421 modes with l=3, 4 and 5 form a nearly continuous band of operating frequencies. Locking was observed as high as the l= 7 mode albeit at lower gain. It should be noted that the experiment was proof-of-principle and that the guiding magnetic field and electron beam parameters had not been optimized. Even so, the idea was shown to merit further investigation to ascertain whether higher gain, bandwidth and efficiency could be achieved.

Table 4.5.3 Performance of 32 GHz Extended Interaction Second Harmonic Inverted Gyrotwystron

Beam Voltage, Current	58 kV, 9.2 A
Magnetic Field (Gun, Circuit)	1.10 kG, 6.75 kG
Saturated Locking Gain	33 dB
Locking Bandwidth, TE_{42l} with l= 3,4,5	1.3 %
Peak Output Power	85 kW
Efficiency	16 %

4.5.5.3 Noise Measurements in a Frequency-doubling Gyro-TWT

Frequency multiplying (FX) gyro-amplifiers [6] usually consist of multiple interaction stages, each one operating at a specified harmonic (s) of the electron cyclotron and input signal frequencies. By convention, a number sequence signifies the operating harmonic of each section (beginning with the input). For example, a "1-2-2 gyroklystron" is a frequency-doubling amplifier consisting of a fundamental input and second harmonic intermediate and output sections. These schemes have the advantage over purely harmonic gyro-devices (those with s> 1 throughout) because the gain of the input section is higher. Thus, stronger electron bunching is achieved with modest input stage length. With sufficient drive power and drift length, nonlinear processes generate harmonics of the drive signal in the beam current. Subsequent sections are excited at s_n times the drive frequency, where the subscript indicates the section number operating at its given harmonic. Since the gain in FX gyro-devices is inherently nonlinear; which can be expressed by $P_{out} = G^s P_{in}^s$ where P_{out} and P_{in} is the output and input powers, respectively, and G is harmonic gain; modulation of the carrier (by applied and noise signals) produces inter-modulation products of order s in the output even in the small signal regime. Applications of FX gyro-devices include millimeter wave amplifiers for coherent radars and high-gradient accelerators, which are typically operated near saturation for high power and efficiency. Also, superior phase stability and low noise are required to achieve high resolution and particle energy, respectively. Therefore, the understanding and characterization of the gain and noise characteristics over a wide dynamic range in these devices is very important.

The concern is that FX noise figure will be excessive since the total output noise power will consist of all harmonic products of the carrier and modulation sidebands including injected and electron shot noise at the input stage. In the small signal regime, estimating FX noise figure is fairly straightforward since the gain as defined above is constant. The saturated gain

characteristic is much more complicated. A modulated input carrier produces nonlinear upper and lower sideband (USB and LSB respectively) products in the output. Around saturation, input amplitude modulation (AM) will be converted to phase modulation (PM). At the University of Maryland, harmonic gain was studied in a frequency doubling gyro-TWT. The results are in good agreement with simple analysis using narrowband signal theory. Here, we will present a brief overview of the analysis and some important experimental results.

We begin by assuming that the F2 gyro-amplifier behaves like a classical frequency doubling circuit. We also consider the noise spectrum as many discrete narrowband signals with a given offset from the carrier frequency. Thus, we can apply narrowband modulation theory to describe the dependence of sideband gain on carrier amplitude. The input and output signals are represented as

$$A_{in} = \tilde{A}_i(t)e^{-i\omega_0 t} + C.C.$$

$$A_{out} = \tilde{A}_o(t)e^{-i2\omega_0 t} + C.C$$

where A_{in} and A_{out} is the amplitude of the input and output envelopes with normalizations given by $P_{in} = \left|\tilde{A}_{ic}\right|^2$ and $P_{out} = \left|\tilde{A}_o\right|^2$, respectively, ω_0 is the carrier angular frequency and C.C. are complex conjugate terms. The relation between the output and input amplitude is $\tilde{A}_o(t) = G_{P_i}\tilde{A}_{ic}^2(t)$. Here, G_{P_i} is the complex, drive-dependent gain. When written in phasor notation $\left|\tilde{A}_o(t)\right|e^{-i2\phi_i} = G_P\left|\tilde{A}_{ic}^2(t)\right|e^{-i\phi_i}$ we see that the output phase is twice the input as expected in a frequency doubler. With these basic definitions in place, the FX output power follows the expected form, namely $P_{out} = \left|G_{P_{in}}\right|^2\left|\tilde{A}_i\right|^4 = \left|G_{P_{in}}\right|^2 P_{in}^2$.

We now consider inter-modulation when the input consists of the carrier and a sideband offset by $\Delta\omega$ with amplitudes A_{ic} and δA respectively. This is consistent with linear noise theory where the input signal is represented by an ideal carrier with additive noise $\tilde{A}_i(t) = \tilde{A}_{ic} + \delta\tilde{A}e^{-i\Delta\omega t}$. Now, the output is given by $\tilde{A}_o(t) = G_{P+\Delta P}(\tilde{A}_{ic} + \delta\tilde{A}e^{-i\Delta\omega t})^2$ where the subscript $P+\Delta P$ means we must account for small perturbations in gain since it depends on the drive level as well. Therefore, we write $\tilde{A}_o(t) = G(\left|\tilde{A}_{ic} + \delta\tilde{A}e^{-i\Delta\omega t}\right|^2)(\tilde{A}_{ic} + \delta\tilde{A}e^{-i\Delta\omega t})^2$ and after expanding,

$$\tilde{A}_o(t) = G(\left|\tilde{A}_{ic}\right|^2 + A_{ic}^*\delta\tilde{A}e^{-i\Delta\omega t} + A_{ic}\delta A^* e^{+i\Delta\omega t} + HOT)(\tilde{A}_{ic}^2 + 2A_{ic}\delta\tilde{A}e^{-i\Delta\omega t} + HOT). \quad (1)$$

The third term in the gain function is a lower intermodulation sideband and HOT refers to high order terms in δA. We can neglect these terms due to their smallness if the signal to noise ratio (SNR) is assumed to be large, which is usually the case in any practical system. By Taylor series expansion, (1) can be written approximately as,

$$\tilde{A}_o(t) \approx G_P(\left|\tilde{A}_{ic}\right|^2)\tilde{A}_{ic}^2 + e^{-i\Delta\omega t}(2G_P A_{ic}\delta\tilde{A} + \frac{\delta G_P}{\delta\left|A_{ic}\right|^2}A_{ic}^*\delta\tilde{A}A_{ic}^2) + e^{+i\Delta\omega t}(\tilde{A}_{ic}^3\delta A^*\frac{\delta G_P}{\delta\left|A_{ic}\right|^2}). \quad (2)$$

Here, we have grouped terms according to their frequency with the coefficients being the carrier, upper and lower sideband gains. Note that the upper sideband is expected to have twice the initial gain as the carrier in the small signal regime while the lower sideband should only appear

where the gain function has a non-zero derivative (near saturation). From (2), the individual sideband gains are

$$g_+ = 2G_P + \left|A_{ic}\right|^2 \frac{\delta G_P}{\delta\left|A_i\right|^2} \tag{3}$$

$$g_- = \left|A_{ic}\right|^2 \frac{\delta G_P}{\delta\left|A_{ic}\right|^2}, \tag{4}$$

and the sideband powers are given by

$$P_{o+,-} = \left|g_{+,-}\right|^2 \left|A_{ic}\right|^2 \left|\delta A\right|^2. \tag{5}$$

If the complex gain function for any given FX device is known either by analysis or experimental measurement, the nonlinear noise gain may be predicted. In the experiment, the carrier and sideband gains and phases are experimentally measured. The derivative of the gain function is computed numerically from the data.

The harmonic gain was experimentally measured in a three-stage frequency doubling gyro-amplifier consisting of a $TE_{01\rightarrow02}$ multi-mode fundamental gyro-TWT input section, radiation-free drift section containing a series of second harmonic buncher cavities and a second harmonic $TE_{02\rightarrow03\rightarrow04}$ multi-mode output section. Table 4 gives the operating parameters, and Fig. 10 shows a schematic of the tube configuration. Harmonic gain was measured as follows. First, an unmodulated carrier was injected into the input. The output power and phase shift were measured while the input power was varied over a 50 dB dynamic range. Figure 11 is a plot of the carrier power, gain and efficiency verses drive power covering the small and large signal regimes. In the above analysis, the harmonic gain of each sideband should depend on the derivative of the gain function. The derivative of the experimentally measured gain function with respect to input power can be computed numerically and substituted into (3) and (4) to compute (5), which gives a semi-empirical prediction for the upper and lower sideband powers. Next, a small amplitude single sideband tone was injected along with a carrier whose power was swept over the dynamic range of the tube. The output sidebands-to-carrier ratio was measured, and the data is plotted in Fig. 12. The experimental data are in good agreement with the calculated values, which are shown for comparison. The results show that the total harmonic power in the sidebands is constant since the USB gain compresses at the same rate the LSB gain increases near saturation. We conclude that the noise figure in frequency doubling gyro-amplifiers is dominated by the noise figure of the driver.

In gyro-amplifiers, the shot noise spectrum should have peaks around harmonics of the cyclotron frequency with spectral density that decreases as the harmonic number increases. With the input signals removed from the gyro-TWT and the input port terminated, the noise spectrum was measured across the gain bandwidth at the fundamental and second harmonic frequencies of the tube. In Fig. 13, the noise spectral density is plotted across the fundamental and second harmonic gain bandwidths. The average noise density is approximately 10 dBm/Hz lower at the second harmonic frequencies. Thus, harmonic and frequency doubling amplifiers have the advantage of low intrinsic noise when operated in the small signal regime.

Table 4.5.4 Frequency Doubling Gyro-TWT Experimental Parameters

Operating Parameter	*Value*
Beam Voltage [kV]	62
Beam Current [A]	5.0
Input Center Frequency [GHz]	16.8
Output Center Frequency [GHz]	33.6
Output Power [kW]	80
RF Pulse Width (FWHM) [μsec]	20
Repetition Frequency (PRF) [Hz]	50
Bandwidth	500 MHz (1.5 %)
Gain (saturated) [dB]	36
Mean Phase Deviation [deg]	0.5
Second Harmonic Efficiency	12 %

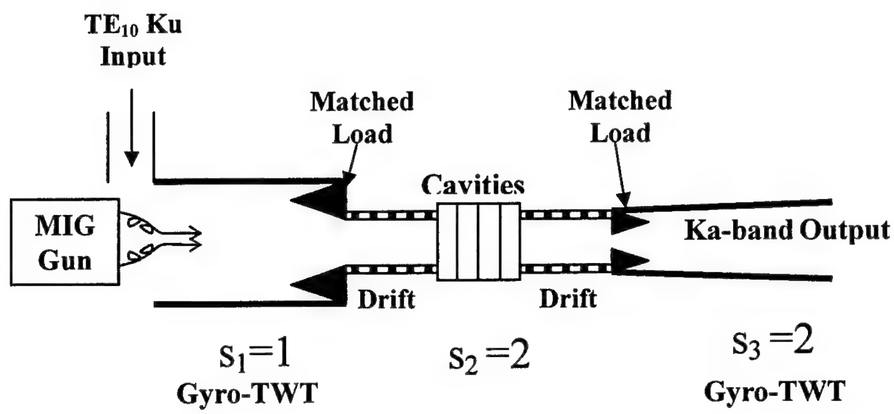

Fig. 4.5.10 Schematic of Frequency Doubling Gyro-TWT

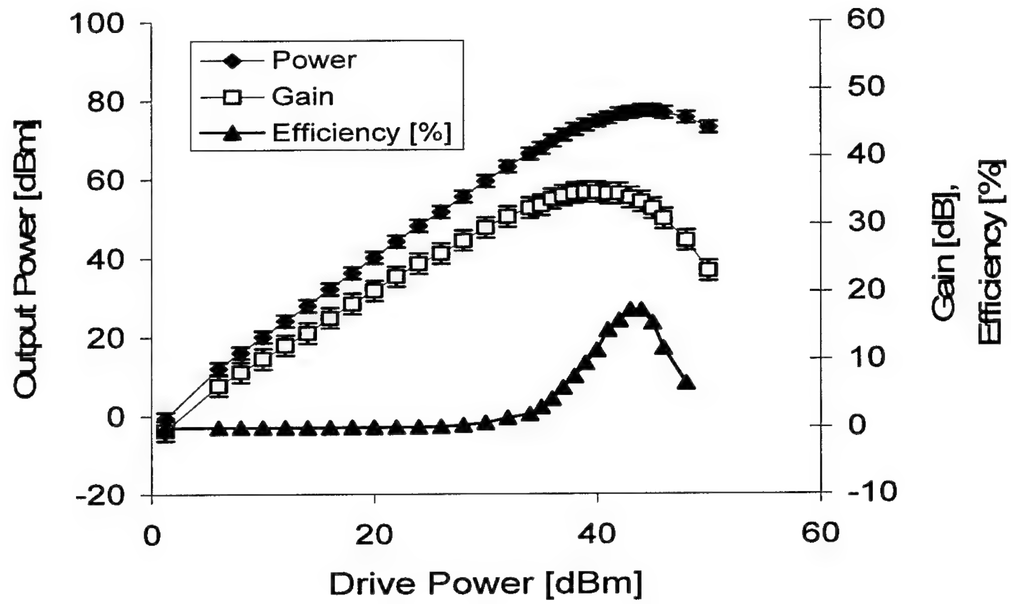

Fig. 4.5.11 Drive Characteristics of the Frequency Doubling Gyro-TWT

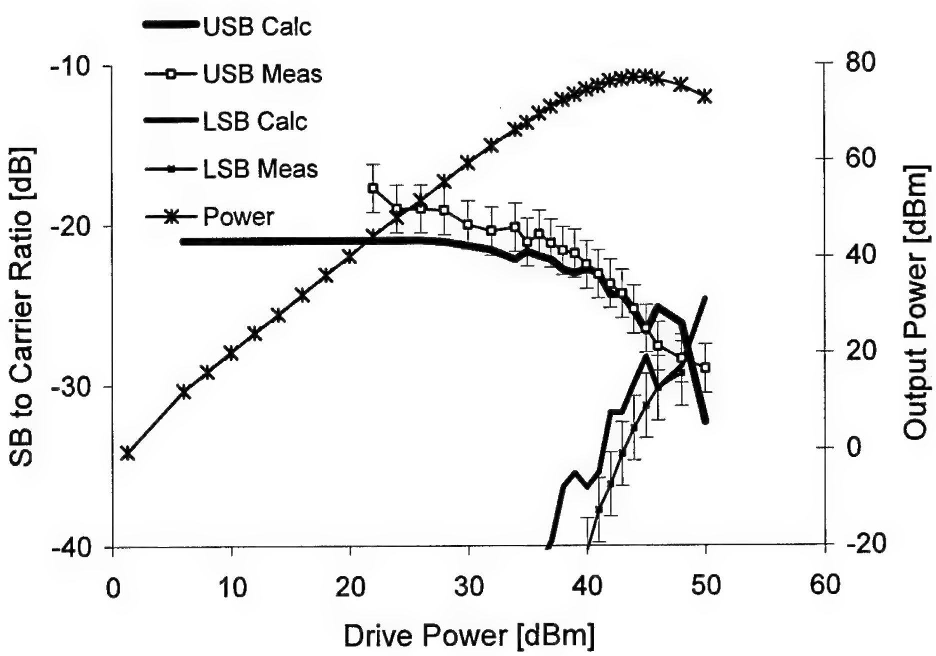

Fig. ***4.5.12 Comparison of Calculated and Measured USB and LSB-to-Carrier Ratio***

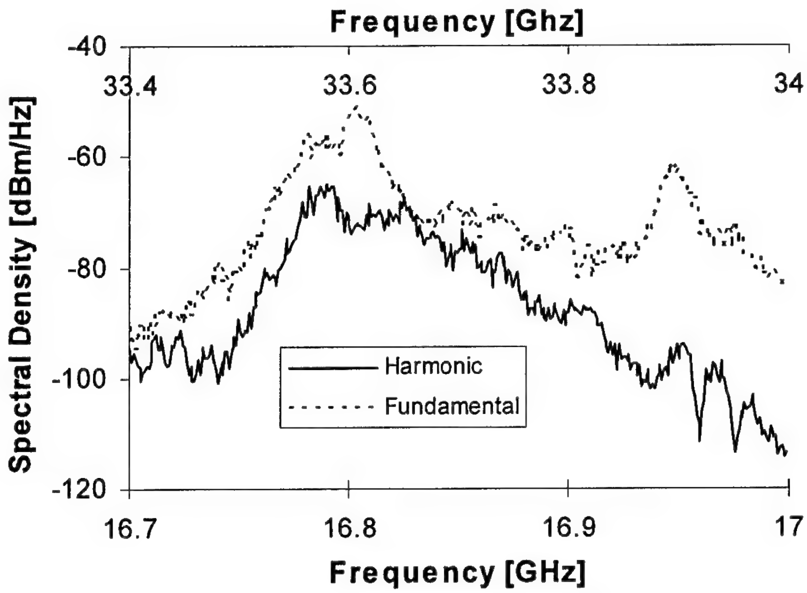

Fig. 4.5.13 Fundamental and Harmonic Intrinsic Noise Spectra

4.5.5.4. Wideband Radial TE_{01} Mode Launcher for Gyro-TWTs

One of the challenges in developing wideband TE-mode gyro-traveling wave tubes is the design of the input mode launcher. In cavity-based gyro-devices, the input mode may be excited by much simpler means (such as coupling apertures) since the circuit is usually operated at one resonant eigenfrequency. Achieving low and reasonably flat VSWR over wide bandwidth (~20%) is critical for stable traveling wave amplification. Not only is flat gain response important for applications such as coherent radar, but, in terms of stability, even small input reflections, especially in concert with other mismatches, can lead to oscillations and unstable gain characteristics. Various designs for multiple aperture TE mode couplers are presented in the literature. Many of these have distinct disadvantages. End-fire TE_{01} couplers, such as the Stanford "rosepetal" launcher (Tantawi), have the input waveguide placed (at the nodes of the transverse field profile) precisely where the electron beam should be located. Longitudinal sidewall couplers add substantially to the length of the input stage and produce marginal purity for high order TE modes. A new wideband radial TE_{01} launcher was developed under the MURI'99 program. The structure has been studied numerically, and a prototype has been constructed and cold tested. Here, the basic design and experimental results will be summarized. Figure 14 shows a photograph of the prototype coupler, which was designed for Ka-band TE01 gyro-TWT inputs. The circuit consists of TE10 rectangular input waveguide, which is split four ways via three H-plane tee sections. Each branch feeds a horn that is directed radially towards a quadrant of the circular TE01 waveguide. The channels and horns are precision CNC machined as mirror images into two plates fitted with accurate alignment pins. Since phase matching of the TE10 propagation paths is critical for high conversion efficiency, the structure is machined from solid plate stock for rigidity. The half pieces are joined along the mid-plane (E-plane) of the

rectangular waveguide to form the completed structure. The vacuum compatible version would be brazed at the joining surface and include a wideband TE10 input window.

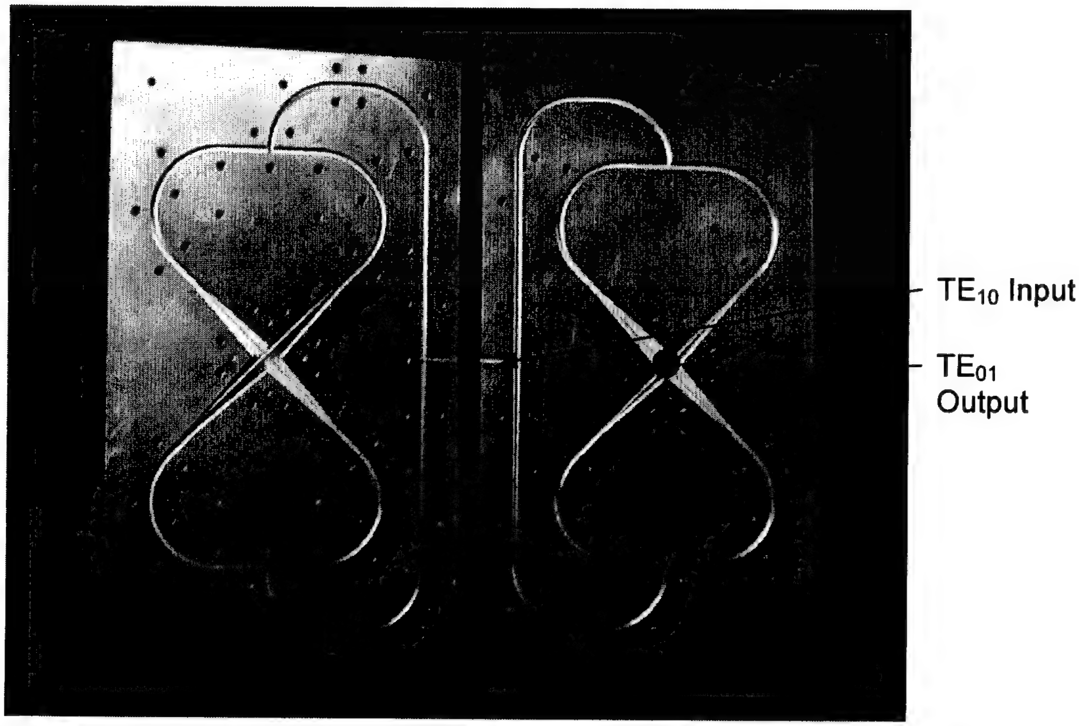

Fig. 4.5.14 Ka-band TE_{01} Mode Launcher

Figure 15 is a plot of the S-parameters verses frequency from an HFSS simulation of the structure. The 1 dB bandwidth is 8.6 GHz, or approximately 24%. The mode purity is excellent. The TE11 and TE21 spurious mode powers are more than 30 dB below the operating mode. Cold test measurements, where 20% bandwidth was achieved, on a scaled Ku-band prototype were in very good agreement with HFSS simulations. The sharp dip at around 40 GHz is caused by conversion of the TE10 to the TE21 mode in the taper section. A design using ridged verses rectangular waveguide may prevent this effect and further improve bandwidth.

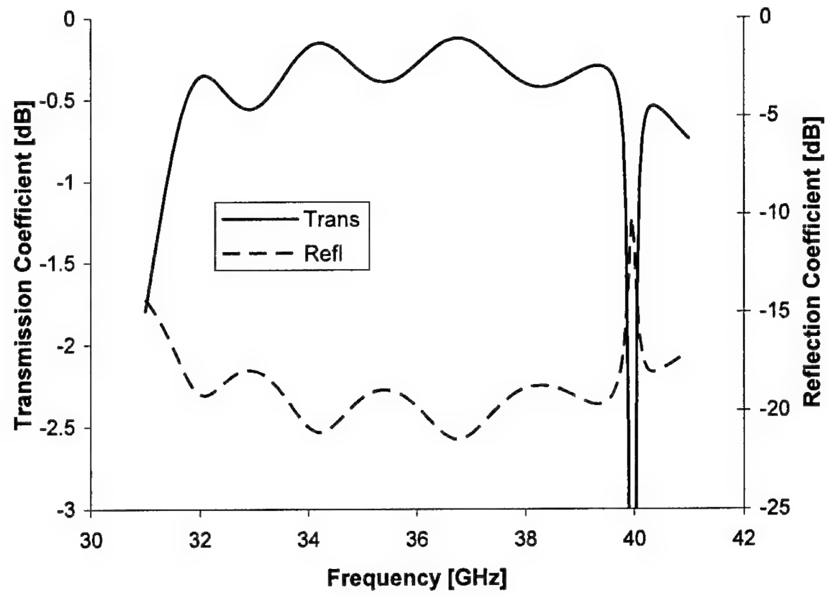

Fig. 4.5.15 $TE_{10} \rightarrow TE_{01}$ Mode Converter Transmission and Reflection

4.5.6 High Thermal Conductivity Materials with Tailored Losses (fabricated by microwave sintering)

Advanced new materials with superior thermal and dielectric properties for support structures, controlled loss buttons, and windows are needed to replace BeO based materials in vacuum microwave sources; BeO dust has been determined to be a carcinogen and BeO structures e no longer being fabricated. These new materials, when available, can lead to improvement in the performance of power microwave devices. Some promising materials have been developed at the University of Maryland under MURI'99. While diamond based materials are hard to beat with respect to thermal conductivity (>1100W/m 0C), cost is a serious issue. The development status of high power millimeter wave windows with emphasis on CVD diamond is described elsewhere [34]. Aluminum nitride (AlN) and its composites are attractive as reasonable cost alternatives. Advanced sintering and synthesis techniques, such as microwave processing, have the potential to take full advantage of the superior intrinsic properties of these materials. As an example, fig. 16 shows the thermal conductivity of microwave processed advanced AlN based ceramics versus benchmarks such as copper, commercial AlN, berylia ceramics and alumina. Advanced microwave processing techniques allows for the development of near single crystal thermal conductivity in AlN. The very low dielectric loss and high thermal conductivity of AlN [35] makes it especially attractive for windows and support structures in power microwave tubes, as well as for electronic packaging of power semiconductors. Combining AlN with a lossy material like TiB2 [36], SiC [37] or C allows development of high thermal conductivity composites with designed (tailored) dielectric losses for controlled loss buttons and support structures where losses are desirable (e.g., helix TWT).

The single crystal value of the thermal conductivity for AlN is close to that of metals like copper, as shown in Fig. 16. However, in commercially available engineering (i.e.

polycrystalline) ceramics the thermal conductivity is generally much lower. Microstructure (number, geometry, and identity of phases) and composition are the key to enhancing thermal conductivity and dielectric properties in polycrystalline materials. The structure of real engineering (i.e. polycrystalline) materials is much more complex than single crystals. Polycrystalline materials have oxide impurities and additives that limit thermal conductivity through low conductivity phases at grain boundaries and surfaces as well as phonon scattering between and within phases. New modeling approaches show us that by controlling and tailoring the microstructural geometry, the resulting thermal conductivity could approach that of single crystals [38-40]. However, it is still very difficult to produce the modeled microstructures in real materials. Currently, development of microstructures that approximate modeled microstructures is largely a result of experimental trial and error. Advanced processing techniques (such as the microwave sintering studied under this MURI program [41]) along with identification and understanding of appropriate additives is critical to the ability to manufacture of designed microstructures. Microwave processing offers the potential to tailor microstructure. Fig.17 shows that the average grain size of ZnO rapidly decreases with increasing heating rate. At the extremely rapid heating rate of 5000 ^{0}C/sec (available with microwave processing), grain growth was suppressed in ZnO so much that the grain size of the densified bulk material is similar to that of the starting powder. It is still an open question whether nano powders will behave in a similar way, but the potential is tremendous. As indicated earlier, the grain size and microstructure control the dielectric and thermal properties (as well as other properties like mechanical, optical, magnetic and acoustic behavior).

Processing additives for AlN ceramics tend to fall into two categories. The first type is additives that enhance densification and development of high thermal conductivity. Yttria (Y_2O_3) is one such material. It forms a liquid phase that scavenges oxide from the AlN grains as it enhances densification through particle-particle rearrangement and enhanced mass transport. All of these increase thermal conductivity. The second type is additives that produce controlled dielectric losses. Lossy materials like TiB_2, SiC or C dispersed in an AlN matrix produce losses. If the continuity of the AlN matrix is maintained and the dispersed materials do not react with the AlN to form solid solutions or low conductivity phases then composites with good thermal conductivity can be formed. Multi-scale modeling [42,43] can allow us to calculate the thermal conductivity and dielectric properties of real materials with complex microstructure (geometry) where simple analytical solutions are not adequate.

Advanced processing is critical to the development of materials with controlled microstructures. For example, the best thermal conductivity in AlN materials is developed after the liquid phase sintering additives have done their job and migrated to multi-grain junctions leaving most AlN grains in intimate contact with one another along most of their boundaries. Microwave processing enhances the rate at which this occurs. This approach led to AlN with a thermal conductivity of 224 W/m^{o}C [35]. Microwave processing also enhances densification and thermal conductivity development in composites. AlN-TiB_2 composites with thermal conductivity of 150 W/m^{o}C were densified in Ar using microwave energy (see Fig. 16 and ref. [36]).

Future challenges include development of economically viable composites with tunable thermal and dielectric properties. These advanced materials also have potential in electronic packaging. Microwave-based processing of novel ceramics could advance the technological and scientific base of advanced microwave tubes. Furthermore, ceramic materials with superior thermal and dielectric properties can also have an impact on commercial and industrial

applications, like electronic packaging of power semiconductors, through the development of commercially viable technologies.

Fig 4.5.16: Thermal conductivity of microwave processed advanced AlN based ceramics versus benchmarks such as copper, commercial AlN, berylia ceramics and alumina.

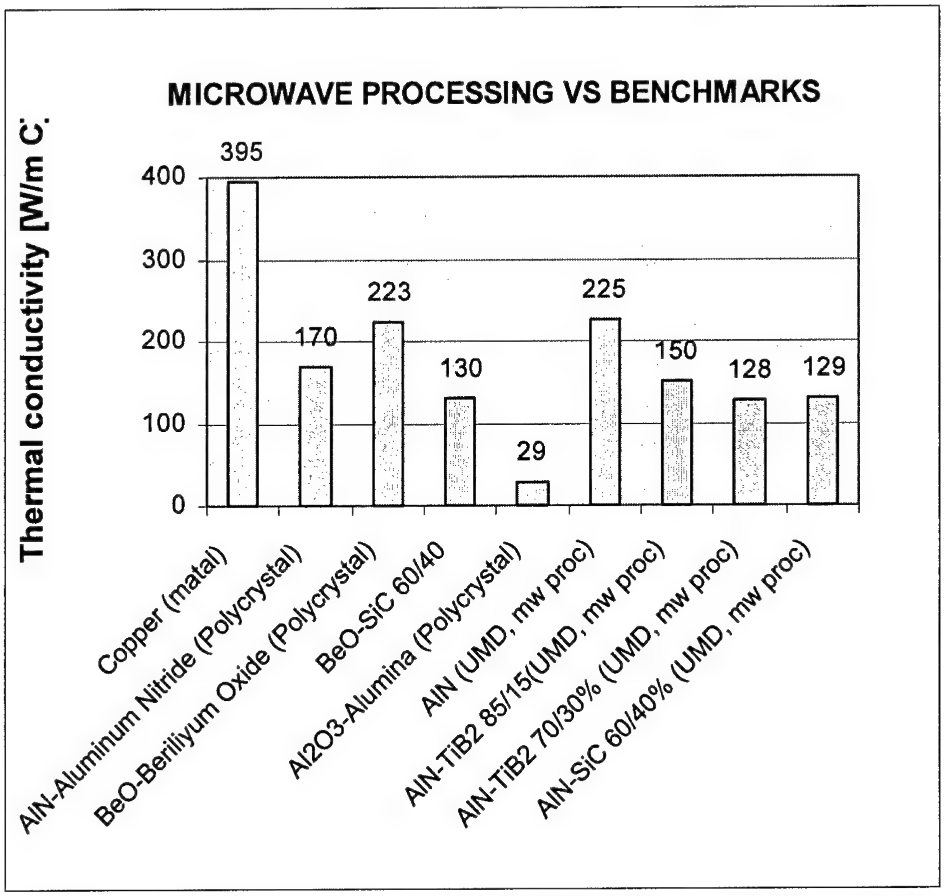

Fig. 4.5.17: The average grain size of ZnO rapidly decreases with increasing heating rate. At the extremely rapid heating rate of 5000 ^{0}C/sec, available only with microwave processing, grain growth was suppressed in ZnO so much that the grain size of the densified bulk material is similar to that of the starting powder

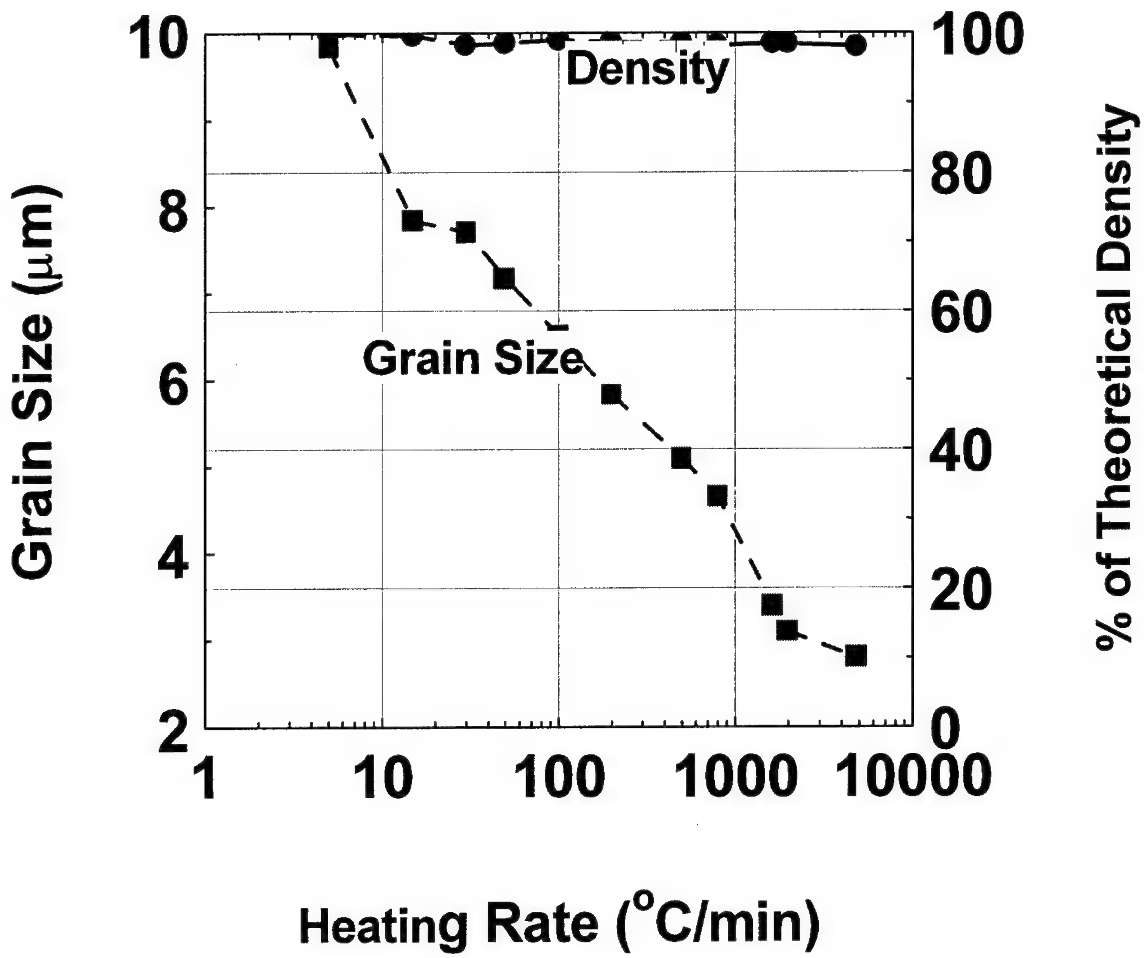

4.5.7 Controlled Chaos In Microwave Tubes

There are strong reasons to believe that the physical phenomenon known as a controlled chaos will be widely used in microwave vacuum electron devices developed for various applications. Before discussing these applications, it makes sense to specify what is meant by "chaos". Chaos designates the deterministic but complicated behavior of some systems, in which arbitrarily small changes in the input produce large changes in the output. Correspondingly, "controlled chaos" designates the phenomenon in which such complicated behavior can be controlled by some means.

There are, at least, two major areas of application of microwave tubes where the use of effects associated with controlled chaos can be very beneficial. Those are: (a) digital communications and (b) direct chaotic radar applications. Let us discuss them in turn.

(a) Digital communications.

Typical communication systems, in which, for instance, such microwave tubes as TWTs are widely used, operate in the so-called linear or small-signal regime. In such systems, any kind of nonlinear effect is extremely undesirable because it causes signal distortion. Therefore the amplifiers (such as TWTs) used in these systems should operate far from saturation, i.e. in the low-efficiency regimes. For such applications as, for instance, satellite communications, where the efficiency is one of the most critical figures of merit, this makes it necessary to use multi-stage collectors for increasing the overall efficiency of the device/system.

In digital communication systems, however, the devices/elements operating in purely nonlinear regimes can also be used in transmitters when properly designed receivers allow users to restore the information. Clearly, devices operating in the saturation regime allow users to greatly increase efficiency. In addition to the greater efficiency, the potential advantages of nonlinear digital communication systems are: light weight, compactness, ability to operate at higher power levels, low probability of interception and low probability of detection. The latter probability is especially low when a device operates in the chaotic regime. For user purposes this chaos should be controlled by some means. Then, at the receiving end, a receiving nonlinear element (e.g. TWT) should be synchronized to the chaotic transmitter resulting in amplification of the received signal with almost no distortion.

Although presently there is active development of such nonlinear electronic devices for transmitting and receiving of RF and optical signals, very little has been done in this regard at microwave frequencies. Nevertheless, even the first studies in the regime of controlled chaos clearly demonstrate the excellent potential of various high-power microwave sources.

(b) Direct chaotic radar applications.

Interest in chaotic waveforms for radar signals is well motivated. The use of chaotic waveforms has the potential of making radar signals ideal for high-accuracy unambiguous ranging with high resistance to jamming as well as low probability of detection. In order to increase the resistance to jamming and reduce the detection probability, chaotic waveforms should have a wide spectrum with minimal discernable features. For the spectrum to be considered wide, it should be, at least, wider than the typical bandwidth of microwave receivers,

which is on the order of several tens of MHz. So, if the radar generates waveforms corresponding to bandwidth on the order of hundreds of MHz to ~1 GHz, then only receivers with properly hopping center frequency will be able to receive these signals. Further, the power should be distributed as uniformly as possible over the band to reduce the probability of detection.

In the subheading of this section we used the term "direct chaotic radar". By "direct chaotic" systems we mean those microwave systems where the chaotic signal is generated directly in the microwave band. Since the radar range increases with transmitted power, it makes sense, of course, to develop high-power microwave sources for a number of applications.

4.5.7.1 State-of-the-art

In regard to the work done on analysis of chaotic oscillations in MVEDs, it should be noted that such regimes in vacuum microwave sources have been studied for more than 20 years. First, the transitions from steady-state operation to oscillations with periodically varying amplitude (automodulation) and then to chaotic oscillations were studied both theoretically and experimentally in backward-wave oscillators (BWOs) [44,45]. As is known, the mechanism responsible for appearance of chaotic oscillations in BWOs is an internal feedback due to the presence of a backward wave propagating towards the cathode, and hence, forming together with electrons streaming towards the collector a feedback loop. Such a loop allows one to consider the BWO as a microwave oscillator with distributed internal feedback. As known devices with distributed internal feedback are prone to various kinds of absolute instabilities.

Then, similar processes were studied in free-electron lasers with external feedback [46-48] and gyrotrons with internal feedback [49,50]. It was shown that in all these devices a sequence of events leads to the onset of chaotic oscillations, which is similar to that known in classical RF oscillators and other nonlinear dynamic systems. That is, there can be phenomena such as period doubling transitions leading to chaos [51].

In addition to systems based on absolute instability, randomization of radiation was also studied in microwave amplifiers with convective instability (TWTs) [52]. It was shown [52,53] that the randomization of an amplified signal in TWTs and other devices based on the resonant interaction between electrons and forward waves can be caused by noise amplification. Another method of generating noise-like signals in microwave oscillators is modulation of an electron beam by a low-frequency signal combined with further mixing of this low-frequency modulation with the high-frequency microwave signal [54].

From the brief overview given above it follows that some basic effects in chaotic operation of microwave tubes are already understood reasonably well. From the brief description of the benefits of using microwave tubes operating in controlled chaotic regimes in digital communication and radar systems it follows that this direction of R&D has great potential. Therefore, the development of microwave vacuum electron devices operating in the regimes of controlled chaos can become an area of active research in the near future.

4.5.8 References

1. G. S. Nusinovich, O. V. Sinitsyn and A. Kesar, "Linear theory of gyro-traveling-wave-tubes with distributed losses", Physics of Plasmas, vol. 8, pp.3427-3433 (July 2001).
2. K. R. Chu et al., IEEE Trans. Plasma Sci., vol. 27, pp.391-404 (April 1999).

3. K. T. Nguyen et al., IEEE Trans. Electron Devices, vol. 48, p.108 (2001).
4. G. S. Nusinovich, W. Chen, and V. L. Granatstein, "Analytical theory of frequency-multiplying gyro-traveling-wave-tubes", Physics of Plasmas, vol. 8, pp.631-637 (Feb. 2001).
5. K. R. Chu et al., IEDM, San Francisco, CA, 9-12 Dec. 1990, p. 699.
6. J. Rodgers, T.M. Antonsen Jr. and V.L. Granatstein, " Harmonic gain and noise in a Frequency Doubling Gyro-amplifier", IEEE Trans. Electron Dev., vol. 50, pp.1785-1792 (Aug. 2003)
7. G. S. Nusinovich and M. T. Walter, "Use of the Kompfner dip effect in multistage gyro-TWTs of high average power", IEEE Trans. Plasma Sci., vol. 30, pp.922-926 (June 2002).
8. O. V. Sinitsyn, G. S. Nusinovich, K. T. Nguyen, and V. L. Granatstein, "Nonlinear theory of the gyro-TWT: comparison of analytical method and numerical code data for the NRL gyro-TWT", IEEE Trans. Plasma Sci., vol. 30, pp.915-921 (June 2002).
9. G. S. Nusinovich, O. V. Sinitsyn, J. Rodgers, T. M. Antonsen, Jr., V. L. Granatstein, and N. C. Luhmann, Jr., "Comparison of multistage gyroamplifiers operating in the frequency-multiplication regime with gyroamplifiers operating at a given cyclotron harmonic", IEEE Trans. Plasma Sci., Special Issue on high-power microwave generation, vol. 32, June 2004 (to be published).
10. H. Guo et al., 25th Int. Conf. on Infrared and Millimeter Waves, Bejing, Sept. 12-15, 2000, pp.317-318.
11. R. S. Symons and J. R. M. Vaughan, IEEE Trans. Plasma Sci., vol. 22, p.713 (1994).
12. G. S. Nusinovich, T. M. Antonsen, Jr., H. Guo, and V. L. Granatstein, "Theory of clustered-cavity gyroklystrons", Physics of Plasmas, vol. 9, pp.4032-4039 (Sept. 2002).
13. O. V. Sinitsyn, G. S. Nusinovich and V. L. Granatstein, "Comparison of two concepts: multi-cavity versus clustered-cavity gyroklystrons", 6th Workshop on High Energy Density and High Power RF, Berkeley Springs, West Virginia, 22-26 June 2003, Eds. S. H. Gold and G. S. Nusinovich, AIP Conf. Proc., vol. 691, AIP, Melville, New York, 2003, pp. 378-385.
14. Y. Miao, T. M. Antonsen, Jr., G. S. Nusinovich, A. N. Vlasov, H. Guo, and V. L. Granatstein, "Prebunching of electrons in harmonic-multiplying cluster-cavity gyro-amplifiers", ibid., pp. 407-416.
15. G. S. Nusinovich, O. V. Sinitsyn, L. Velikovich, M. Yeddulla, T. M. Antonsen, Jr., A. N. Vlasov, S. R. Cauffman, and K. Felch, "Startup scenarios in high-power gyrotrons", IEEE Trans. Plasma Sci., Special Issue on high-power microwave gerenation, vol. 32, June 2004 (to be published).
16. P. Mardahl and K. Cartwright, "Simulations of a 95 GHz, 100 kW CW Gyrotron Interaction Cavity using 3D PIC", The 31st IEEE Int. Conf. on Plasma Science, June 28 – July 1, 2004, Baltimore, MD, paper 5P24.
17. C. S. Kou et al., Phys. Rev. Lett., vol. 70, p.924 (1993).
18. N. S. Ginzburg, S. P. Kuznetsov, and T. N. Fedoseeva, Radiophys. Quantum Electron., vol. 21, p.728 (1979).
19. B. P. Bezruchko, S. P. Kuznetsov, and D. I. Trubetskov, JETP Lett., vol. 29, 162 (1979).
20. G. S. Nusinovich, A. N. Vlasov, and T. M. Antonsen, Jr., "Nonstationary phenomena in tapered gyro-backward-wave oscillators", Phys. Rev. Lett., vol. 87, paper 218301 (19 Nov. 2001).

21. A. Singh, A. Valfells, C. Robey, J. Goldstein, M. J. Kolander and V. L. Granatstein "Advancements in Codes for Computer Aided Design of Depressed Collectors and Tracing of Backscattered Electrons, Part I. Optimization of Depressed Potentials and Tracking of Multiple Orders of Backscatter", IEEE Transactions on Plasma Science, June 2002, pp. 1265-1270

A. Valfells, A. Singh, M. J. Kolander and V. L. Granatstein, "Advancements in
22. Codes for Computer Aided Design of Depressed Collectors and Tracing of Backscattered Electrons, Part II. Improvements in Modeling of the Physics of Secondary Electron Emission and Backscattering", IEEE Transactions on Plasma Science, June 2002, pp.1271-1276.

A. Singh and V.L. Granatstein, "Computer Aided Design of Depressed Collectors
23. For High Power Electron Tubes", Proc. 6th Workshop on High Energy Density and High Power RF, Berkeley Springs, WV, June 22-26, 2003, (AIP Conf. Proc. 691), pp.127-135.
24. 24.A. Singh, A. Valfells, M. Kolander and V.L. Granatstein, "Improvements in
25. Depressed Collector Performance By Modifications to Electrode Geometry vis-a-vis
26. Trajectories of Backscattered Electrons", IEEE Trans. Plasma Science, June 2004
27. (to be published).

A. T. Lin, K. R. Chu, C.C. Lin, C.S. Kou, D.B. McDermott and N. C. Luhmann, Jr., *Int. J. Electron.*, vol. 72, p.873, 1992.
28. K. R. Chu, H. Y. Chen, C. L. Hung, T. H. Chang, L. R. Barnett, S. H. Chen and T. T. Yang, *Phys. Rev. Lett.*, vol. 81, no. 21, pp. 4760-4763, Nov., 1998.
29. H. Guo, D. S. Wu, G. Liu, Y. H. Miao, S. Z. Qian and W. Z. Qin, "Special complex open-cavity and low-magnetic-field high-power gyrotron" *IEEE Trans. Plasma Sci.,* vol. 18, no. 3, June, 1990, pp.326-333.
30. Y. Carmel, K. R. Chu, M. Read, A. K. Ganguly, D. Dialetis, J. S. Levine and V. L. Granatstein, "Realization of a stable and highly efficient gyrotron for controlled fusion research", *Phys. Rev. Lett.*, vol. 50, no. 2, p.112, Jan., 1983.
31. H. Guo, D. J. Hoppe, J. Rodgers, R. M. Perez, J. P. Tate, B. Conroy, V. L. Granatstein, A. M. Bhanji, P. Latham, G. S. Nusinovich, M. L. Naiman and S. H. Chen, "Phase locking of a second-harmonic gyrotron oscillator using a quasi-optical circulator to separate injection and output signals", *IEEE Trans. Plasma Sci.*, vol. 23, pp. 822-832, Oct., 1995.
32. H. Guo, S. H. Chen, V. L. Granatstein, J. Rodgers, G. S. Nusinovich, M. Walter, B. Levush and W. J. Chen, "Operation of a highly overmoded, harmonic-multiplying, wideband gyrotron amplifier", *Phys. Rev. Lett.*, vol. 79, no. 3, pp. 515-518, 1997.
33. J. Rodgers, H. Guo, V. L. Granatstein, S. H. Chen, G. S. Nusinovich, M. Walter and J. Zhao, "High efficiency, phase locked operation of the harmonic-multiplying inverted gyrotwystron amplifier", *IEEE Trans. Plasma Sci.,* vol. 27, no. 2, pp.412-421, April, 1999.
34. J. Rodgers, H. Guo, G. S. Nusinovich and V. L. Granatstein, "Experimental study of phase deviation and pushing in a frequency doubling, second harmonic gyro-amplifier", IEEE Trans. Electron Devices, vol. 48, no. 10, pp.2434-2441, Oct. 2001.
35. J. Zhao, G. S. Nusinovich, H. Guo, J. Rodgers and V. L. Granatstein, "Studies of a three-stage inverted gyrotwystron", *IEEE Trans. Plasma Sci.*, vol. 28, no. 3, pp.657-664, June, 2000.
36. Manfred Thumm, "Development of output windows for high power, long pulse

37. gyrotrons and ED wave applications", Int'l J. of Infrared and Millimeter Waves,
38. Vol. 19, No 1, pp 3-14 (1998).
39. G. Xu, T. Olorunyolemi, O. Wilson, I. Lloyd and Y. Carmel, "Microwave
40. sintering of high-density, high thermal conductivity AlN", J. Mater. Res., vol. 17,
41. No. 11 (Nov. 2002).
42. G. Xu, Y. Carmel, T. Olorunyolemi, I. Lloyd and O. Wilson, "Microwave
43. sintering and properties of AlN/TiB_2 composites", J. Mater. Res., Vol. 18, No. 1
44. pp. 66-76 (2003).
45. Gengfu Xu, "Unique high temperature microwave sintering of AlN based
46. ceramics with high thermal conductivity", Ph.D. dissertation, University of
47. Maryland, May 2002.
48. J. Calame, A. Birman, Y. Carmel, D. Gershon, B. Levush, A. Sorokin, V.
49. Semenov, D. Dadon, P. Martin and M. Rosen, "A dielectric mixing law for
50. porous ceramics based on fractal boundaries", J. Appl. Phys, v.80, n.7, pp3892-
51. 4000 (1996).

A. Birnboim and Y. Carmel, " Simulation of microwave sintering of ceramic
52. bodies with complex geometry", J. Am. Ceram. Soc., v.82, n.11, pp. 3024-3030
53. (1999).

A. Birnboim, T. Olorunyolemi and Y. Carmel, "Calculating the thermal
54. conductivity of heated powder compacts", J. Am. Ceram, Soc., v.84, n.6,
55. pp.1315-1320 (2001)
56. G. Xu, I. Lloyd, Y. Carmel, T. Olorunyolemi and O. Wilson, "Microwave
57. sintering of ZnO at ultra high heating rates", J. Mater. Res. Vol. 16, No. 10,
58. pp. 2850-2858 (2001).
59. See for example S. Yip, "Synergistic science", Nature Materials, Vol. 2, pp3-5
60. (Jan 2003). www.nature.com/naturematerials, and references therein.

A. Haslam, D. Moldovan, S. R. Phillpot, D. Wolf and H. Gleiter, "Combined
61. atomistic and mesoscale simulation of grain growth in nanocrystaline thin films",
62. computational Materials Science, v.23, pp.15-32 (2002).
63. N. S. Ginzburg, S. P. Kuznetsov, and T. N. Fedoseeva, "Theory of transients in relativistic backward-wave tubes", Radiophys. Quantum Electron., v.21, pp.728-738 (1978).
64. B. P. Bezruchko, S. P. Kuznetsov, and D. I. Trubetskov, "Experimental observation of stochastic self-oscillations in the electron beam – backscattered electromagnetic wave dynamic system", JETP Lett., v.29, p.162 (1979).
65. Ya. L. Bogomolov, V. L. Bratman, N. S. Ginzburg, M. I. Petelin, and A. D. Yunakovsky, "Nonstationary generation in free-electron lasers", Optics Comm., v.36, pp.209-213, (1981).
66. T. M. Antonsen, Jr., "Nonlinear Dynamics in a Free Electron Laser", in "Nonlinear Dynamics and Particle Acceleration", Tsukuba, Japan, 1990, Eds. Y. H. Ichikawa and T. Tajima, Conf. Proc. No. 230, Particles and Fields Series 45, AIP, New York, 1991, pp.106-115.
67. H. P. Freund and T. M. Antonsen, Jr., "Principles of Free-Electron Lasers", Chapman and Hall, London, U.K., 2nd Edition, 1996, Chapter 11.
68. N. S. Ginzburg, G. S. Nusinovich, and N. A. Zavolsky, "Theory of non-stationary processes in gyrotrons with low-Q resonators", Int. J. Electron., v.61, pp.881-894, (1986).

69. N. A. Zavolsky and G. S. Nusinovich, "Nonstationary processes in a gyrotron with a beam-dependent microwave field structure", Sov. J. Comm. Techn. Electron., v.36, pp.117-122, (1991).
70. E. Ott, "Chaos in Dynamical Systems", Cambridge University Press, 1993.
71. N. S. Ginzburg, A. S. Pikovskii, and A. S. Sergeev, "Randomization of Electromagnetic Radiation in Systems with Convective Instability in the Electron Beam", Sov. J. Comm. Techn. Electron., v.34 , pp.38-46, (1989).
72. V. Dronov, M. R. Hendrey, T. M. Antonsen, Jr., and E. Ott, "Communication with a Chaotic Traveling Wave Tube Microwave Generator", *Chaos,* v.14, n.1, pp.30-37, March 2004.
73. V. L. Vaks, N. S. Ginzburg, A. S. Sergeev, A. V. Smorgonskii, V. V. Kholos,
74. and A. O. Shuleshov, "The use of Modulation in Microwave Oscillators to
75. Obtain Stochastic Output Signals", J. Comm. Techn. Electron., v.39, No.11,
76. pp.1-5, (1994)

4.5.9 Publications

4.5.9.1 Books

1. G.S. Nusinovich, "Introduction to the Physics of Gyrotrons", The Johns Hopkins University Press, 2004, ISBN 0-8018-7921-3.

4.5.9.2 Papers in Scientific Journals

1. G. Nusinovich, O. Sinitsyn, L. Velikovich, M. Yeddulla, T. Antonsen, Jr., A. Vlasov, S. Cauffman and K. Felch, "Start-up scenarios in high-power gyrotrons", Invited Paper, IEEE Trans. Plasma Sci., June 2004 (to be published)

2. Y. Miao, T.M. Antonsen,Jr., G.S. Nusinovich, A.N. Vlasov, H. Guo and V.L. Granatstein, "Prebunching of electrons in harmonic-multiplying cluster-cavity gyro-amplifiers", ibid.. (to be published)

3. G.S. Nusinovich, O.V. Sinitsyn, J. Rodgers, T.M. Antonsen, Jr., V.L. Granatstein and N.C. Luhmann, Jr., "Comparison of multistage gyroamplifiers operating in the frequency-multiplication regime with gyroamplifiers operating at a given cyclotron harmonic", ibid. (to be published)

4. A. Singh, A. Valfels, M. Kolander and V.L. Granatstein, "Improvements in depressed collector performance by modifications to electrode geometry vis-à-vis trajectories of backscattered electrons", ibid. (to be published).

5. G. Xu, Y. Carmel, T. Olorunyolemi, Y. Carmel, and I. Lloyd, O. Wilson, "Microwave sintering and the properties of AlN/TiB_2 composites", J. Mater. Research v.18, pp. 66-76 (2003)

6. G. Xu, T. Olorunyolemi, Y. Carmel, I. Lloyd, O. Wilson, “Design and construction of insulation configuration for ultra-high temperature microwave processing of ceramics”, J. Am. Ceram. Soc., v. 85, n.3, pp. 2082-2086 (2003)

7. J. Rodgers, T. Antonsen Jr. and V. Granatstein, "Harmonic gain and noise in a frequency doubling gyro-amplifier", IEEE Trans. Electron Devices v.50, pp.1785-1792 (2003)

8. G.S. Nusinovich, T.M. Antonsen, Jr., H. Guo and V.L. Granatstein, "Theory of clustered-cavity gyroklystron", Physics of Plasmas v.9, pp. 4032-4139 (2002)

9. T. Olorunyolemi, A. Birnboim, Y. Carmel, O. Wilson, I. Lloyd, S. Smith and R. Campbell, "Thermal conductivity of ZnO: from green to sintered state", J. American Ceramic Society v.85, pp.1249-1253 (2002)

10. G. Xu, T. Olorunyolemi, O. Wilson, I. Lloyd and Y. Carmel, "Microwave sintering of high-density, high thermal conductivity AlN", J. Mater. Research v.17, pp.2837-2845 (2002)

11. G. Xu, I. Lloyd, Y. Carmel, T. Olorunyolemi and O. Wilson, "Microwave sintering of ZnO at ultra high heating rate" J. Mater. Research v.16, pp.2850-2858 (2002)

12. O. Sinitsin, G. Nusinovich, K. Nguyen and V.L. Granatstein, "Nonlinear Theory of the Gyro-TWT: comparison of analytical method and numerical code data for the NRL gyro-TWT", IEEE Trans. Plasma Sci., v.16, pp. 915-921 (2002)

13. G.S. Nusinovich and M. Walter, " Use of the Kompfner Dip Effect in Multi-stage Gyro-TWTs of High Average Power", ibid., pp. 922-926.

14. J. Rodgers, H. Guo, G.S. Nusinovich and V.L. Granatstein, "Experimental studies of phase deviation and pushing in a frequency-doubling, second harmonic gyro-amplifier", IEEE Trans. Electron Devices **v.48,** pp.2434-2441 (2001)

15. G.S. Nusinovich, J. Rodgers, W. Chen and V. L. Granatstein, “Phase Stability in Gyro-Traveling –Wave-Tubes”, ibid., pp.1460-1468

16. G. Nusinovich, O. Sinitsin & A. Kesar, “Linear Theory of Gyro-TWTs with Distributed Losses”, Physics of Plasmas, v.**8,** pp.3427-3433 (2001)

17. G. Nusinovich, A.Vlasov, and T. Antonsen, “Nonstationary Phenomena in Tapered Gyro-Backward-Wave Oscillators”, Phys. Rev. Lett., v. **87,** pp. 1-4, (2001)

18. D. Gershon, J.P. Calame and A. Birnboim, “Complex Permittivity Measurements and the Mixing Laws of Alumina Composites”, J. Appl. Phys., v. **89** pp. 8110-8116 (2001)

19. D. Gershon, J.P. Calame and A. Birnboim, "Complex Permittivity Measurements and the Mixing Laws of Porous Alumina", J. Appl. Phys, **v. 89**, pp. 8117-8120 (2001)

.

20. G. Xu, I. Lloyd, Y. Carmel, T. Olorunyolemi, O. Wilson, "Microwave Sintering of ZnO at ultra high heating rates", J. Material Research, v. 16, pp.2850-2858 (2001).

21. G.S. Nusinovich, J. Rodgers, W. Chen and V.L. Granatstein, "Phase Stability in Gyro-Traveling-Wave-Tubes", IEEE Trans. Electron Devices, v.48, pp.1460-1468 (2001)

22. G.S. Nusinovich, W. Chen and V.L. Granatstein, "Analytical Theory of Frequency-Multiplying Gyro-Traveling-Wave-Tubes", Phys. Plasmas 8 (2001) 631.

23. J. Zhao, H. Guo, G.S. Nusinovich, J. Rodgers and V.L. Granatstein, "Studies of a Three-Stage Inverted Gyrotwystron", IEEE Trans. Plasma Sci., v. 28, 657-664 (2000)

24. A.T. Lin, H. Guo and V.L. Granatstein, "Dynamic Simulation of Mode-Selective Interaction Cavity for Wide-Band High-Power Gyrotron Applications", ibid., 782-789

25. J. Zhao, G.S. Nusinovich, H. Guo, J.C. Rodgers and V.L. Granatstein, " Axial Mode Locking in a Harmonic-multiplying, Inverted Gyrotwystron", ibid., pp. 597-605

4.5.9.3 Presentations at Conferences

1. A. Singh and V.L. Granatstein, "Towards estimation of the effects of misalignment of electron beam injected into a high power gyrotron with depressed collector", 5th IEEE Int. Vacuum Electronics Conf. (IVEC 2004), Monterey, CA, April 27-29, Book of Abstracts, pp.202-203.

2. Y. Miao, T.M. Antonsen, Jr., G.S. Nusinovich, A.N. Vlasov, H. Guo and V.L. Granatstein, "Prebunching of electrons in harmonic –multiplying cluster-cavity gyro-amplifiers", 2004 IEEE Int. Conf. on Plasma Science (ICOPS 2004), Baltimore, MD, July 1, 2004, Conf. Record, p.267.

3. O.V. Sinitsin, J. Rodgers, G.S. Nusinovich and V.L. Granatstein, "Effects of operation of a buncher cavity at the second cyclotron harmonic on gyroklystron efficiency", ibid., p.341

4. J. Rodgers, G. Nusinovich, H. Guo, W. Chen and V. Granatstein. "Harmonic Gain and Noise in Frequency Multiplying Gyro-amplifiers", 6th Workshop on High Energy Density and High Power RF, June 22-26, 2003, Berkeley Springs, WV (AIP Conf. Proc. 691) pp.243-250.

5. O. V. Sinitsyn, G. S. Nusinovich and V. L. Granatstein, "Comparison of Two Gyroklystron (GKL) Concepts: Four-Cavity Conventional GKL vs Clustered-Cavity GKL", ibid., pp.378-385.

6. Y. Miao, T.M. Antonsen, Jr., H. Guo, G. Nusinovich and V. Granatstein, " Prebunching of Electrons in Harmonic-Multiplying Clustered-Cavity Gyro-Amplifiers", ibid., pp.407-416.

7. A. Singh and V.L. Granatstein, "Computer Aided Design of Depressed Collectors for High Power Electron Tubes", ibid., pp.127-135.

8. G. S. Nusinovich, H. Guo, T. M. Antonsen, Jr. and V.L. Granatstein, "Concept and theory of clustered-cavity gyroklystrons", ibid. pp.403-407.

9. O.V. Sinitsin, J. Rodgers, G.S. Nusinovich and V.L. Granatstein, "Effects of operation of a buncher cavity at the second cyclotron harmonic on gyroklystron efficiency", ibid., p.341

10. Y. Carmel, A. Birnboim, T. Olorunyolemi, I. Lloyd and O. Wilson, "Multi-scale dielectric and thermal properties of composites: modeling and experiments", 3rd World Congress on Microwave and Radio Frequency Applications, 22-26 September, 2002, Sydney, Australia.

11. G. S. Nusinovich, M. Yedulla, L. Velikovich, T. M. Antonsen, Jr., A. N. Vlasov, S. Cauffman and K. Felch, "Start-Up Scenarios in High-Power Gyrotrons (Invited Keynote)", 27th Int. Conf. on Infrared and Millimeter Waves, Sept. 22-26, 2002, San Diego, CA, Conf. Digest, p.329-330.

12. G.S. Nusinovich, O.V. Sinitsyn, J. Rodgers, V.L. Granatstein, and N.C. Luhmann, Jr., "Comparison of two gyroklystrons concepts: frequency multiplication versus operation at a given cyclotron harmonic", Digest of the 3rd IEEE Int. Vacuum Electronics Conf., INVEC-2002, April 23-25, 2002, Monterey, CA, p.87-88.

13. J.Rodgers, T.M. Antonsen, Jr., V.L. Granatstein, T.H. Chang, K.R. Chu, "Improved Phase and Gain Stability in Gyro-Traveling-Wave Amplifiers with Detuned Cyclotron Resonance Mismatch", ICOPS-2002 IEEE conference Record-Abstracts, The 29th IEEE Int. Conf. On Plasma Science, Banff, Alberta, CA, May 26-30, 2002, p.132, paper21309.

14. G.S. Nusinovich, O.V. Sinitsyn, and V.L. Granatstein, "Comparison of Twon Concepts of Gyro-Traveling-Wave Tubes (gyro-TWTs)", Ibid., p.132, Paper 2B10.

15. G.S. Nusinovich and M. Walter, " On the use of Kompfner dip effect in gyro-TWTs", Digest of the 26th Int. Conf. On Infarared and Millimeter Waves, Toulouse, France, Sept. 2001, p.97.

16. G.S. Nusinovich and O.V. Sinitsyn, "Theory of gyro-TWTs with distributed losses", ibid., p.102

17. G.S. Nusinovich and A.N. Vlasov, "Nonstationary phenomena in gyro-backward-wave-oscillators", ibid., p.52

18. V.L. Granatstein, H.Guo, Y. Miao, G.S. Nusinovich, J. Rodgers, "Frequency-doubling Gyro-amplifiers using a TE Cluster Cavity", 43rd APS-DPP Annual Meeting, Oct. 29- Nov. 2, 2001, Long Beach, CA, APS Bulletin, Oct. 2001, vol.46, No.8, p.214, Paper L02-7.

19. O. Sinitsyn , G.S. Nusinovich, V.L. Granatstein, and K. Nguyen, " Theory of the gyro-TWT with distributed losses", ibid, p.124, Paper FP1-89.

20. Y.Y. Miao, H. Guo, J. Rodgers and V.L. Granatstein, "TE0node Clustered-cavities and Extended Interaction Cavities for Wideband Gyro-ampliofiers", 28th IEEE Int. Conf. on Plasma Science, Las Vegas, NV, June 17-22, 2001, Conference Record, p.514

21. H. Guo, Y.Y. Miao, J. Rodgers, V. Granatstein,Y.G. Ding, R.S. Wu, J.R. Luo, D.S. Wu, Y.L. Lin, Y.H. Miao, Y.N. Sao, W. Guo and A.T. Lin, " Studies of a TE04 Mode, Wideband, Triplet Gyrotron Amplifier with Harmonic Multiplication", ibid., p.520

22. H. Guo, J. Rodgers, J. Zhao, Y.Y. Miao, W.J. Chen and V.L. Granatstein, " Latest Progress in Studies of Harmonic Multiplying Gyro-amplifiers", @5th Int. Conf on IR and Millimeter Waves, Beijing, China, Sept. 12-15, 2000, Book of Abstracts, pp. 317-318

23. H. Guo, V. Granatstein, J. Rodgers, J.J. Zhao, W.J. Chen and Y. Miao, " Progress in Experimental Studies of Harmonic Multiplying Gyro-amplifiers", 27th IEEE Int. Conf. on Plasma Science, New Orleans, LO., June4-7 2000, Conference Record, p.202

4.6 University of Michigan

4.6.1 Significant Achievements

4.6.1.1. 4A. Magnetron Noise Reduction- U. Michigan

This is a breakthrough of first magnitude. A novel, simple, low-cost, and effective method was discovered whereby noise in kW magnetrons was suppressed. Two patent applications are being filed. Noise in crossed-field devices is an outstanding problem that defies cure. Very significant effort, in experimentation and in modeling, has been put forth by DoD in the last 15 years to reduce the noise in crossed-field amplifiers, such as those used in the Patriot and Aegis radars. Despite the heroic effort by the who's-who in crossed-field devices, no practical solution on CFA noise has previously emerged.

The UM work in the MURI MVE program offered an innovative approach. Instead of studying the CFA directly, we provided an in-depth study of noise in the ubiquitous microwave oven magnetron. U-Michigan discovered a simple way to completely eliminate both the close-in and the sideband noise. U-Michigan also discovered that the startup of the magnetron may be hastened, especially when N/2 magnetic periods are utilized, where N is the number of magnetron cavities. These results have been demonstrated for both new and old kW magnetrons. No significant degradation in power or efficiency is observed. It is expected that this novel technique of noise reduction may be extended to DoD crossed-field amplifiers, as CFA and magnetrons share many similarities in the noise characteristics. This invention is also expected to have far reaching consequences on reducing magnetron interference with communications systems that operate in the unlicensed 2.4 GHz spectrum (e.g., cordless phones, Bluetooth), extremely close to the 2.45 GHz oven frequency. Our newly discovered noise-reduction technique may also be applied to magnetrons used for homes, industrial heating and lighting. Multiple publications, Invited Talks (IVEC, ICOPS), Press Releases (APS, ABCnews.com, AIP, etc.), TV and radio interviews have covered this unprecedented advance.

A Patent Application was Filed: "Low Noise, Crossed-Field Devices Such as a Microwave Magnetron Having an Azimuthally-Varying Axial Magnetic Field and Microwave Oven Utilizing Same"

4.6.1.2. 4B. Analytic theory of higher dimensional Child-Langmuir Law - U. Michigan

For 90 years, there has been no useable analytic theory of Child-Langmuir Law beyond 1-D. Without exception, all 2D theories are very complicated; the results are neither transparent nor useable. Answering this need, U Mich developed such a simple scaling law, which gave the maximum current density that can be emitted over a finite patch of the cathode surface before the onset of a virtual cathode. The theory was simple and elegant, developed from first principles and agrees with simulations. Immediately after its publication, this scaling law was used by NRL scientists to successfully interpret the current measured from their cathode on ELECTRA. This work stimulated many studies elsewhere.

4.6.1.3. 4C. First theory of klystron intermodulation - U. Michigan

U Mich developed a general theory that accurately evaluates the intermodulation products, which result from an input signal with multiple frequency components. In high power

amplifiers, these IM products are a crucial limitation in modern analog and digital communications. The code has been validated with a series of collaborative experiments with our MURI partner, U of Wisconsin. Also with UW, a novel method, by injecting a weak signal, to suppress 3-rd order intermod has been demonstrated.

4.6.1.4. 4D. Heating of thin film on microwave windows

To what extent a thin film of contaminants would lead to excessive heating of high power rf windows have never been quantified, by a scaling law. U Mich investigators provided such a scaling law, which surprisingly predicts that a thin film of contaminants (much thinner than the skin depth) may absorb up to a 50 percent of incident rf power. This theory also provides a novel scaling law for the resulting temperature rise.

4.6.2. Progress

4.6.2.1. a) Magnetron Noise Reduction

4.6.2.1.1 5A. Magnetron Noise Reduction

This is a breakthrough of first magnitude. A novel, simple, low-cost, and effective method was discovered whereby noise in kW magnetron was suppressed. Two patent applications are being filed. Noise in crossed-field devices is an outstanding problem that defies cure. Very significant effort, in experimentation and in modeling, has been put forth by DoD in the last 15 years to reduce the noise in crossed-field amplifiers. These amplifiers are used in the Patriot and Aegis radars. Despite the heroic effort by the who's-who in crossed-field devices, no practical solution on CFA noise has emerged. The MURI MVE program offers an attractive solution. Instead of studying the CFA directly, we provided an in-depth study of noise in the ubiquitous microwave oven magnetron. We discovered a simple way to completely eliminate both the close-in and the sideband noise. We also discovered that the startup of the magnetron may be hastened. These results have been demonstrated for both new and old kW magnetrons. No significant degradation in power or efficiency is observed. It is expected that this novel technique of noise reduction may be extended to DoD crossed-field amplifiers, as CFA and magnetrons share many similarities in the noise characteristics. This invention is also expected to have far reaching consequences on several communications systems that operate in the unlicensed 2.4 GHz spectrum (e.g., cordless phones, Bluetooth), extremely close to the 2.45 GHz used in microwave ovens. Our newly discovered noise-reduction technique may also be applied to magnetrons used for industrial heating and lighting. Multiple publications, Invited Talks (IVEC, ICOPS), Press Releases (APS, ABCnews.com, AIP, etc.), TV and radio interviews have covered this unprecedented advance.

4.6.2.1.2. 5B. Analytic theory of higher dimensional Child-Langmuir Law

For 90 years, there has been no useable analytic theory of Child-Langmuir Law beyond 1-D. Without exception, all 2D theories are very complicated; the results are neither transparent nor useable. However, a simple analytic 2D theory is of fundamental interest because electron emission is often restricted to finite patches on the cathode surface. Moreover, modern cathodes,

such as ferroelectric cathodes, laser-triggered cathodes, and field emitter arrays, etc., have at times displayed the puzzling phenomenon that the emission current densities are higher than that predicted by the familiar 1D Child-Langmuir law. There is thus a pressing need for the development of a 2D Child Langmuir Law.

Answering this need, U Mich developed such a simple scaling law. It gave the maximum current density that can be emitted over a finite patch of the cathode surface before the onset of a virtual cathode. The theory was simple and elegant, developed from first principles. It was shown to agree with simulation results. Immediately after its publication, this scaling law was used by NRL scientists to successfully interpret the current measured from their hibachi cathode on ELECTRA [Hegelar et al., Phys. Plasmas, 9, 4309, (2002)].

4.6.2.1.3 5C. First theory of klystron intermodulation

U Mich developed a general theory that accurately evaluates the intermodulation products which result from an input signal with multiple frequency components. In high power amplifiers, these IM products may reach unacceptable levels, thereby distorting the information being transmitted. This problem is acute for demanding modern analog and digital communications applications.

Prior to this work, virtually all large signal klystron simulation codes treated only single tone input signals. One basic problem in the development of a multi-signal klystron code is that of resolving the narrow spacing of the IM products from the carriers. Our newly developed algorithm got rid of this difficulty. It was also able to accurately account for charge overtaking and the space charge effects. The code has been validated with a series of collaborative experiments with our MURI partner, U of Wisconsin. Also with UW, a novel method, by injecting a weak signal, to suppress 3-rd order intermod has been demonstrated. Calculations have been performed, using our newly developed klystron intermod code, to interpret this U Wisconsin experiment on intermod

suppression. This joint UW-UM collaboration was published in Physical Review Letters.

Because of this work, and of his pioneering simulation studies in beam loading, U Mich graduate student Craig Wilsen received the IEEE Outstanding Graduate Student Award. These works were documented in his Ph.D. thesis.

The advance of the multi-signal code, its demonstrated ability to account for charge-overtaking, plus our work on beam-loading of cavities, are being applied to the multi-beam klystron (MBK) by U Mich student Richard Kowalczyk. MBK is now actively pursued at NRL. In fact, Dr. Baruch Levush of NRL has already approached U Mich PI's in having Richard Kowalczyk to do an internship at NRL on the multibeam klystron. Richard Kowalczyk already performed an internship at L-3 on this topic.

4.6.2.1.4. 5D. Heating of thin film on microwave windows

The extent to which a thin film of contaminants would lead to excessive heating of high power rf windows has never been quantified, in particular in terms of a scaling law. U Mich investigators provided such a scaling law, which surprisingly predicts that a thin film of contaminants (even much thinner than the skin depth) may absorb up to a 50 percent of the incident rf power. It also provides a novel scaling law for the resulting temperature rise. When this new result was presented to our industrial partner, Northrop-Grumman/Litton (now L3), in

August, 2002, Dr. Al Theiss excitedly announced to the audience that this theory might explain the unexpected window failure that occurred significantly below the rated power. Note that this window failure has long been a puzzle (and worry) to Northrop-Grumman/ Litton/ L-3, which are heavily sponsored by DoD. Our work also stimulated Dr. Howard Jory of CPI to perform measurements on one of his broken diamond windows.

Thin film heating is of significant interest to DoD's HPM program. Thin film coatings of conductive materials with low secondary electron emission (SEE) yields, such as Ti, TiN or Cr_2O_3, are often deposited on the windows to prevent the occurrence of multipactor. Too-thin a film may not suppress SEE, whereas too-thick a film may lead to excessive Ohmic heating. The scaling laws mentioned above then provide a guide for the optimization of the film thickness, in particular when the film thickness is in the nanometer range.

4.6.2.1.5 5E. Theory of Crossed-Field Electron Flow

The maximum injection current in an insulated, relativistic diode has been computed for the first time. Surprisingly, the space-charge limited condition is not the limiting condition. This finding was confirmed by MAGIC code simulations. Fundamental properties of cycloidal crossed-field flows were examined. The multiplicity of the solutions among the n-th order Slater orbits and the Brillouin flow is clarified. It is concluded that ALL Slater orbits are either highly unstable or simply physically inaccessible. The most probable state in a crossed-field diode is the Brillouin flow superimposed by a weak turbulent background. These statements hold regardless of the diode voltage (i.e., relativistic or not, as long as the diode is magnetically insulated).

4.6.2.1.6 5F. Injection Locking of Magnetrons

A reflection amplifier system was constructed, similar to that employed by Brown. The oscillator magnetron was directed through a circulator and a tuning stub section to a matched load. The tuning stubs are utilized as a high power splitter, to reflect a portion of the microwave power. The circulators direct the reflected microwave power into a second magnetron, which acts as the amplifier. Another circulator is used to avoid reflections into the oscillator magnetron, to avoid frequency pulling. Microwave power and spectrum are monitored at appropriate points in the system corresponding to oscillators and amplifier. Initial experiments were performed to verify magnetron operation as a reflection amplifier.

These experimental data were compared with Adler's equation: the amplifier frequency corresponds exactly to the oscillator (drive) frequency for power levels above 10 W, in good agreement with Adler's equation. Furthermore, the magnetron's microwave output power scales linearly versus drive power above the level predicted by Adler's equation.

A major focus of this research program has been the identification of the "quiet" versus "noisy" state of magnetrons. These states are believed to hold the keys to the understanding of crossed-field noise. The quiet state was achieved by operating the magnetron with the heater turned off after the full microwave power was achieved. Note that the effect of the magnetic perturbations was to reproduce the quiet microwave spectrum from a magnetron.

4.6.3 Students Educated Under MURI'99

4.6.3.1 U. Michigan Graduate Students Working on MURI-Related Research

Student	Type and Date of Degree	Dissertation Title	Status
Craig Wilsen	Ph.D. 2001	Theory of Intermodulation in HighPower Microwave Amplifiers	Engineer: L-3
V. Bogdan Neculaes	Ph.D. Expected 2004	Low-Noise Magnetrons	UMi Grad Student
Richard Kowaczyk	Ph.D. Expected 2005	Design Studies of Multi-Beam Klystrons	UMi Grad Student (DoE Fellowship) L-3 Summer Intern
Herman Bosman	Expected Ph.D. 2004	Theory of RF Window Failure	UMi Grad Student (DoE Support)
Nick Jordan	Ph.D. Expected 2007	Magnetron Experiments & Simulation	UMi Grad Student L-3 Summer Intern
P. Pengvanich	Ph.D. expected 2007	Magnetron Theory	UMi Grad Student
Wilkin Tang	Ph.D. expected 2008	RF Heating of Window Contaminants	UMi Grad Student DoE Support L-3 Summer Intern
Michael Jones	Ph.D. expected 2005	Magnetron Simulation and Experiments	UMi Grad Student AFOSR support

4.6.4 List of Publications and Presentations

Patent Application Filed: "Low Noise, Crossed-Field Devices Such as a Microwave Magnetron Having an Azimuthally-Varying Axial Magnetic Field and Microwave Oven Utilizing Same"

Publications

1) M.C. Jones, V.B. Neculaes, W. White, Y.Y. Lau, and R.M. Gilgenbach, "Simulation of rapid startup in microwave magnetrons with azimuthally varying axial magnetic fields", Applied Physics Letters, 84, p1016, (2004).
2) "Limiting Current in a Relativistic Diode Under the Condition of Magnetic Insulation", M. Lopez, Y.Y. Lau, R.M. Gilgenbach, D.W. Jordan, J.W. Luginsland, Physics of Plasmas, 10, 4489, (2003)
3) "Low-noise microwave magnetrons by azimuthally varying axial magnetic field", V.B. Neculaes, R.M. Gilgenbach, and Y.Y. Lau, Applied Physics Letters, 83, p1938 (2003).
4) "Suppression of Third Order Intermodulation in a Klystron by Third Order Injection", S. Bhattacharje, C. Marchewka, J. Welter, R. Kowaczyk, C.B. Wilsen, Y.Y. Lau, J.H. Booske, A. Singh, J.E. Scharer, R.M. Gilgenbach, M.J. Neumann, and M.W. Keyser, Phys. Rev. Letters 90 (2003) March 7

5) "Microwave Absorption in a Thin Film", H. Bosman, Y.Y. Lau, R.M. Gilgenbach, Applied Physics Letters, 82 1353 (2003) MARCH
6) "A simulation study of beam loading on a cavity", C. Wilsen, J. Luginsland, Y.Y. Lau, T.M. Antonsen, D.P. Chernin, P.M. Tchou, M.W. Keyser, R.M. Gilgenbach, and L.D. Ludeking, IEEE Trans. Plasma Science, Special Issue on High Power Microwaves, 30, p1160, 2002
7) A Note on Current Modulation from Nonlinear Electron orbits", C.B. Wilsen, Y.Y. Lau, D. Chernin, and R.M. Gilgenbach, IEEE Transaction on Plasma Science, Special Issue on High Power Microwave Generation, 30, p1176, 2002
8) "Single Surface Multipactor on a Dielectric Surface", R. Anderson, W. Getty, M.L. Brake, Y.Y. Lau, R.M. Gilgenbach, and A. Valfells, Review of Scientific Instruments, **72**, 3095 (2001).
9) Theory of Intermodulation of a klystron", Y.Y. Lau, D.P. Chernin, C. Wilsen, and R.M. Gilgenbach, IEEE Trans. Plasma Science, 28 959 June (2000)
10) Y. Y. Lau, "A simple theory on the two-dimensional Child-Langmuir Law", Phys. Rev. Lett. **87**, (Dec. 10, 2001 issue).
11) J. W. Luginsland, Y. Y. Lau, R. J. Umstattd, and J. J. Watrous, "Beyond the Child Langmuir Law: The Physics of Multi-Dimensional Space-Charge-Limited Emission", Phys. Plasmas, 2002

(1) Student Conference Call Presentations
University of Michigan
1) Mike Lopez, UM, presented at main MURI Teleconference
2) Herman Bosman, UM, presented at MURI Student Teleconference
3) Bogdan Neculaes, MURI Teleconference: "Low Noise Magnetron by Azimuthally Varying Axial Magnetic Field"

1. V.B.Neculaes, R.M. Gilgenbach, and Y.Y. Lau, "Low-noise microwave magnetrons by azimuthally varying axial magnetic field", *Applied Physics Letters*, **83**, p.1938 (2003).
2. M.C. Jones, V.B. Neculaes, W. White, Y.Y. Lau, and R.M. Gilgenbach, "Simulation of rapid startup in microwave magnetrons with azimuthally varying axial magnetic fields", *Applied Physics Letters,* **84**, p.1016, (2004).
3. M. Lopez, Y.Y. Lau, R.M. Gilgenbach, D.W. Jordan, J.W. Luginsland, "Limiting Current in a Relativistic Diode Under the Condition of Magnetic Insulation", *Physics of Plasmas*, **10**, p.4489, (2003).
4. S. Bhattacharje, C. Marchewka, J. Welter, R. Kowaczyk, C.B. Wilsen, Y.Y. Lau, J.H. Booske, A. Singh, J.E. Scharer, R.M. Gilgenbach, M.J. Neumann, and M.W. Keyser, "Suppression of Third Order Intermodulation in a Klystron by Third Order Injection", *Phys. Rev. Letters*, **90** (2003) March 7.
5. H. Bosman, Y.Y. Lau, R.M. Gilgenbach, "Microwave Absorption in a Thin Film", *Applied Physics Letters*, **82**, p.1353 (2003) MARCH
6. C. Wilsen, J. Luginsland, Y.Y. Lau, T.M. Antonsen, D.P. Chernin, P.M. Tchou, M.W. Keyser, R.M. Gilgenbach, and L.D. Ludeking, "A simulation study of beam loading on a cavity", *IEEE Trans. Plasma Science, Special Issue on High Power Microwaves*, **30**, p1160, 2002.
7. C.B. Wilsen, Y.Y. Lau, D. Chernin, and R.M. Gilgenbach, "A Note on Current Modulation

from Nonlinear Electron orbits", *IEEE Transaction on Plasma Science, Special Issue on High Power Microwave Generation*, **30**, p1176, 2002.

8. Y.Y. Lau, D.P. Chernin, C. Wilsen, and R.M. Gilgenbach, "Theory of Intermodulation of a klystron", *IEEE Trans. Plasma Science*, **28**, p.959 June (2000).
9. Y. Y. Lau, "Simple theory for the two-dimensional Child-Langmuir Law", *Phys. Rev. Lett.*, **87**, (Dec. 31, 2001 issue).
10. J. W. Luginsland, Y. Y. Lau, R. J. Umstattd, and J. J. Watrous, "Beyond the Child-Langmuir Law: The Physics of Multi-Dimensional Space-Charge-Limited Emission", *Phys. Plasmas*, **9**, 2371, 2002.

4.7 MURI Book Project

As noted in the Director's Overview, a major emphasis over the past few years and involving the entire MURI Consortium as well as numerous contributors from Industry and Government Laboratories has been the preparation of a definitive book entitled "Modern Microwave and Millimeter-Wave Power Electronics" to be published by IEEE Press with the proceeds and royalties flowing from this book to benefit the research activities of US graduate students in the field of microwave vacuum electronic devices (MVED) research. The intended audience of this cutting edge book is primarily comprised of electrical engineers and/or systems engineers interested in long-distance (high power) communications and/or radar systems as well as those involved in nonlethal microwave defensive systems.

The book is being written to familiarize solid-state-trained electrical engineers **and electronic systems engineers** with the rich field of MVED technology. This helps fill a significant void in current EE solid-state-dominated education that has existed for more than a decade. There exists no competing book that delivers such comprehensive coverage at this level.

At the time of this report, the book manuscript has been completed and submitted to IEEE Press for review. Galley proofs are expected in August and the book publication is scheduled for the end of the year. The book will have a length of approximately 500 pages and is organized into fifteen (15) chapters:

The book begins by carefully detailing the differences between solid state and vacuum electronic microwave sources, pointing out what parameter ranges are ideally suited to solid state but also what ranges are beyond the capabilities of solid state for practical applications. This provides the fundamental motivation for why the book should be purchased and read.

The second chapter is devoted to the exceptionally rich history of MVED development, illustrating the progressive leaps in physical understanding that lead to today's wealth of alternative sources.

The **next four chapters** describe in detail the four principal types of MVEDs available to modern electrical engineers. Pains are taken not to duplicate previously available material but rather to provide a rich reference source to that existing coverage, simultaneously filling the many gaps in information that exist. An entire chapter is devoted to the "Traveling-Wave Tube (TWT)" which forms the backbone for satellite and airborne communications, as well as for most military electronic counter-measures systems, and for many commercial and military radar systems.

Chapter 7 is particularly noteworthy since it will be **the first** comprehensive write-up to appear in any book to-date on what is probably the most exciting and promising area of MVED R&D, namely that of miniaturized MVEDs for high frequency radiation. This area is crucial for any engineers interested in high bandwidth data/voice communications over large distances when transmitter size and/or weight are important (e.g. – for airborne, man-portable, or satellite-based systems).

Chapter 8 treats the important subject of cathodes (i.e.- electron-beam sources) for producing ever-higher current densities of emitted electrons for higher current e-beams. It also discusses how novel cathode alternatives could be employed in realistic electron-guns for producing the types of beams to drive the various classes of MVEDs.

Chapter 9 will provide the reader with the most careful yet comprehensive explanation of the crucial issue of how to achieve linear amplification of microwave signals - a must for communications engineers and systems designers.

Chapter 10 describes in detail the wealth of computer modeling and simulation tools available to the MVED engineer for the virtual prototyping of specific devices. This subject is crucial for gaining a full appreciation of how MVEDs are designed before any "metal is cut."

The **next two chapters** review the new structures and materials that are available to handle new MVED designs that require higher power densities and/or superior control.

Chapter 13 reviews the important area of High Power Microwave (HPM) sources that has been discussed in great detail in the 2001 IEEE Press book entitled, "High-Power Microwave Sources and Technologies." This chapter reminds the reader of the main differences between the HPM and MVED worlds and then goes on to highlight the two major research areas that dominate the HPM field at this time, namely those of electrode materials and computer modeling.

Chapter 14 discusses the issue of individual MVED unit cost. Methods are clearly illustrated whereby unit cost can be dramatically reduced for individual MVEDs - and how this has already been accomplished for the widespread "cooker" magnetrons used in microwave ovens. Case study data from operational experience is presented that contradicts the popular but overly-optimistic assumption that solid-state-based microwave power electronic systems guarantee superior functionality and reliability for lower system capital or operating costs.

Chapter 15 brings the book to a close by giving an overview of future possibilities for MVEDs and the plethora of promising applications open to them.

The actual book outline together with the responsible "Chapter Masters" follows below:

Chapter 1 (Introduction and Overview). **John Booske** (University of Wisconsin)

Chapter 2 (Historical Highlights). **Neville Luhmann, Jr**. (University of California, Davis) and **Gregory Nusinovich** (University of Maryland)

Chapter 3 (Klystrons). **George Caryotakis** (Stanford Linear Accelerator Center at Stanford University)

Chapter 4 (Traveling Wave Tubes). **John Booske** (University of Wisconsin)

Chapter 5 (Gyro-Amplifiers). **Bruce Danly** (US Naval Research Laboratory)

Chapter 6 (Crossed-Field Devices). **Ronald Gilgenbach** (University of Michigan, Ann Arbor)

Chapter 7 (Microfabricated MVEDs). **Glenn Scheitrum** (Klystron Department at the Stanford Linear Accelerator Center at Stanford University)

Chapter 8 (Advanced Electron Beam Sources). **Ryan Umstattd** (Department of Physics and Information Systems at the US Naval Postgraduate School, Monterey, CA).

Chapter 9 (Linear Amplification). **Kenneth Kreischer is** (Northrup-Grumman, Rolling Meadows, IL).

Chapter 10 (Computational Modeling). **Lars Ludeking** (Mission Research Corporation, Newington, VA) and **Thomas Antonsen** (Department of Electrical and Computer Engineering and Department of Physics at the University of Maryland, College Park, MD).

Chapter 11 (Next-Generation Microwave Structures & Circuits). **Richard (**MIT Fusion Research Center, Massachusetts Institute of Technology, Cambridge, MA).

Chapter 12 (Advanced Materials). **David Abe** is (US Naval Research Laboratory, Washington, DC).

Chapter 13 (HPM Sources). **Thomas Hussey** (High Power Microwave Division of the Directed Energy Directorate of the US Air Force Research Laboratory, Kirtland AFB, Albuquerque, NM) and **Don Shiffler** is a Senior Research in the same division and same location.

Chapter 14 (MVED Manufacturing TechnologiesNeville C. Luhmann ,Jr. (US Naval Weapons Support Center, Crane, IN).

Chapter 15 (Emerging Applications & Future Possibilities). **Victor Granatstein**(Electrical and Computer Engineering at the University of Maryland, College Park, MD). and **Robert Barker** (US Air Force Office of Scientific Research)

The complete Table of Contents follows below:

"Modern Microwave & MM-Wave Power Electronics"

CONTENTS

(as of 6 July 2004)

Chapter 12. Advanced Materials Technologies for MVEDs

Chapter 13. High Power Microwave (HPM) Sources

Chapter 14. Affordable Manufacturing

Chapter 15. Emerging Applications and Future Possibilities

INDEX

ABOUT THE EDITORS

APPENDICES

The following appendices to Chapters 3, 4, 6, and 9 respectively may be found in appropriate digital format on this book's Internet website at http://www.xxxxx.yyyyy/zzzz/